

**Phosphorylation sites on specific
neuronal proteins can control the mode of synaptic
vesicle exocytosis and thereby regulate synaptic
transmission**

by

Deeba Singh

A thesis submitted in partial fulfilment for the requirements for the degree of
Doctor of Philosophy at the University of Central Lancashire

December, 2017

© Copyright by Deeba Singh Oct, 2017

All Right Reserved

Dedication

I dedicate this thesis to my beloved mother

&

To the loving memory of my father.

Declaration



Concurrent registration for two or more academic awards

I declare that while registered as a candidate for the research degree, I have not been a registered candidate or enrolled student for another award of the University or other academic or professional institution.

Material submitted for another award

I declare that no material contained in the thesis has been used in any other submission for an academic award and is solely my own work.

Signature of candidate

Deeba Singh (B.Sc)

Type of award

Doctorate of Philosophy, Ph.D.

School

School of Pharmacy and Biomedical Sciences,

University of central Lancashire

Acknowledgements

I would like to express my deepest gratitude to my supervisor, Dr. Anthony Ashton for his full support, understanding, expert guidance, patience and encouragement throughout my study. His positive attitude and confidence in my research has inspired me and given me the confidence. I would also like to thank my second supervisor, Dr. Jaipaul Singh for his insightful comments.

I would like to express my gratitude to my family; my Mom and brother for their unconditional love and support and to my Dad, who would have been very proud today. I am deeply indebted to the sacrifices made by my family on my behalf.

I would also like to thank my friends; Sonam, Shraddha, Dilip, Reshmi, Vivianna, Pratik, Shweta and Florina for constantly motivating me to get my PhD done and helping me sail through this phase. A special mention to Adam and Stephen for their help and support, this wouldn't have been possible without them. Also, I would like to thank Swati, Sushant, Tazeen, Doyel, Vaibhav, Gina, Rohan, Charmi, Priyanka and Shreya for keeping me entertained.

In conclusion, I would like to thank UCLan for the equipment and services provided. Also, a big thank you to the technical staff for providing a helping hand whenever needed.

Abstract

Synaptic vesicles (SVs) can exocytose via Full fusion (FF) or by Kiss-and-Run (KR) mechanisms. In this thesis, synaptosomes prepared from adult rat cerebrocortex demonstrated that these modes can be switched by regulating the intracellular calcium levels and/or protein phosphorylation reactions. The stimuli employed were: 30 mM K⁺ (HK), 1 mM 4-aminopyridine (4AP) and 5 μM ionomycin (ION) together with 5 mM Ca²⁺. In this model employed, myosin-II and dynamins can regulate the closure of the fusion pore of the readily releasable pool (RRP) of SVs during KR but are independent of each other's actions.

In biochemical assays, synaptosomes were maximally labelled with FM2-10 dye such that both the RRP and the RP were loaded and such terminals were subsequently evoked to release the dye and this was compared to the endogenous release of glutamate (GLU). Results show that the rise in [Ca²⁺]_i at the active zone produced by HK5C activates PKC isoforms, which in turn cause phosphorylation of myosin-II and dynamins. It is hypothesised that dynamins are active at relatively lower increases in [Ca²⁺]_i that do not activate PKCs whereas myosin-II is active at relatively higher increases in [Ca²⁺]_i that activate certain PKCs. Such activation of PKC stimulates myosin-II -but inhibits the action of dynamins – and it is this active protein that can close the fusion pore. ION5C, however, activates dynamin(s) but not myosin-II, and under such conditions dynamin can close the fusion pore. This dynamin-dependent KR mode is independent of clathrin because this is not perturbed by the blockade of clathrin action using the drug, pitstop2TM and the HK5C evoked myosin-II-dependent KR is independent of both clathrin and dynamin. Therefore, the KR

mechanism described, herein, is distinct from ultra-fast endocytosis that has both a dynamin and clathrin dependence. Pre-treatment of synaptosomes with DYN and/or pitstop2TM prior to the initial pre-stimulation with HK5C inhibits all dynamin and clathrin dependent processes so that SVs that recycle after the HK5C pre-stimulation would be perturbed if they had such a requirement. Indeed, following this treatment some SVs were not released by ION5C, although, the 4AP5C evoked GLU release is not affected and it would appear that the 4AP5C sensitive pool (the RRP) can still release following blockade of dynamin and clathrin. This demonstrates that the RRP underwent KR during the first pre-stimulus (actually via a myosin-II- dependent process) and was available to release again during the second round, and again this cannot be via ultra-fast endocytosis.

The role of cAMP and PKA pathways in regulating the modes was investigated. Adenylate cyclase activation by forskolin inhibits the release of the RP but switches all the RRP vesicles to KR when evoked by 4AP5C. Adenylate cyclase inhibition by 9-Cyclopentyl-Adenine (9-Cp-Ade) has no effect on GLU release or exocytotic mode. Forskolin's action on the RP is due to a specific increase in cAMP, because pre-treatment of synaptosomes with 9-Cp-Ade before forskolin prevents the forskolin action. The PKA activator, Sp-5,7-dichloro-cBIMPs (cBIMPS) does not affect evoked GLU release although it does switch some of the RP to a KR mode whereas inhibiting PKA with KT 5720 has no effect on GLU release but induces the RRP to undergo FF. Clearly, forskolin's action on both the RP and the RRP SVs is distinct from PKA activation and it may work through activating the exchange protein directly activated by cAMP (EPAC). Previous experiments have showed that inhibition of protein phosphatase 2A (PP2A) by okadaic acid (OA) switches the RRP to FF for all stimuli, but OA pre-

treatment before forskolin failed to prevent 4AP5C switching some SVs in the RRP from FF to KR. This suggests that an adenylate cyclase pathway can override the OA-sensitive pathway.

The Seahorse extracellular flux analyser was used to measure various mitochondrial respiration parameters (basal, ATP production, spare capacity, maximum respiration, proton leakage and non-mitochondrial respiration). Employing 0.3 and 3 μM phenyl arsine oxide appears to perturb the spare respiratory capacity, whilst 0.1 μM did not. This indicated that we were previously using too high a concentration of this drug to study modes of exocytosis. Such a result led to the testing of the drugs employed in this study on exocytosis to check that they did not produce a non-specific effect on the bioenergetics of the synaptosomes: 9-Cp-Ade, Blebb, Go 6983, cBIMPs, forskolin or OA did not change the mitochondrial respiratory parameters indicating that any exocytotic effects shown were specific.

The specific phosphorylation of Ser-778, Ser-774 and Ser-795 on dynamin 1 was investigated using well characterized commercial antibodies and western blotting. It was concluded that the phosphorylation of Ser-774 and Ser-778 showed no correlation with dynamin's activity towards regulating closure of the fusion pore although these sites may well correlate with clathrin dependent endocytosis and bulk endocytosis. However, the phosphorylation of Ser-795 on dynamin may play an important role in the inhibition of dynamin's activity towards closing the fusion pore during KR. Phosphorylation on Ser-795 may be under the regulation of PKC as demonstrated using a PKC activator, phorbol myristate acetate, and an inhibitor, Go 6983. Therefore, endogenous PKC activation may phosphorylate this site when a very high $\Delta[\text{Ca}^{2+}]_i$ is achieved at the active zone. It was difficult to obtain a conclusion as to which PKC isoform

could regulate the mode of SV exocytosis by phosphorylation of Ser-795 on dynamin due to the low phosphorylation levels obtained whilst employing Go 6983 and Go 6976.

Contents

Dedication	1
Declaration.....	2
Acknowledgements.....	3
Abstract.....	IV
List of Figures	XIV
List of Tables.....	XXII
List of abbreviations	XXIII
Chapter 1	1
Introduction	1
1.1 Background	2
1.2 Synaptic vesicles	4
1.3 synaptic vesicle pools.....	8
1.4 Overview of synapse and active zone (AZ)	10
1.5 Synaptic vesicle cycle.....	12
1.6 Different modes of exocytosis and endocytosis.....	14
1.6.1 Full fusion	14
1.6.2 Kiss-and-run	16
1.6.3 Overview of CME.....	18
1.6.4 Overview of ADBE	20
1.6.5 Overview of ultrafast endocytosis	23

1.7	Dynamins.....	26
1.8	Myosin-II	30
1.9	Ca ²⁺ dependent regulation of exocytosis (Refer to Figure 1.5).....	35
1.9.1	Step 1) SNARE proteins, the engine of membrane fusion	35
1.9.2	Step 2) Priming the SNARE engine	36
1.9.3	Step 3) Ca ²⁺ -dependent triggering starts the SNARE engine:	37
1.10	cAMP-dependent Protein Kinase A (PKA).....	42
1.11	Working hypothesis	44
Chapter 2		45
Materials and Methods.....		45
2.1	Introduction.....	46
2.2	Materials used	46
2.1	Preparation of synaptosomes:	49
2.2.	The measurement of the release of endogenous glutamate.....	51
2.3	FM 2-10 dye release assay	57
2.4	Statistical analysis	62
2.5	Bioenergetics assay (mitochondrial stress test).....	62
2.6	Statistical analysis	67
2.7	Western blotting.....	68
2.7.1	Sample preparation.....	68
2.7.2	Electrophoresis	69
2.7.3	Western blotting.....	70

2.7.4 Re-probing / stripping the PVDF membrane	71
2.7.5 S.E.M.i-quantification of blots:	72
Chapter 3	74
Investigating the Role of Protein Kinase C.....	74
3.1 Background results	75
3.1.1 Introduction	75
3.1.2 Interpretation of background results.....	84
3.2 Introduction to chapter 3	85
3.3 Results.....	86
3.4 Discussion	97
3.4.1 Dynamins and Myosin-II regulate the fusion pore.....	97
3.4.2 PKCs regulate the action of dynamins and myosin-II	98
3.4.3 KR is independent of CDE	101
3.4.4 Dynamin-I regulates the fusion pore	101
Chapter 4	103
Effect of pre-treatment of 160 μ M DYN and 15 μ M Pitstop2 TM	103
4.1 Introduction.....	104
4.1.1 Brief summary of results presented earlier on in this study.....	104
4.1.2 Further investigations into the distinct modes of SV exocytosis.....	107
4.2 Results.....	108
4.3 Discussion	115
4.3.1 Dynamin dependent and clathrin dependent recycling	115

4.3.2 RRP SVs recycle independent of clathrin and dynamins	116
4.3.3 RP is not available for release if the action of dynamins and clathrin is inhibited prior to prestimulation with HK5C	117
4.3.4 RRP SVs can recycle independently of the RP	118
4.3.5 KR is distinct to ultrafast endocytosis.....	118
Chapter 5	120
Investigating the Role of Protein Kinase A.....	120
5.1 Introduction.....	121
5.2 Results.....	122
5.3 Discussion	149
5.3.1 Effect of Inhibition of PKA using KT 5720	149
5.3.2 Effect of activation of PKA using cBIMPS	150
5.3.3 Effect of double treatment of cBIMPS and KT 5720	150
5.3.4 Effect of activation of adenylate cyclase using Forskolin	151
5.3.5 Effect of double treatment of 9-Cp-Ade and Forskolin	152
5.3.6 Effect of double treatment of KT 5720 and Forskolin	153
5.3.7 Effect of double treatment of Forskolin and Okadaic acid.....	154
5.4 Conclusion.....	155
Chapter 6	156
Bioenergetics	156
6.1 Introduction.....	157
6.2 Mitochondrial stress test assay.....	157
6.3 Results.....	161

6.3.1 Determining the appropriate concentration of phenylarsine oxide (PAO).....	161
6.3.2 Effect of various concentrations on mitochondrial respiration parameters.....	164
6.4 Discussion	178
Chapter 7	182
Phosphorylation Studies	182
7.1 Investigating the role of phosphorylation of dynamins in switching the mode of synaptic vesicular exocytosis.....	183
7.1.1 Introduction.....	183
7.2 Results.....	186
7.2.1 Investigating the role of Ser-774, Ser-778 and Ser-795 in KR exocytosis.....	186
7.2.2 Phospho-serine-778 content of dynamin 1	188
7.2.3 Phospho-serine-774 content of dynamin 1	191
7.2.4 Phospho-Ser-795.....	194
7.2.5 Regulation of phospho-Ser 795 on dynamin 1 by Ph est and determination as to whether this is due to activation PKC	196
7.2.6 The effect that pre-treatment with the conventional PKC inhibitor, Go 6976, has on phosphorylated Ser795 of dynamin as revealed by OA treatment	199
7.2.7 The effect that pre-treatment with the broad spectrum PKC inhibitor Go 6983 has on phospho-Ser795 of dynamin as revealed by OA treatment.....	205

7.2.8 Investigating the role of PKA on phosphorylation of Ser-778 and Ser-774 on Dynamin 1	211
7.2.9 Phospho-serine -774 content of dynamin 1 following manipulation of PKA and PP2B.....	213
7.2.10 Phospho-serine -778 content of dynamin 1 following manipulation of PKA and PP2B.....	221
7.3 Discussion	228
Chapter 8	231
General Discussion and Conclusion.....	231
8.1 General discussion and conclusion	232
8.2 Future directions	235
References.....	238
Appendix 1	250
Appendix 2	253
Appendix 3.....	259
Appendix 4.....	261

List of Figures

- Figure 1.1:** A diagram showing the events involved in neurotransmission. 4
- Figure 1.2.1:** Molecular model of outside view of an average synaptic vesicle. 6
- Figure 1.2.2:** Image shows the physical parameters and composition of an average synaptic vesicle as explained in section 1.2. 7
- Figure 1.3:** A diagram showing the three synaptic vesicle pools namely ready release pool (RRP), reserve pool and silent pool. 9
- Figure 1.4:** A diagram showing 3D model of synaptic architecture. 11
- Figure 1.5:** Figure shows events that orchestrate neurotransmitter release at the synapse (full fusion) 13
- Figure 1.6.1:** Schematic diagram showing release of neurotransmitters from synaptic vesicles via a full fusion mechanism. 15
- Figure 1.6.2:** Diagrammatic representation of the comparison between kiss-and run and full fusion 16
- Figure 1.6.3:** CME involves several morphologically distinct steps from clathrin coat binding, invagination of the coated bud, constriction and fission of the neck of CCV and subsequent uncoating of the CCV. 19
- Figure 1.6.4:** Schematic comparison of the three forms of endocytosis: a) CME b) KR c) ADBE. 22
- Figure 1.6.5:** Diagram showing the process of ultrafast endocytosis. 24
- Figure 1.6.6:** Diagram showing a comparison between CME, ultrafast endocytosis and KR. 25
- Figure 1.7.1:** Domain organization of dynamin and their function. 27
- Figure 1.7.2:** Diagram illustrating the functions of dynamin in CME. 29
- Figure 1.8.1:** A diagram depicting the domain structure of myosin-II. 32
- Figure 1.8.2:** Diagrammatic representation of regulation of activity of NMII 34
- Figure 1.9:** Domain structure of PKC isoforms. 41

Figure 2.1.1: Schematic representation of synaptosome formed from isolated nerve terminal	50
Figure 2.1.2: Schematic representation of the steps undertaken for preparation of synaptosomes.	51
Figure 2.2.1: Schematic representation of the order in which samples were added to the microtiter plate for this assay	54
Figure 2.2.2: General schematic representation of the sample preparation timeline to study the effect of (A) treatment with various drugs; or (B) treatment with combination of two drugs; or (C) treatment with combination of two drugs before the pre-stimulation step; on evoked Glu by the stimulus of interest	56
Figure 2.3.1: Schematic representation of the order in which samples were added to the microtiter plate for this assay and has been explained above.	59
Figure 2.3.2: Figure 2.3.2 General schematic representation of the sample preparation timeline to study the effect of (A) treatment with various drugs; or (B) treatment with combination of two drugs; on FM2-10 dye release by the stimulus of interest	60
Figure 2.5.1: Schematic representation of the Xfp utility plate and cartridge. This asS.E.M.bly is also supplied with a clear lid which is placed on top of the sensory cartridge which is removed during measurements.	63
Figure 3.1: The effect of 160 μ M DYN on Glu release evoked by (A) HK5C (B) ION5C and (C) 4AP5C.	76
Figure 3.2: The effect of 160 μ M DYN on FM2-10 dye release evoked by (A) HK5C, (B) ION5C and (C) 4AP5C	78
Figure 3.3: The effect of 50 μ M Blebb on Glu release evoked by (A) HK5C, (B) ION5C, and (C) 4AP5C	80
Figure 3.4: The effect of 50 μ M Blebb on FM2-10 dye release evoked by (A) HK5C, (B) ION5C and (C) 4AP5C	82
Figure 3.5: The effect of 1 μ M Go 6983 on Glu release evoked by HK5C. Data are mean + S.E.M., n= 5 different experiments	83
Figure 3.6: The effect of 1 μ M Go 6983 on FM2-10 dye release evoked by HK5C	86
Figure 3.7: The effect of 1 μ M Go 6983 followed by 50 μ M Blebb on Glu release evoked by HK5C	87

Figure 3.8: The effect of 1 μ M Go 6983 followed by 50 μ M Blebb on FM2-10 dye release evoked by HK5C	88
Figure 3.9: The effect of 1 μ M Go 6983 followed by 160 μ M DYN on Glu release evoked by HK5C	89
Figure 3.10: The effect of 1 μ M Go 6983 followed by 160 μ M DYN on FM2-10 dye release evoked by HK5C	90
Figure 3.11: The effect of 15 μ M pitstop2 TM on Glu release evoked by ION5C	92
Figure 3.12: The effect of 15 μ M pitstop2 TM on ION5C evoked FM2-10 dye release	93
Figure 3.13: The effect of 15 μ M pitstop2 TM plus 160 mM DYN on Glu release evoked by ION5C.	94
Figure 3.14: The effect 15 μ M pitstop2 TM or 15 μ M pitstop2 TM plus 160 μ M DYN on FM2-10 dye release evoked by ION5C	95
Figure 4.1: The effect of 1 μ M BAF on HK5C, ION5C and 4AP5C evoked glutamate release.	105
Figure 4.2: The effect that 160 μ M DYN treatment before pre-stimulation exerts on the subsequent ION5C evoked glutamate release.	108
Figure 4.3: The effect that 15 μ M pitstop2 TM treatment before pre-stimulation exerts on the subsequent ION5C evoked glutamate release	109
Figure 4.4: The effect that 160 μ M DYN treatment before pre-stimulation exerts on the subsequent 4AP5C evoked glutamate release.	110
Figure 4.5: The effect that 15 μ M pitstop2 TM treatment before pre-stimulation exerts on the subsequent 4AP5C evoked glutamate release	112
Figure 4.6: The effect that 160 μ M DYN plus 15 μ M pitstop2 TM treatment before pre-stimulation exerts on the subsequent 4AP5C evoked glutamate release	113
Figure 5.1: The effect of 2 μ M KT 5720 on glutamate release. No significant difference in the glutamate release is observed between control and KT 5720-treated terminals for any of the three stimuli, (A) HK5C, (B) ION5C and (C) 4AP5C are employed.	121
Figure 5.2: The effect of 2 μ M KT 5720 on FM 2-10 dye release.	123

Figure 5.3: The effect of 50 μ M cBIMPS on glutamate release. cBIMPS produces no significant difference in the glutamate release for any of the three stimuli employed: HK5C, ION5C and 4AP5C	125
Figure 5.4: The effect of 50 μ M cBIMPS on FM 2-10 dye	127
Figure 5.5: The effect of 2 μ M KT 5720 and 50 μ M cBIMPS on FM 2-10 dye release	129
Figure 5.6: Comparison of the effect of 2 μ M KT 5720 plus 50 μ M cBIMPS vs 2 μ M KT 5720 on HK5C evoked FM 2-10 dye release.	130
Figure 5.7: Comparison of the effect of 2 μ M KT 5720 and 50 μ M cBIMPS vs 50 μ M cBIMPS on HK5C evoked FM 2-10 dye release.	130
Figure 5.8: The effect of 100 μ M 9-Cp-Ade on glutamate release.	132
Figure 5.9: The effect of 100 μ M 9-Cp-Ade on FM 2-10 dye release.	134
Figure 5.10: The effect of 100 μ M forskolin on glutamate release	136
Figure 5.11: The effect of 100 μ M 1,9-dideoxy-forskolin on HK5C evoked glutamate release.	138
Figure 5.12: The effect of 100 μ M forskolin on 4AP5C evoked FM 2-10 dye release	139
Figure 5.13: The effect of 100 μ M 9-Cp-Ade and 100 μ M forskolin on 4AP5C evoked glutamate release	140
Figure 5.14: The effect of 100 μ M 9-Cp-Ade plus 100 μ M forskolin on 4AP5C evoked FM2-10 release.	140
Figure 5.15: Comparing the effect of 100 μ M 9-Cp-Ade plus 100 μ M forskolin with 100 μ M forskolin alone on 4AP5C evoked FM 2-10 dye release	141
Figure 5.16: The effect of 2 μ M KT 5720 followed by 100 μ M forskolin on 4AP5C evoked FM2-10 dye release	143
Figure 5.17: The effect of 0.8 μ M OA on 4AP5C evoked FM2-10 dye release	144
Figure 5.18: The effect of 0.8 μ M OA plus 100 μ M forskolin on 4AP5C evoked FM2-10 dye release	145
Figure 5.19: A comparison of the effect of 100 μ M forskolin with 100 μ M forskolin plus 0.8 μ M OA on 4AP5C evoked FM 2-10 dye release	146
Figure 6.1: Measurement of mitochondrial respiration through sequential injections of various compounds	156

Figure 6.2: The effect of modulators on ETC cycle	157
Figure 6.3: The effect of 3 μM PAO on the bioenergetics of synaptosomes	159
Figure 6.4: Comparison of the effect exerted by 1 μM and 0.3 μM of PAO on the bioenergetics of synaptosomes	160
Figure 6.5: The effect of 0.1 μM PAO on the bioenergetics of synaptosomes. Error bars indicate S.E.M.	161
Figure 6.6: Comparison between the effect exerted by 0.1 μM , 0.3 μM and 3 μM PAO and control on the spare respiratory capacity	162
Figure 6.7: Comparison between the effect exerted by 0.1 μM , 0.3 μM and 3 μM PAO and control on the average ATP production	163
Figure 6.8: Comparison between the effect exerted by 0.1 μM , 0.3 μM and 3 μM PAO and control on the average proton leak	164
Figure 6.9: Comparison between the effect exerted by 0.1 μM , 0.3 μM and 3 μM PAO and control on the average maximum respiration	165
Figure 6.10: Top: effect of 50 μM cBIMPS on synaptosomes as shown by the mito stress test. Bottom (clockwise): Effect of 50 μM cBIMPS on spare capacity, ATP production, maximum respiration and proton leakage	167
Figure 6.11: Top: effect of 100 μM forskolin on synaptosomes as shown by the mito stress test. Bottom (clockwise): Effect of 100 μM forskolin on spare capacity, ATP production, maximum respiration and proton leakage	168
Figure 6.12: Top: effect of 100 μM 9-Cp-Ade on synaptosomes as shown by the mito stress test. Bottom (clockwise): Effect of 100 μM 9-Cp-Ade on spare capacity, ATP production, maximum respiration and proton leakage	169
Figure 6.13: Top: effect of 1 μM Cys A on synaptosomes as shown by the mito stress test. Bottom (clockwise): Effect of 1 μM Cys A on spare capacity, ATP production, maximum respiration and proton leakage	170
Figure 6.14: Top: effect of 2 μM KT 5720 on synaptosomes as shown by the mito stress test. Bottom (clockwise): Effect of 2 μM KT 5720 on spare capacity, ATP production, maximum respiration and proton leakage	171
Figure 6.15: Top: effect of 50 μM blebb on synaptosomes as shown by the mito stress test. Bottom (clockwise): Effect of 50 μM blebb on	172

spare capacity, ATP production, maximum respiration and proton leakage	
Figure 6.16: Top: effect of 1 μ M Go 6983 on synaptosomes as shown by the mito stress test. Bottom (clockwise): Effect of 1 μ M GO 6983 on spare capacity, ATP production, maximum respiration and proton leakage	173
Figure 6.17: Top: effect of 0.8 μ M OA on synaptosomes as shown by the mito stress test. Bottom (clockwise): Effect of 0.8 μ M OA on spare capacity, ATP production, maximum respiration and proton leakage	174
Figure 7.1: Schematic representation of the various ways in which biological responses can be altered	182
Figure 7.2: Schematic diagram showing the domain structure and phosphorylation sites for dynamin 1	184
Figure 7.3: The effect of OA, Cys A, KN-93, Ph est, and Blebb drug treatments on phosphorylation of ser-778 of dynamin 1 following the application of HK5C stimulation for 15 sec	187
Figure 7.4: Reprobing blots presented in Figure 7.3 with anti-dynamin 4E67	187
Figure 7.5: Bar chart showing changes produced in p-Dyn778 phosphorylation after the various drug treatments and comparing basal (Lo to HK5C).	188
Figure 7.6: The effect of OA, Cys A, KN-93, Ph est, and Blebb drug treatments on phosphorylation of ser-774 of dynamin 1 following the application of HK5C stimulation for 15 sec	190
Figure 7.7: Reprobing blots presented in Figure 7.6 with anti-dynamin 4E67 (top and bottom blot) or anti-synaptophysin (middle blot).	190
Figure 7.8: Bar chart showing changes produced in p-Dyn774 phosphorylation after the various drug treatments and comparing basal (Lo to HK5C).	191
Figure 7.9: The effect of OA, Cys A, KN-93, Ph est, and Blebb drug treatments on phosphorylation of ser-795 of dynamin 1 following the application of HK5C stimulation for 15 sec	193
Figure 7.9a: Over-exposed image of bottom blot in Figure 7.9. Faint bands can be observed with OA treated samples and dark bands can be observed with Ph est treated samples	193

Figure 7.10: Reprobing blots presented in Figure 7.9 with anti-dynamin 4E67.	194
Figure 7.11: Effect of Ph est and GO 6983 + Ph est treatment on phosphorylation of Ser-795 on dynamin 1 following the application of HK5C stimulation for 15 sec	195
Figure 7.12: Reprobing blots presented in Figure 7.11 with anti-dynamin 4E67	196
Figure 7.13: The effect of OA, GO 6976, OA+Go 6976 drug treatments on the phosphorylation of Ser-795 on dynamin 1 seen after stimulation	198
Figure 7.14: Reprobing blots shown in Figure 7.13 with anti-dynamin 4E67	199
Figure 7.15: 15 Bar chart showing the changes produced in p-Dyn795 phosphorylation following 2 s stimulation in samples treated with OA or OA plus Go 6976	200
Figure 7.16: Bar chart showing the changes produced in p-Dyn795 phosphorylation following 15 s stimulation in samples treated with OA or OA plus Go 6976	201
Figure 7.17: Bar chart showing the changes produced in p-Dyn795 phosphorylation following 120 s stimulation in samples treated with OA or OA plus Go 6976	202
Figure 7.18: The effect of OA, GO 6983, OA+Go 6983 drug treatments on the phosphorylation of Ser-795 on dynamin 1 seen after stimulation	204
Figure 7.19: Reprobing blots shown in Figure 7.18 with anti-dynamin 4E67	204
Figure 7.20: Bar chart showing the changes produced in p-Dyn795 phosphorylation following 2 s stimulation in samples treated with OA or OA plus Go 6983	205
Figure 7.21: Bar chart showing the changes produced in p-Dyn795 phosphorylation following 15 s stimulation in samples treated with OA or OA plus Go 6983	207
Figure 7.22: Bar chart showing the changes produced in p-Dyn795 phosphorylation following 120 s stimulation in samples treated with OA or OA plus Go 6983.	208
Figure 7.23: The effect of Cys A, cBIMPS, KT 5720 drug treatments on phosphorylation of Ser-774 in dynamin 1 following the application of basal (Lo), HK5C and ION5C stimuli across various time points.	212
Figure 7.24: Reprobing blots presented in Figure 7.23 with anti-dynamin 4E67. The blots show similar levels of total dynamin.	212

Figure 7.25:	Bar chart showing the stimulus evoked time dependent reduction in phospho-Ser774 in non-drug treated synaptosomes.	214
Figure 7.26:	Bar chart showing the stimulus evoked time dependent reduction in phospho-Ser774 in Cys A treated synaptosomes.	215
Figure 7.27:	Bar chart showing the stimulus evoked time dependent reduction in phospho-Ser774 in cBIMPS treated synaptosomes.	216
Figure 7.28:	Bar chart showing the stimulus evoked time dependent reduction in phospho-Ser774 in KT 5720 treated synaptosomes.	218
Figure 7.29:	The effect of Cys A, cBIMPS, KT 5720 drug treatments on phosphorylation of Ser-778 in dynamin 1 following the application of basal (Lo), HK5C and ION5C stimuli across various time points.	220
Figure 7.30:	Reprobing blots presented in Figure 7.29 with anti-dynamin 4E67. The blots show similar levels of total dynamin	220
Figure 7.31:	Bar chart showing the stimulus evoked time dependent reduction in phospho-Ser778 in non-drug treated synaptosomes.	222
Figure 7.32:	Bar chart showing the stimulus evoked time dependent reduction in phospho-Ser778 in Cys A treated synaptosomes.	223
Figure 7.33:	Bar chart showing the stimulus evoked time dependent reduction in phospho-Ser778 in cBIMPS treated synaptosomes.	224
Figure 7.34:	Bar chart showing the stimulus evoked time dependent reduction in phospho-Ser778 in KT 5720 treated synaptosomes.	225
Figure 8.1:	A schematic representation of the action of PKCs.	230

List of Tables

Table 2.1: Pair of antibodies used with their final dilution factor	48
--	----

List of abbreviations

+S.E.M.	Standard error of mean (positive)
±S.E.M.	Standard error of mean (positive and negative)
4AP	4-Aminopyridine
4AP5C	4AP with 5 mM extracellular Ca ²⁺
9-Cp-Ade	9-Cyclopentyladenine monomethanesulfonate
ADBE	Activity dependent bulk endocytosis
AZ	Active zone
BAF	Bafilomycin A1
BAR	Bin-Amphiphysin-Rvs
Blebb	Blebbistatin
Ca ²⁺	Calcium
CaM	Calmodulin
CaMKII	Ca ²⁺ /CaM-dependent protein kinase type II
cAMP	Cyclic adenosine monophosphate
CaN/PP2B	calcineurin/protein phosphatase 2B
cBIMPS	Sp-5,6-Dichloro-cBIMPS
CCV	Clathrin coated vesicle

CDE	Clathrin dependent endocytosis
CDK5	Cyclin-dependent kinase 5
CME	Clathrin mediated endocytosis
Con	Control
Cys A	Cyclosporin A
DAG	Diacylglycerol
DYN	Dynasore
EPAC	Exchange protein directly activated by cAMP
FCCP	Carbonyl cyanide-p-trifluoromethoxyphenylhydrazone
FF	Full-collapse fusion mode of exocytosis
GDH	Glutamate dehydrogenase type II
Glu	Glutamate/Glutamic acid
GSK-3	Glycogen synthase kinase
HK	High K ⁺ ion concentration, external
HKxC	HK with x mM extracellular Ca ²⁺
ION	Ionomycin
IONxC	ION with x mM extracellular Ca ²⁺
KDa	Kilodalton
KR	Kiss-and-run mode of exocytosis

Max	Maximum
MES	2-(N-morpholino)ethanesulfonic acid
min	Minute (s)
MLC	Myosin light chain
MLCK	Myosin light chain kinase
NADP ⁺	β-Nicotinamide adenine dinucleotide 2'-phosphate, Oxidised form
NADPH	β-Nicotinamide adenine dinucleotide 2'-phosphate, reduced form
NMHC	Myosin heavy chain
NMII	Non-muscle myosin II
NMJ	Neuromuscular junction
NSF	N-ethylmaleimide sensitive factor
OA	Okadaic acid
OCR	Oxygen consumption rate
PAGE	Polyacrylamide gel electrophoresis
PAO	Phenylarsine oxide
Ph Est/PMA	Phorbol esters/ phorbol 12-myristate 13-acetate
PI(4,5)P ₂	Phosphatidylinositol 4,5-bisphosphate
PIP ₂	Phosphatidylinositol 4,5-bisphosphate
PIP ₂	Phosphatidylinositol biphosphate

PKA	Protein Kinase A
PKC	Protein Kinase C
PLC	Phospholipase C
PP1	Protein phosphatase 1
PRD	Proline rich domain
PVDF	Polyvinylidene fluoride
RP	Reserve pool
RRP	Ready releasable pool
RT	Room temperature
SDS	Sodium dodecyl sulphate
Sec or s	Second(s)
-SEM	Standard error of mean (negative)
Ser	Serine
SNAP	Synaptosomal-associated protein
SNARE	Soluble NSF-Attachment Protein Receptor
SV	Synaptic vesicle
Thr	Threonine

Chapter 1

Introduction

1.1 Background

For over a century, the neuron doctrine (put forth in early 1900s) -which states that the neuron is the structural and functional unit of the nervous system- has provided the fundamental essence for neuroscience. Santiago Ramón y Cajal is identified as the leading protagonist of the neuron doctrine and he made detailed observations about the functional contact points between neurons, later described as 'synapses' by Sherrington in 1897 (Yuste, 2015; Guillery, 2005). The synapse is the point at which one neuron communicates with another neuron and is composed of the presynaptic terminal, the synaptic cleft and the postsynaptic terminal. Communication between neurons is known as synaptic transmission which can be either electrical or chemical and the neurons can receive either an excitatory or inhibitory signal. These synaptic connections can process and exchange prodigious amounts of information over a distributed neural network in the matter of milliseconds (Marois and Ivanoff, 2005). The approximate distance between pre and post synaptic membrane in an electrical synapse is 4nm. Synaptic delay is virtually absent across the gap junctions, which are specialized protein structures that conduct the flow of ionic current from presynaptic to postsynaptic terminal. Electrical synapses have bidirectional transmission and are employed to transmit rapid and stereotyped depolarizing signals. In a chemical synapse, the distance between the pre and post synaptic membrane is 20-40nm. It has a synaptic delay of at least 0.3 ms but usually 1-5 ms or longer and has a unidirectional transmission. Chemical synapses can amplify the neuronal signal and also mediate either excitatory or inhibitory changes post-synaptically. They can also produce electrical changes that can last from milliseconds to minutes in the post synaptic cell. The majority of the synapses in the brain are chemical (Kandel, 2013). On arrival of an action

potential, the neurotransmitter that is present pre-synaptically is released in a calcium-dependent manner due to the opening of voltage-gated calcium channels in response to presynaptic depolarization (Martini, 2007). The neurotransmitter which is stored in synaptic vesicles is released to activate specific receptors present post-synaptically. The amount of neurotransmitter released is directly proportional to intensity of the stimulation. This release of transmitter occurs at the active zone. These active zones contain proteins that perform specialized functions like priming and docking of the synaptic vesicles, recruiting the appropriate calcium channels and certain other proteins and mediating short and long-term plasticity. The regions on either side of the active zones are called peri-active zones where some forms of endocytosis take place to replenish the pool of vesicles (Martini, 2007; Sudhof and Rizo, 2011). This has been demonstrated in figure 1.1.

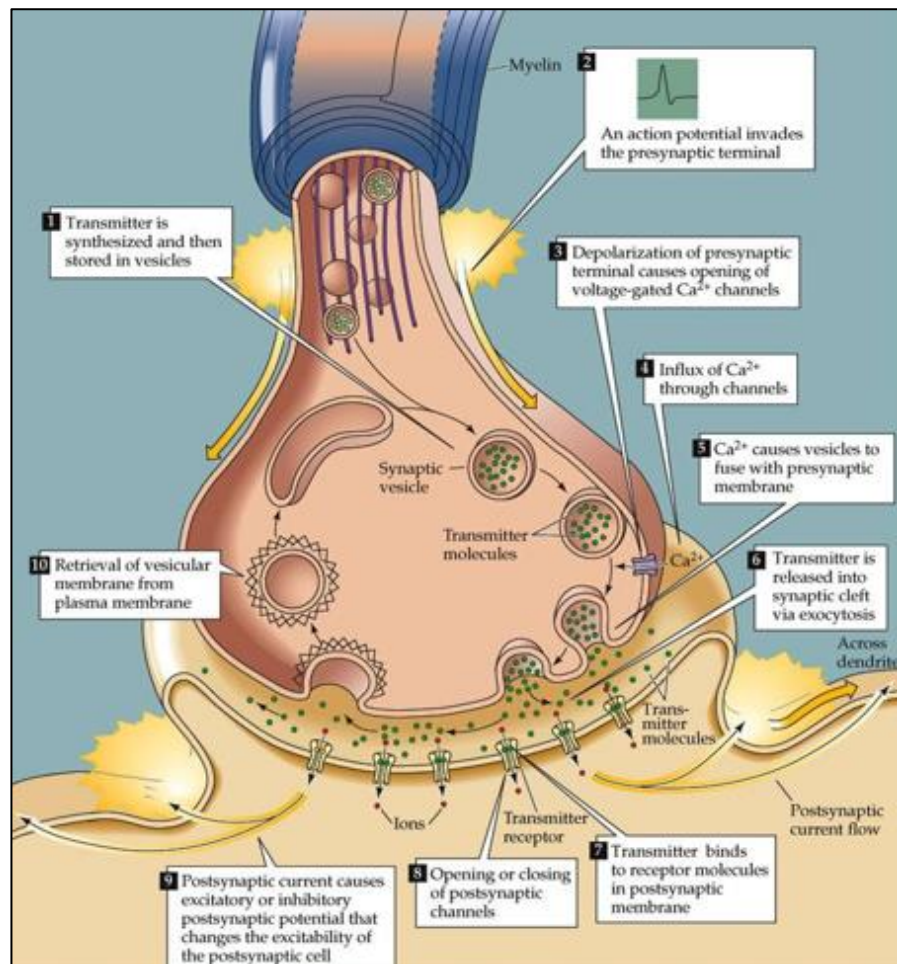


Figure 1.1 A diagram showing the events involved in neurotransmission (Sudhof and Rizo, 2011).

1.2 Synaptic vesicles

Synaptic vesicles are organelles present in synaptic boutons that play a critical role in neurotransmission. They are the best characterized of all organelles. Palade and Palay (1954) presented the first electron microscopy images that confirmed the existence of synaptic vesicles. Later Whittaker and Sheridan (1965) performed biochemical analyses to isolate acetylcholine from synaptic vesicles. Takamori *et al.*, (2006) used various molecular, biophysical, electron microscopy and modelling techniques to determine a quantitative description of the synaptic vesicle using rat brain homogenate as shown in figure 1.2.2. Synaptic vesicles have an average size of 40nm and can hold 1790 molecules of glutamate at a concentration of 150mM (this varies for other

neurotransmitters). Synaptic vesicles contain a diverse array of trafficking proteins as shown in figure 1.2.1. With the exception of V-ATPase which is present only in one or two copies, vesicles contain multiple copies of proteins required for membrane traffic and uptake of neurotransmitter (Takamori *et al.*, 2006). Takamori *et al.*, (2006) have shown that synaptic vesicles are biochemically homogenous in that all SVs contain the same constituents. However, Crawford and Kavalali (2015) have suggested that synaptic vesicles are not homogenous organelles and possess intrinsic molecular differences and different interaction partners (Crawford and Kavalali, 2015). Future studies are necessary to ascertain the possibility of molecular heterogeneity and distinct biochemical fingerprints (Alabi and Tsein, 2012). Hua *et al.*, (2011) have shown that v-SNARE distribution differs in synaptic pools which serves as a molecular tag in distinguishing different synaptic pools. (Hua *et al.*, 2011).

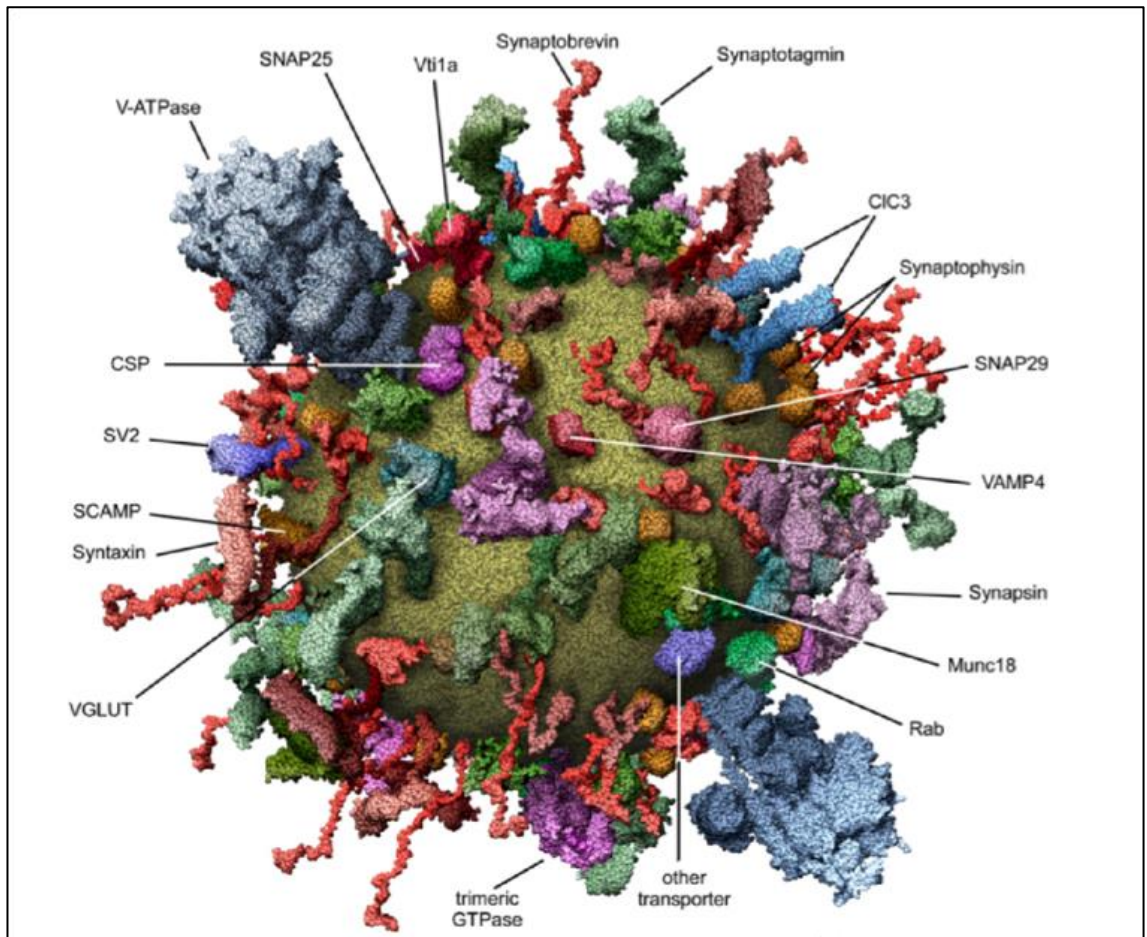


Figure 1.2.1 Molecular model of outside view of an average synaptic vesicle (Takamori *et al.*, 2006).

Physical Parameters	
Density (g/ml)	1.10
Outer diameter (nm)	41.6
Inner aqueous volume (l)	19.86×10^{-21}
Number of neurotransmitter molecules (at 150 mM)	1790
Mass (g) ^a	29.6×10^{-18}
Mass (MDa) ^a	17.8
Protein:phospholipids (w:w)	1.94
Phospholipids:cholesterol (mol:mol)	1:0.8
Transmembrane domains (number/% of surface coverage) ^b	600/20.0
Protein Stoichiometry (Copies/Vesicle)	
Synaptophysin	31.5
Synaptobrevin/VAMP2	69.8
VGLUT1 ^c	9.0
VGLUT2 ^c	14.4
Synapsins	8.3
Syntaxin 1	6.2
SNAP-25	1.8
Synaptotagmin	15.2
Rab3A	10.3
SV2	1.7
Synaptogyrin	2.0
SCAMP1	0.8
CSP	2.8
V-ATPase ^d	1.4
NSF (hexamer)	0.2
Membrane Lipids	
Phospholipids total (number/% of surface coverage)	6992/50.4
Phosphatidylcholine	2524
Phosphatidylethanolamine (C1-ester/C1-ether)	1621/1311
Phosphatidylserine	857
Phosphatidylinositol	132
Sphingomyelin	516
Cholesterol	5663
Hexosylceramide	108
Mean values are shown.	
^a Calculated indirectly using the vesicle number and the sum of protein and lipid masses. In agreement with this result, a mass of $(26.4 \pm 5.8) \times 10^{-18}$ g was measured directly with STEM, which corresponds to 15.9 ± 3.5 MDa.	

Figure 1.2.2 Image shows the physical parameters and composition of an average synaptic vesicle as explained in section 1.2 (Takamori *et al.*, 2006)

1.3 synaptic vesicle pools

Birks and MacIntosh (1961) put forth the concept that synaptic vesicles are not functionally equivalent after they investigated acetylcholine release from cat sympathetic ganglia and discovered that some vesicles underwent exocytosis more easily than others. Later Elmqvist, *et al.*, (1965) obtained similar results with human intercostal muscles. Chemical synapses have a distinctive feature of an assembly of synaptic vesicles in the presynaptic terminal. These vesicles participate in a cycle which allows sustained activity of the nerve terminal. Vesicle pools have been extensively investigated in all major synaptic preparations, including synapses as different as the *Drosophila* larval neuromuscular junction (NMJ), goldfish retinal bipolar cells, the frog NMJ, the mammalian calyx of Held (a giant synapse in the auditory system), and cultured hippocampal synapses cells (Rizzoli and Denker, 2010).

In all these synapses, three major synaptic pools have been proposed which have been given a varied array of names. For this thesis, they will be referred to as ready releasable pool, reserve pool and silent pool as shown in figure 1.3. The ready releasable pool is situated closest to the active zone and is recruited for release upon arrival of low frequency stimulation. Before these vesicles can exocytose, the vesicles are primed and docked. The second category of synaptic vesicle pool is the reserve pool. It is spatially distant from RRP and is released once RRP has been exhausted. The third type of synaptic vesicle pool that is thought to exist is the silent pool. This silent pool makes up almost eighty percent of the total vesicle pool. It is situated farthest from the active zone and does not release under normal physiological conditions. The number of vesicles belonging to each pool differs across synapses (Ashton and Ushkaryov, 2005).

Besides, the aforementioned three pool model, several other pool models have been proposed. Out of these, the main pools are spontaneous pool which release without stimulation, super-pool of vesicles which are shared between boutons and surface pool of vesicles which are stranded or deposited in a state of fusion with the plasma membrane and are available for compensatory retrieval from there in response to exocytosis of other vesicles. These new concepts provide a new outlook in the functioning of synaptic vesicles but due to lack of understanding about their exact mechanism these concepts prove to a debatable issue (Mochida, 2015).

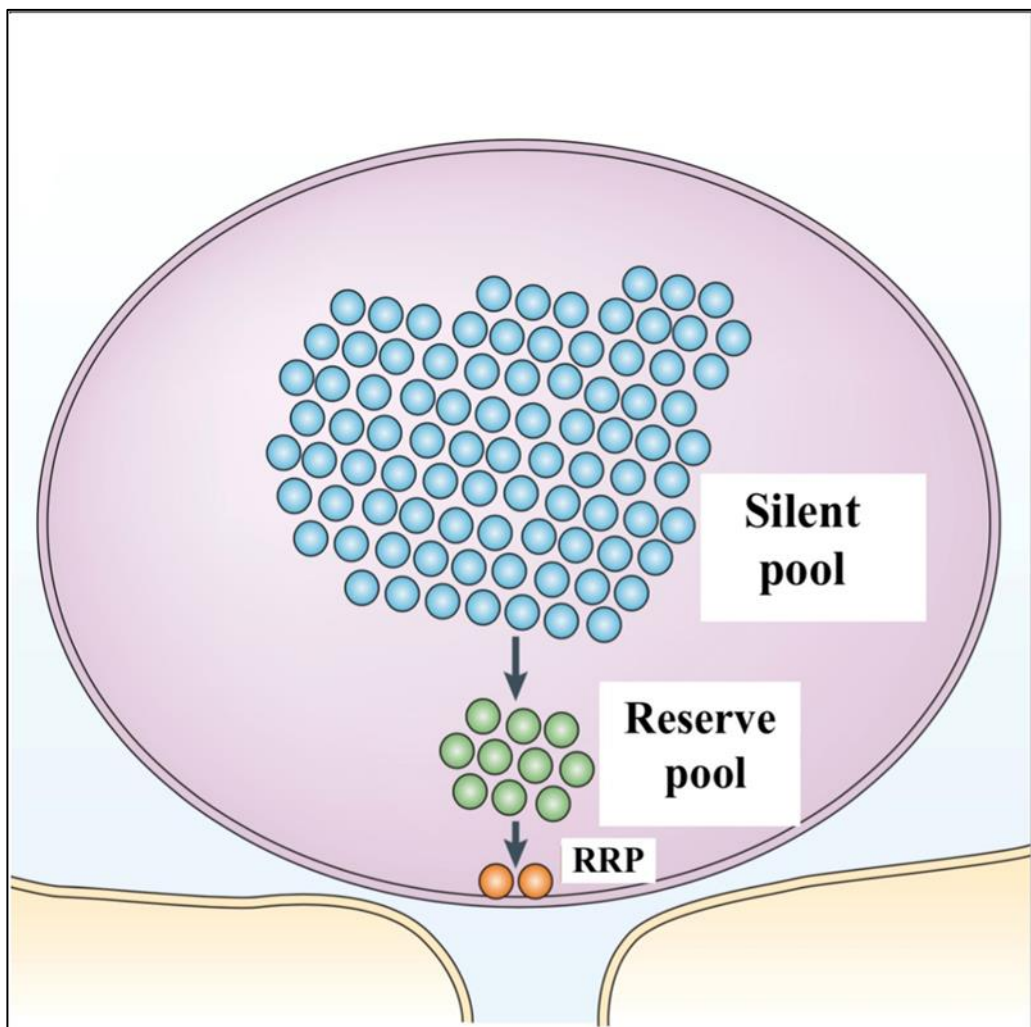


Figure 1.3 A diagram showing the three synaptic vesicle pools namely ready release pool (RRP), reserve pool and silent pool (Rizzoli and Betz, 2005).

1.4 Overview of synapse and active zone (AZ)

The intercellular junctions between a presynaptic neuron and a postsynaptic cell, the latter of which can also be a neuron, represent synapses. Synapses receive information in the form of an action potential and transmit it to the postsynaptic cell through the release of neurotransmitter. Thus, they act as “computational devices” that help in transmission of action potential encoded information (Sudhof, 2012). The information received at the synapse can, in the form of action potential trains, bring about use-dependent changes in the postsynaptic neuron. These changes can either be long-term or short-term; termed as long-term plasticity or short-term plasticity respectively. Synapses differ from each other in various parameters like neurotransmitter type, release probability and post synaptic receptor composition. There are various types of neurons in the mammalian brain, which form a multitude of synapses that display distinguished properties depending on the pre and postsynaptic neurons. Thus, there are hundreds of distinct types of synapses with unique computational properties (Sudhof, 2012). The strength of synaptic transmission and its regulation rely on the complex set of proteins that are required for synaptic function and that contribute to the active zone and the postsynaptic density. Wilhelm *et al.*, (2014) have performed a detailed characterization using fluorescence microscopy for localization of proteins, quantitative immunoblotting and mass spectrometry for determining protein numbers and electron microscopy for measuring organelle numbers, sizes and positions using the cortex and cerebellum of adult rats as shown in figure 1.4. Using these techniques, they generated a 3D model of an average synapse which shows 300,000 proteins in atomic detail.

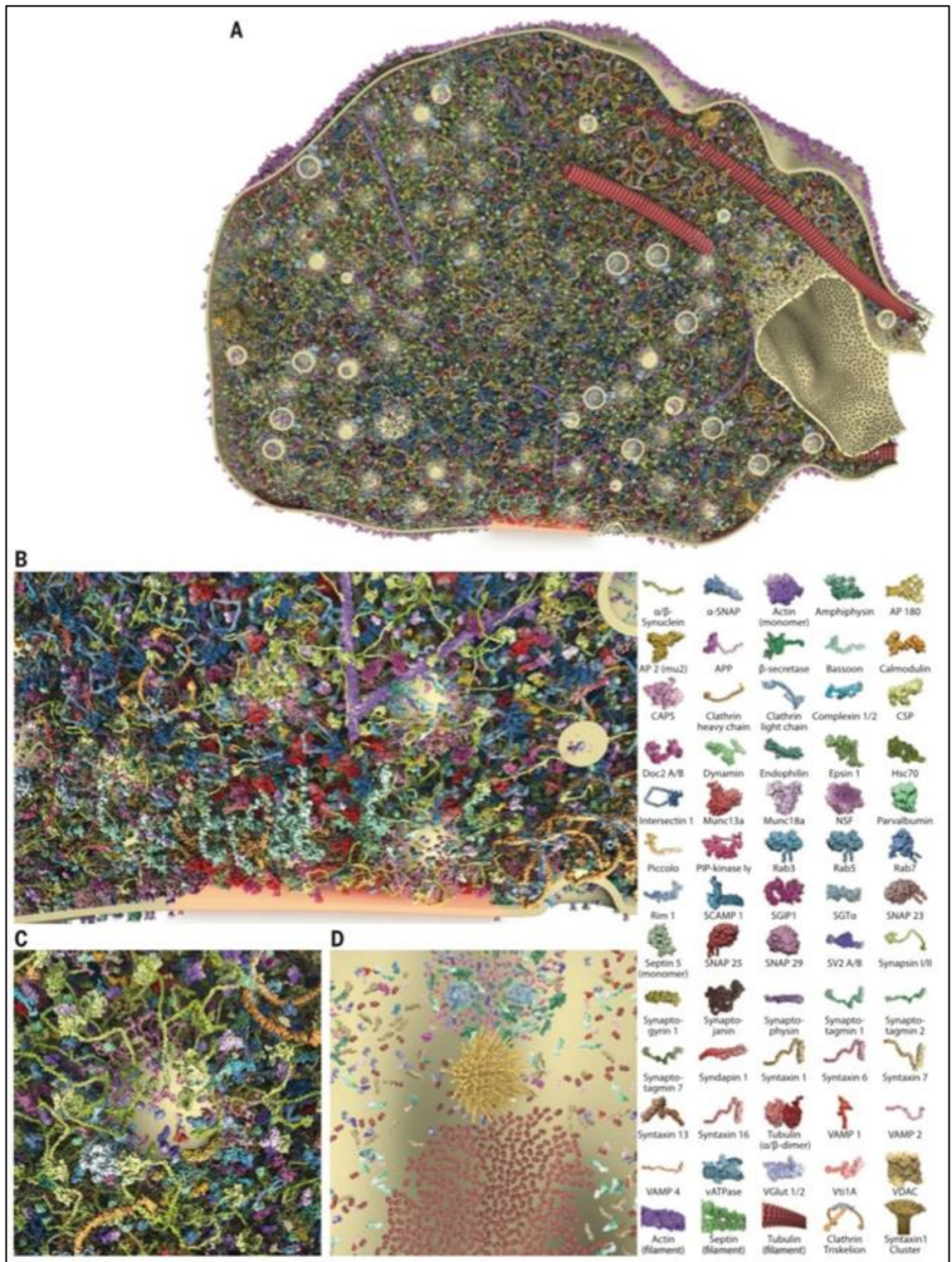


Figure 1.4 A diagram showing 3D model of synaptic architecture. A) A section of synaptic bouton, showing 60 proteins B) High zoom view of active zone area C) High zoom view of vesicle cluster D) High zoom view of a section of plasma membrane in the vicinity of AZ. The graphical legend to the right indicates the different proteins (Wilhelm *et al.*, 2014).

The presynaptic bouton is a specialized site characterized by the presence of active zones. In vertebrates the active zones are mainly disc-like structures with a diameter of 0.2-0.5 μm . Active zones are flanked by peri-synaptic zones on either side. They allow a presynaptic action potential to lead to the release of a chemical signal with high spatial and temporal precision (Kittel and Heckmann, 2016). The active zone contains a set of specialized proteins which are described later in sections 1.7-1.9.

1.5 Synaptic vesicle cycle

The synapses formed by neurons are independently regulated. The major event in the synaptic vesicle cycle is exocytosis by membrane fusion. The presynaptic boutons contain numerous synaptic vesicles filled with neurotransmitter. On arrival of an action potential, the predocked vesicles at the active zone undergo a Ca^{2+} -dependent fusion at the active zone resulting in neurotransmitter release through the formation of a fusion pore. Fusion pores help regulate the rate and the amount of release of neurotransmitter. The exocytosed vesicles are then retrieved via endocytosis for refilling the neurotransmitter and are also docked and primed for re-release (Jackson *et al.*, 2015). The events of the conventionally discussed synaptic vesicle cycle are discussed in the legend for figure 1.5.

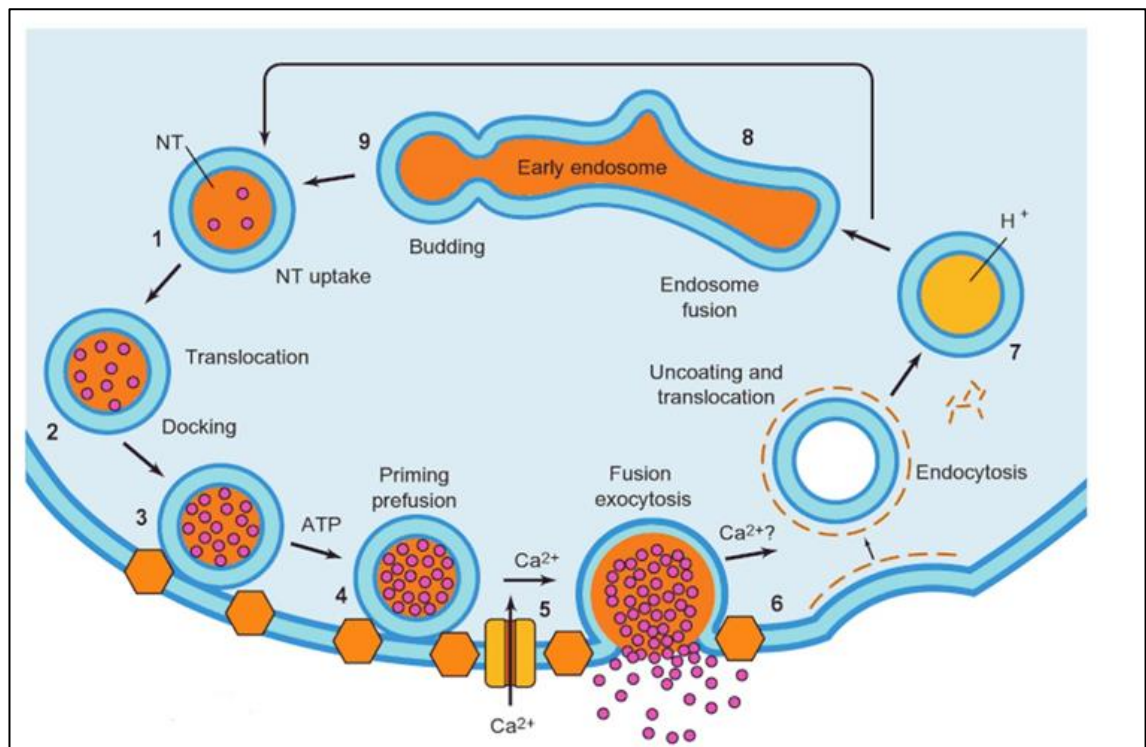


Figure 1.5 Figure shows events that orchestrate neurotransmitter release at the synapse (full fusion): 1) Synaptic vesicles are filled with neurotransmitter using specific transporters in the SV membrane. This process is ATP dependent. 2) The synaptic vesicles are moved to the active zone 3) They are then docked at the AZ 4) and primed for fusion event 5) On arrival of an action potential, there is an influx of calcium through the opening of the voltage gated calcium channels that triggers the fusion of the synaptic vesicles to the plasma membrane for release of transmitter release 6) The vesicles then move away from the active zone and gathered in coated pits for endocytosis 7) The coated vesicles begin to acidify and the clathrin coat is removed by a chaperone 8) The endocytosed vesicles are then fused with an early endosome for sorting and reconstitution 9) with SV then ready for re-use (Brady and Siegel, 2012).

1.6 Different modes of exocytosis and endocytosis

This conventional model only takes into account the full fusion mode of exocytosis when in fact, there are two forms of exocytosis: full fusion (FF) and Kiss-and-run (KR).

1.6.1 Full fusion

Full fusion was initially described in 1973 by Heuser and Reese at the frog neuromuscular junction (NMJ). In this mode, the SVs manifest a complete aqueous continuity between vesicle lumen and external medium and full lipid continuity vesicle membrane and plasma membrane, causing near-instantaneous neurotransmitter release at the active zone as shown in figure 1.6.1 (Harata *et al.*, 2006). The collapsed membrane then moves away from the active zone and is retrieved by clathrin-mediated endocytosis, slow recycling via endosomal compartments or bulk endocytosis. This process has also been implicated in CNS terminals (Sankaranarayanan and Ryan, 2000).

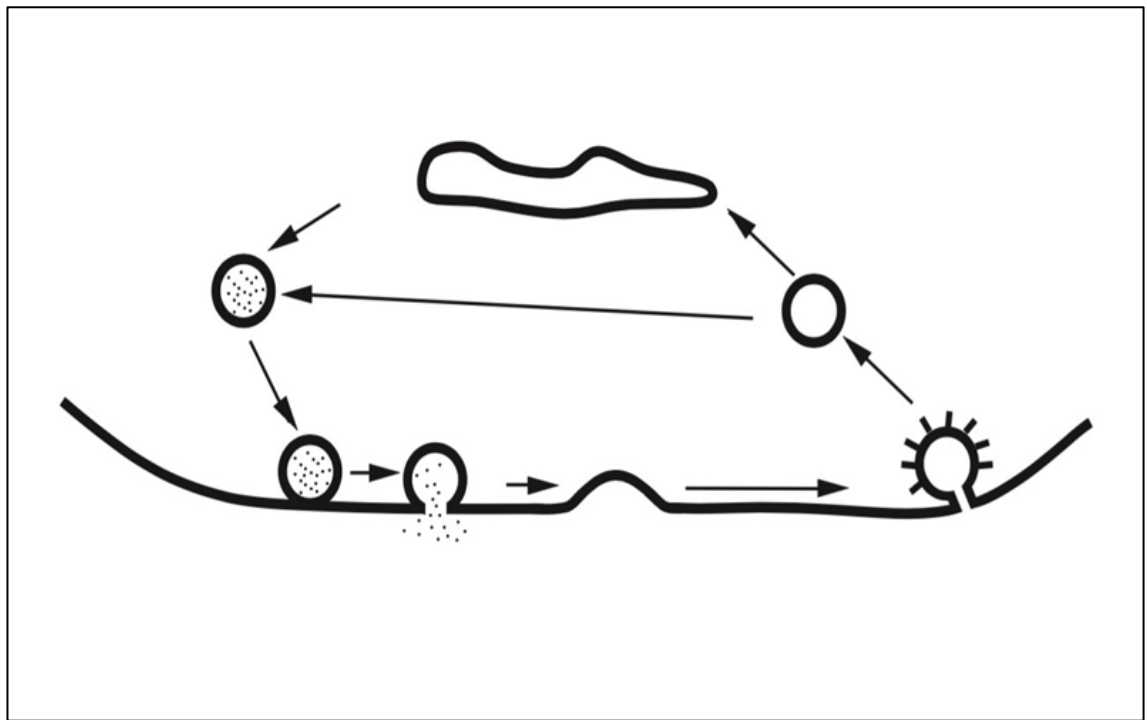


Figure 1.6.1 Schematic diagram showing release of neurotransmitters from synaptic vesicles via a full fusion mechanism. The synaptic vesicles then diffuse laterally and are retrieved via clathrin-mediated endocytosis or endosomal recycling. (Wu *et al.*, 2007).

This process would put tremendous pressure on the RRP vesicles to maintain a speedy and efficient exocytosis process because the endocytosed vesicles would have to quickly return to the interior and then through the following endocytosis steps in quickly and be primed and ready for release in order to maintain the signal downstream, this would mean that the vesicles race back and forth and in the process restore the complement of proteins and lipids required for release; a quick exocytosis process called kiss-and run helps solve the kinetic dilemma of the RRP vesicles allowing them to release the neurotransmitter and help maintain the signal.

1.6.2 Kiss-and-run

KR or non-classical mode of fusion was also discovered in 1973 by Ceccarelli and colleagues at the frog NMJ. KR results in the formation of a transient pore for release of neurotransmitter, without complete loss of identity of SVs and cessation of this would occur by closing of the fusion pore. Thus, the SVs are available for rapid re-use.

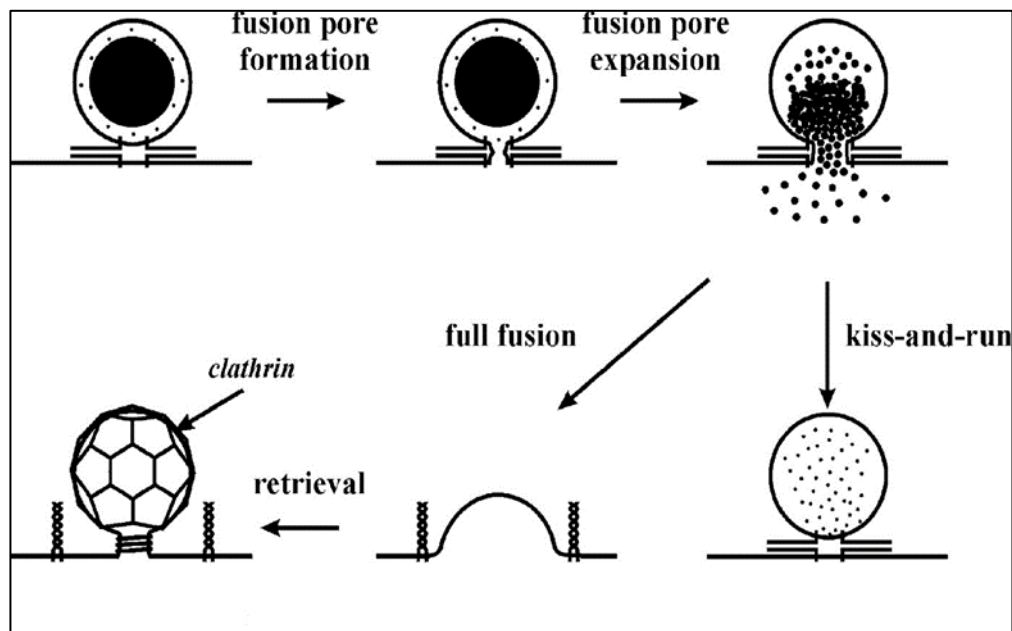


Figure 1.6.2 Diagrammatic representation of the comparison between kiss-and-run and full fusion. (Burgoyne *et al.*, 2001).

Harata *et al.*, (2006) have proposed that KR helps to conserve the resources during periods of stimulation and this ensures that the synapses are ready for high frequency firing with a full quota of fusion-competent vesicles. These processes co-exist in nerve terminals with frequency of stimulation being the deciding factor. KR and FF are at variance with each other (as shown in figure 1.6.2) on various factors like lack of lipid and protein continuity when the SV fuses with the plasma membrane or vesicle location after fusion. KR still remains a debatable concept. Harata *et al.*, (2006) have shown the prevalence

of KR in the hippocampal cells by using bromophenol blue to quench the incompletely released FM dye. He *et al.*, (2006) have performed capacitance measurements at giant synapses to demonstrate the prevalence of KR while Zhang *et al.*, (2009) have used recycling of quantum dots in SVs technique to show KR. KR mode of exocytosis involves the endocytic stage where the fusion pore closes (Harata *et al.*, 2006).

Ashton *et al.*, (unpublished data) have shown that a switch in the mode of exocytosis can be brought about by modulating $[Ca^{2+}]_i$ and protein phosphorylation. Strong stimulation of nerve terminals causes the RRP to undergo KR while the RP fuses via FF.

In synapses at a given time period, the number of vesicles undergoing exocytosis can surpass the reserve of precursor synaptic vesicles delivered from the cell body. Thus, to balance the demand and supply of vesicles, nerve terminals have developed efficient endocytic ways for recapturing and reusing membranes that have fused with the plasmalemma for neurotransmitter release. Electrophysiological studies using extracellular endocytic tracers performed at the frog NMJ by Heuser and Reese and Ceccarelli and colleagues have given rise to two schools of thought: one holding that vesicles acquire tracers directly via a reversible exo/endocytic sequence in which they consistently maintain their biochemical identity during transient continuity with plasma membrane, the other that synaptic vesicles acquire tracers indirectly via the formation of clathrin coated vesicles which are spatially and temporally separate from exocytosis and reverse a temporary loss of vesicles' individual identity upon merger with plasma membrane (Heuser, 1989) Depending on the intensity of stimulation at various synapses the time taken for endocytosis can vary (Saheki, and De Camilli, 2012). There are in fact four different forms of SV

endocytosis: a) clathrin mediated endocytosis (CME) b) KR (mentioned earlier) c) bulk endocytosis/ activity dependent bulk endocytosis (ADBE) and d) ultrafast endocytosis.

1.6.3 Overview of CME

Clathrin mediated endocytosis is a ubiquitous process occurring in all eukaryotic cell types to internalize nutrients, antigens, pathogens and recycling receptors. In nerve terminals, clathrin coated vesicles (CCVs) bud off from the presynaptic plasmalemma at the peri-active zone. After full fusion of SVs they are translocated into the cell. This process requires sequential and progressive assembly of CCVs which serve to converge the cargo proteins and lipids into the emerging vesicle thereby providing a self-propelled medium to deform the membrane into a vesicular bud as shown in figure 1.6.3. Pitstop (2-(4-Aminobenzyl)-1,3-dioxo-2,3-dihydro-1H-benzo[de]isoquinoline-5-sulfonic acid sodium salt) serves as an inhibitor for CME by selectively inhibiting ligand association with the clathrin terminal domain (Kleist *et al.*, 2011). Work by Heuser and Reese (1973) suggested that clathrin coated vesicles fuse to an internal endosome from which SVs are pinched off. However, more recent findings suggest that the coated vesicles simply lose the clathrin coat and the SV is recovered.

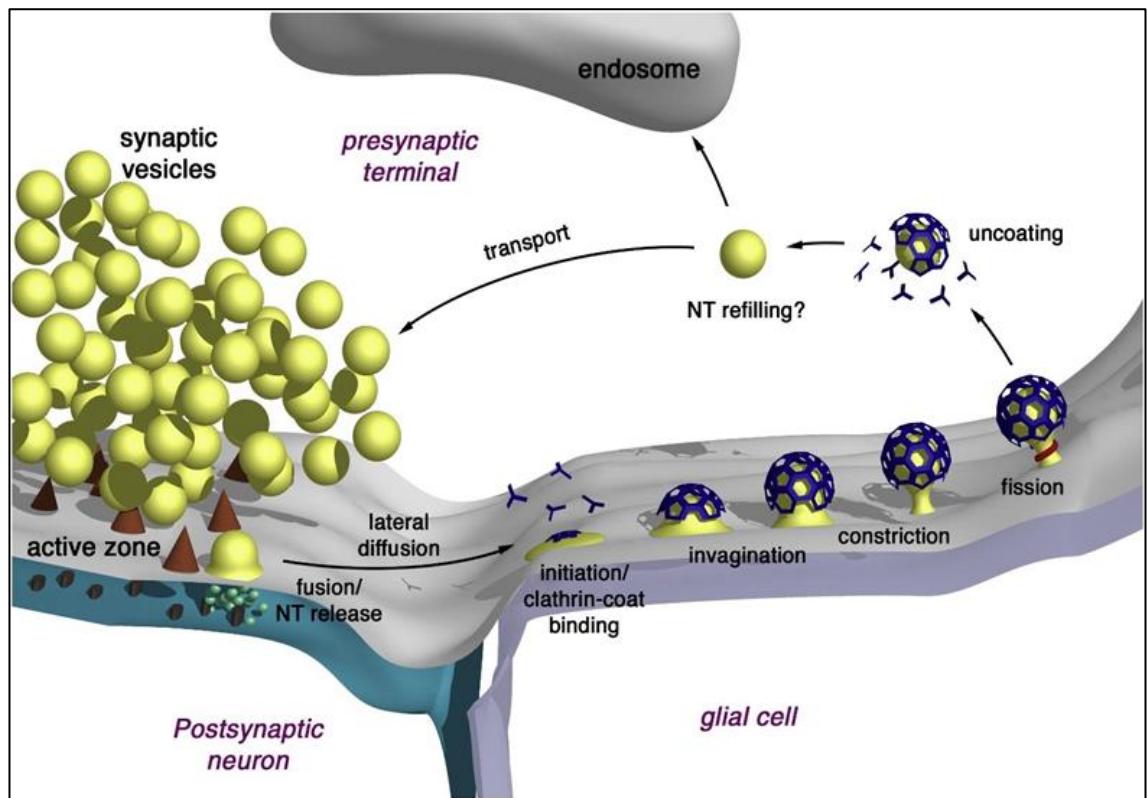


Figure 1.6.3 CME involves several morphologically distinct steps from clathrin coat binding, invagination of the coated bud, constriction and fission of the neck of CCV and subsequent uncoating of the CCV. An endosome intermediate is not required for CME (Shupliakov and Brodin, 2010).

The clathrin coat consists of two layers, one being the inner layer of adaptors and the outer layer comprised of a clathrin lattice. The inner layer is made up of various proteins that may contain, a membrane binding and folded module with flexible arms and this may terminate into a small folded module. The former part binds to the cytoplasmic exposed domains of the membrane proteins and to the head group of PI(4,5)P₂ while the arms serve as a link for the clathrin heavy chain and other adaptors as well as other endocytic factors. The outer clathrin lattice layer is composed of a triskelion shaped scaffold protein made up trimers of heavy chains with three bound light chains (Saheki and De Camilli, 2012; Takei and Haucke, 2001; Kononenko and Haucke, 2014; Shupliakov *et al.*, 2002).

Initiation of the clathrin coat assembly is aided by the accumulation of PIP₂ and adaptor proteins for example AP-2 at the invagination site. Accessory proteins help form protein-protein interactions to assist the assembly of the clathrin coat. As the clathrin coat assembles around the budding vesicles the membrane acquires an increasing curvature until a deeply invaginated coated pit is formed.

Growth of CCVs requires BAR domain proteins and actin reorganization. Constriction and fission of the coated pit requires the GTPase dynamin. Uncoating of the clathrin layer is an ATP-dependent step requiring Hsc70 ATPase and its DnaJ-like cofactor auxilin (Saheki and De Camilli, 2012; Takei and Haucke, 2001; Kononenko and Haucke, 2014; Shupliakov *et al.*, 2002).

The time constant for CME is 15-20 seconds while for KR the fusion pore closes with 0.5 seconds. KR mode of exocytosis/endocytosis bypasses the need for CME or any other form of endocytosis.

1.6.4 Overview of ADBE

The concept of ADBE was first reported by Miller and Heuser in 1984 at amphibian NMJ (Clayton and Cousin, 2009). This pathway is activated during intense stimulation conditions, wherein a large number of SVs fuse with the plasma membrane in a short period of time. The excess plasmalemma is captured by the formation of plasma membrane infoldings. These infoldings later undergo fission to form cisternae and intracellular vacuoles. The endosome-like compartments which form in response to synaptic vesicular exocytosis may contain the proteins and lipids which are abundantly present in the plasma membrane. These endosome-like intermediates eventually disappear as new SVs are formed, thereby suggesting a precursor-product relationship between the newly formed SVs and these organelles (Saheki and

De Camilli, 2012). The SVs bud from these endosomes in clathrin and adaptor protein dependent manner (Cheung and Cousin, 2013). Cousin and colleagues have suggested that the ADBE form of endocytosis replenishes the reserve pool of vesicles (Cheung and Cousin, 2013). The time constant and speed for this process is still a debatable issue. This process is recruited during intense stimulatory conditions when clathrin dependent machinery is saturated and persists for minutes after termination of the stimulation. This process in comparison to CME is much slower thereby placing the nerve terminal in a dangerous situation to rapidly correct the large increase in membrane area produced by this process (Clayton *et al.*, 2008). Figure 1.6.4. shows a schematic comparison between CME, KR and ADBE.

ADBE is dependent on two events: activation of calcium/calmodulin dependent protein phosphatase, calcineurin, which in turn dephosphorylates GTPase dynamin I during intense stimulation, which results in an interaction with F-BAR protein syndapin. Thereby necessitating the dependence of this process on extracellular calcium (Cheung and Cousin, 2013). The exact molecular machinery behind this process is unknown. Although bulk endocytosis does occur, the molecular mechanisms elucidated by Cousin and colleagues is now questioned. They have emphasised the role of dynamin I in the process and its regulation by phosphorylation. However, bulk endocytosis still occurs in KO mice which lack dynamins I or I and III (Cheung and Cousin, 2013).

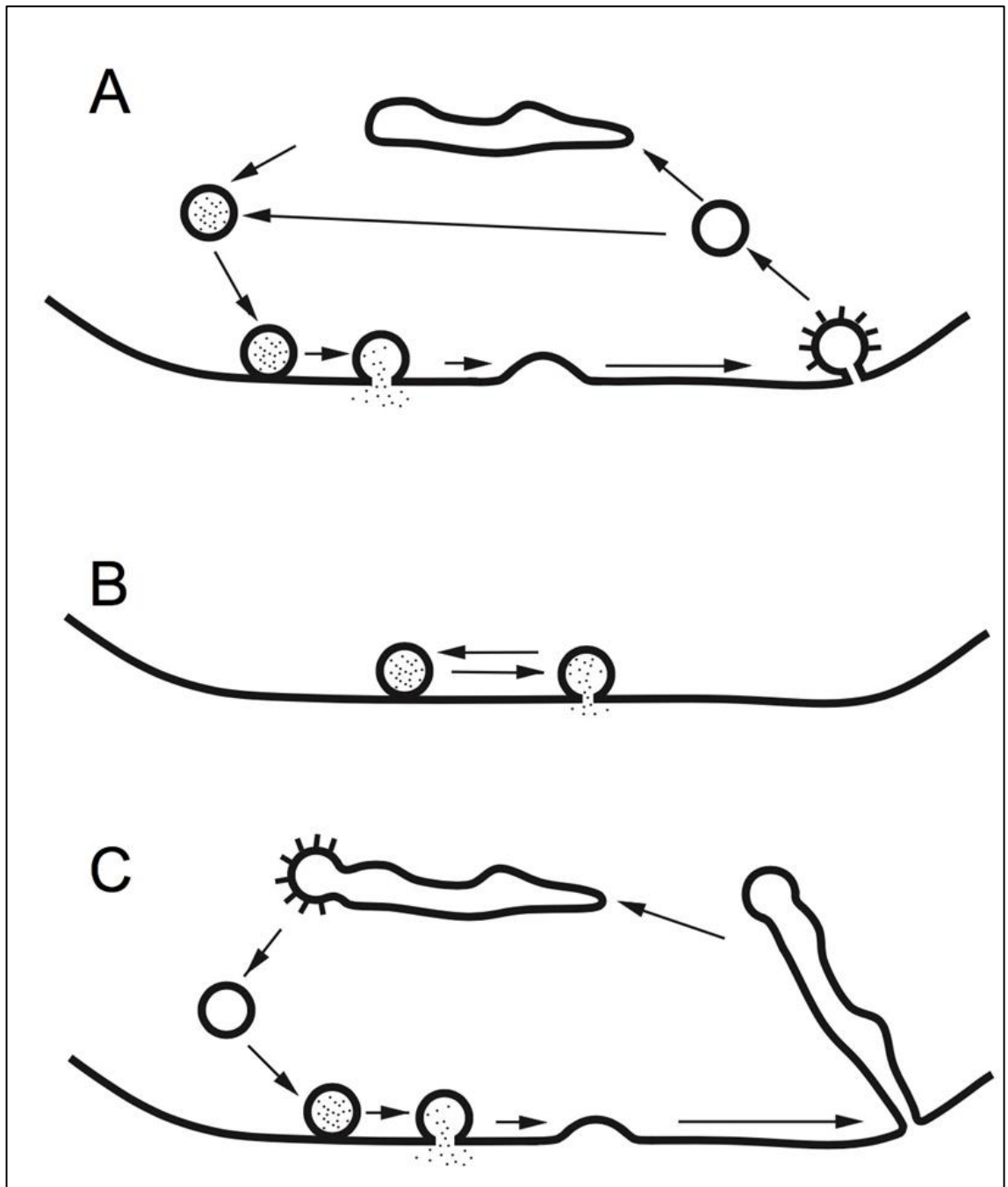


Figure 1.6.4 Schematic comparison of the three forms of endocytosis: a) CME b) KR c) ADBE (Wu *et al.*, 2007).

1.6.5 Overview of ultrafast endocytosis

The concept of ultrafast endocytosis was put forth by Watanbe *et al.*, (Watanbe *et al.*, 2013) in recent experiments in *C.elegans* and mouse hippocampal neurons. In this process as shown in figure 1.6.5, the docked vesicles fully collapse into the plasma membrane synaptic and are retrieved by endocytic invaginations that appear 50-100 ms after SV fusion. The transition from synaptic vesicle to synaptic endosome takes one second after stimulation. After 3 seconds coated vesicles pinch off from the endosome. These coated vesicles transition to small diameter SVs 5-6 seconds after stimulation. This process occurs at the interstitial zone, which is a region adjacent to the AZ and is less densely packed with proteins and cytoskeletal elements and surrounding this zone is the periaxonal zone, where ADBE and CME take place. The endocytic invaginations formed are approximately 80nm in diameter, which is equivalent to four SVs rather than one, thus differing from KR. This form of endocytosis has been observed in mild stimulatory conditions (most experiments use only one action potential). Also, the time taken for this recycling process is around 5 secs whereas KR is only limited by the time it takes for SV to reload with neurotransmitter which is only about 1 secs. KR may still be a faster recycling mechanism than ultrafast endocytosis which may only occur under such low stimulation conditions. Figure 1.6.6. highlights the differences between CME, ultrafast endocytosis and KR The exact molecular mechanism for this process is unknown, however, some studies have indicated that dynamin, actin and endophilin may help regulate this process (Watanbe *et al.*, 2013; Watanbe *et al.*, 2014; Kononeko. and Haucke, 2014; Zhou *et al.*, 2014; Saheki, and De Camilli, 2012).

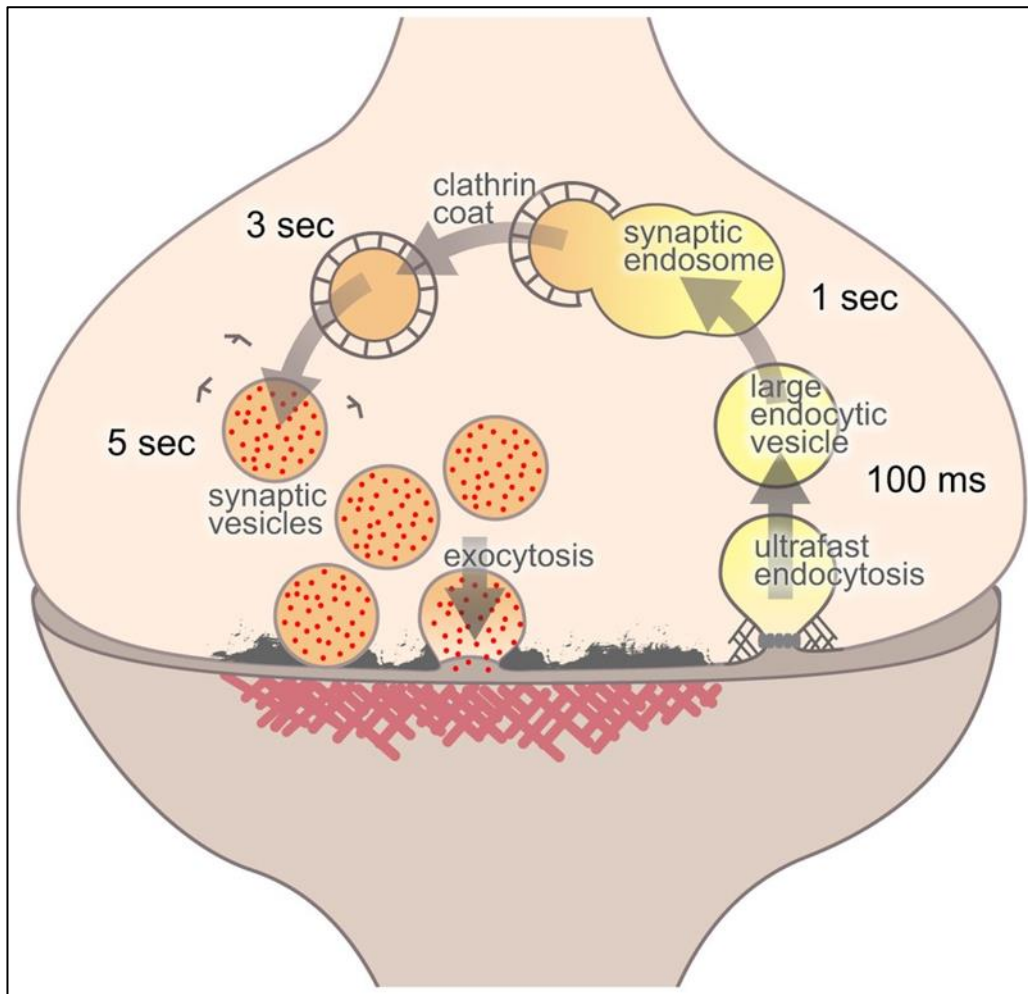


Figure 1.6.5 Diagram showing the process of ultrafast endocytosis (Watanabe *et al.*, 2014).

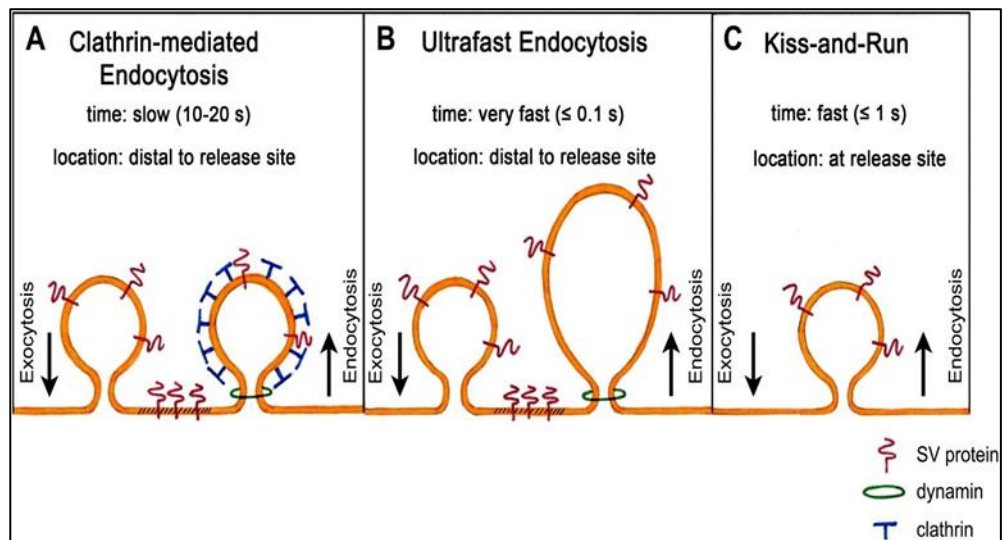


Figure 1.6.6 Diagram showing a comparison between CME, ultrafast endocytosis and KR. A and B are dynamin and clathrin dependent later in this thesis we show that KR also is dynamin dependent. The timings relate to when the invagination pinches off from the membrane and not the recycling time for a SV to be reavailable for further rounds of SV exocytosis (Kononeko. *et al.*, 2013).

1.7 Dynamins

Dynamin derived from the word 'dynamic' was named so to demonstrate its molecular motor-like properties and was first isolated as a microtubule binding protein which on addition of ATP caused the microtubules to slide past each other (Sheptner, and Vallee, 1989). Dynamin is a 100 KDa protein that plays an important role in endocytosis. Three dynamin genes can be found in mammalian genomes. These proteins have the same domain organization and share 80% of the homology but have distinctive expression patterns. Dynamin I has a high expression level in neurons but not in non-neuronal tissues however it can be detected in cultured cell lines. Dynamin 2 has a ubiquitous expression level. Dynamin 3 like dynamin 1 can be found in neurons but has a relatively lower expression level, it can also be found in testis and in lower levels in lungs as well. These three different isoforms form different protein-protein interactions and have different quantitative properties, which include affinities for SH3-domain proteins, GTPase activity levels, oligomerization efficiency rates and lipid binding properties which in turn affect the membrane fission rate (Liu *et al.*, (2011))

Dynamin belongs to a family of GTPases which are known as dynamin-like proteins (DLPs) also called dephosphins. Its domain structure and the function of each domain are shown in figure 1.7.1. Dynamins are cytosolic proteins, having an amino terminal G domain; a 'middle' or 'stalk' region; a pleckstrin homology domain (PH domain); a GTPase effector domain (GED) and a proline-rich carboxy terminal region, typically referred to as the proline-rich domain (PRD). The PH domain mediates the interaction between dynamin and lipids in membranes, in particular it interacts with phosphoinositide phospholipids. GED interacts with the G domain and PRD helps in protein-

protein interactions. Dynamins hydrolyze GTP and the rate depends on its interaction with other molecules, regulated by the phosphorylation state of dynamin.

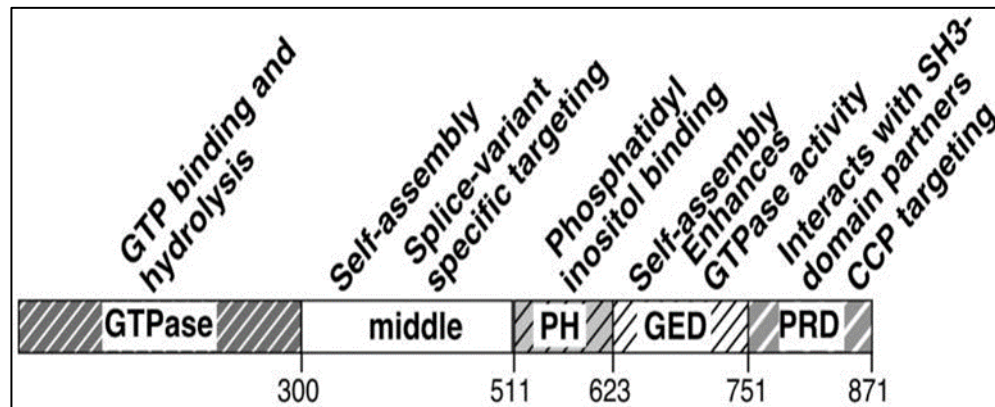


Figure 1.7.1 Domain organization of dynamin and their function (Courtesy: Mettlen, *et al.*, 2011)

Dynamins form dimers in solutions and these dimers form tetramers at higher concentrations. This polymerization creates a spiral array and is the result of side by side placement of dimers through interactions of the stalk tips. This spiral forms around membrane invaginations and through GTP hydrolysis, scission of the invagination in vesicles can occur. The angle at which dynamins interact determines the diameter of the vesicle neck, also called fusion pore (FP). The core is formed by the stalks and the BSE and G domains of each dimer project towards the adjacent rungs of the dynamin helix. It is after this asS.E.M.bly that G-domain dimerization takes place across adjacent rungs. Once the dynamin polymerization is complete around the neck of the endocytic intermediate, its GTP-hydrolysis-dependent structural reorganization triggers constriction. There are three models that have been proposed regarding the mechanism of dynamin for membrane fission which are the twistase model,

constrictase model and the poppase model. Dynamin may contribute to multiple forms of endocytosis, but its action is best understood in the context of clathrin mediated endocytosis as described in figure 1.7.2. During the formation of endocytic buds, a subset of scaffold proteins, and clathrin adaptors are first recruited to the phosphoinositol lipid containing regions of the plasma membrane. These components help to cluster cargo, inducing membrane curvature and also have actin-nucleating properties. This coat subsequently grows through the clathrin lattice which in turn recruits additional cargo adaptors and endocytic factors. Dynamin then begins to accumulate around this growing pit. This assembly then results in deep invagination of the bud and formation of a narrow neck. The next step in this process is recruitment of BAR domain proteins which in turn causes dynamin to rapidly accumulate at bud necks to mediate fission (Ferguson & Camilli 2012), Mettlen *et al.*, (2011) have proposed another role for dynamin wherein dynamin functions as a regulatory GTPase. And the GTP bound dynamin serves to regulate the effectors that control vesicle formation. The self-assembling property activates an internal GAP domain (GED) that exerts a negative control on dynamin function and terminates dynamin-effector interactions.

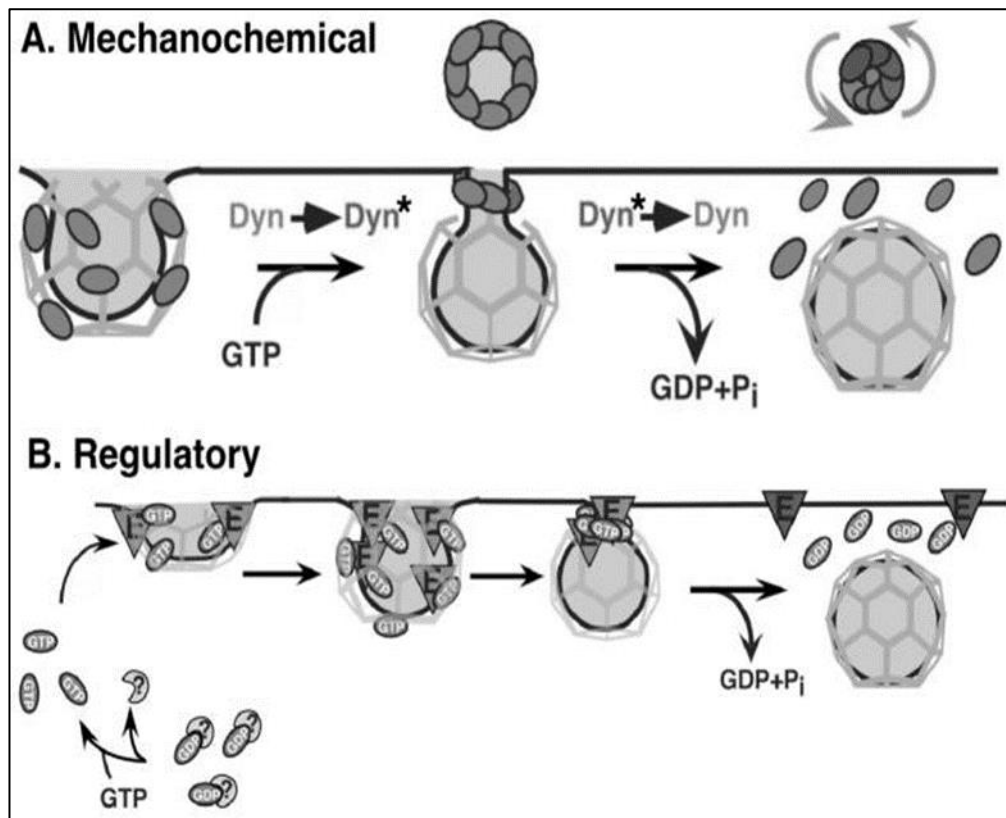


Figure 1.7.2 Diagram illustrating the functions of dynamin in CME. A) the mechanochemical function acts to bring about membrane fission. B) The regulatory function acts to terminate the dynamin-effector interactions (Mettlen *et al.*, 2011).

Ferguson and Camilli (2012) have suggested that dynamin 1 phosphorylation depends, at least in part, on CDK5, and, upon nerve stimulation, dynamin is rapidly dephosphorylated by calcium and calmodulin-dependent phosphatase calcineurin; thereby facilitating endocytosis (Ferguson & Camilli 2012). The action of calcineurin (PP2B) can be inhibited by the action of cyclosporine A. Graham, *et al.*, (2007) have shown that in synaptosomes dynamin I has seven phosphorylation sites *in vivo*: Ser774, Ser778, Ser822, Ser851, Ser857, Ser512, and Ser347. On further analysis, it was found that the Thr780 phosphorylation site does not undergo phosphorylation *in vivo* but does so *in vitro*. Moreover, their quantification analysis led to the conclusions that Ser774

and Ser778 were the major sites of phosphorylation (Graham *et al.*, 2007). Not much information is available for dynamin 2 and dynamin 3. However, since dynamin 1 and 3 share common mechanisms it is believed that dynamin 3 is phosphorylated at the equivalent sites as dynamin 1.

Besides endocytosis dynamin also interacts with the cytoskeleton and plays an important role in cytokinesis. The absence of dynamin 2 show links to tissue specific diseases like Charcot-Marie disease and centronuclear myopathy (CNM). Mutations in dynamin 1 specifically affect the nervous system. The dynamin1 gene can be considered a target for idiopathic causes of epilepsy (Ferguson & Camilli, 2012). Also, the invasive activity of pancreatic ductal carcinoma was associated with upregulation in dynamin 2 expression (Ferguson & Camilli, 2012).

The action of dynamins 1 and 2 can be inhibited by DYN (3-Hydroxynaphthalene-2-carboxylic acid (3,4-dihydroxybenzylidene)hydrazide). Dynole-34-2TM(2-Cyano-*N*-octyl-3-[1-(3-dimethylaminopropyl)-1*H*-indol-3-yl]acrylamide) acts as a dynamin 1 inhibitor. Dyngo-4a (3-Hydroxy-*N'*[(2,4,5trihydroxyphenyl)methylidene]naphthalene-2-carbohydrazide) inhibits dynamin 2.

1.8 Myosin-II

Each molecule of myosin-II is made up of 6 polypeptide chains, which are arranged as dimers of heavy chains; each dimer is associated with one essential light chain (ELC) and one regulatory light chain (RLC); this light chain is associated with the heavy chain in a tight non-covalent fashion. In mammals, three different genes for non-muscle myosin heavy chains (NMHC) have been identified which in turn give rise to three myosin II protein complexes called IIA,

IIB and IIC. Each NMHC can be divided into various structurally defined domains with each domain performing a different function. Figure 1.8.1 shows the domain structure of myosin-II. The N-terminal portion of the NMHC peptide forms a globular head, which is also referred to as the motor domain because it mediates the ATPase- and actin-binding activities of the molecule. The ELC and RLC associate with the heavy chains via interaction with IQ motifs that reside near the C-terminal end of the globular head, in a region often referred to as the neck domain. After the neck domain is an α -helical coiled-coil rod/tail domain, which mediates heavy chain homodimerization and filament assembly, and the molecule terminates with a nonhelical tailpiece (NHT) of approximately 34-44 amino acids (Sandquist and Means 2008).

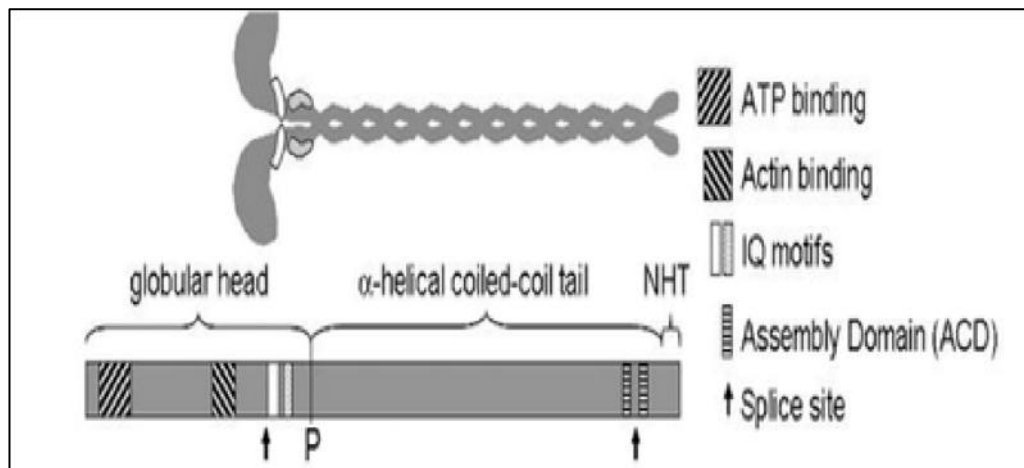


Figure 1.8.1 A diagram depicting the domain structure of myosin II (Sandquist and Means, 2008).

All these three isoforms perform two basic functions which are assembly into bipolar filaments and contraction of F-actin in an ATP-dependent manner. The functions performed by non-muscle myosin can be regulated through various ways, the best characterised method being phosphorylation of RLC at Ser19. Phosphorylation on Ser19 of the RLC stimulates the actin-activated ATPase of myosin-II and promotes the assembly of myosin-II into filaments. One of the key enzymes regulating the phosphorylation status of the RLC is Rho kinase (ROCK), which can directly phosphorylate the RLC as well as phosphorylate and inactivate the targeting subunit of the myosin light chain phosphatase. The other method of regulating myosin II is through PKC. When activated by phorbol esters (PMA), PKC can phosphorylate Ser1/2 residues of RLC *in vivo* and it can also phosphorylate Thr9 *in vitro*. This PKC phosphorylation, not only inhibits the rate of MLCK phosphorylation, but also inhibits the ATPase activity of myosin-II once it is phosphorylated by MLCK (Bresnick 1999). In case of heavy chains of myosin-IIa, Ser1916 and Ser1943 are phosphorylated by PKC and casein kinase II respectively; whereas, on the other hand, Ser1939 and Ser1941 of

myosin-IIb are phosphorylated by PKC (Bresnick 1999). Myosin-II has been proved to be involved in the mobilization of RP to near the synaptic membrane (Ryan, 1999).

Recently, it has been suggested that dephosphorylated myosin-II can act as a molecular motor by hindering the dilation of fusion pores thereby possibly regulating the size of the pore. Moreover, it can also regulate the amount of vesicular release by manipulating the duration of the fusion pore opening (Aeeco *et al.*, 2008; Aoki *et al.*, 2010). It should be noted that the PKC phosphorylations of these other sites may be involved in activation of myosin II. Thus, it will clearly depend upon what amino acids are phosphorylated as to what specific roles myosin II may play. A diagrammatic representation of regulation of NM II has been shown in the figure 1.8.2; wherein various proteins like TRPM7 (transient receptor potential melastatin 7), PKCb, PKC, PKCz and CK II have been shown to regulate the activity of NMHC. Human RLC is encoded by myosin heavy chain 9 (MYH9), NMHC IIB by MYH10 and NMHC IIC by MYH14. Kinases PKC, MLCK, ROCK, MRCK/CDC42BP (myotonic dystrophy kinase-related CDC42-binding kinase, ZIPK/ DAPK3 (leucine zipper interacting kinase) and citron kinase can regulate the activity of RLC (Vincente-Manzanares M. *et al.*, (2010)). The action of myosin II can be inhibited by the action of Blebb (\pm)-1,2,3,3a-Tetrahydro-3a-hydroxy-6-methyl-1-phenyl-4*H*-pyrrolo[2,3-*b*]quinolin-4-one).

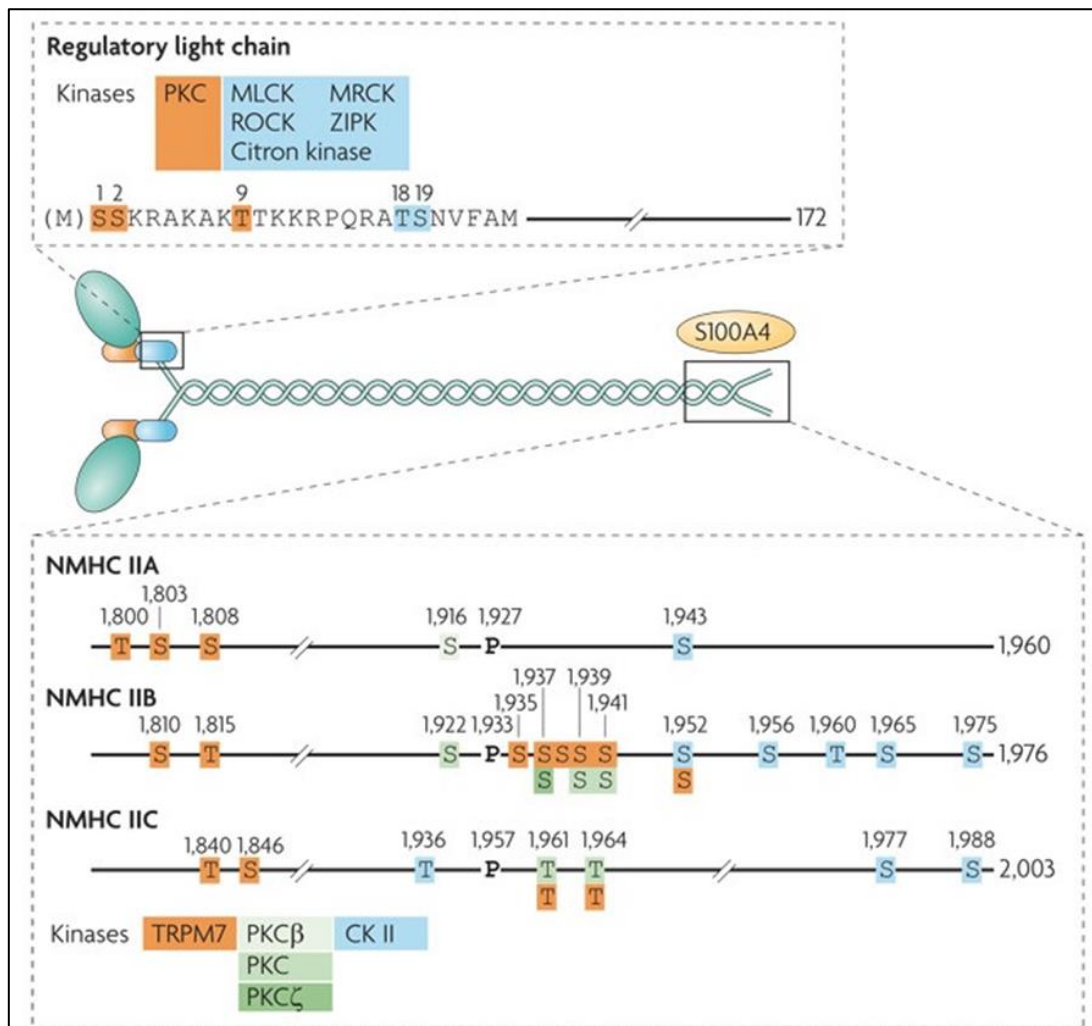


Figure 1.8.2 Diagrammatic representation of regulation of activity of NM II (Vicente-Manzanares *et al.*, 2010).

1.9 Ca²⁺ dependent regulation of exocytosis (Refer to Figure 1.5)

A rapid increase in intracellular Ca²⁺ acts as a trigger for exocytosis. In neurons, the proteins that form a part of the exocytotic machinery are: soluble N-ethylmaleimide-sensitive factor attachment protein (SNAP) receptors (SNAREs), ATPase N-ethylmaleimide-sensitive factor (NSF) and its co-factor α -SNAP, Munc18/Sec1, Munc13, synaptotagmins and Rab3 and its effectors.

1.9.1 Step 1) SNARE proteins, the engine of membrane fusion

Role of SNAREs

SNAREs belong to the family of membrane proteins which regulate membrane fusion and are characterised by the presence of SNARE motif which consists of approximately 60 amino acids and has a α -helical coiled coil domain structure. There are 36 SNAREs in the human genome. Based on their localisation on the plasma membrane whether vesicular or target membrane, they were previously classified as v-SNAREs and t-SNAREs. Fassheur *et al.*, (1998) have reclassified SNAREs into R-SNAREs and Q-SNAREs depending on the conserved arginine or glutamine sequence respectively in the SNARE motif. Synaptobrevin (Vesicle-associated membrane protein (VAMP-2)) which is a R-SNARE contains a single SNARE motif, syntaxin 1 which is Q-SNARE also contains a single SNARE motif while SNAP-25 (25-kDa synaptosomal associated protein) which is a Q-SNARE contains two SNARE motifs, these three proteins come together to form the SNARE complex. Neuronal SNAREs form protein-protein interactions with Munc18/Sec1, Munc13, synaptotagmins and complexin. Post exocytosis, the SNARE complex is disassembled and individual proteins are recycled. This process is mediated by the action of α -

SNAP and ATPase activity of NSF (Jahn and Fasshauer, 2012; Barclay *et al.*, 2005; Seino and Shibasaki, 2005).

1.9.2 Step 2) Priming the SNARE engine

Munc18/Sec 1 or SM proteins belong to the family of hydrophobic proteins with no recognizable motifs. Unc-18 was first discovered in *C.elegans* and later discovered in yeast as Sec1. The mammalian homologs of Unc-18 and Sec1 are named Munc-18 and Sec1 respectively. There are seven homologs present in the human genome. Munc18 acts as a negative regulator of the SNARE complex assembly by binding to the H_{abc} domain of syntaxin 1 in its closed formation (Jahn and Fasshauer, 2012; Barclay *et al.*, 2005; Seino and Shibasaki, 2005).

Munc-13 has a phorbol ester (PMA) binding domain (C1) and two calcium binding C2 domains that flank the MUN domain. Munc-13 acts as a positive regulator of the SNARE complex by hindering the binding of Munc-18 to syntaxin 1, through regulating the activity of the H_{abc} domain on syntaxin 1, thus activating the formation of SNARE complex. This process helps with synaptic transmission by priming the synaptic vesicles. Munc-13 can also interact with Rim and Doc2. Munc-13 can bind to calmodulin to form a Ca²⁺ sensor, which has been described to control short-term synaptic plasticity (Jahn and Fasshauer, 2012; Barclay *et al.*, 2005; Seino and Shibasaki, 2005).

RIM functions as the central organiser of the active zone. It contains a zinc finger motif and two C2 domains. RIM interacts with Rab3 once SVs have docked with GTP-bound Rab3. In this way, orchestrating the attachment site of SVs (Jahn and Fasshauer, 2012; Barclay *et al.*, 2005; Seino and Shibasaki, 2005).

1.9.3 Step 3) Ca²⁺-dependent triggering starts the SNARE engine:

Synaptotagmins were initially named p65 but after cloning renamed as synaptotagmins. There are 13 isoforms of synaptotagmins and they are characterised by the presence of two C2 domains. This is a rigid motif with calcium binding loops; C2A, which binds to two calcium ions and C2B, which binds to three calcium ions, and are linked to each other and the membrane by flexible linkers. In the presence of Ca²⁺, the C2 domains interact with acidic phospholipid enriched membranes. The binding of synaptotagmin to syntaxin or syntaxin-bound SNARE complex occurs via C2 domains (Jahn and Fasshauer, 2012; Barclay *et al.*, 2005; Seino and Shibasaki, 2005).

Calmodulin (CaM) is a Ca²⁺ effector protein with two EF-hand domains on both its N and C terminals connected to each other by a short linker region. Each of the EF domains bind to Ca²⁺ with low affinities. The basic function of calmodulin is to exert regulatory effects of Ca²⁺. Even though calmodulin has 4 Ca²⁺-binding sites, the cytosolic calcium level rarely saturates these sites. However, fluctuation of cytosolic Ca²⁺ levels can also lead to competitive binding of CaM to its targets. The major targets of CaM are CaMKII (Ca²⁺/CaM-dependent protein kinase type II) and calcineurin (CaN).

CaMKII is a serine/ threonine kinase mainly found in neurons, it plays an essential role in synaptic function, synaptic plasticity and memory consolidation. Its activity was first described by Schulman and Greengard in the late 1970s. In mammals, it is encoded by genes *a*, *b*, *g* and *d*. The former two isozymes are abundantly expressed in neurons. Each of these isozymes produce multiple splice variants. CaMKII is made up of 12 monomers, each derived from either of the four genes. Each of these monomers assemble to form the holoenzyme

which gives rise to numerous combinations for the haloenzyme structure. Each of the homomers can form dodecamers each of which can bind to CaM. In its basal state, it is inactive due to the action of the auto-inhibitory domain which causes steric block of substrate binding. Binding of Ca^{2+} to calmodulin results in alteration of the domain adjacent to it, which in turn results in a conformational change, leading to the activation of CaMKII. Prior to the phosphorylation of the exogenous substrates, the activated kinase causes the intersubunit to undergo rapid autophosphorylation at a site located within the autoinhibitory domain at Thr286. This step has three important functions: a) promotes the binding of CaMKII with PSD, partly through its interaction with NMDA receptor b) it decreases the dissociation rate of Ca^{2+} CaM at the post-synaptic membrane c) retaining a substantial kinase activity even after the dissociation of Ca^{2+} -CaM. Thus, a sustained CaMKII activity is achieved independent of the action of Ca^{2+} and CaM, and persists till the appropriate protein phosphatase dephosphorylates Thr286. The binding of PSD-CaMKII can be modulated by action of protein phosphatase 1 (PP1) (Shifman *et al.*, 2006; Griffith, 2004; Liu and Murray, 2012; Ghosh and Giese, 2015; Barclay *et al.*, 2005; Seino and Shibasaki, 2005; Soderling, and Derkach, 2000).

Protein phosphatases play a major role in signal transduction pathways. They functionally counteract protein kinases. In mammalian cells the major serine/threonine phosphatase catalytic subunits consist of four forms namely PP1 (protein phosphatase 1), PP2A (protein phosphatase 2A), PP2B (protein phosphatase 2B (CaN)) and PP2C (protein phosphatase 2C). They are classified so based on their substrate specificity, dependence on metal ions and sensitivity to inhibitory agents. PP1 and PP2A are not dependent on any divalent cations while PP2B and PP2C are Ca^{2+} and Mg^{2+} dependent respectively. PP1, PP2A and PP2B share the homologous catalytic subunits and are complexed with one or more regulatory subunits. PP2C is found in minor amounts in tissues (Hugh *et al.*, 2006; Yamamoto *et al.*, (1999)).

CaN is formed of two subunits; CaNA (60 kDa) and CaNB (20 kDa) (Fraga, *et al.*, 2010). CaNA forms the CaM-binding catalytic subunit while CaNB forms the regulatory Ca^{2+} -binding subunit. The catalytic subunit contains some phosphatase activity. It has a unique domain structure which distinguishes it from other phosphatases; a catalytic domain in N-terminal half, a regulatory part consisting of a CaNB-binding domain and a CaM-binding domain, an autoinhibitory domain. The CaNB subunit binds tightly to subunit A and activates it. The CaNB subunit is formed of four EF-hand Ca^{2+} -binding motifs. CaN regulates the Ca^{2+} signalling pathways indirectly through the action of other signalling proteins and also helps in regulating intracellular Ca^{2+} channels which are located in different subcellular Ca^{2+} stores. CaN also regulates the activity of dynamins (Fraga, *et al.*, (2010)).

PKCs are a large family of multi gene protein serine/threonine kinases that sit at the crossroads of various signal transduction pathways and their role has been implicated in various cellular functions. Previously it was thought that activation of PKC enzymes was through proteolysis, however, experiments with tumour promoting-PMA has helped in the identification of 15 PKC isoenzymes. These 15 isoenzymes can be classified into three groups based on their structure and cofactor regulation; conventional, novel and atypical. α , β I, β II and γ belong to the conventional isoforms while δ , ϵ , η and θ belong to the novel isoforms and $M\zeta$ and ι/λ refer to the atypical isoforms. Irrespective of the disparity between these isoforms the term PKC refers to the entire family. Like all other kinases, PKC has a regulatory and catalytic subunit. The catalytic subunit contains a highly conserved domain which consists of ATP/substrate-binding and catalysis motifs. The regulatory domain helps maintain the inactive conformation of the enzyme. The domain structure of the isoforms has been shown in figure 1.9. cPKCs are activated by the action of DAG and calcium. Hydrolysis of PIP_2 (phosphatidylinositol 4,5 biphosphate) by PLC (phospholipase C) forms DAG and IP3 (inositol 1,4,5-triphosphate). IP3 then diffused through the cell and binds to IP3-sensitive Ca^{2+} channels located in the ER, thereby increasing the cytosolic calcium levels. cPKCs then bind to these calcium ions which mediate its translocation to the cell membrane aiding its interaction with DAG through the C1 domain. The resulting conformational change brings about the phosphorylation of its substrates. nPKCs are activated by the action of DAG only. The C1 domains of nPKCs have a higher affinity for DAG than cPKCs thus allowing their direct recruitment to the membrane. Activation of aPKCs is independent of the action of calcium and DAG, such aPKCs are activated by

lipid metabolite second messengers (Wu-Zhang and Newton, 2013, Mochly-Rosen *et al.*, 2012; Khalil, 2010; Steinberg, 2008).

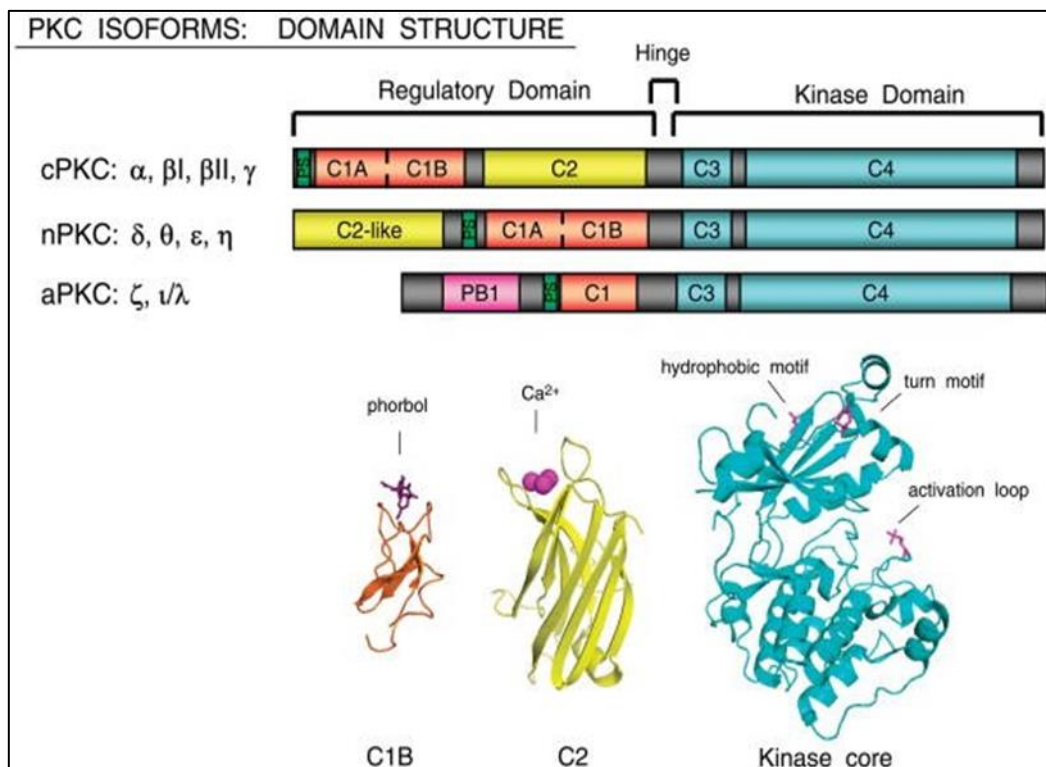


Figure 1.9 Domain structure of PKC isoforms. (Steinberg, 2008) Top: PKCs contain a conserved domain structure (shown in teal) and more variable regulatory domains. All the regulatory domains contain a pseudosubstrate motif, depicted in green, NH_2 terminal to the C1 domain (shown in pink). The C1 domains, shown in orange, function as sensors for PMA/ DAG in cPKCs and nPKCs. The C1 domain in aPKCs does not bind to DAG nor PMA. C2 domains, shown in yellow act as calcium-dependent phospholipid binding sites in cPKCs. nPKCs have a C2 domain which does not bind to calcium. The PKC δ -C2-like domains a phosphotyrosine binding module. The grey regions shown above are the variable regions.

Bottom: ribbon diagrams of the domains.

1.10 cAMP-dependent Protein Kinase A (PKA)

cAMP is known as a universal secondary messenger that plays a major role in cellular responses to extracellular signals. It regulates a range of biological activity for example controlling axon guidance, axonal regeneration, sensory function and memory. Adenyl cyclases when activated by G protein-coupled receptors coupled to $G_{\alpha s}$ produce cAMP (Sieburth and Wang, 2013). The molecular targets for cAMP are PKA, cAMP-GEF/EPAC, CNG and HCN channels (Seino and Shibasaki 2005).

PKA is an enzyme which plays a major role in neuronal processes like learning and memory, synaptic plasticity and regulation of neuronal excitability (Zhong *et al.*, 2009) It was amongst the first kinases to be characterised. PKA is a heterotetrameric protein consisting of two identical regulatory subunits and two catalytic subunits (Seino and Shibasaki 2005). PKA isozymes are encoded by four genes for regulatory subunit ($R1\alpha$, $R1\beta$, $R2\alpha$ and $R2\beta$) and four genes for the catalytic subunit ($C\alpha$, $C\beta$, $C\gamma$ and PrKX). The regulatory subunits can form homodimers and heterodimers, which adds to the molecular diversity of PKA. A-kinase anchoring proteins (AKAPs) mediate the localisation and specificity of PKA. The inactive holoenzyme is a R_2C_2 tetramer. The regulatory subunits contain a phosphate binding cassette which binds to cAMP cooperatively on two sites A and B, in the inactive form the catalytic subunit inhibit this interaction. In the inactive form, only site B is exposed for cAMP binding. On stimulation, cAMP binds to site B on both the regulatory subunits thereby inducing the binding of cAMP with the A site on both the regulatory subunits. Thus, the binding of four cAMP molecules results in a conformational change and dissociation into a regulatory subunit dimer with 4 bound cAMP molecules

and two catalytic monomers which in turn are catalytically active, thereby causing the phosphorylation of its substrates (Seino and Shibasaki, 2005).

Turner *et al.*, (1999) have suggested that protein phosphorylation plays an important role in synaptic plasticity. Thus, modulating the action of various protein phosphatases and kinases can alter neurotransmitter release. For example, Nagy *et al.*, (2002) have shown that phosphorylation of SNARE SNAP-25 at Ser187 expedites vesicle recruitment and thereby modulates the formation of the SNARE complex and in PC12 cells this process leads to exocytosis (Yamamori *et al.*, 2014; Gao *et al.*, 2016; Kohansal-Nodehi, 2016). Also, Gao *et al.*, (2016) have also shown that phosphorylation of SNAP-25 at Thr138 disrupts the SNARE complex and thus prevents exocytosis. Liu *et al.*, (1994) have shown that dynamin is dephosphorylated by calcineurin and this dephosphorylation of dynamin alters its interactions with the binding proteins involved in endocytosis (Clayton and Cousin, 2009) Thus, it can be concluded that protein phosphorylation and dephosphorylation can alter neurotransmitter release and can also regulate mode of exocytosis (Henkel and Kornhuber, 2001). In this study, the role of dynamins and myosin-II has been investigated in 'kiss-and-run' mode of exocytosis. In addition to these proteins the action of various other kinases and phosphatases (for e.g. PKA, PP2A) has been studied. Regulation of exocytosis is fundamental to cellular signalling and is associated to an array of disorders like epilepsy, diabetes, asthma and hypertension (Sim *et al.*, 2003). Thus, these protein phosphatases can serve as potential targets for treatments of these diseases (Sim *et al.*, 2003).

1.11 Working hypothesis

The mode of SV exocytosis can be regulated by the $[Ca^{2+}]_i$ that the exocytosing vesicles are exposed to, and that this may be by regulating the phosphorylation and/or dephosphorylation of certain proteins involved in the closure of the fusion pore through regulation of Ca^{2+} -sensitive kinases and phosphatases.

Main aim

The main aim of this study was to determine the role of dynamins and myosin-II in regulation of SV exocytosis and to ascertain the role of various phosphatases and kinases that could mediate this process. Also, identifying the phosphorylation sites on dynamins under the effect of various drug treatments that would mediate a switch in the mode of exocytosis.

Specific aims

- To determine the role of PKCs in regulation of fusion pore
- To investigate the effect of 160 μ M DYN and 15 μ M pitstop 2TM pre-treatment on the mode of exocytosis.
- To investigate the role of PKA and cAMP pathway in regulation of fusion pore
- To investigate the effect of various drug treatments on bioenergetics of neuron.
- Identifying the role of phosphorylation of ser774, ser778 and ser779 on dynamin I under the effect of various kinases and phosphatases in bringing about a switch in the mode of exocytosis.

Chapter 2

Materials and Methods

2.1 Introduction

Nerve terminal depolarisation brings about influx of Ca^{2+} and release of neurotransmitter from the synaptic vesicles via KR or FF. Understanding the factors that determine the mode of release is important in determination of the synaptic function. This study aims to determine the factors that bring about a switch in the mode of exocytosis by using biochemical assays and molecular biology techniques. The biochemical part consisted of using endogenous glutamate release assay and FM dye release assay in combination with various drug treatments. One of the factors that plays a role in bringing about a switch in the mode of synaptic vesicle exocytosis is by post-translational modification of proteins namely dynamins and myosin-II through phosphorylation or dephosphorylation. The molecular biology part consisted of using western blot to decipher the phosphorylation sites on dynamin that are involved in regulating the switch in the mode of exocytosis. Understanding the metabolic profile of synaptosomes is important for studying synaptic function. For assessing this, mitochondrial stress test was performed using a Seahorse Xfp flux analyser by employing various modulators and inhibitors which helped give an insight about the metabolic profile of the synaptosomes. The method used for this entire study was established by Ashton *et al.*, (unpublished study).

2.2 Materials used

Stimuli employed: 30 mM K^+ , 5 μM ionomycin or 1 mM 4-aminopyridine in the presence of 5 mM $[\text{Ca}^{2+}]_e$ (HK5C, ION5C and 4AP5C respectively).

Reagents used for preparing buffers:

For Lo: 125mM NaCl, 5mM KCl, 1mM MgCl₂, 20mM Hepes and
10mM glucose; pH 7.4

For homogenisation buffer: 320 mM sucrose, 10 mM Hepes; pH 7.4

For Bioenergetics buffer: 3.5 mM KCl, 120 mM NaCl, 1.3 mM CaCl₂,
0.4 mM KH₂PO₄, 1.2 mM Na₂SO₄, 2 mM MgSO₄, 15 mM
glucose, 2 mM glutamine, 1 mM pyruvate.

For Wash Buffer: 3% dried skimmed milk powder, 1% Tween-20 in
TBS; pH 7.4

For blocking buffer: 3% dried skimmed milk powder, 1% Tween-20 in
TBS; pH 7.4

Drugs used [all dissolved in Dimethyl sulfoxide (DMSO)]: Okadaic Acid (OA)
(0.8 µM), Cyclosporin A (Cys A) (10 µM), Phorbol 12-myristate 13-
acetate (Ph est) (1 µM), DYN (DYN) (160 µM), Blebb (blebb) (50
µM), KN-93 (10 µM), GO 6983 (1 µM), Pitstop2TM (15 µM),
phenylarsine oxide (PAO) (0.1 µM), dyngo-4a (50 µM), dynole-34-2
(20 µM), Go 6976 (1 µM), Forskolin (100 µM), 9-Cp-Ade (100 µM) KT
5720 (2 µM), 1,9-dideoxyforskolin (100 µM), Sp-5,6-dichloro-cBIMPS
(50 µM), rotenone/actimycin (0.5 µM), carbonyl cyanide 4-
(trifluoromethoxy)phenylhydrazone (FCCP) (2 µM), oligomycin (2
µM).

Other reagents used: 1 mM NADPH, 36 mUnits of GDH, 100 µM FM 2-10 dye,
NuPAGE sample reducing agent, NuPAGE MES SDS running buffer,
Unstained MagicMarkTM XP Western Protein Standard, Restore plus
Western blotting stripping buffer, Supersignal West dura extended

duration chemiluminescence substrate, 4 mg/ml BSA, 50% solution of PEA (polyethyleneamine, NaOH, 1 mM advasep-7, coomassie protein stain, Instant Blue, Bradford's reagent, Lithium Dodecyl Sulphate sample buffer, calibration buffer, Restore Western Blot Stripping buffer, dried skimmed milk powder, iBlot Transfer Stack (regular size), MagicMark™ XP Western Protein Standard, NuPAGE antioxidant, NuPAGE®Novex® 4-12% Bis-Tris Midi Protein Gels (12+2 well), Xf plate, Nicholls buffer.

Equipment used: Tecan GENios Pro TM plate reader, motor driven homogeniser, Avanti J-25 centrifugation machine, PowerEase 500 power pack, NU-PAGE gel system, iBlot® 7-Minute Blotting System, ChemiDoc XRS+, Seahorse Xfp analyser, non-CO₂ incubator

Antibodies used:

Table 2.1: Pair of antibodies used with their final dilution factor

Primary antibody	dilution factor	Secondary antibody	dilution factor
p-Dynamin (Ser-778)	1:400	Donkey anti-sheep HRP-conjugate	1:5000
p-Dynamin (Ser-774)	1:1000		1:5000
p-Dynamin (Ser-795)	1:100		1:5000
Dynamin-I (4E67)	1:1000	Goat anti-mouse HRP-conjugate for dynamin 4E67	1:5000

- Dynamin I (4E67) is a mouse monoclonal antibody raised against amino acids 1-750 of Dynamin I of human origin (protein accession number: Q05193). The exact epitope recognized by this antibody has not been determined

- p-Dynamin I (Ser-774), is a sheep polyclonal antibody raised against Ser-774 phosphorylated Dynamin I of rat origin (protein accession number: P21575)
- p-Dynamin I (Ser-778), is a sheep polyclonal antibody raised against Ser-778 phosphorylated Dynamin I of rat origin (protein accession number: P21575)
- p-Dynamin I (Ser-795), is a goat polyclonal antibody raised against Ser-795 phosphorylated Dynamin I of human origin (protein accession number: Q05193)
- The exact peptide sequences used to develop these polyclonal antibodies are considered proprietary. However, since these antibodies are phospho-specific, the peptide sequence for each one is a very short peptide surrounding the specific phosphorylated amino acid residue (Santacruz Biotechnology)

2.1 Preparation of synaptosomes:

For this study cerebrocortical synaptosomes -pinched off nerve terminals- prepared from adult male Wistar rats were used as a model system for studying synaptic release. Synaptosomes were first prepared by Whittaker and colleagues in the late 1950s and were instrumental in studying synaptic structure and its functional components (Whittaker,1965). For preparation of synaptosomes, one adult male Wistar rat was humanely killed by cervical dislocation and the cerebral cortex was extracted and placed in an isotonic sucrose solution (referred to here as homogenisation buffer 320 mM sucrose, 10 mM HEPES; pH 7.4; 4⁰C) The rat tissue was then homogenised using a motor driven homogeniser. The Teflon homogeniser disrupts the neurons in such a way that the nerve terminals can reseal themselves to form closed sacs.

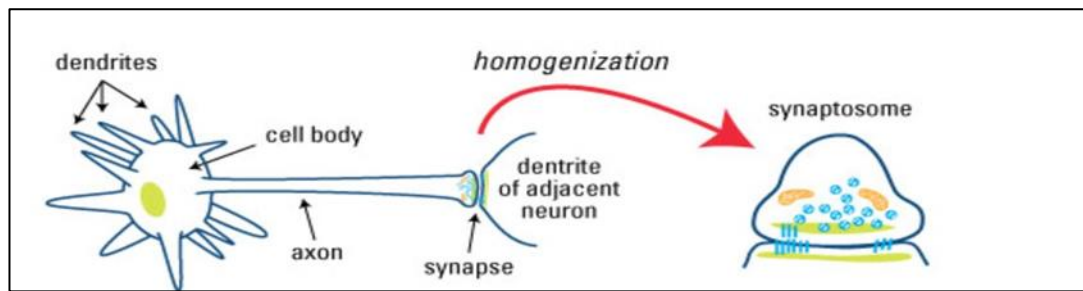


Figure 2.1.1 Schematic representation of synaptosome formed from isolated nerve terminal (Wu, Opperman, Kaboord, 2012)

The homogenate obtained after this initial disruption is a mix of isolated nerve terminals, nuclear debris, membrane fragments and myelin (Sihra, 1995). Hence, differential centrifugation was carried out at 1941 x g for 10 min at 4⁰C to eliminate nuclear debris. The supernatant obtained was then centrifuged at 21025 x g for 20 min at 4⁰C. The crude pellet obtained was then suspended in modified Tyrodes' buffer (referred as Lo; 125 mM NaCl, 5 mM KCl, 1 mM MgCl₂, 20 mM Hepes, 10 mM glucose; pH 7.4) and then centrifuged again at 21075 x g for 20 min at 4⁰C. The crude mitochondrial/ synaptosomal pellet (P2) was then re-suspended in 8 ml of Lo. This synaptosomal fraction was kept oxygenated at 40C until aliquots were used for various measurements.

Synaptosomes contain the complete presynaptic terminal including mitochondria and synaptic vesicles plus some postsynaptic membrane including the postsynaptic density. Synaptosomes serve as a good model to study synaptic function because they represent a quasi in vitro model for neurotransmitter release as they contain functional ion channels, receptors enzymes and proteins (Atlas, 2014).

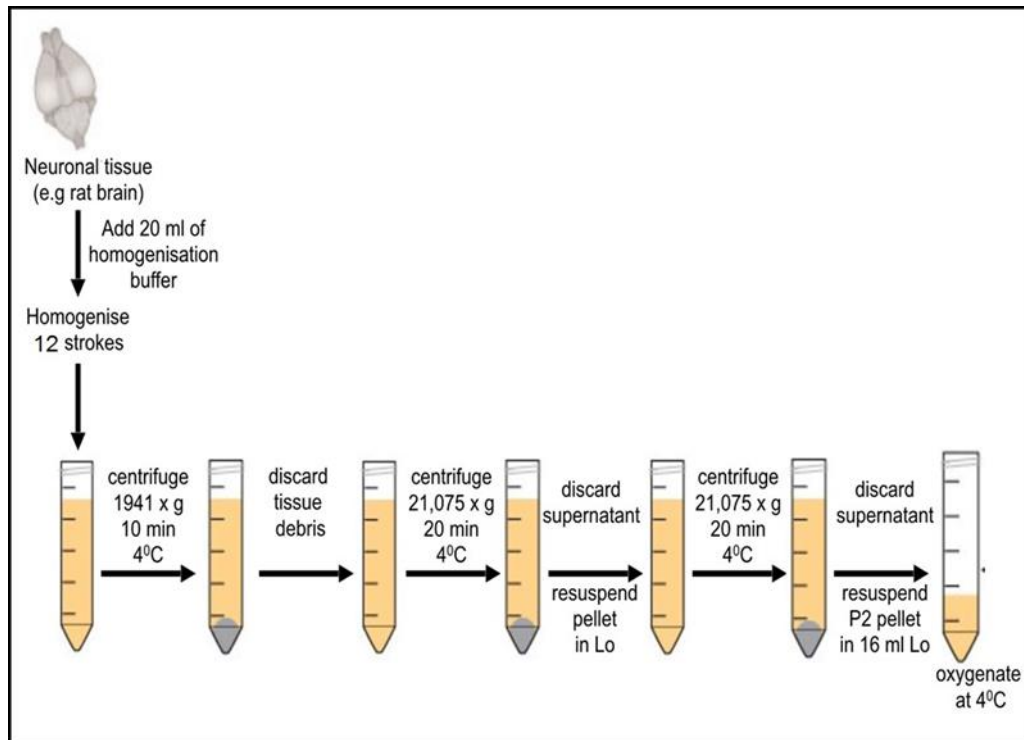


Figure 2.1.2 Schematic representation of the steps undertaken for preparation of synaptosomes.

2.2. The measurement of the release of endogenous glutamate

Aliquots (2ml) of synaptosomes suspension were centrifuged (9589 x g for 45 sec) and resuspended in 1 ml of Lo buffer at room temperature (RT). The synaptosomes were then stimulated for 90 sec at this temperature by adding 275 μ l high potassium buffer (referred here as HK5C); 130 mM K^+ and 25mM $[Ca^{2+}]_e$ plus 1 mM $MgCl_2$, 20mM HEPES): the final concentration was 30 mM K^+ and 5mM $[Ca^{2+}]_e$. This step induces the exocytosis of all releasable vesicles. The synaptosomes were then centrifuged, resuspended in Lo buffer and incubated at RT for 10min. These steps were performed to make the GLU assay comparable to the FM 2-10 dye release assay. The required drug or equivalent amount of solvent was then added to the synaptosomal suspension

for 5-10 min at 37⁰C. The synaptosomes were centrifuged, resuspended in 1ml Lo at RT and centrifuged again. Finally, the synaptosomes were resuspended in 1.6 ml of Lo that contained the relevant amount of drug or solvent. The drug was always included in the final resuspension unless it was found to interfere with the actual assay (either the GLU or FM dye release assay) in which case it was not added back: the drugs not added back were DYN, Blebb, dyngo and pitstop2TM.

121 µl aliquots of the synaptosomal suspension together with 20 µl of Lo was added to a row of wells (12 samples) of a 96 well black microtitre plate with a transparent bottom. 10 µl of 20mM NADP⁺ (final concentration of 1mM) and 9 µl of glutamate dehydrogenase type II (GDH: E.C. 1.4.13) (4 mUnits) was then added and these wells were incubated for 10 min at RT. GLU released from synaptosomes incubated in the physiological buffer medium containing GDH and NADP⁺ will react with the enzyme to produce α-ketoglutarate and at the same time NADP⁺ gets converted to NADPH: it is the latter compound that is detected fluorometrically. During this initial 10 min incubation, any GLU present in the extracellular buffer (prior to stimulation) will react and produce a background fluorescence. This background fluorescence can be subtracted so that upon evoked GLU release the fluorescence increase can be determined. This GLU assay can detect release within seconds and provides a rapid real-time detection of GLU (Nicolls and Sihra, 1987). After the initial 10 min incubation period, wells 1-5 were treated with the relevant stimulus with 5 mM Ca²⁺ (40µl of HK5C or ION5C or 4AP5C) whilst 40 µl of the corresponding stimulus without Ca²⁺ (HK0 or 4AP0 or Lo) was added to wells 6-12. The endogenous GLU release was measured using the Tecan Genios ProTM plate reader. The settings used were excitation wavelength (λ) 340 nm, emission

wavelength (λ) 465 nm, gain was 70 (this represents the required setting for sufficient assay sensitivity. The machine was set for 21 cycles which means that each individual well (wells 1-9) was read and then this was repeated 20 more times: this number of cycles was sufficient to detect all the evoked GLU release. The machine was set so that the plate was shaken for 3 sec before the wells were measured, and between cycles the plate was shaken for 1 sec. Following these measurements, 10 μ l of buffer was added to wells 7-9 and 10 μ l of 1mM GLU (freshly prepared from 679mM stock glutamate) was added to wells 10-12. The change in fluorescence upon the addition of this amount of GLU (10 nmol) was measured using the same settings for 15 cycles for wells 7-12. This was actually an excess time period for measurement since normally all the 10 nmol of GLU had been detected and produced a maximal fluorescence after about 8 cycles. GLU release obtained from wells 1-5 and 6-9 were averaged and the latter value subtracted from the former to provide a measure of the amount of evoked GLU release from the synaptosomes. This was in arbitrary fluorescent units (AFU). The AFU measured upon the addition of 10 nmol GLU enables one to convert the release data from AFU to nmol of GLU released. Furthermore, as 10 nmol GLU was added after the measurement of each row of the microtitre plate (different treatments for the synaptosomes) this quantity of fluorescence could be used to correct for the sensitivity of the assay in each row (this can vary slightly between rows). Such normalization of the data allows direct comparisons between rows representing different conditions within the same experiment and this can also be utilized between different experiments to ensure all samples measured are corrected to similar sensitivity. A schematic representation of this has been shown in Figure 2.2.2 (A).

	1	2	3	4	5	6	7	8	9	10	11	12
A CON	STIM					STIM ₀			STIM ₀			
B Drug	STIM					STIM ₀			STIM ₀			
C Con	STIM					STIM ₀			STIM ₀			
D Drug	STIM					STIM ₀			STIM ₀			
E Con	STIM					STIM ₀			STIM ₀			
F Drug	STIM					STIM ₀			STIM ₀			
G Con	STIM					STIM ₀			STIM ₀			
H Drug	STIM					STIM ₀			STIM ₀			

Figure 2.2.1 Schematic representation of the order in which samples were added to the microtiter plate for this assay (see below for further explanation). The order for drug treated and control rows was shuffled in a cyclic manner for independent experiments. In order to ensure that every drug was averaged for the response to the same age of synaptosomes (from time of preparation).

For double drug treatments for e.g. for Go 6983 and DYN. The protocol slightly differs in the usual way that there are two sequential 5 min 37°C pre-treatments with drugs. This was designed to use the first 5 min period to add a drug on its pathway (e.g. inhibition of PKCs with Go 6983) prior to a second 5 min period when there is an addition of drugs that act on, in this example on, dynamins. Obviously, as a control the first 5 min incubation period would just have solvent added and for the total control, relevant amounts of solvent would be added during the first and the second incubation period. Note that Go 6983 is incubated with the synaptosomes for 10 mins at 37°C and the results for this drug alone include the addition of an amount of solvent equivalent to the addition of the other drug during the second 5 min incubation period and this has been and this has been schematically represented in the figure 2.2.2.(B).

For chapter 4, a slightly different protocol was followed wherein the synaptosomes were treated with DYN or pitstop 2 or a mixture of both the drugs prior to pre-stimulation with HK5C and this has been schematically represented in the figure 2.2.2 (C).

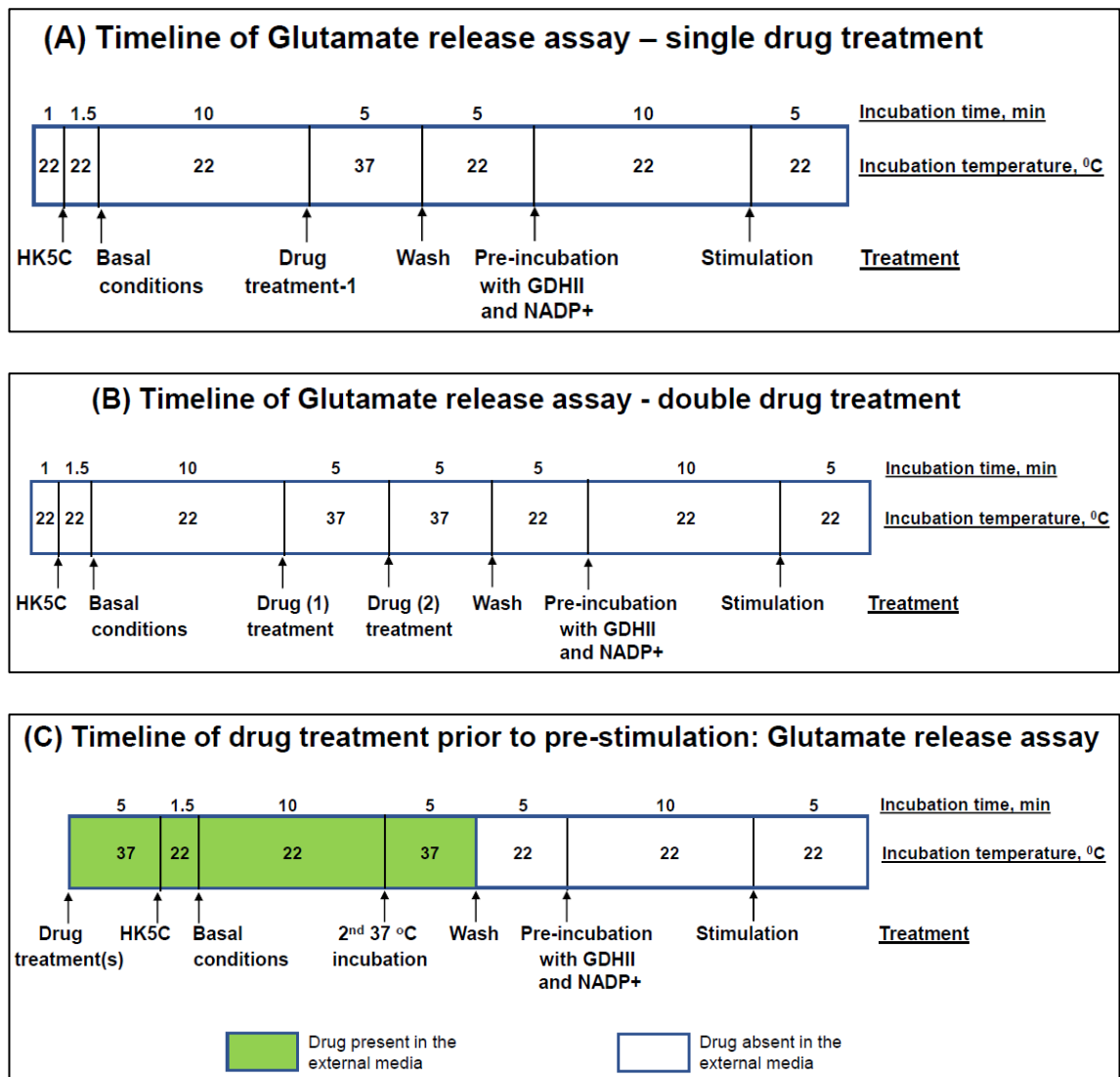


Figure 2.2.2 General schematic representation of the sample preparation timeline to study the effect of (A) treatment with various drugs; or (B) treatment with combination of two drugs; or (C) treatment with combination of two drugs before the pre-stimulation step; on evoked Glu by the stimulus of interest.

Please note that in experiments involving double drug treatments, all the experiments performed as in (B) were performed with treatment of drugs in series (i.e. in two series of steps), whereas, for those in (C), this double drug treatment was performed in a single step.

2.3 FM 2-10 dye release assay

1 ml of synaptosomes were gassed with O₂ at RT for 15 min at RT and subsequently centrifuged (see section 2.2) and resuspended in 1 ml of Lo buffer at RT (Final volume is 1.1 ml as the pellet has some volume). 2.2 µl of 50 mM FM 2-10 dye was then added (final concentration 100 µM) and following a 60 sec incubation 275 µl of buffer containing 130 mM K⁺ and 25 mM Ca²⁺ (plus 1 mM Mg²⁺ and 20 mM Hepes) was added (to give a final concentration of 30 K⁺ and 5 mM Ca²⁺) and synaptosomes were incubated for a further 90 sec at RT. This step ensures exocytosis of all releasable SVs and their subsequent labelling with FM 2-10 dye. The synaptosomes were then centrifuged and resuspended in 1 ml Lo containing 100 µM FM 2-10 dye and incubated for 10 min at RT: this step ensures that all recycled SVs have FM dye bound to their luminal domain. Subsequently, the synaptosomes were incubated for 5-10 min at 37°C with the desired drug or equivalent amount of solvent. 4 µl of 250 mM advasep-7 (1 mM final concentration) was then added to the synaptosomes before their centrifugation. Advasep-7 serves as a soluble high affinity scavenger for FM dye and this reduces the background fluorescence. Indeed, it has a higher affinity for FM dye than the dye has for membranes and so advasep-7 strips dye from the plasma membrane. However, the seven negative charges on this molecule make it membrane impermeable, so this drug cannot remove dye from the internalized SVs (Kay *et. al.*, 2007). The synaptosomes were then washed by centrifugation and resuspension to ensure the removal of most of the plasma membrane bound dye and finally the terminals were resuspended in 1.5 ml of Lo buffer containing the appropriate concentration of the relevant drug or solvent. In some cases, the drug was not included in the final resuspension (see 2.2). 160 µl aliquots of this suspension were added to

wells 1-8 of a black micotitre plate which had a black bottom. The measurements were taken using a Tecan Genios Pro™ plate reader. The settings used were excitation wavelength (λ) 485 nm, emission wavelength (λ) 555 nm, gain was 40 (this represents the required setting for sufficient assay sensitivity). The machine was set for 461 cycles which means that each individual well was read 461 times which took 120 sec: this number of cycles was sufficient to detect all the evoked FM2-10 dye release. In this assay, the actual machine injected 40 μ l of the stimulus or the basal buffer into the well (so final volume in well was 200 μ l). Prior to any measurements, the two injectors in the plate reader were primed: one contained the relevant stimulus and the other contained Lo. Four wells were then injected with the stimulus and four wells were injected with the basal buffer. Each well was measured separately following the 40 μ l injection. This process was then repeated using another row of the micotitre plate following the preparation of dye loaded drug treated synaptosomes. Each condition was repeated twice in the same experiment. One row had the stimulation added to wells 1-4 and Lo added to wells 5-8 but on the second repeat of the condition Lo was injected into wells 1-4 and the stimulus added to wells 5-8. This ensured that the age of the synaptosomes (since first made) was taken into account and no artifacts were created from such a factor. When the experiment was repeated the order of the various drug treatment was changed again to counteract the age of the synaptosomes from when they were first prepared. To determine the specific FM2-10 dye evoked released, the corrected average data from basal samples was subtracted from the corrected average data from stimulated samples. Prior to this all individual wells were corrected such that they had the same starting value of FM 2-10 dye fluorescence. This normalization procedure ensured that all experiments were

directly comparable. A schematic representation of this has been shown in Figure 2.3.2 (A).

	1	2	3	4	5	6	7	8	9	10	11	12
A CON	STIM				STIM₀							
B Drug	STIM				STIM₀							
C Con	STIM				STIM₀							
D Drug	STIM				STIM₀							
E Con	STIM				STIM₀							
F Drug	STIM				STIM₀							
G Con	STIM				STIM₀							
H Drug	STIM				STIM₀							

Figure 2.3.1 Schematic representation of the order in which samples were added to the microtiter plate for this assay and has been explained above. The order for drug treated and control rows was shuffled in a cyclic manner for independent experiments.

For double drug treatments with FM 2-10 dye release assay the protocol followed was similar to the protocol followed for double drug treatment for glutamate release assay as shown in Figure 3.2.2 (B).

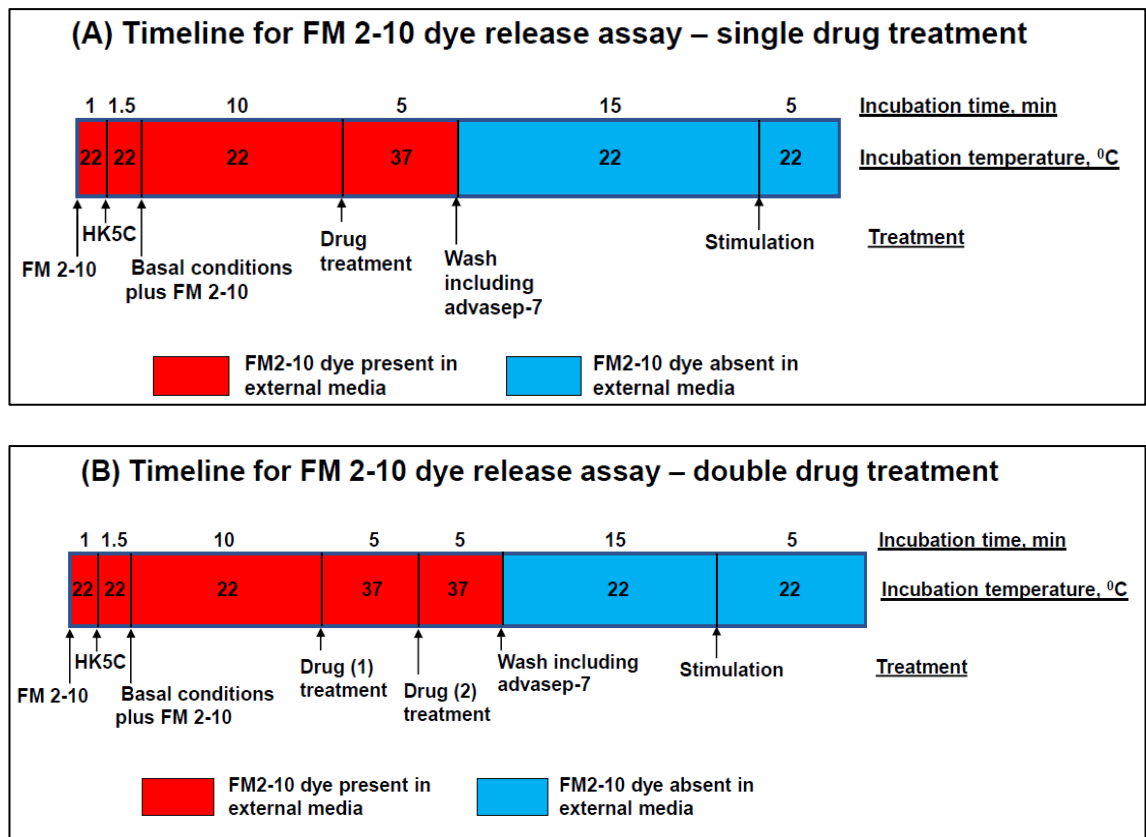


Figure 2.3.2 General schematic representation of the sample preparation timeline to study the effect of (A) treatment with various drugs; or (B) treatment with combination of two drugs; on FM2-10 dye release by the stimulus of interest.

2.4 Statistical analysis

The results presented are the average of several independent experiments (n). All basal values from such multiple experiments were averaged as were all the stimulated values. Then average basal value was subtracted from average stimulated values, the statistical analysis was performed using Microsoft Excel and GraphPad Prism software. The values were statistically analysed by comparing control and test values using unpaired student's t-test. $p < 0.05$ was considered as significant. The results were presented in a graphical format as a percentage of maximum control. For ease of presentation, selective data points at an interval of 10 sec have been shown, wherein the error bar indicates the standard error of mean (S.E.M). In chapters 3-7, 'n' if shown in the figures as part of the results includes replicates of the same experiment while 'n' represented below the figures as part of the legend indicates the number of independent experiments, the latter in this study is 3 unless stated otherwise. Also, the control in this entire thesis indicates non-drug treated synaptosomes unless stated otherwise. It should be noted that for all the 4AP5C experiments the error bars seem larger but this is simply because 4AP5C only induces the release of the RRP and so this is a smaller amount of Glu release but we have shown the figures as a percentage of the maximal control release induced by 4AP5C, unless stated otherwise.

2.5 Bioenergetics assay (mitochondrial stress test)

Mitochondrial respiratory activity of synaptosomes via direct measurement of oxygen consumption rate can be monitored using Seahorse Xf Cell Mito Stress test. The parameters measured are through injection of various modulators and inhibitors which target the electron transport chain thereby measuring basal

respiration, ATP production, maximal respiration, proton leakage and spare capacity.

Synaptosomes (P2 pellet) obtained by the aforementioned method were suspended in 4.5 ml of Lo buffer. 0.02 ml aliquot of synaptosomes were then centrifuged at 9589 x g for 45 sec. The synaptosomal pellet obtained was then resuspended in 1.2 ml bioenergetics buffer (3.5 mM KCl, 120 mM NaCl, 1.3 mM CaCl₂, 0.4 mM KH₂PO₄, 1.2 mM Na₂SO₄, 2 mM MgSO₄, 15 mM glucose, 2 mM glutamine, 1 mM pyruvate) plus 4 mg/ml of bovine serum albumin at 4°C. There is no buffer present in this solution as proton production would not be measurable in presence of a buffer. The pH of this solution was adjusted with a small amount of NaOH (the pH of the solution was adjusted as the synaptosomes are acclimatized to a neutral pH and any change in pH would cause a change in the metabolic profile). The synaptosomes were initially suspended in Lo buffer but it was later observed that the in the later steps synaptosomes did not adhere to the plate hence Nicholls buffer was preferred over Lo buffer. This buffer was employed because it is the one that has been characterized for use with synaptosomes and the Seahorse Xfp analyser (Brand and Nicholls, 2011).

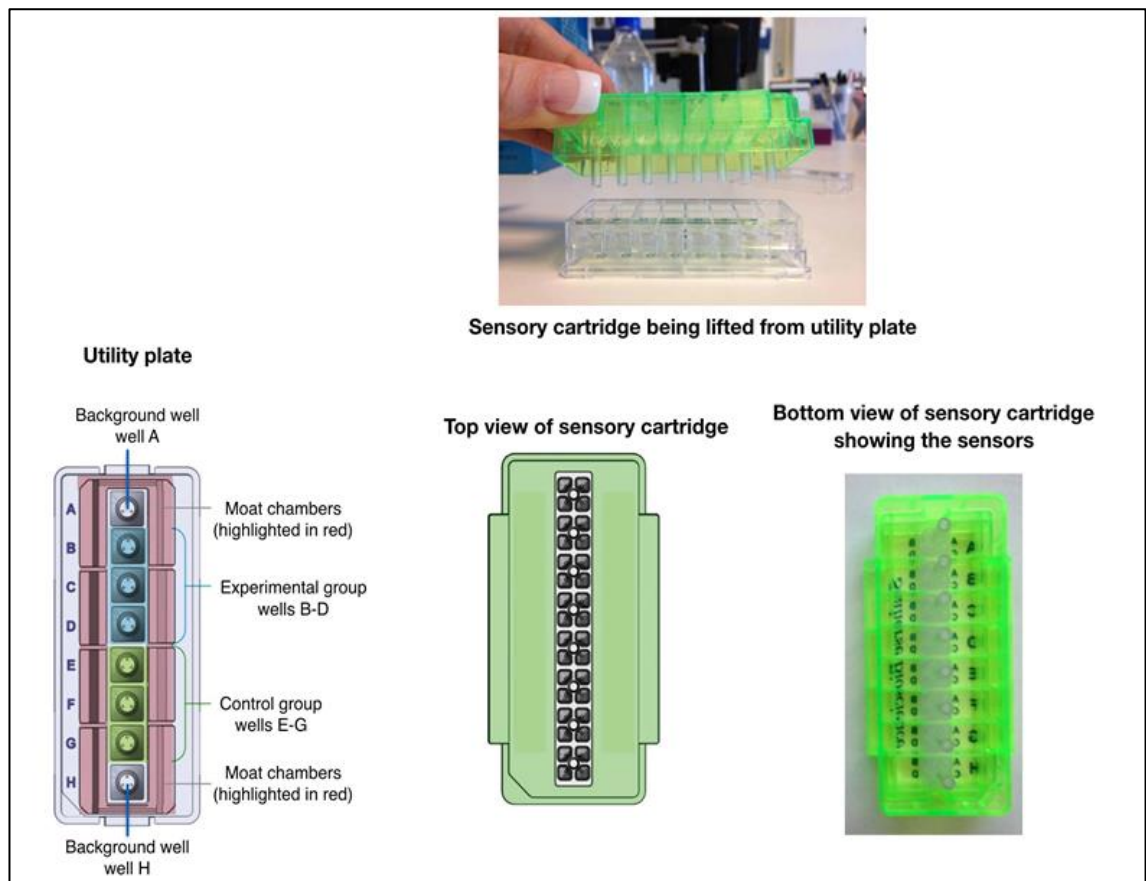


Figure 2.5.1 Schematic representation of the Xfp utility plate and cartridge. This asS.E.M.bly is also supplied with a clear lid which is placed on top of the sensory cartridge which is removed during measurements.

6 x 0.175 ml aliquots of the synaptosomal suspension were added to wells B-G of the Xf plate. Wells B-D act as the experimental wells while wells E-G act as the control wells. Wells A and H act as background wells. The purpose of the background wells is to filter out artefacts, such as temperature and buffering capacity that affect the oxygen and pH (changes not due to metabolic activity of the synaptosomes). Also, they serve as a starting point for troubleshooting the assay with unexpected results, to point out changes due to temperature fluctuations or potential thermal problems. Moat chambers prevent evaporation when the plate is incubated in a non-CO₂ incubator at 37⁰C overnight (explained below) or when running the assay

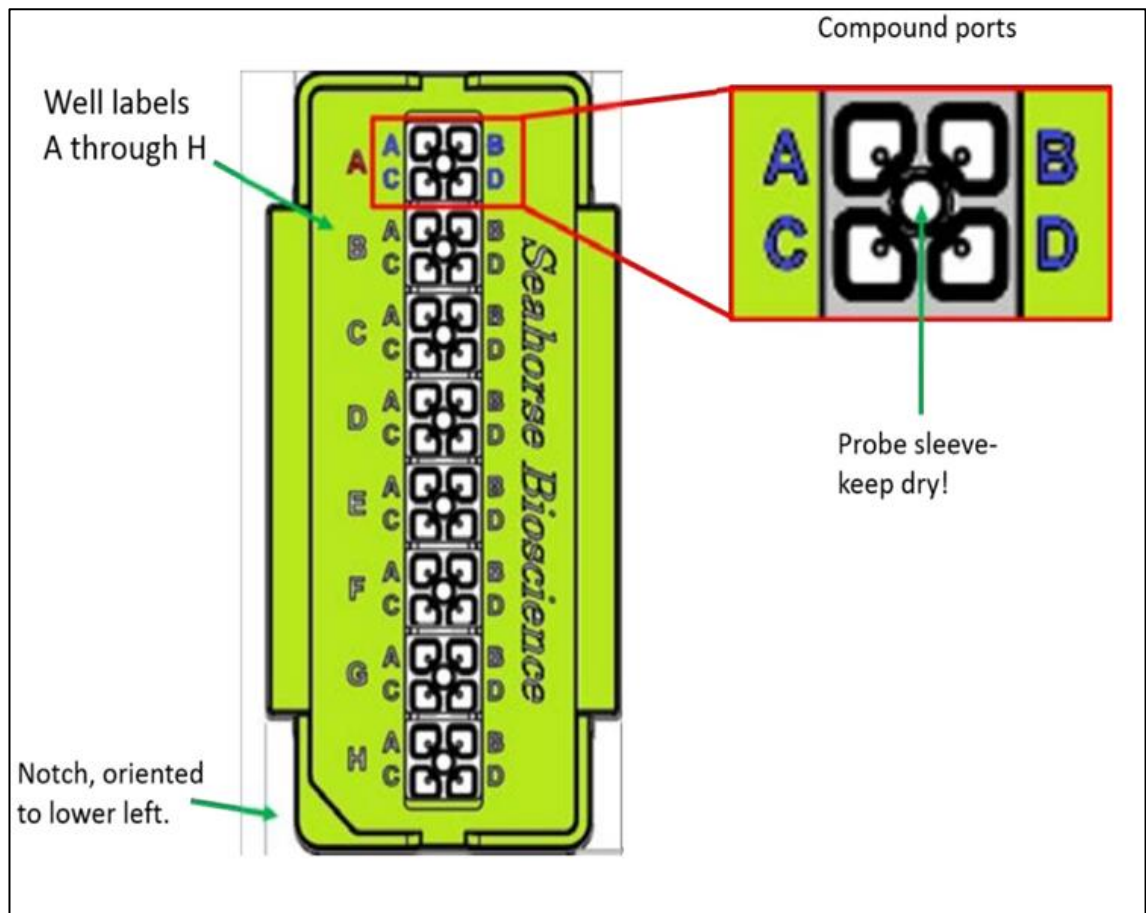


Figure 2.5.2 Schematic representation of the top of the sensory cartridge showing the drug ports. Port A loaded with optimised concentration of oligomycin, Port B: loaded with optimised concentration of FCCP. Port C loaded with optimised concentration of Actimycin A/ Rotenone (Seahorse manual).

A day prior to running the assay, wells A-H of two utility plates were pretreated with 1:1500 of 50% solution of PEA (polyethyleneamine) and incubated at room temperature. This helps the synaptosomes adhere to the bottom of the plates. The solution was then removed and the plates were allowed to dry. The sensor probes were hydrated by adding 200 μ l of calibration buffer to wells A-H (PBS, pH 7.4, supplied by Seahorse Biosciences). 400 μ l of calibration buffer was added to the moat chambers. The cartridge was then placed over the utility plate and the entire asS.E.M.bly was then placed in a sealed box with moist paper towels (to prevent evaporation) and then placed in a non-CO₂ incubator

at 37⁰C overnight. After the sensor probes were hydrated (on the day of the assay) keeping the cartridge in the utility plate for one of the cartridges the drug ports are loaded with the relevant drug concentrations of oligomycin, FCCP, actimycin A/ rotenone in the relevant port. This entire assembly was then placed in the Seahorse Xfp Flux analyzer and allowed to equilibrate at 37⁰C for 12 min. After the equilibration was done, the sensor cartridge was placed on the other utility plate which contained the adhered drug treated synaptosomes. These were prepared as outlined next.

After the synaptosomes were aliquoted onto the utility plate pretreated with PEA, the synaptosomes on the plate were centrifuged at 2000 X g for 20 min at 40C. This was done to adhere the synaptosomes to the plate. Wells A and H have no synaptosomes aliquoted into them. The supernatant from the wells was discarded. 0.2 ml of bioenergetics buffer (37⁰C) containing the relevant drugs or DMSO was added to wells B-G. The synaptosomes were incubated for 5 min at 37⁰C. The solution was then decanted and 0.175 ml of fresh bioenergetics buffer containing BSA (37⁰C) was added. These samples were added to the sensor cartridge that had been equilibrating in the analyzer washed with such buffer before the final buffer addition. The relevant programme was then used to measure:

- a) 3 x 3 min measurements of basal oxygen consumption and proton production;
- b) following the automatic injection of 0.025 ml of 16 µM oligomycin from port A to all wells, 3 x 3 min measurements of oxygen consumption and proton production (final concentration of oligomycin is 2 µM)

- c) following the automatic injection of 0.025 ml of 18 μM FCCP from port B to all wells, 3 x 3 min measurements of oxygen consumption and proton production (final concentration of FCCP is 2 μM)
- d) following the automatic injection of 0.025 ml of 5 μM of rotenone/actimycin A from port C to all wells, 3 x 3 min measurements of oxygen consumption and proton production (final concentration of rotenone/actimycin A is 0.5 μM)
- e) The machine converts all the data from changes in oxygen consumption or proton production into plots and rates. This data was analyzed using wave 2 software

2.6 Statistical analysis

The results presented are the average of 2-3 independent set of experiments (n). The data was analyzed using wave 2 software and Microsoft Excel. The Mito stress test report generator automatically calculates the key metrics that determine the mitochondrial function of each group. The key metrics are spare respiratory capacity, coupling efficiency, basal response, ETC accelerator response and ATP coupler response. It gives a graphical representation of the data which is then exported to MS Excel where the error bars represent SD. The control and the experimental group values obtained were analyzed using unpaired student's t-test. $p < 0.05$ was considered significant. From the raw data, we can average several experiments. As the machine does 3 x 3 min measurements we can average all these data points or we can average those that represent either the maximum or minimum values (depending on the port addition). We can manually determine from such multiple experiments; a) basal bioenergetics; b) maximal respiratory capacity; c) spare respiratory capacity; d) proton leakage; e) non-mitochondrial respiration.

2.7 Western blotting

2.7.1 Sample preparation

The first step in western blotting workflow is sample preparation which sets the foundation for the quality of results. The initial steps for sample preparation were carried out in the same manner as described in section 2.1. After which the synaptosomes were treated with the drug or DMSO for 5-10 mins at 37⁰C and suspended in 1 ml Lo then centrifuged at 9589 x g for 45 sec (as described in glutamate assay). The synaptosomes were re-suspended in 225 µl of Lo buffer plus the relevant amount of drug or DMSO (except for DYN, Blebb, dyngo, pitstop). 25 µl aliquot from this suspension was used to determine the protein concentration of the sample using Bradford assay and the remaining 200 µl was used for sample preparation. This 200 µl suspension was distributed as 2 x 100 µl aliquots, one of which was treated with the required stimulus and the other with Lo buffer. Depending the conditions being tested, the stimulation was applied for either 2, 15, 30 or 300 sec (these stimulation periods were chosen as RRP exocytoses in 2 sec, the changes produced at 15 sec represent the cellular processes preparing dynamin I for endocytic processes e.g. CME, the changes produced at 30 sec would represent the dephosphorylation changes that lead biochemical interactions which are preparing dynamin I to contribute to CME and since we measure FM dye release for about 5 min changes produced at 300 sec would help in comparison) was immediately after which 1X NuPAGE LDS (lithium dodecyl sulphate) sample buffer and 1X dithiothreitol were added to solublise the proteins and reduce the di-sulphide bridges. The same process was carried out for the non-stimulated samples in which L0 was added for the various time points. 1X NuPAGE LDS sample buffer and 1X dithiothreitol were added. The samples were then vortexed using

a bench top vortex mixer and heated at 70⁰C for 10 min. The samples were then stored at -20⁰C. The desired final protein concentration was 1.5 mg/ml and the samples were diluted depending on the results obtained from the Bradford assay.

2.7.2 Electrophoresis

Prior to each electrophoresis run, the samples were re-heated for 10 min at 70⁰C. To separate the proteins based on molecular weight, Novex NuPAGE SDS-PAGE gel system with NuPAGE Novex 4-12% Bis-Tris Midi Protein Gels (12+2 wells) were used. The gel tank components were assembled and 1X NuPAGE MES SDS buffer was used as running buffer and checked for leakage. Then 45 µl of the relevant sample (67.5 µg protein) was loaded in to each of the sample wells. For the two marker lanes, either 7 µl of diluted MagicMark XP western protein standard (dilution 1:7) or 7 µl of Novel sharp unstained protein standard was loaded depending if the latter process was to carry out western blotting or to carry out coomassie protein stain. After loading the gels, the lid was placed on the tank and the assembly was connected to the PowerEase 500 power pack and the relevant settings were chosen. Electrophoresis was carried out at 120 mA (constant current). The gels were electrophoresed for 1 hour and 20 min.

This gel system was preferred as LDS sample buffer minimises the Asp-Pro cleavage and when LDS containing samples are heated to 70⁰C the pH changes to 8 from 8.5, which serves as an ideal condition for protein reduction, alkylation and also helps in preserving the protein integrity. The precast gels give a good separation of proteins and also employ a neutral pH thereby minimising protein modifications. Also, this gel system reduces the sample run time. (Invitrogen)

After the electrophoresis run was complete, either protein staining or western blotting (described below) was carried out. For coomassie protein staining, InstantBlue was used. The gel was incubated with this stain for 15 min and the bands were visualised using ChemiDoc XRS+. This stain gave better signal to noise ratio and hence was preferred over other protein stains.

2.7.3 Western blotting

For carrying out western blotting iBlot 7-Minute Blotting system was used which consisted of iBlot Gel Transfer Device and iBlot Gel Transfer Stacks. After the electrophoresis was complete the gel was placed on a PVDF membrane (polyvinylidene fluoride) and the transfer stacks were layered to perform blotting of proteins. The transfer stacks function as ion reservoirs that contain the anode and cathode buffers incorporated into the gel matrix thereby eliminating the need for pre-made buffers. The stacks also contain the electrodes. The asS.E.M.bly was placed on the blotting surface of the transfer device and P3 program was selected. The transfer device helps in efficient transfer of proteins onto the PVDF membrane in 7 minutes thus providing a quick method for performing western blotting. After the transfer was complete the PVDF membrane was blocked using 30 ml of blocking buffer (3% dried skimmed milk powder, 1% Tween-20 in TBS; pH 7.4) for 60 min at RT. This blocking step helps enhance the specific signal for antigen-antibody interaction while decreasing the background noise ratio. After this incubation step, blocking buffer was drained and the membrane was incubated with the 5ml of primary antibody solution (appropriate primary antibody concentration, 1% dried skimmed milk powder, 1% Tween-20 in TBS) for 30 min at RT and for 30 min at 37⁰C. The antibody solution was then removed and the blot was washed 6 times with an interval of 5 min between the washes using 25 ml of wash buffer

for each wash (0.05% Tween-20, 25mM Trizma base, 0.15M NaCl; pH 7.3-7.4). The wash buffer was drained and the membrane was incubated with the 5ml of secondary antibody solution (appropriate secondary antibody concentration, 1% dried skimmed milk powder, 1% Tween-20 in TBS) for 30 min at RT and for 30 min at 37°C. The antibody solution was removed and the blot was washed 6 times with an interval of 5 min between the washes using 25 ml of wash buffer for each wash. After this step, the membrane was incubated with 3 ml of SuperSignal west dura chemiluminescent substrate for 5 min. The PVDF membrane was then visualised using ChemiDoc XRS+ image lab software.

2.7.4 Re-probing / stripping the PVDF membrane

After visualising the membrane, the membrane was washed 3 times using 25 ml of wash buffer with an interval of 5 minutes in between the washes. After washing the membrane, the wash buffer was drained and the membrane was incubated with 15 ml of Restore Western Blot Stripping buffer at RT. After the incubation, the membrane was washed 4 times using was 25 ml of wash buffer with an interval of 5 minutes in between the washes. The wash buffer was then drained and the membrane was then incubated with the desired primary antibody followed by washing and then incubation with the desired secondary antibody followed by washing again (as described above). The membrane was first probed for the desired phosphorylated residue and then stripped and probed with dynamin-I 4e67 antibody. The stripping buffer provides efficient removal of chemiluminescent substrate, primary antibody and secondary antibody as they bind to the membrane surface and the stripping buffer dissociates this bond leaving the PVDF membrane intact. The stripping step thus helps eliminate the need to run the samples again and helps cut down the cost.

2.7.5 S.E.M.i-quantification of blots:

For estimating the protein quantities for each visualized band on the blotted membranes, ChemiDoc XRS+ image lab software was used. For each membrane that was visualized, six images at multiple exposure times were taken. This was done to eliminate any error arising due to the time taken for each band to appear. As there were various drug treatments loaded on one gel, the time taken for all the bands to appear for the desired antibody may differ.

Thus, as the exposure time was increased the band intensity showed a linear increase as well. However, overexposure would give a false representation of the true intensity of a band, so it was important to have an exposure time which was in the linear range of detection. Differences between gels were expressed to the maximum intensity lane and a correction factor was used when probing the equivalent phosphorylated tracks. To give a true representation of the amount of phosphorylation, each band for each drug treatment was compared to the corresponding dynamin-I 4e67 value. Dynamin-I 4e67 recognizes the total dynamin-I content for each band and is a good control.

For carrying out S.E.M.i-quantification of membranes, volume analysis tool was used. This tool helps draw a border around each band of interest which then subtracts the intensity of pixels around the border (the background) from the intensity of pixels observed for that band. This is represented as adjusted internal volume. These values are then exported to Excel where each band is expressed as a percentage of a particular selected band (control basal band). This gives a relative quantity of amount of protein present. The value obtained for each band was then compared to dynamin-I 4e67 value and thus expressed as a ratio. For each drug treatment, the value obtained for the stimulated sample was compared to the unstimulated control of the same drug treatment

and expressed as a percentage which was then represented as a histogram plot.

This process was repeated for 2-3 independent experiments and the values obtained were averaged together and represented as a histogram plot with the error bars representing standard error of mean. The statistical significance was carried out using unpaired student t-test wherein $p < 0.05$ was considered significant.

Also, for ease of presentation only the region of the blot that contains dynamin is shown in the results as the rest of the blot was blank (see representative blot in appendix 3). The results shown are obtained from 3 independent experiments unless otherwise stated.

Chapter 3

Investigating the Role of Protein Kinase C

3.1 Background results

3.1.1 Introduction

Previous work in the Ashton laboratory (e.g. Dilip Bhuva PhD thesis 2014) had shown that in cerebrocortical synaptosomes, SVs could undergo distinct exocytotic modes KR or FF and that these could be switched by various conditions including activation/inhibition of kinases/phosphatases. Ca^{2+} seemed to be important in regulating the mode and the Ca^{2+} dependent kinases, CaMKII and PKC, have both been implicated in regulating this process. Excitingly, the use of specific drugs implicated some phospho-proteins as being possible mediators of the closure of the fusion pore that produces KR exocytosis. Perturbation of the activity of such proteins can lead to the pore expanding – instead of closing – which leads to the vesicular membrane being fully inserted into the plasma membrane and this represents the FF mode.

The two phospho-proteins that appear to play a role in regulating KT were dynamins (1 and 2) and non-muscle myosin-II. Dynamins action was investigated using the drug, DYN (Macia *et al.* 2006) which inhibits the dynamin family (160 μM perturbs the action of dynamins fully in nerve terminals (shown ahead in this chapter). It specifically blocks the GTPase activities of dynamin-I and dynamin-II (Chung *et al.* 2010; Hosoi *et al.* 2009; Zhu *et al.* 2010) such that they cannot perform their normal roles. The other phospho-protein is non-muscle myosin II (Neco *et al.*, 2008; Chandrasekar *et al.*, 2013) whose action can be inhibited using 50 μM Blebb (e.g. Chandrasekar *et al.*, 2013).

This introduction aims to provide the rationale behind this study. This chapter includes some figures that summarize the results obtained with DYN (Figure 3.1

and 3.2) and Blebb (Figure 3.3 and 3.4). Such results help explain the premise behind many of the experiments carried out in this chapter. Figure 3.1-3.4 are background results but these experiments were performed again depending on the experiment, this was done to for maintaining controls for the experiments.

In order to understand the results, herein, it is necessary to just remind the reader of what comparison between evoked Glu release and FM2-10 dye release reveals. FM 2-10 dye will only be maximally released from the preloaded SVs if the SV undergoes the FF mode of exocytosis. This is because, the disassociation of FM2-10 dye from the fused SV lipid membrane requires more time which can only occur during FF mode of exocytosis. The fluorescence of FM 2-10 dye decreases 20-fold when it is released into the extracellular matrix. Thus, there will be decrease in fluorescence of FM2-10 dye only when SV undergoes FF mode of exocytosis, and not when undergoing KR. On the other hand, the glutamate can be fully and quickly released even if exocytosis is via a transiently open fusion pore as observed during KR. Thus, the release of glutamate occurs during both, KR and FF whereas the release of FM2-10 dye requires FF mode of exocytosis for its release (Omiatek *et al.*, 2010; Zhang *et al.*, 2007). Thus, if a drug has no effect on the glutamate release but can affect the FM2-10 dye release, then one can say that the drug is affecting the mode of SV exocytosis.

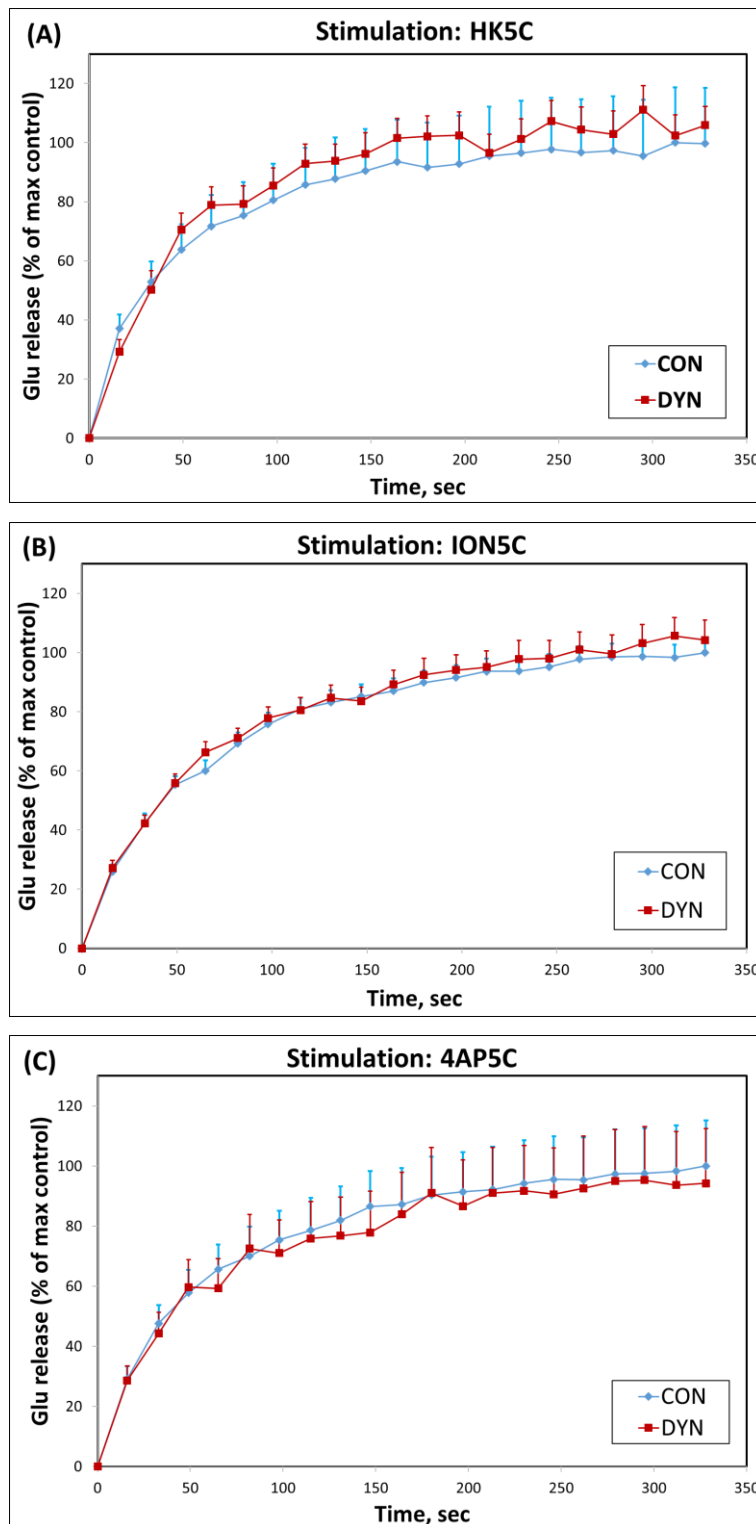


Figure 3.1 The effect of 160 μM DYN on Glu release evoked by (A) HK5C (B) ION5C and (C) 4AP5C. Data are mean +S.E.M. from 5 different experiments (i.e. n=5). There is no significant difference between drug treated and control terminals.

Figure 3.1 demonstrates that DYN treatment (after SV recycling), under any of the three stimulations, had no effect on the total Glu released from the synaptosomes, irrespective of the SV pool.

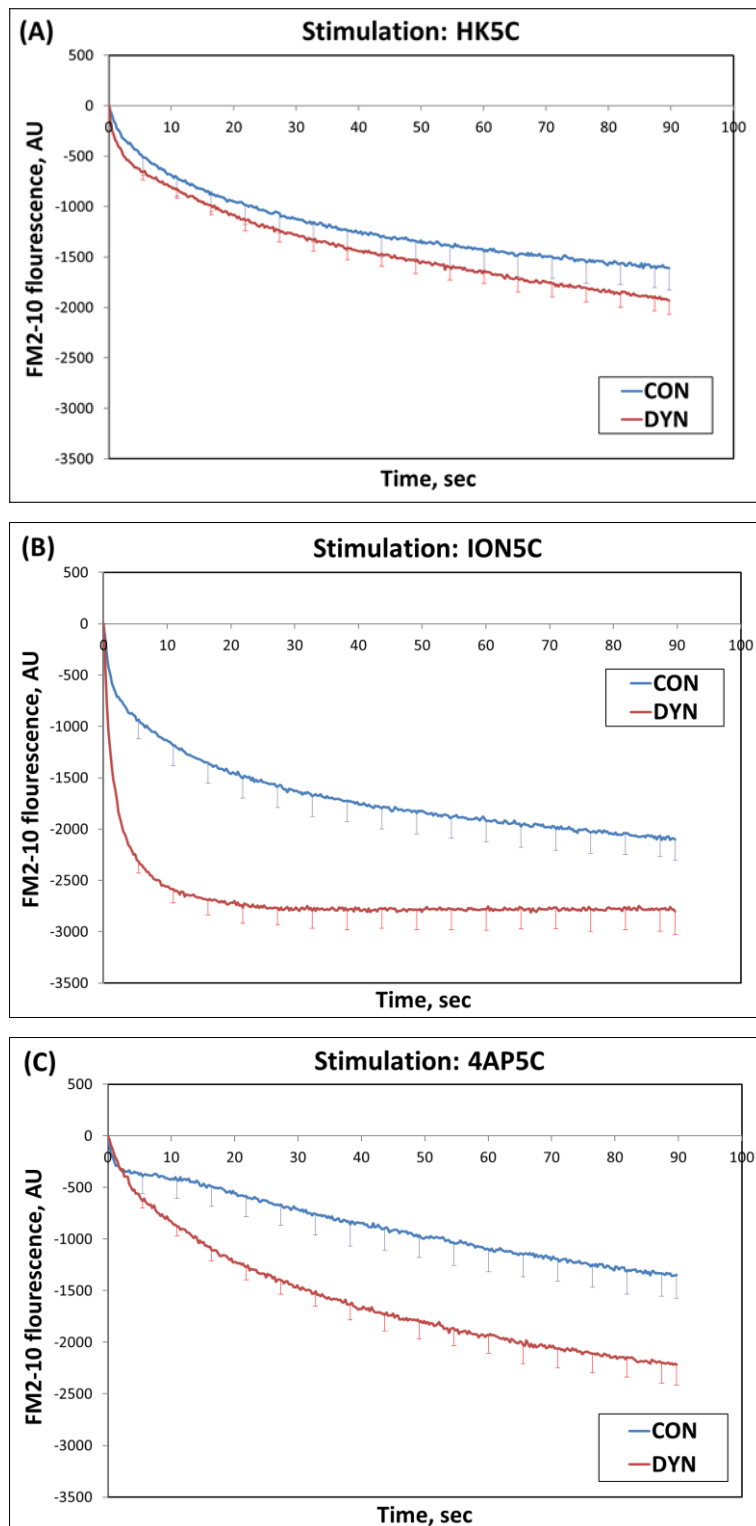


Figure 3.2 The effect of 160 μM DYN on FM2-10 dye release evoked by (A) HK5C, (B) ION5C and (C) 4AP5C. Data are mean \pm S.E.M. from 5 different experiments (i.e. $n=5$).

Panel A of figure 3.2 shows no significant change in the FM 2-10 dye release, when HK5C is used as stimulus for control and DYN treated terminals. Panels B and C show a significant increase in FM 2-10 dye release for DYN treated synaptosomes when employing ION5C and 4AP5C as stimuli.

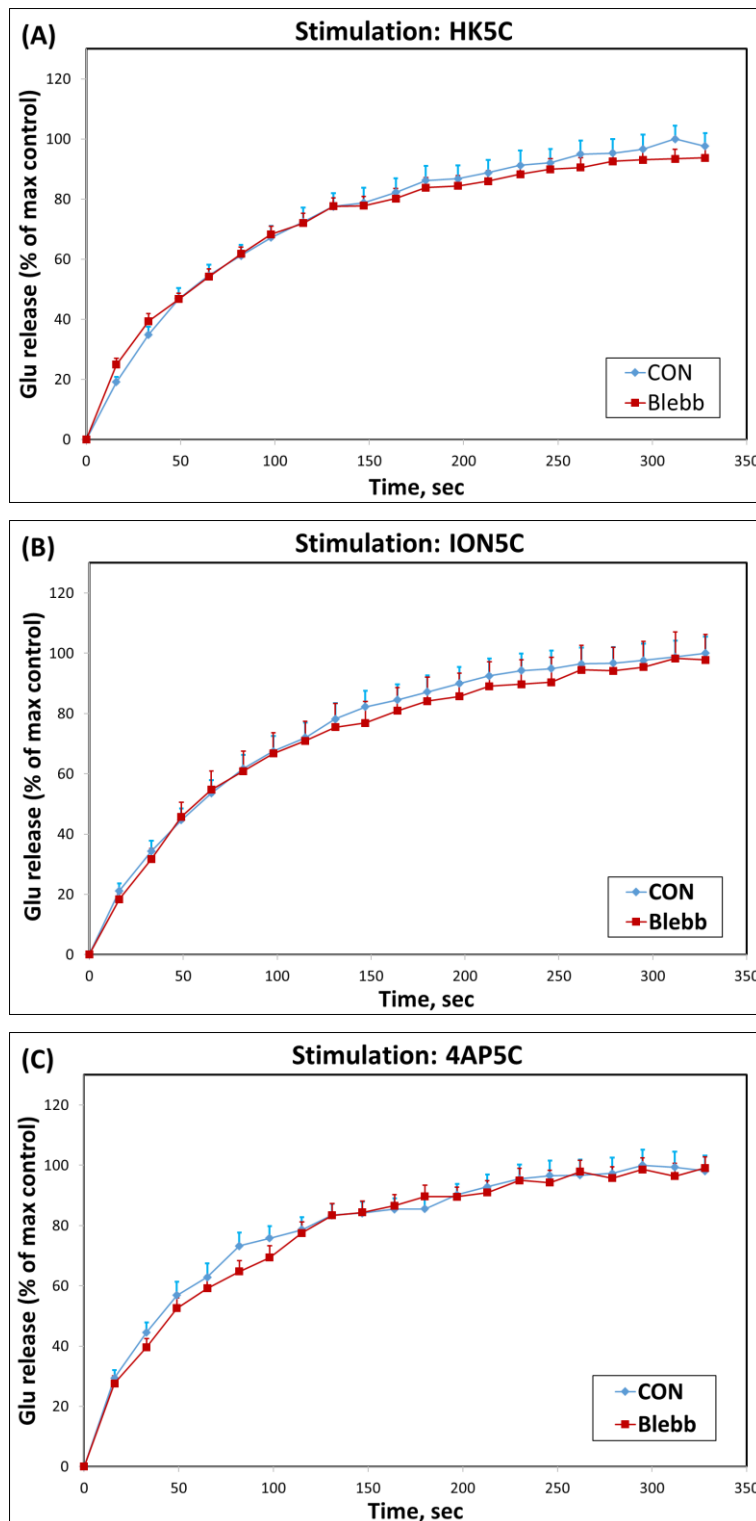


Figure 3.3 The effect of 50 μ M Blebb on Glu release evoked by (A) HK5C, (B) ION5C, and (C) 4AP5C. Data are mean +S.E.M. from 5 different experiments (i.e. n=5). There is no significance difference between drug treated and control terminals.

This Blebb treatment did not perturb the Glu release evoked by any of these stimuli and, therefore, inhibition of myosin II does not perturb the release of the RRP or RP of SVs.

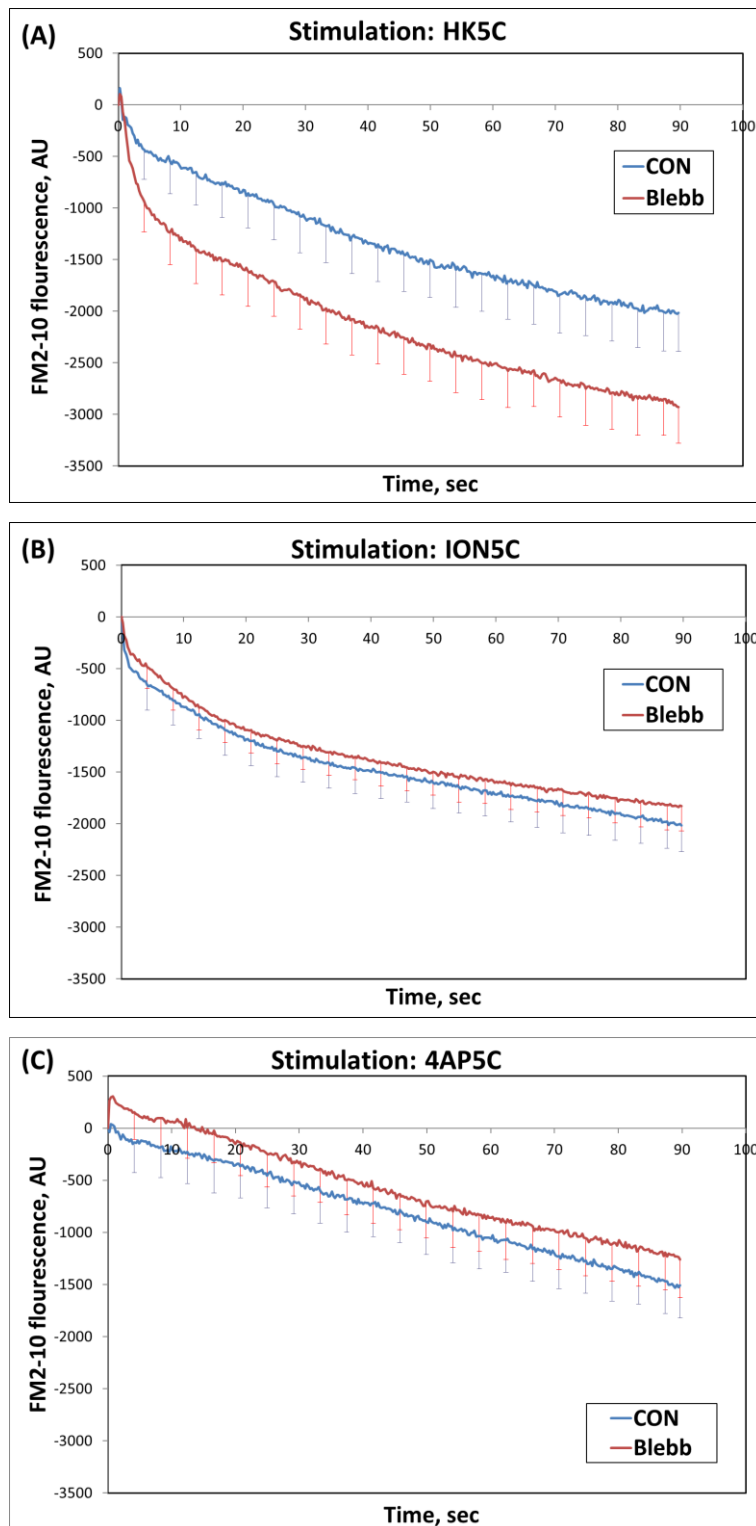


Figure 3.4 The effect of 50 μ M Blebb on FM2-10 dye release evoked by (A) HK5C, (B) ION5C and (C) 4AP5C. Data are mean \pm S.E.M. from 5 different experiments (n=5).

Panel A of figure 3.4 shows a significant increase in the FM 2-10 dye release for Blebb treated terminals compared to control when HK5C is used as stimulus. However, panels B and C of figure 3.4 show no change in the FM 2-10 dye release when control and Blebb treatment are compared for stimulation by ION5C or 4AP5C.

These results confirm that myosin-II does play a role in switching the mode of synaptic vesicular exocytosis but only for the HK5C stimulus.

3.1.2 Interpretation of background results

Thus, inhibition of dynamins significantly increased the FM 2-10 dye release for ION5C and 4AP5C stimulation. Therefore, dynamins are required for the closure of the fusion pore during KR exocytosis of the RRP of SVs induced by these stimuli whilst such SVs are switched to FF in the absence of active dynamins. HK5C induces KR independently of the activity of dynamins and it was found that in this case myosin-II is responsible for the closure of the fusion pore during HK5C stimulation evoked KR release of the RRP of SVs.

This was an interesting finding but we really wanted to know why there was difference in the proteins that regulated the fusion pore depending upon the stimulus employed. Therefore, we hypothesised that the high Ca^{2+} concentration levels induced by HK5C at the active zone enables myosin-II to be activated and this closes the fusion pore such that the release of the RRP SVs is via KR. However, ION5C and 4AP5C do not achieve these high levels of Ca^{2+} at the active zone and so myosin-II is not activated, and therefore myosin-II plays no significant role in the fusion mode evoked by these stimuli.

The results also indicate that these high levels of Ca^{2+} - induced by HK5C - must inactivate dynamins otherwise, when non-muscle myosin-II is blocked, the dynamins could still close the fusion pore.

3.2 Introduction to chapter 3

As we had previously determined that various calcium dependent kinases (and a calcium dependent phosphatase) can regulate the mode of exocytosis, it was hypothesised that these same kinases may be involved in activating myosin-II and inactivating dynamin. Thus, in this chapter the role that PKCs may play was investigated by using Go 6983 (*3-[1-[3-(dimethylamino)propyl]-5me-thoxy-1H-indol-3-yl]-4-(1H-indol-3-yl)-1H-pyrrole--2,5-dione*) (Young *et al.*, 2005) through FM 2-10 dye release assay and glutamate assay. This is a broad-spectrum PKC inhibitor and 1 μM Go 6983 inhibits all PKCs including the three categorised classes conventional, novel and atypical (Lanuza *et al.*, 2014).

The determination of a dynamin dependence for the mode of exocytosis of the RRP SVs under distinct stimulation conditions meant that it was vitally important to determine whether the closure of the fusion pore via dynamin exhibited distinct properties from other dynamin-dependent processes. It has been well characterized that CME has a dynamin requirement (Saheki and De Camilli, 2012) and recently ultra-fast endocytosis has been shown to have a dynamin requirement (Watanabe *et al.*, 2013). Intriguingly, although these processes are distinct they both depend upon clathrin action (e.g. Watanabe *et al.* 2014). Thus, if one can show that the RRP SVs exocytose independent of clathrin then this would suggest that the KR exocytotic mechanism described, herein, is distinct from these two other processes. Fortunately, a drug has been produced recently that specifically inhibits clathrin dependent processes by blocking the

terminal domain of the protein so it can no longer form productive clathrin coats. This drug is called Pitstop2TM (von Kleist *et al.*, 2011). Thus, in this chapter we investigated whether the dynamin-dependent KR mode of RRP could be perturbed by blockade of clathrin processes using Pitstop2TM.

3.3 Results

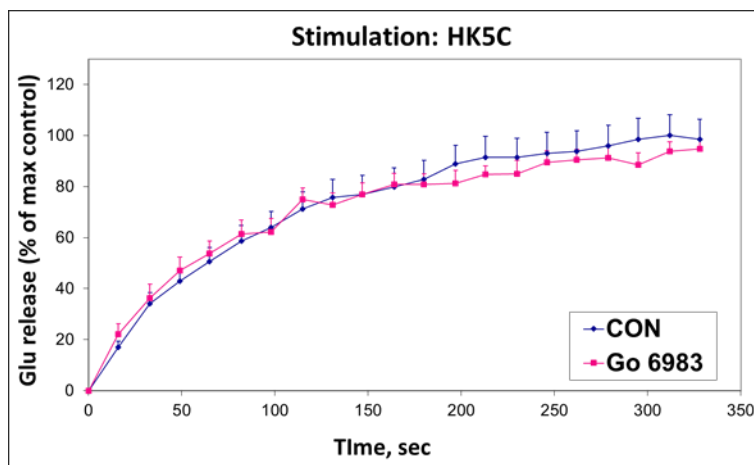


Figure 3.5. The effect of 1 μ M Go 6983 on Glu release evoked by HK5C. Data are mean + S.E.M., n= 5 different experiments. There is no significant difference between drug treated and control terminals.

Clearly, endogenous PKCs are apparently not involved in regulating the total number of SVs undergoing fusion from either the RRP or the RP, since pre-treatment with Go 6983 does not significantly decrease the amount of Glu released (Figure 3.5).

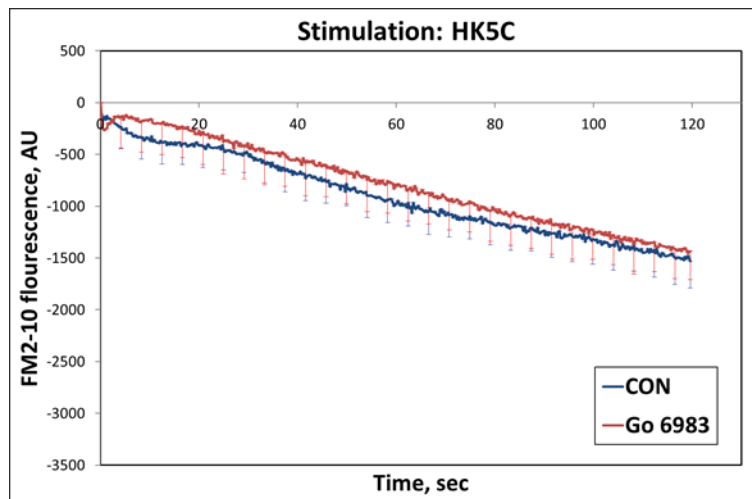


Figure 3.6 The effect of 1 μ M Go 6983 on FM2-10 dye release evoked by HK5C. Data are mean \pm S.E.M., $n=3$ different experiments. There is no significant difference between drug treated and control terminals.

This result would on face value also suggest that activation of endogenous PKCs by the application of HK5C does not regulate the fusion mode of the RRP or the RP SVs. This is because there is neither more FM dye release (due to conversion of the RRP to FF) or less FM dye release (due to conversion of the RP to KR).

The release of HK5C evoked Glu was measured following the treatment with both Go 6983 and Blebb (Figure. 3.7).

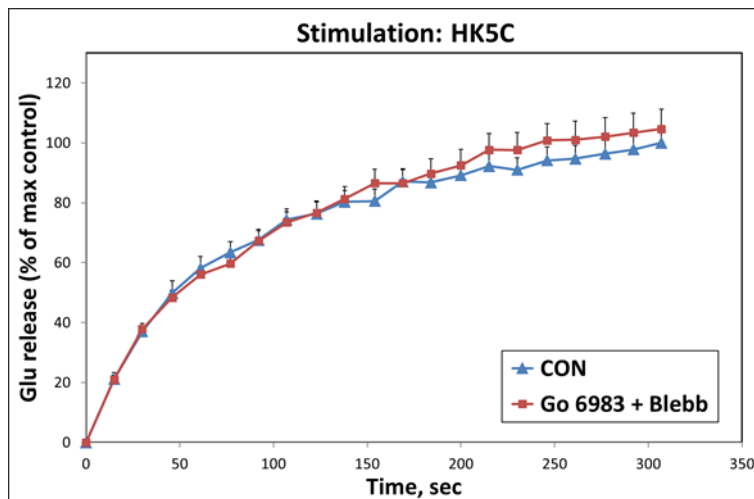


Figure. 3.7. The effect of 1 μ M Go 6983 followed by 50 μ M Blebb on Glu release evoked by HK5C. Data are mean +S.E.M., n= 3 different experiments. There is no significant difference between drug treated and control terminals.

The double drug treatment of inhibiting endogenous PKCs and blocking myosin-II activity fails to perturb the total number of SVs exocytosing from the RRP and the RP induced by the application of HK5C. Thus, we can use the same drug treatment to investigate whether this can regulate the modes of exocytosis of these SVs.

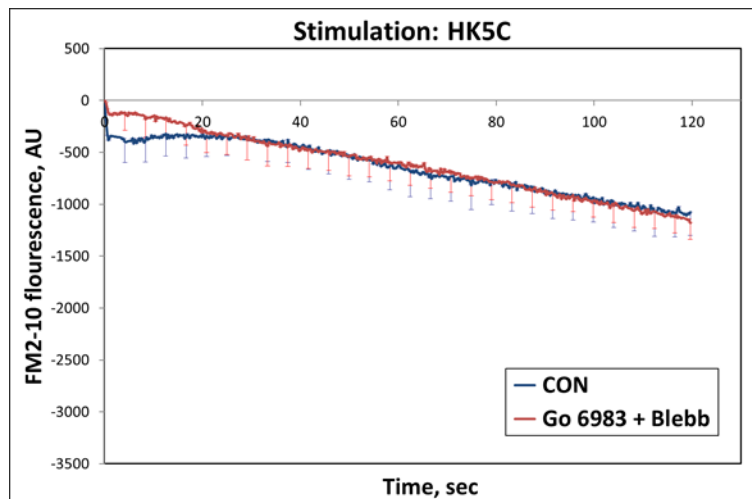


Figure. 3.8. The effect of 1 μ M Go 6983 followed by 50 μ M Blebb on FM2-10 dye release evoked by HK5C. Data are mean \pm S.E.M., n=3 different experiments. There is no significant difference between drug treated and control terminals.

results in Figure 3.8 (in conjunction with the results in Figure 3.7) when compared to Figure 3.4 clearly show that inhibition of PKCs with Go 6983 prevents the fusion pore for RRP SVs from being regulated by myosin-II as Blebb no longer prevents the fusion pore closing and KR still occurs. This result indicates that under the double drug treatment conditions another protein must be able to close the fusion pore and induce KR.

We pointed out in the introduction to this chapter that HK5C must not only activate myosin-II to close the fusion pore of the RRP SVs but that it must also inactivate the dynamins. Clearly, as inhibition of PKCs prevents myosin-II acting on the fusion pore (Figure 3.7 and 3.8) then it could well be that it is also the HK5C activated PKCs that normally inactivate dynamins. Thus, we investigated the effect that the double treatment with Go 6983 and DYN would have on HK5C evoked Glu release (Figure 3.9).

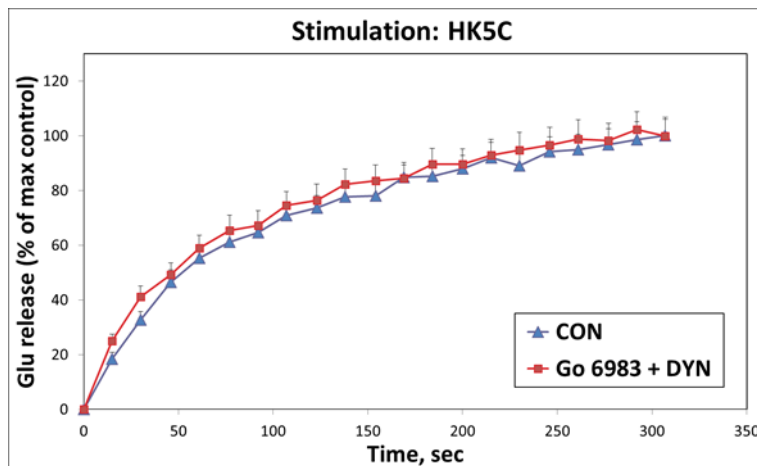


Figure. 3.9. The effect of 1 μM Go 6983 followed by 160 μM DYN on Glu release evoked by HK5C. Data are mean +S.E.M., n=3 different experiments. There is no significant difference between drug treated and control terminals.

The double drug treatment of inhibiting endogenous PKCs and blocking dynamins did not prevent the SVs exocytosing from the RRP and the RP induced by the application of HK5C. Thus, we can use the same drug treatment to investigate whether this treatment can regulate the modes of exocytosis of such SVs.

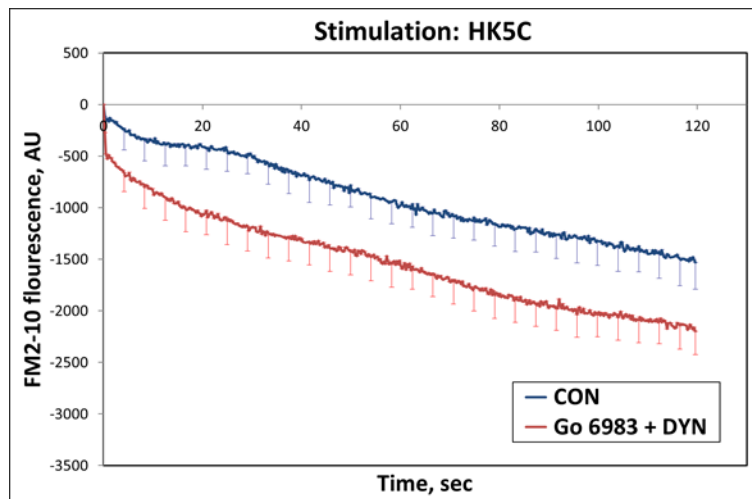


Figure. 3.10. The effect of 1 μM Go 6983 followed by 160 μM DYN on FM210 dye release evoked by HK5C. Data are mean \pm S.E.M. from 3 different experiments (i.e. $n=3$). There is a significant increase in the HK5C evoked FM 2-10 dye release for Go 6983 plus DYN treated terminals compared to the non-drug treated control.

As shown in Pre-treatment with Go 6983 (inhibitor of PKCs) and DYN (inhibitor of Dynamin I & II) switched all of the exocytosing SVs to FF mode, including those belonging to RRP. From Figure 3.6 and Figure 3.8, it can be concluded that when PKCs and Myosin-II are inhibited, the RRP still undergoes KR. This means that there must be a protein involved in closure of the fusion pore of these RRP SVs causing them to undergo KR mode of exocytosis. From Figure 3.10, it can be deduced that inhibition of PKCs and Dynamins causes the RRP vesicles to exocytose via FF mode.

A comparison between the action of HK5C following Blebb treatment (Figure. 3.4) and following Go 6983 plus DYN (Figure. 3.10) would suggest that there was an approximately equal amount of extra FM2-10 dye released compared to the control conditions. This represented all the RRP SVs switching to a FF mode. However, in view of speculation elsewhere in this thesis that the RRP could be heterogeneous (see Chapter 5) it was important to confirm that the Go

6983 - by blocking PKCs - was able to convert the RRP SVs such that they all now exhibited dynamin sensitivity. In order to do this, we compared the result highlighted in Figure 3.10 with an experiment where we showed the dynamin sensitive of ION5C evoked release of the RRP of SVs (Figure 3.2).

By comparing Figure 3.10 and Figure 3.2, it would appear that the increase in FM2-10 dye release following the relevant drug treatments are similar. This would suggest that inhibiting PKCs converts all the HK5C evoked RRP SVs so that the mode of exocytosis is now dynamin sensitive.

Synaptosomes were pre-treated with 15 μ M Pitstop2TM using the single drug addition protocol as outlined in chapter 2. This drug perturbs clathrin dependent processes and this enable one to investigate the role of clathrin in regulation of the mode of exocytosis of SVs. The terminals were evoked to release neurotransmitter with the usual dynamin-dependent stimulus, ION5C, as the purpose of this study was to investigate whether clathrin contributed to the dynamin-dependent closure of the fusion pore of RRP SVs during KR.

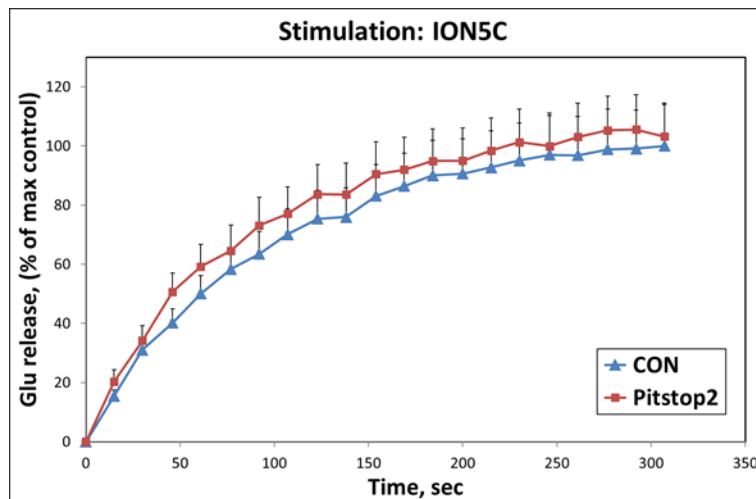


Figure. 3.11. The effect of 15 μ M pitstop2TM on Glu release evoked by ION5C. Data are mean +S.E.M., n= 5 different experiments (i.e. n=5). There is no significant difference between drug treated and control terminals.

The amount of release induced by ION5C was statistically the same in the control and pitstop2TM treated terminals. This indicates that the RRP and RP SVs both still release their Glu content by exocytosing with the presynaptic plasma membrane.

Clearly, as pitstop2TM treatment did not prevent the exocytosis of the RRP and the RP, we were then able to determine whether such treatment perturbed the mode of exocytosis of these pools of SVs (Figure 3.12).

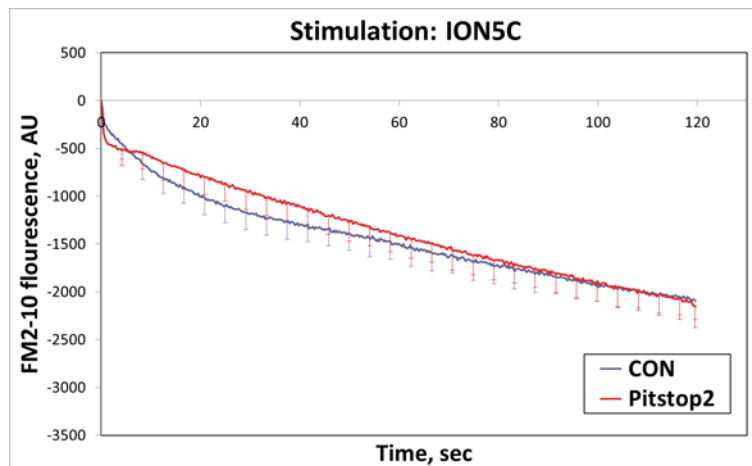


Figure. 3.12. The effect of 15 μM pitstop2TM on ION5C evoked FM2-10 dye release. Data are mean \pm S.E.M., $n = 5$ different experiments. There is no significant difference between drug treated and control terminals.

This result would appear to suggest that the dynamin-dependent closure of the fusion pores of the RRP SVs that leads to KR with ION5C stimulation is not perturbed when clathrin activity is blocked. This would suggest that KR is dynamin-dependent but clathrin-independent when studied with ION5C.

However, there remained the possibility that pitstop2TM treatment may change the requirements for KR independently of the dynamins as we found when myosin-II dependence for HK5C was switched to dynamin dependency by inhibition of PKCs (see above). Thus, we carried out a double drug treatment with Pitstop2TM and DYN to determine if the latter drug still switched the mode of the RRP SVs to FF (Figure 3.13 and 3.14)

In these experiments, Pitstop2TM and DYN were added at the same time in single drug incubation protocol similar to the protocol followed for Figure 3.1 except that both drugs were added at the same time.

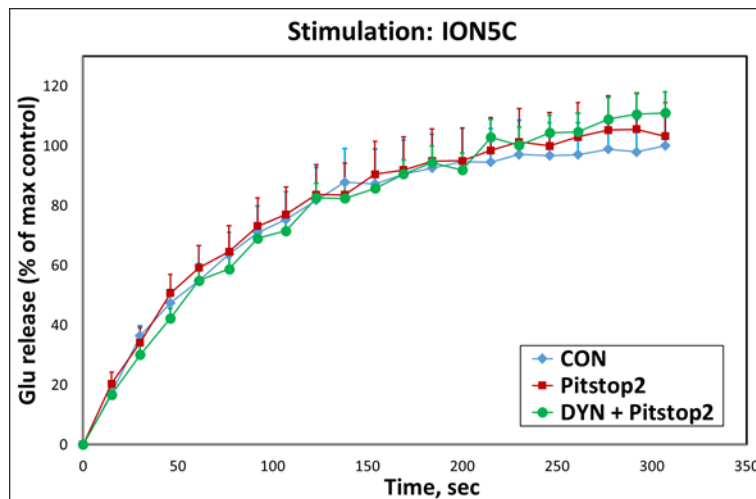


Figure. 3.13. The effect of 15 μM pitstop2TM plus 160 mM DYN on Glu release evoked by ION5C. Data are mean +S.E.M., n= 5 different experiments. There is no significant difference between drug treated and control terminals.

The joint treatment did not affect the maximum release of Glu induced by ION5C which represents the RRP and the RP SVs exocytosing their neurotransmitter content. Thus, we were able to see whether this double treatment had any effect upon the mode of exocytosis of the RRP SVs (Figure 3.14).

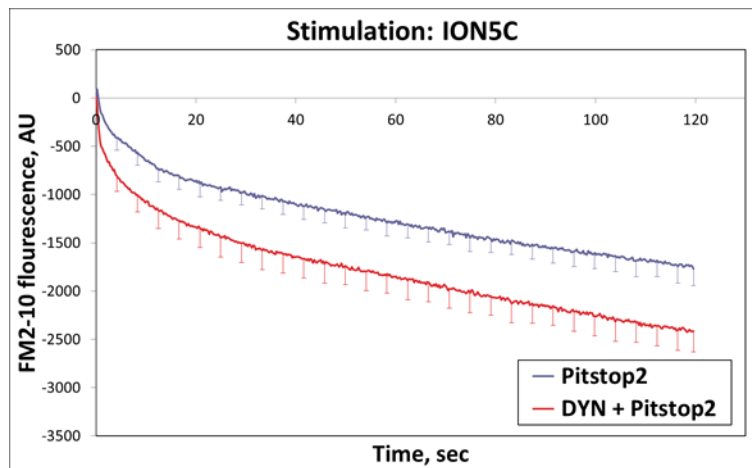


Figure. 3.14. The effect 15 μ M pitstop2TM or 15 μ M pitstop2TM plus 160 μ M DYN on FM2-10 dye release evoked by ION5C. Data are mean \pm S.E.M. from experiments.

It would seem that pitstop2TM did not prevent DYN from switching the mode of the RRP SVs to FF when ION5C is used as the stimulus. This would suggest that the action of dynamin on closing the fusion pore is totally independent of its action in a different endocytotic pathway that also involves clathrin (CME or ultrafast endocytosis).

There is a significant increase in the ION5C evoked FM 2-10 dye release for pitstop2TM plus DYN treated terminals compared to pitstop2TM alone, results of three independent experiments (i.e. n=3).

3.4 Discussion

3.4.1 Dynamins and Myosin-II regulate the fusion pore

In order to investigate the role of dynamins, 160 μM DYN (DYN) was used as demonstrated by figure 3.1. It was found that 160 μM DYN had no effect on the glutamate released upon HK5C, ION5C and 4AP5C stimulations. These results indirectly support Ashton *et al.*'s unpublished data that all the three stimuli induce only a single round of SV release. This is because it has been confirmed by various studies that the dynamins are required for the clathrin-dependent endocytosis (Hosoi *et al.*, 2009). If the stimuli employed induced more than one round of release, then a decrease in the glutamate release would be observed upon the inhibition of dynamins. However, the results showed that this was not the case thereby indicating that all three stimuli only induced a single round of release.

In contrast, inhibition of dynamins significantly increased the FM 2-10 dye release upon ION5C and 4AP5C stimulation indicating that dynamins are required for the closure of the fusion pore during these stimuli and their inhibition would cause all the SVs undergoing KR to switch to FF mode of exocytosis (shown in figure 3.2).

The role of myosin-II was assessed by specifically inhibiting it, using 50 μM Blebb. It was found that even though it did not affect the glutamate release under any of the three stimuli (Figure 3.3); it increased the amount of FM 2-10 dye released under HK5C stimulation (Figure 3.4). This signifies that myosin-II is responsible for the closure of the fusion pore during HK5C stimulation resulting in the KR mode of exocytosis.

These results together with the Ashton *et. al.*, unpublished data (see Introduction to background results) would suggest that the dynamins are responsible for the KR of RRP vesicles during ION5C and 4AP5C stimuli and that myosin-II is responsible for the KR of RRP during the HK5C stimulation. Furthermore, these results also suggest that dynamins may be active and therefore responsible for the KR, only during lower $[Ca^{2+}]_i$ at the active zone as produced during ION5C and 4AP5C stimulations. Myosin-II may be active, and therefore responsible for the KR, only during higher $[Ca^{2+}]_i$ at the active zone as produced during HK5C stimulation. Thus, it can be summarised that dynamins and myosin-II are involved in the KR mode of exocytosis.

These results may relate to the functional state that a particular terminal may find itself in which would be defined by the amount of stimulation it may have or be receiving. From our arguments about levels of Ca^{2+} at the active zone, it can be seen that such synaptic activity could change the mode requirements for the distinct proteins that we have outlined. Further as these both are (Dynamins & Myosin-II) phospho-proteins this means that secondary messenger pathways could regulate the mode by regulating dynamins and/or myosin-II.

3.4.2 PKCs regulate the action of dynamins and myosin-II

Synaptic transmission is highly regulated by processes of short- and long-term synaptic plasticity, as well as by intracellular second-messenger cascades. A particularly important signalling cascade that targets the presynaptic compartment of synapses is the PKC pathway (Lou *et al.*, 2008). An example of this is that Ahmed and Siegelbaum (2009) have shown that PKC can enhance N-type channel activity directly and antagonize signalling cascades that inhibit N-type channel opening (Ahmed and Siegelbaum, 2009). This type

of information led us to question whether there could there be a role of PKC activation towards myosin-II regulating the fusion pore of the RRP SV.

Double treatment of synaptosomes with 1 μ M Go 6983 and 50 μ M blebb revealed that if PKC is inhibited, myosin-II cannot regulate the mode of exocytosis from the RRP SVs. This suggests that PKC is involved in the KR mode of exocytosis and regulates the activation of myosin-II. Herein, this occurs when HK5C is used as the stimulus but this may occur *in vivo* under strong stimulation conditions that a nerve terminal might experience under certain physiological situations.

In previous studies conducted in Ashton laboratory (Dilip Bhuvu, PhD thesis 2014) it has been shown that under such strong stimulation conditions activation of certain PKCs can inhibit dynamin and so this protein cannot regulate the fusion pore of the RRP SVs as so it does not contribute to KR. Clearly, this would also occur under certain physiological conditions. However, lower stimulation conditions will not only fail to activate myosin-II but they will also fail to inactivate dynamins.

This chapter showed that HK5C also exhibited dynamin-dependent regulation of the fusion pore leading to KR of the RRP SVs if certain PKCs are not activated (the specific PKC isoforms are still unknown). Clearly, when these enzymes are stimulated they can inactivate the dynamins (see chapter 7).

In summary, HK5C produces a large increase in $[Ca^{2+}]_i$ at the AZ and a subsequent generalized lower increase in Ca^{2+} throughout the nerve terminal. This elevated presynaptic calcium concentration causes activation of certain isoforms of PKC (yet unknown) which in turn results in phosphorylation of myosin-II thereby activating it. Dynamins belong to a family of dephosphins

which means that dynamins are active when dephosphorylated. Activation of PKC inhibits the action of dynamin. In this way, PKC acts as a regulator for closure of the fusion pore during KR mode of exocytosis by activating myosin-II and inhibiting dynamins when HK5C is employed. Myosin-II and dynamins both are capable of inducing the closure of the fusion pore of the RRP of SVs. Dynamins and Myosin-II are able to regulate the mode of fusion pore in a Ca^{2+} dependent manner, with each protein requiring distinct changes in $[\text{Ca}^{2+}]_i$. Thus, dynamins are generally active only during lower $[\text{Ca}^{2+}]_i$ at the AZ whereas myosin-II is active only when a relatively higher $[\text{Ca}^{2+}]_i$ is achieved at the active zone (Ashton *et al.*, unpublished work).

Another important result conducted by Ashton *et al.*, not reported in this thesis, is further proof about the regulation of dynamins and myosin-II by PKCs. The data presented here utilised the PKC inhibitor, Go 6983. However, you can activate certain PKCs utilising the active phorbol ester (Ph est) (Parfitt and Madison, 1993; Lou *et al.*, 2008). Ashton and colleagues have found that pre-treatment of synaptosomes with 40 nM PMA does not affect the ION5C evoked release of the RRP and the RP. However, it was found that such treatment prevented dynamins from exerting its induction of FF for the RRP. This suggests that the PKC activation inactivated the dynamins. This indicates that PMA activates myosin-II to now close the fusion pore and induce KR but this is blocked by blebb. Thus, both ION5C and HK5C can under different circumstances have the same protein requirement for closing the fusion pore during KR of the RRP SVs (Refer chapter 8, Figure 8.1 for a diagrammatic summary).

3.4.3 KR is independent of CDE

ION5C was employed as a stimulus to determine whether clathrin had a role to play in regulating the dynamin-dependent KR mode. One could argue that 4AP5C could be used as part of RRP which undergoes KR which is also dynamin-dependent. However, this contribution of KR to the release is much less when compared to ION5C and it would be more difficult to produce statistically significant data with 4AP5C and one would perhaps need to do many experiments. Similarly, in chapter 6 we have demonstrated that this latter stimulus may work differently on distinct sub-populations of RRP SVs and this could also complicate the analysis. HK5C could not be used as stimulus as RRP undergoes KR under the influence of myosin-II; which is not linked to clathrin dependent endocytosis. The results employing ION5C, pitstop2TM and DYN indicate that the action of dynamin is independent of the clathrin which implies that KR is independent of CDE. It also suggests that the KR mode studied, herein, is probably distinct from ultra-fast endocytosis which has a dynamin and clathrin dependent requirement (Watanabe *et al.*, 2013,2014). It should be noted that in some preliminary experiments the double stimulation protocol was used in which DYN was used prior to pitstop2TM or alternatively pitstop2TM was used prior to DYN. Under any of these conditions pitstop2TM failed to perturb the action of DYN on dynamins. Thus, this is extra evidence for the KR mode being able to be regulated by dynamins but not being regulated by clathrin.

3.4.4 Dynamin-I regulates the fusion pore

In other studies, conducted by Ashton *et al.*, but not reported in this thesis, the dynamin isoform that seems to regulate the mode of exocytosis was investigated using some drugs that are specific for certain isoforms at specific

concentrations. 20 μM Dynole-34-2TM is reported to be specific for dynamin-I GTPase action whilst 50 μM Dyngo-4aTM is specific for the GTPase activity of dynamin 2 (Robertson *et al.*, 2014). Careful comparison between these two drugs reveals that Dynole-34-2TM induces the RRP SV to switch to FF with ION5C stimulation whilst Dyngo-4aTM has no effect. This is an important observation because it highlights that the major dynamin present in nerve terminals – dynamin-I – is the protein that regulates the fusion pore whilst dynamin-II which is ubiquitously expressed throughout the body but is present at very low levels in central nerve terminals doesn't appear to play a role.

Chapter 4

Effect of pre-treatment of 160 μM DYN and 15 μM Pitstop2TM

4.1 Introduction

4.1.1 Brief summary of results presented earlier on in this study

A distinguishing feature of SVs is their Ca^{2+} dependency. The three stimuli used for this study are Ca^{2+} dependent and induce SV exocytosis by distinct mechanisms (Rizo & Rosenmund, 2008). As mentioned earlier, at the active zone HK5C produces a relatively fast and large increase in $[\text{Ca}^{2+}]_i$ in comparison to ION5C and 4AP5C which do not produce such a large increase in Ca^{2+} at this region. This is due to the strategic localization of voltage-dependent Ca^{2+} channels here (Ashton *et al.*, unpublished). However, HK5C and ION5C induce release of both releasable SV pools with exocytosis of RRP by KR and the RP undergoing FF, whilst 4AP5C results in the exocytosis of RRP by a mixture of KR and FF (see Figure 3.2 & 3.4; Ashton *et al.*, unpublished).

All the above conclusions have depended upon the fact that these stimuli are present during the release period such that the terminals are constantly stimulated with no period of recovery unlike the situation with trains of action potentials in the brain. As a consequence, in this study, SVs undergo only one round of release. That only one round or release of these pools occurs has been determined by several methods. Bafilomycin A (BAF), when applied acutely at 1 μM in conjunction with a stimulus to rat synaptosomes, it does not interfere with the initial glutamate release of SVs undergoing exocytosis, but inhibits the re-uptake of glutamate when these SVs recycle (Ikeda and Bekkers, 2009; Ashton *et al.*, unpublished). It would seem that this concentration and the short time period (5 mins) does not interfere with the Glu content of non-released SVs but once these have released their content and, following

recycling into the terminal, they are then unable to reload with Glu because the proton gradient required for this has been inhibited by BAF (Ikeda and Bekkers, 2009). Therefore, if the stimuli employed induced several rounds of release of recycled and reloaded vesicles then there would be a difference between CON and BAF treated samples. Figure 4.1 indicates that this is not the case and there is no difference between control and BAF treated samples.

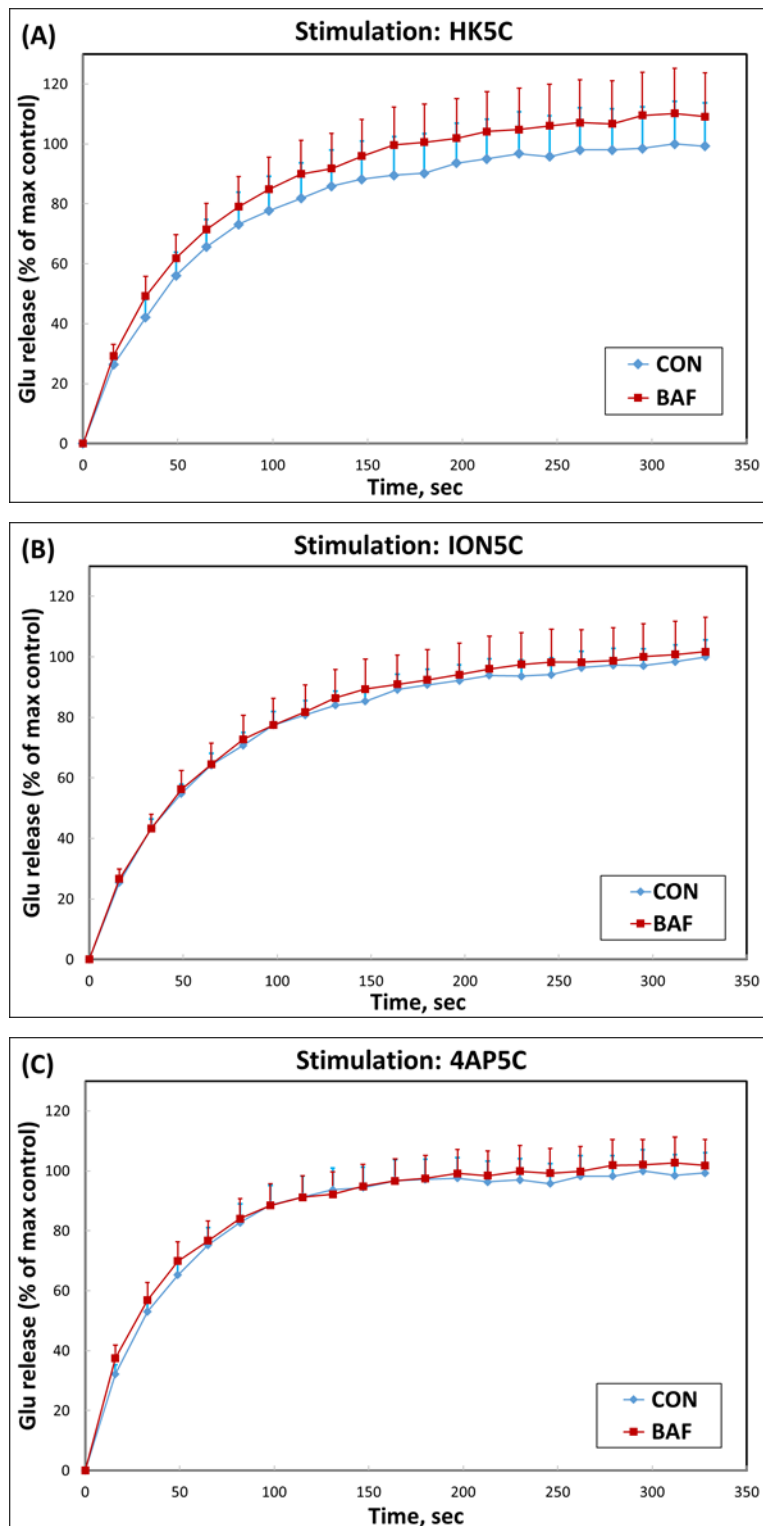


Figure 4.1. The effect of 1 μ M BAF on HK5C, ION5C and 4AP5C evoked glutamate release. (Ashton *et al.*, unpublished) Error bars represent positive S.E.M., n=3 independent experiments).

This finding indicates that only one round of SV fusions takes place after the application of the stimulus. This is actually a prerequisite for comparing stimulated Glu release and stimulated FM2-10 dye release.

4.1.2 Further investigations into the distinct modes of SV exocytosis

It has been established that both the RRP and RP of SVs can be released by exocytosis even when dynamin or clathrin-dependent processes have been blocked. This actually demonstrates again that the stimuli employed only induce one round of release of these pools. If there were recycling, reloading and re-release of SVs during the stimulation period then any SVs recycling by a dynamin or clathrin-dependent process would fail to be released and so DYN or pitstop2TM treatment would reveal this but they fail to do so. Clearly, all SVs can exocytose and release their Glu content although they might not be able to recycle via these protein specific processes.

All our experiments involve a pre-stimulation with HK5C which induces the RP and RRP SVs to exocytose. Following removal of the stimulus, these SVs can be made available for re-release by recycling, reloading and re-priming.

Indeed, it should be noted that this pre-stimulation is the means by which the SVs are loaded with FM2-10 dye. Such dye will label all the SVs whether they undergo KR or FF during this period. This is due to the property of the dye because whilst it has a fast association rate with the lipid membrane, it has a much slower dissociation rate (departition). Therefore, FM2-10 dye will label SVs even if they recycle by KR in <0.5 sec although a further round for release induced by a subsequent stimulation will mean that such KR SVs will not release their dye content.

We can actually test whether this pre-stimulation mechanism induces some SVs to undergo a clathrin and/or dynamin-dependent component that is distinct from those SVs undergoing KR. This simply involves pre-treating the synaptosomes with DYN or pitstop2TM prior to performing this pre-stimulation with HK5C. It is fortuitous that HK5C stimulation of the RRP of SVs is via a dynamin-independent myosin II-dependent KR mechanism since such SVs will still recycle when dynamins are blocked. Such an experiment would also confirm that some SVs do have a dynamin requirement for recycling and similarly that these same SVs have a clathrin-dependent requirement for vesicular endocytosis. Such results would also confirm that DYN and pitstop2TM do act on these processes and that these drugs in our experiments are active i.e. these would represent positive controls to prove that these drugs are working in our preparation.

4.2 Results

The main aim of this chapter was to establish that KR is distinct to ultra-fast endocytosis. This was done by treating synaptosomes with 160 μ M DYN (Figure 4.2, 4.4) or 15 μ M pitstop2TM (Figure 4.3, 4.5) or a mixture of the two drugs (Figure 4.6).

Synaptosomes were treated with DYN prior to the pre-stimulation with HK5C, followed by a second round of release evoked by ION5C (Figure 4.2).

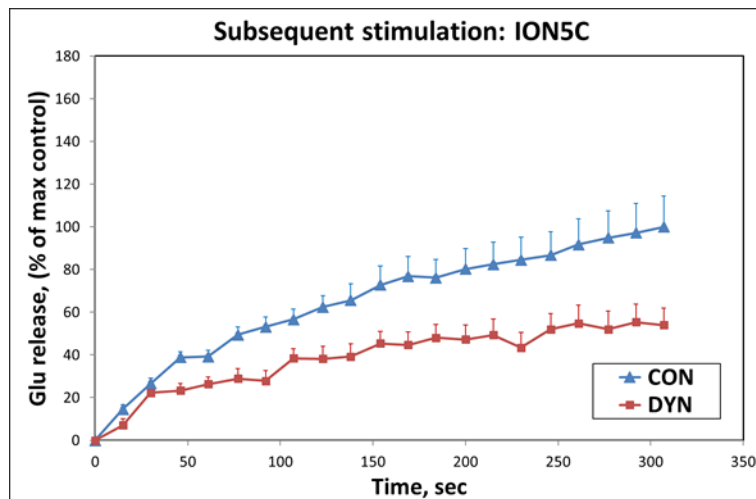


Figure 4.2 The effect that 160 μM DYN treatment before pre-stimulation exerts on the subsequent ION5C evoked glutamate release. Glutamate release has been expressed as percentage of maximum control. Error bars indicate S.E.M. The results were repeated with 3 individual experiments with numerous independent measurements (i.e. $n \geq 3$). $p < 0.05$ was considered significant.

A significant decrease in ION5C evoked Glu release can be observed when synaptosomes were pretreated with 160 μM DYN prior to the prestimulation with HK5C compared to the non-drug treated control. This indicates that some SV recycling must have a dynamin-dependent requirement and this can include CME (Takei *et al.*, 2005), bulk endocytosis (Clayton *et al.*, 2010) or ultrafast endocytosis (Watanabe *et al.*, 2013). Herein, the stimuli employed for the pre-stimulation is HK5C which can induce a dynamin-independent KR mode of exocytosis for the RRP SVs. Synaptosomes were treated with pitstop2TM prior to the pre-stimulation with HK5C, followed by a second round of release evoked by ION5C (Figure 4.3).

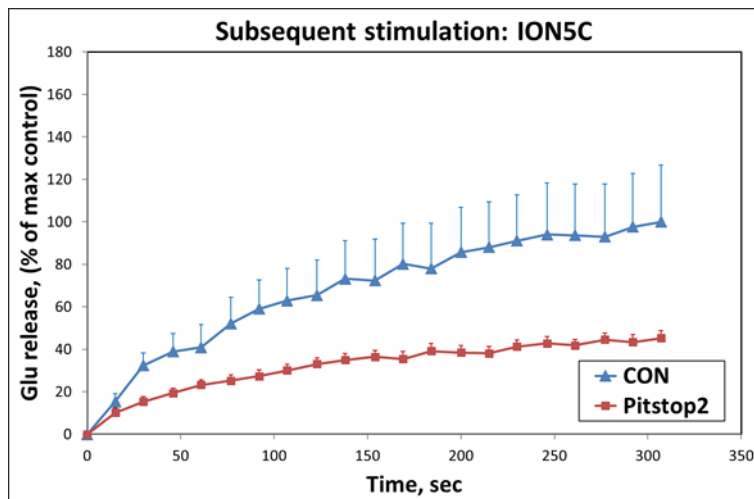


Figure 4.3 The effect that 15 μM pitstop2TM treatment before pre-stimulation exerts on the subsequent ION5C evoked glutamate release. Glutamate release has been expressed as percentage of maximum control. Error bars indicate S.E.M. The results are representative of at least 3 individual experiments (i.e. $n \geq 3$), $p < 0.05$ was considered significant).

A significant decrease in ION5C evoked Glu release can be observed when synaptosomes were pretreated with 15 μM pitstop2TM prior to the pre-stimulation with HK5C compared to the non-drug treated control. This indicates that some SV recycling must have a clathrin-dependent requirement and this obviously includes CME but it also includes ultrafast endocytosis.

By comparing Figure 4.2 and Figure 4.3 the glutamate release occurs from a pool of SVs that do not require CME, bulk endocytosis or ultra-fast endocytosis for recycling.

HK5C induces all the RRP to undergo KR and as it is speculated that this mode is clathrin independent (it still occurs when pitstop2TM is added later on following the pre-stimulation step), it would seem that the SVs that are still able to exocytose (as seen in Figure 4.3) must have been those that represented the RRP SVs. Similarly, as HK5C induces KR of the RRP that is dynamin

independent then it would appear that the SVs that are still able to exocytose (as seen in Figure 4.2) must also be those that represented the RRP SVs. We can test to see whether the SVs available for release following the blockade of dynamin or clathrin before the pre-stimulation, do represent the RRP since we can stimulate with 4AP5C which exclusively releases just this pool (Figure 4.4,4.5 and 4.6).

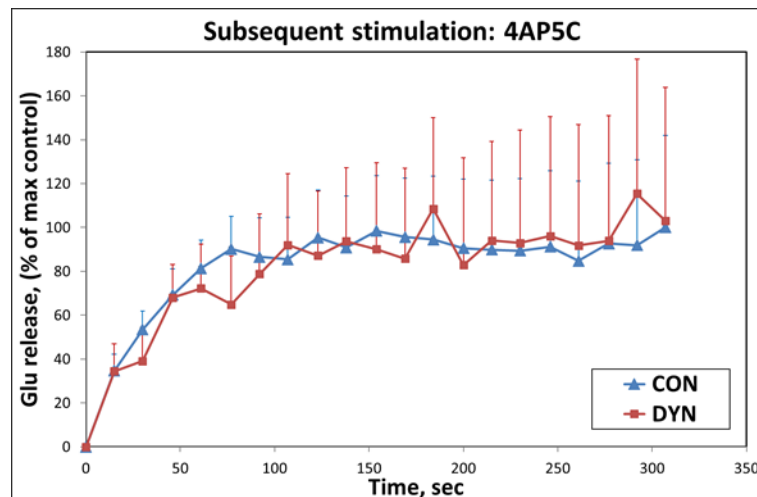


Figure 4.4. The effect that 160 μM DYN treatment before pre-stimulation exerts on the subsequent 4AP5C evoked glutamate release. Glutamate release has been expressed as percentage of maximum control. Error bars indicate S.E.M. The results were repeated with 3 individual experiments with numerous independent measurements (i.e. $n \geq 3$), $p < 0.05$ was considered significant). The difference was not significant.

Compared to the non-drug treated control, there was no significant decrease in 4AP5C evoked Glu release observed when synaptosomes were pretreated with 160 μM DYN prior to the pre-stimulation with HK5C. This suggests that the

inhibition of dynamins does not perturb the release of the 4AP5C-sensitive pool
which is the RRP.

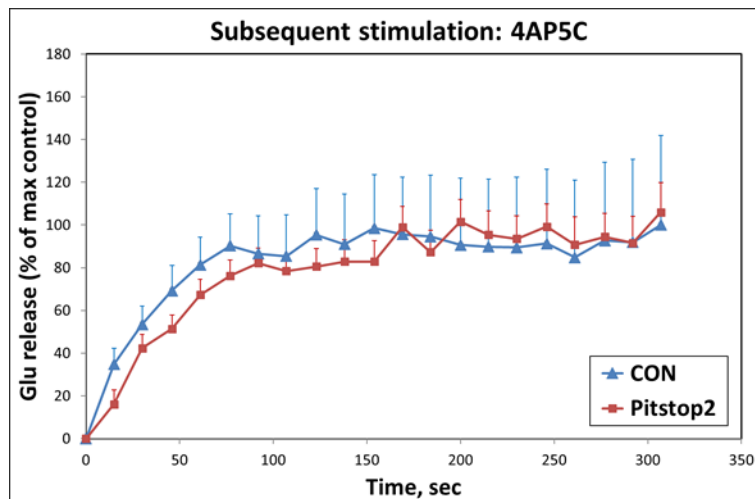


Figure 4.5. The effect that 15 μM pitstop2TM treatment before pre-stimulation exerts on the subsequent 4AP5C evoked glutamate release. Glutamate release has been expressed as percentage of maximum control. Error bars indicate S.E.M. The results were repeated with 3 individual experiments with numerous independent measurements. The difference was NS. $p < 0.05$ was considered significant.

Following blockade of clathrin-dependent processes with pitstop2TM and the succeeding HK5C evoked exocytosis and subsequent recycling, and reloading of SVs, there was no significant difference in the 4AP5C evoked Glu release compared to the non-drug treated control. This suggests that the inhibition of clathrin does not perturb the release of the 4AP5C-sensitive pool which is the RRP.

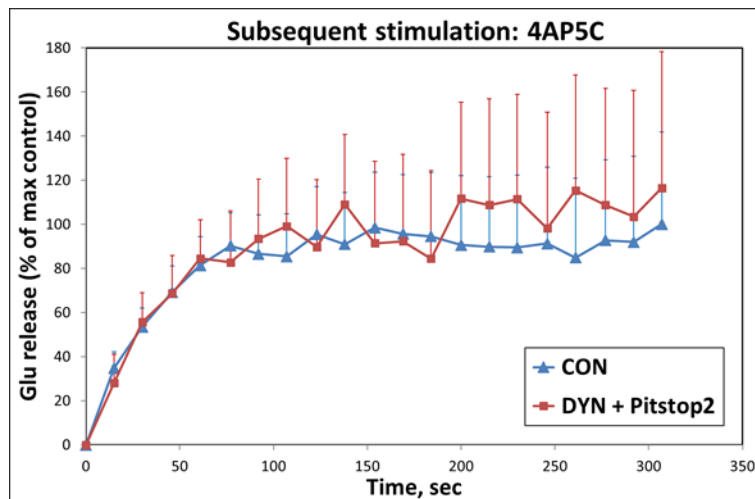


Figure 4.6. The effect that 160 μM DYN plus 15 μM pitstop2TM treatment before pre-stimulation exerts on the subsequent 4AP5C evoked glutamate release. Glutamate release has been expressed as percentage of maximum control. Error bars indicate S.E.M. The results were repeated with 3 individual experiments with numerous independent measurements (i.e. $n \geq 3$). The difference was NS. ($p < 0.05$ was considered significant).

Pre-treatment of synaptosomes with DYN and pitstop2TM perturbs all dynamin and clathrin-dependent processes, but subsequent HK5C pre-stimulation, and further (after recovery) 4AP5C evoked Glu release indicated that even this double drug treatment did not perturb the amount of release induced by 4AP5C relative to the non-drug treated control. Clearly, the 4AP5C sensitive pool (the RRP) can still occur following blockade of these two major endocytotic proteins.

4.3 Discussion

4.3.1 Dynamin dependent and clathrin dependent recycling

The results indicate that some SVs that normally recycle after the pre-stimulation (and get loaded by FM2-10 dye) can be prevented from re-releasing if prior to the initial pre-stimulation dynamins are inhibited. Similarly, some SVs that recycle after the pre-stimulation are unavailable for re-release if clathrin is inhibited. These results indicate that there are dynamin-dependent recycling processes for some SVs as well as some clathrin dependent processes for some SVs. As there are two processes that require both clathrin and dynamin (CDE and ultra-fast endocytosis) and a third that may only require dynamin (bulk endocytosis) it is interesting that the amount of release induced by ION5C (Figure 4.2 and Figure 4.3) is similar whether clathrin or dynamins are inhibited before the pre-stimulation step. This may indicate that the pools that are perturbed are those which depend upon both proteins and that bulk endocytosis may not be participating during the stimulation induced by HK5C. Another possibility is that the bulk endocytosis also has a clathrin requirement. Finally, the role of dynamin in bulk endocytosis (Clayton *et al.*, 2010) is actually very controversial and experiments with dynamin knock out mice suggest that this pathway might not actually require dynamin (Wu *et al.*, 2014). Despite these problems the results clearly indicate that there appears to be some SVs that can recycle in the absence of functional dynamins. This fits in with work with single (Lou *et al.*, 2008) and double knockout mice (Raimondi *et al.*, 2011) for dynamins 1 and 3 where it is apparent that some SVs can recycle and rerelease even in the absence of these dynamins (with the caveat that the tiny amount of dynamin 2 present does not contribute to this recycling). The results also

highlight that DYN and pitstop2TM are active and working on their expected substrates to produce a particular phenotype.

4.3.2 RRP SVs recycle independent of clathrin and dynamin

The nature of the SV pool that was available for release, even after inhibiting dynamin and clathrin prior to the pre-stimulation step, was examined by exclusively stimulating the RRP SVs with 4AP5C. It would appear that the pool of SVs that was available for release was the RRP as the drug treatments did not perturb 4AP5C evoked Glu release (Figure 4.4, 4.5 and 4.6). As during the pre-stimulation with HK5C the RRP would have recycled by a KR mechanism that was independent of dynamin – it is dependent on myosin-II activity – it would seem that the simplest explanation is that the pool of SVs released by 4AP5C (or by ION5C) is these RRP SVs that had recycled by a KR mechanism.

Before these experiments, we knew that the RRP SVs could undergo exocytosis by a KR mechanism. However, we had not checked whether such SVs would actually be available for a second round of release, but results suggest that such vesicles are available. Thus, it would seem that the RRP SVs can recycle and re-release independently of clathrin and dynamin. Data with the FM2-10 dye release would suggest that such SVs probably undergo KR during the first round of HK5C stimulation (the pre-stimulation when dye is taken up) and then undergo KR again during the second round but this is dependent upon the stimulus (e.g. ION5C and HK5C would induce RRP to undergo KR whilst with 4AP5C some of the RRP undergoes KR and some undergoes FF).

Obviously, if an experiment was designed to do three stimulations one might find that the third round (following the same initial pre-treatment) still induce the RRP to fully release (if you use HK5C, second stimulus and ION5C or HK5C for

third stimulus) whilst clearly the use of 4AP5C in the second stimulus may only allow a sub-population of SVs to be released during the third stimulation period: this would be those SVs that underwent KR in the second round whilst those that underwent FF would be blocked.

4.3.3 RP is not available for release if the action of dynamins and clathrin is inhibited prior to prestimulation with HK5C

If the RRP SVs are those that can recycle independently of dynamins and clathrin following the inhibition of these proteins prior to the pre-stimulation with HK5C, then the pool of SVs that is no longer able to release is the RP. This fits in perfectly with the ideas presented throughout this thesis. It was always expected that those SVs that undergo FF would recycle by CME or via dynamin-dependent bulk endocytosis. Thus, the RP SVs would no longer recycle during the protocol employed herein and so they would be unavailable for release during the second stimulation. In fact, this result may help us justify the claim that the KR mode can be switched to FF by various conditions (as outlined throughout this thesis). There was always the possibility that when more FM210 dye released was induced by various drug treatments what actually was happening was that the fusion pore opening time was extended (or closure time slowed down) so that the dye eventually departed and was released. This would still indicate that KR existed but would not indicate a switch to FF. Furthermore, you could go further and say that the RP that appeared to be undergoing FF actually just had a longer pore opening time. However, if this is the case it would be hard to explain why the RP SVs did not recycle following inhibition of clathrin and/or dynamin as all forms of KR (including extended opening of the pores) is supposed to be clathrin independent.

Furthermore, the preliminary results obtained with 3 μ M PAO (refer to chapter 6) by Ashton and colleagues, not published and not reported herein; suggest that whilst KR is not perturbed by reducing the levels of PIP₂, FF is totally inhibited. This result - which is currently being reinvestigated as 3 μ M PAO interferes with synaptosomal bioenergetics (as stated in chapter 7 and appendix 1)- indicates that for the vesicular membrane to fully insert into the plasma membrane during FF requires intact levels of PIP₂ whereas the production of the fusion pore and KR does not have such a requirement. This can be explained by the fact that many proteins are regulated by binding to the PIP₂ and may play a role in exocytosis/endocytosis (e.g. synaptojanin; Voronov *et al.*, 2008). It is much more difficult to understand why the extension of the fusion pore opening time would require intact levels of PIP₂ whilst its actual initial production does not.

4.3.4 RRP SVs can recycle independently of the RP

These results also suggest that the RRP SVs can recycle independently of the RP and be available for release again. This was a major conclusion of a paper by Ashton and Ushkaryov (2005) that showed that the synaptosomes could keep recycling and re-releasing the RRP of SVs independently of the RP. Indeed, it was suggested in this paper that one possibility for such RRP SVs recycling and re-releasing was because they were undergoing KR. We have now provided more evidence for this (Ashton and Ushkaryov, 2005).

4.3.5 KR is distinct to ultrafast endocytosis

Even though, this is a small chapter the results obtained are very important for the whole debate about KR. Recently, ultra-fast endocytosis has been described which apparently allows SVs to re-enter the terminals within 30 msec (Wantanabe *et al.*, 2013, 2014). These authors believe that such a mode means

that there is absolutely no need for a KR mode because this has been suggested to recycle in a slower period of <500 msec. KR was originally argued for on the basis that it allowed SVs to recycle much more quickly than CDE or bulk endocytosis and that this mechanism would help maintain synaptic transmission during periods of prolonged stimulation where these other two mechanisms might not be able to keep up with the demand for SV recycling. Clearly, those studying ultra-fast endocytosis believe it can allow this fast recycling and so one does need to evoke the idea of KR. This is actually disingenuous to the KR mode because whilst vesicular membranes recycle in about 30 msec by the ultrafast mechanism, such vesicular membranes fuse to form an endosome and subsequently SVs are pinched off from there, and then they can load up with neurotransmitter and be able to contribute to synaptic transmission again. However, this seems to take at least 5 sec which is slower than how quickly a KR SV may be able to release neurotransmitter again (approximately 2 sec: rate limiting step is reloading with neurotransmitter).

The most important result from this chapter is that the KR mechanism that we are studying is not the same as the ultra-fast endocytosis that has been recently described. Ultrafast endocytosis has both a dynamin dependence (Watanabe *et al.*, 2013) and a clathrin dependence (Watanabe *et al.*, 2014). However, the mode we are studying does not require clathrin and the fusion pore can be closed by a non-dynamin-dependent mechanism (depending upon the stimulus employed).

Chapter 5

Investigating the Role of Protein Kinase A

5.1 Introduction

cAMP plays the role of a critical secondary messenger involved in synaptic transmission. Binding of the appropriate ligand to the G-protein-coupled receptor, located on the cell surface, results in the intracellular production of cAMP through adenylyl cyclase associated with that particular receptor. This then allows cAMP to diffuse through the cytoplasm and bind to its targets, the most studied one being PKA. Thus, PKA pathway serves an important intracellular signalling pathways (Yao and Sakaba, 2010). The main aim of this chapter was to investigate if this pathway could regulate synaptic vesicular exocytosis, various activators and inhibitors were employed.

Much research has been carried out on the role of both cAMP and PKA on neurotransmitter release (Leenders and Sheng, 2005). Some of the studies have found a direct link between changes in cAMP levels and activation/deactivation of PKA whilst others have investigated PKA-independent processes requiring changes in cAMP (e.g. exchange proteins directly activated by cAMP, (EPAC)- see chapter 1 for more information on EPAC). In some studies, the target for the PKA that might regulate release is known. cAMP has been shown to regulate release (e.g. Santafe *et al.*, 2009). It has been suggested that cAMP can regulate the Ca^{2+} sensitivity of certain SVs (Yao and Sakaba, 2010). Other groups have also shown that cAMP and PKA can regulate the population of silent synapses (Crawford and Steven Mennerick, 2012). This latter result may be related to a novel form of synaptic plasticity that has been described, in which release sites which are switched off during low-frequency depression can be reactivated. This reactivation involves PKA induced phosphorylation of synapsin I (Doussau *et al.*, 2010). Indeed, PKA-mediated synapsin I phosphorylation is a central modulator of Ca^{2+} -dependent

synaptic activity (Menegon *et al.*, 2006). EPAC has been shown to be a second target for cAMP and activation can enhance neurotransmitter release (Gekel and Neher, 2008). Finally, cAMP has been shown to regulate the fusion pore of vesicles undergoing exocytosis from rat lactotrophs (Calego *et al.*, 2014).

5.2 Results

{(9S,10S,12R)-2,3,9,10,11,12-Hexahydro-10-hydroxy-9-methyl-1oxo-9,12-epoxy-1H-diindolo[1,2,3-fg:3',2',1'-kl]pyrrolo[3,4-][1,6]benzodiazocine-10-carboxylic acid hexyl ester} (i.e. KT 5720) is a cell permeable inhibitor of cAMP dependent protein kinase A (E.C.2.7.11.11). It blocks PKA signalling through competitive inhibition at the active site on target protein (Huang *et al.*, 2000). PKA is an enzyme which performs a variety of functions in eukaryotic cells by adding phosphates to proteins to “target sites” (Huang *et al.*, 2000). For this study, the effect of 2 μ M KT 5720 (see Huang *et al.*, 2000) on synaptic vesicular exocytosis was investigated through its action on the glutamate and FM 2-10 dye release assays (Figure 5.1 and 5.2).

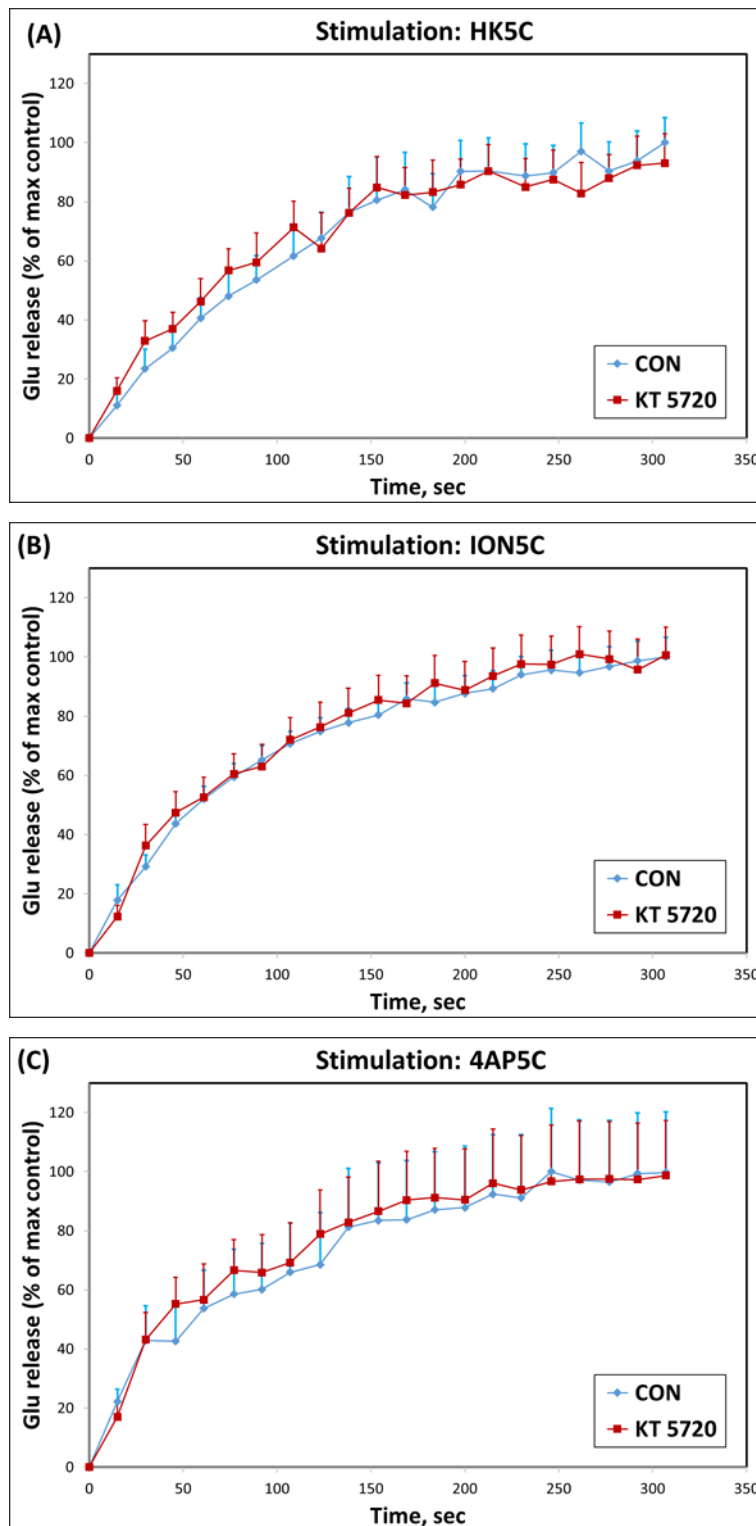


Figure 5.1. The effect of 2 μ M KT 5720 on glutamate release. No significant difference in the glutamate release is observed between control and KT 5720-treated terminals for any of the three stimuli, (A) HK5C, (B) ION5C and (C) 4AP5C are employed. The data points represent the glutamate released and are expressed as a percentage of the maximum control release. The error bars represent S.E.M. These are the results of 3 independent experiments (i.e. performed on different days) with numerous independent sample replicates (i.e.

prepared on same day) per experiment and a $p < 0.05$ was considered significant.

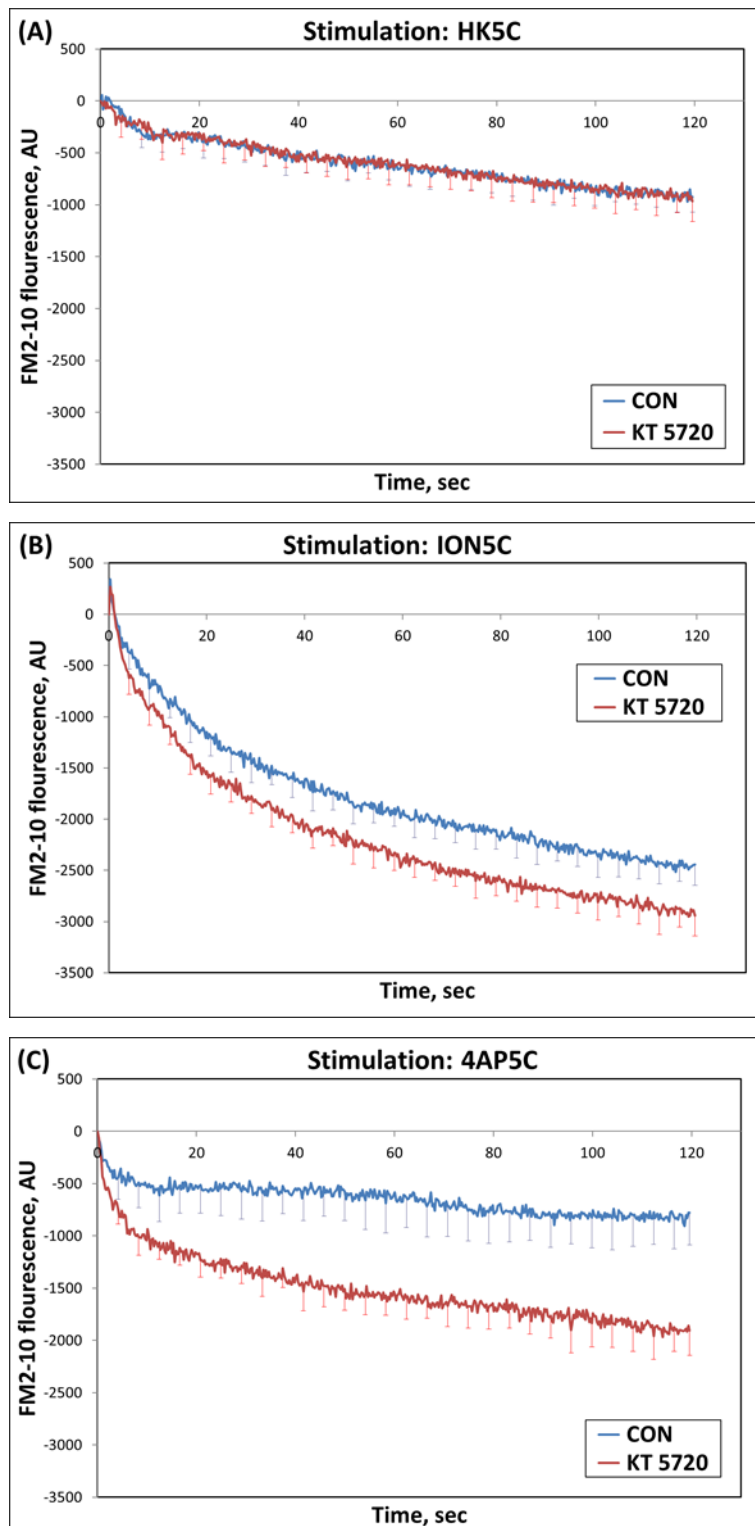


Figure 5.2. The effect of 2 μM KT 5720 on FM 2-10 dye release. The error bars represent S.E.M.. These are the results of 3 independent experiments (i.e. performed on different days) with numerous independent sample replicates (i.e. prepared on same day) per experiment and a $p < 0.05$ was considered significant.

No significant change in FM2-10 dye release is observed with HK5C release with or without KT 5720 treatment. However, when ION5C and 4AP5C are employed as stimuli a significant increase in the FM2-10 dye release is observed in the KT 5720 treated terminals: the p value was less than 0.0001 for both stimuli. The data points represent the FM dye released and are expressed as a percentage of maximum control release.

Clearly, inhibition of PKA causes the SVs to undergo more FF for ION5C and 4AP5C.

5,6-dichloro-1-β-D-ribofuranosylbenzimidazole-3',5'-cyclicmonophosphorothioate (i.e cBIMPS) is a selective, cAMP-analogue protein kinase activator. For this study, the effect of 50 μM cBIMPS (Kidokoro *et. al.*, 2004) on synaptic vesicular exocytosis was investigated through its action on glutamate and FM 2-10 release from synaptosomes (Figure 5.3 and 5.4).

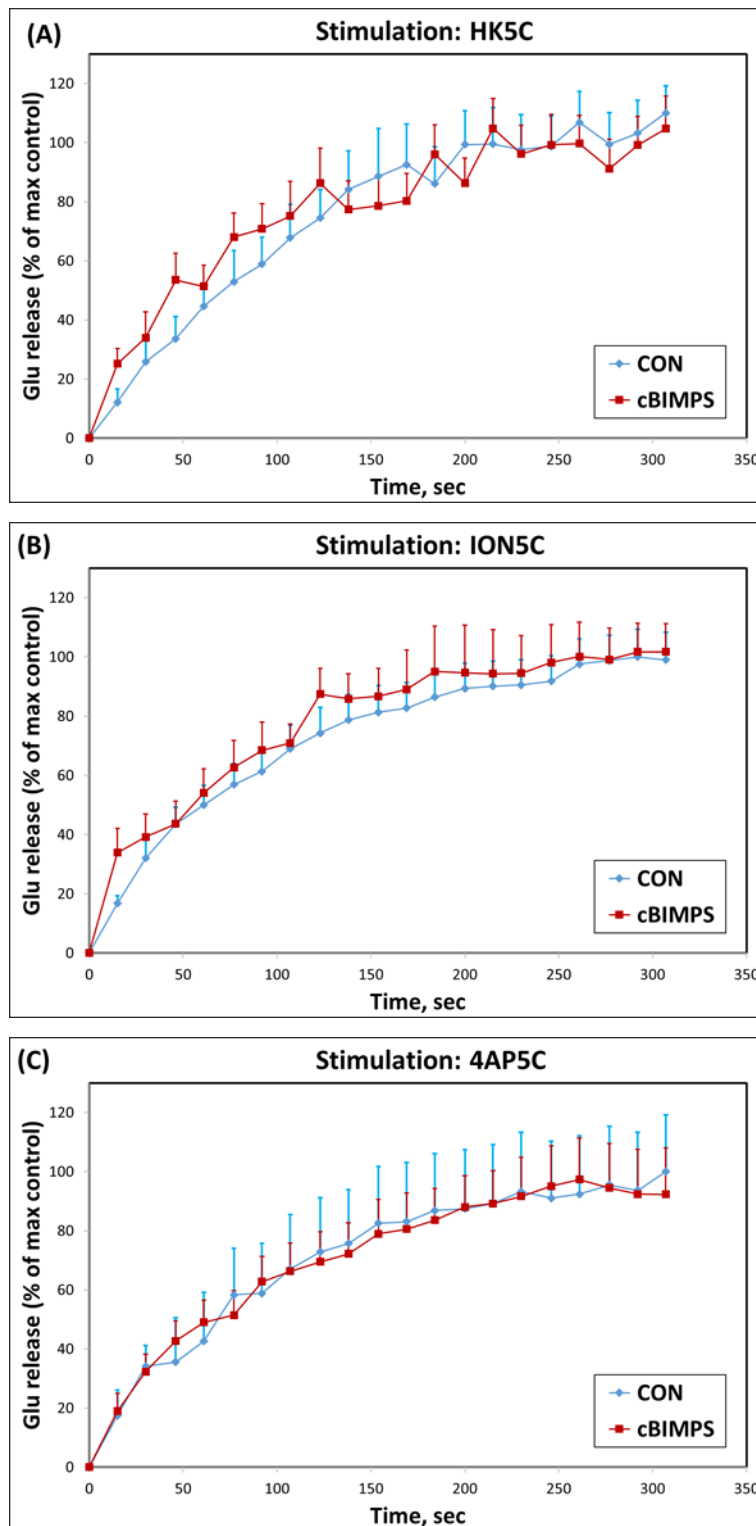


Figure 5.3. The effect of 50 μ M cBIMPS on glutamate release. cBIMPS produces no significant difference in the glutamate release for any of the three stimuli employed: HK5C, ION5C and 4AP5C. The data points represent the glutamate released and are expressed as a percentage of maximum control release. The error bars represent S.E.M. These are the results of 3 independent experiments (i.e performed on different days) with numerous independent

sample replicates (i.e. prepared on same day) per experiment and a $p < 0.05$ was considered significant.

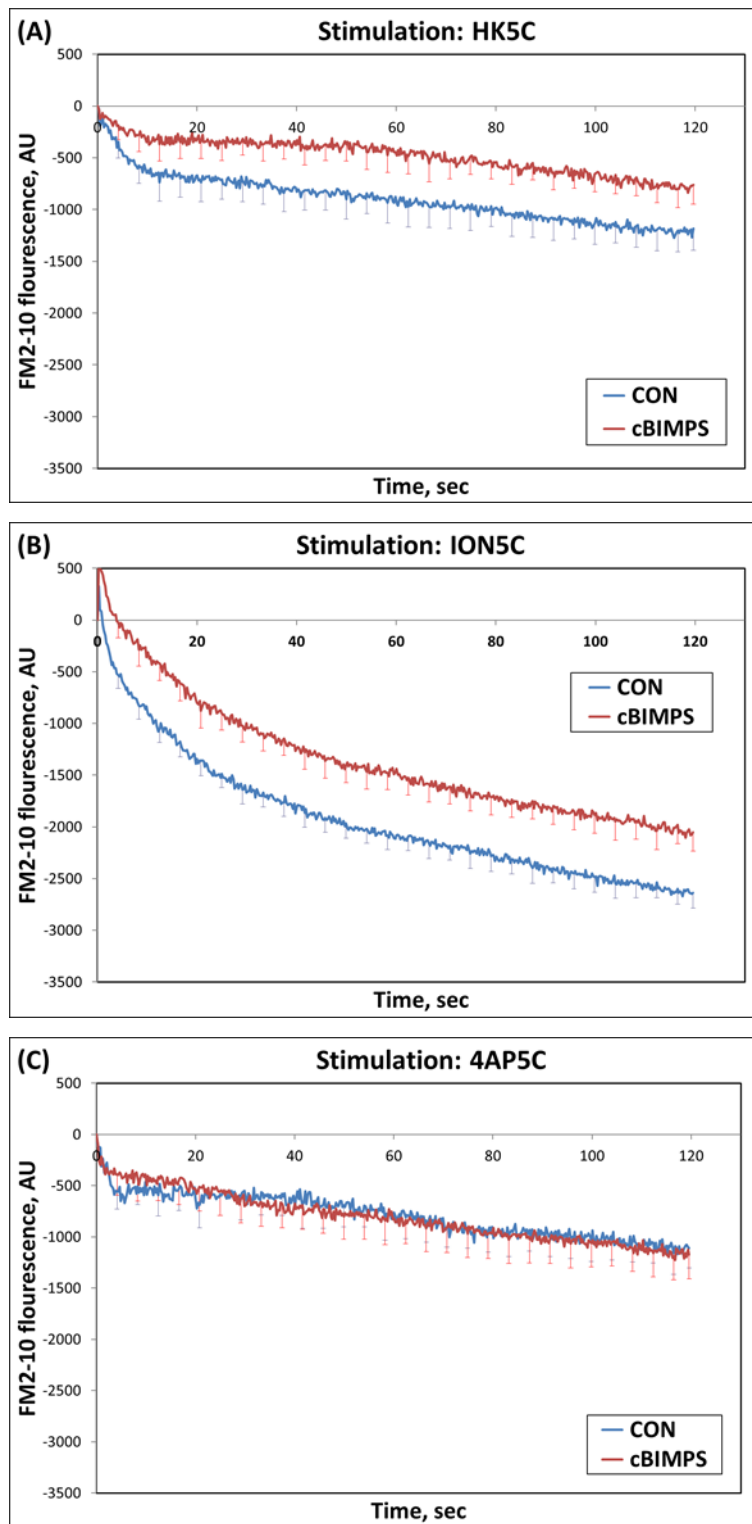


Figure 5.4. The effect of 50 μM cBIMPS on FM 2-10 dye. No significant change in FM2-10 dye release is observed for 4AP5C stimulation following cBIMPS treatment. However, when ION5C and HK5C are employed as stimuli, a significant decrease in the FM2-10 dye release is observed after such drug treatment: p value was less than 0.0001 for both. The data points represent the FM dye released and are expressed as a percentage of maximum control. The error bars represent S.E.M. These are the results of 3 independent experiments

(i.e performed on different days) with numerous independent sample replicates (i.e. prepared on same day) per experiment and a $p < 0.05$ was considered significant.

These results indicate that activation of PKA causes most of the SVs to undergo KR with HK5C and ION5C and that this action is specific for the RP since 4AP5C does not release the RP. In order to show that the cBIMPS action is specific and does activate PKA, we tested whether cBIMPs exerted any action following blockade of PKA with KT 5720 (Figure 5.5, 5.6 and 5.7).

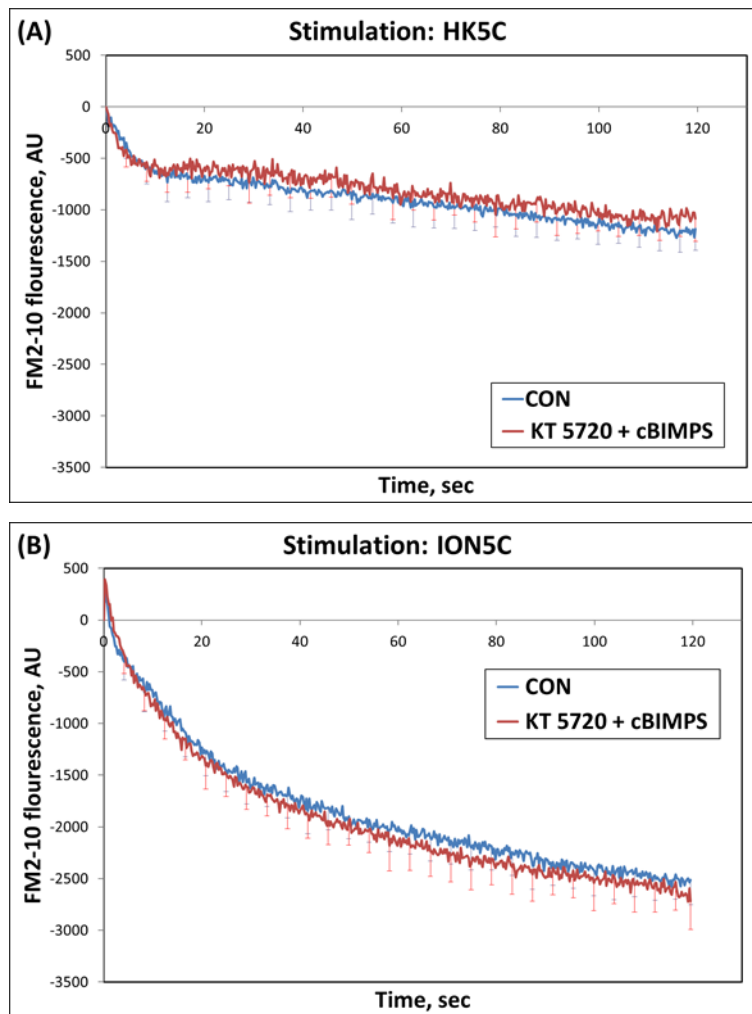


Figure 5.5. The effect of 2 μ M KT 5720 and 50 μ M cBIMPS on FM 2-10 dye release. Pretreatment with KT 5720 followed by cBIMPS produces no significant change in the release of FM dye induced by HK5C or ION5C compared to the non-drug treated control. The data points represent the FM dye released and are expressed as a percentage of maximum control. The error bars represent S.E.M.. These are the results of 3 independent experiments (i.e performed on different days) with numerous independent sample replicates (i.e. prepared on same day) per experiment and a $p < 0.05$ was considered significant.

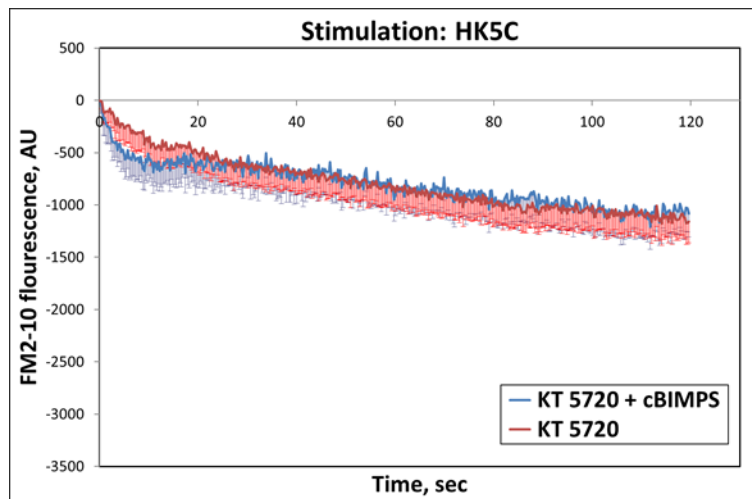


Figure 5.6. Comparison of the effect of 2 μM KT 5720 plus 50 μM cBIMPS vs 2 μM KT 5720 on HK5C evoked FM 2-10 dye release. There is no change in FM 2-10 dye release between the conditions: $p=0.4$ These are the results of 3 independent experiments (i.e. performed on different days) with numerous independent sample replicates (i.e. prepared on same day) per experiment and a $p<0.05$ was considered significant.

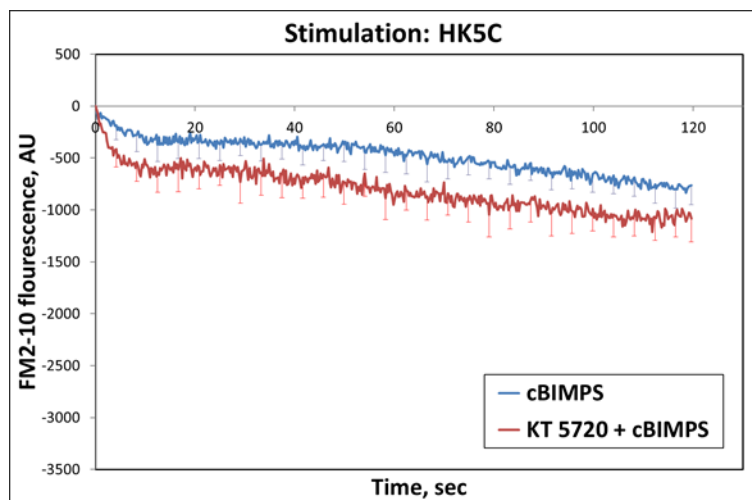


Figure 5.7. Comparison of the effect of 2 μM KT 5720 and 50 μM cBIMPS vs 50 μM cBIMPS on HK5C evoked FM 2-10 dye release. The FM dye release for the double treatment of 2 μM KT 5720 and 50 μM cBIMPS was significantly greater than the FM dye release for 50 μM cBIMPS alone. The error bars represent S.E.M.. The p value obtained was < 0.01 . These are the results of 3 independent experiments (i.e performed on different days) with numerous independent sample replicates (i.e. prepared on same day) per experiment and a $p<0.05$ was considered significant.

9-Cyclopentyladenine mesylate; or mononmethanesulphonate i.e. 9-CP-Ade is a cell permeable and non-competitive adenylate cyclase (AC) inhibitor that targets the P site domain (Johnson *et. al.*, 1997).

For this study the effect of 100 μ M 9-Cp-Ade (Fresco *et al*, 2004) on synaptic vesicular exocytosis was investigated through its action on glutamate and FM 2-10 dye release assay (Figure 5.7 and Figure 5.8).

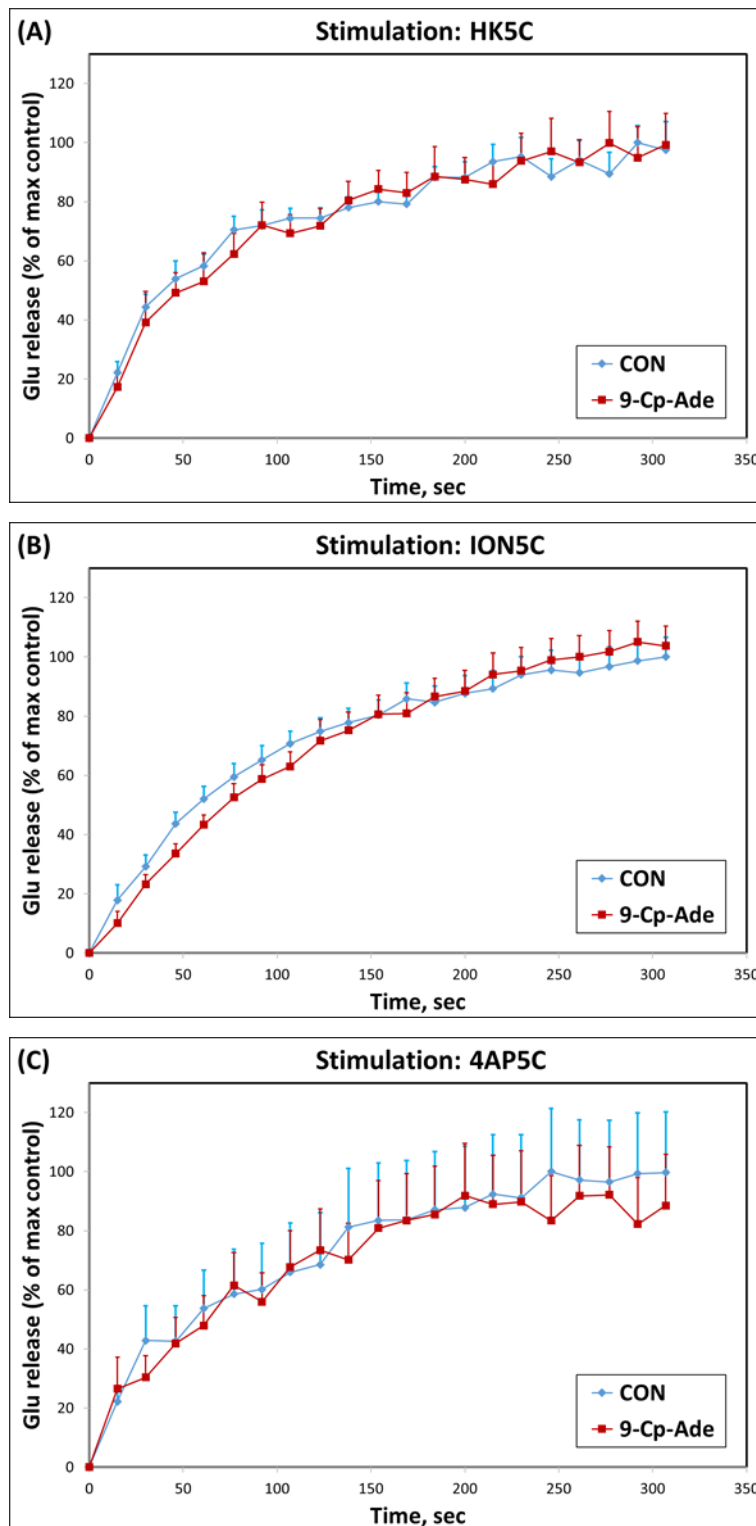


Figure 5.8. The effect of 100 μ M 9-Cp-Ade on glutamate release. No significant difference in the glutamate release is observed when comparing control to 9Cp-Ade treated terminals for any of the three stimuli are employed. The data points represent the glutamate released and are expressed as a percentage of maximum control release. The error bars represent S.E.M. These are the results of 3 independent experiments (i.e performed on different days) with

numerous independent sample replicates (i.e. prepared on same day) per experiment and a $p < 0.05$ was considered significant.

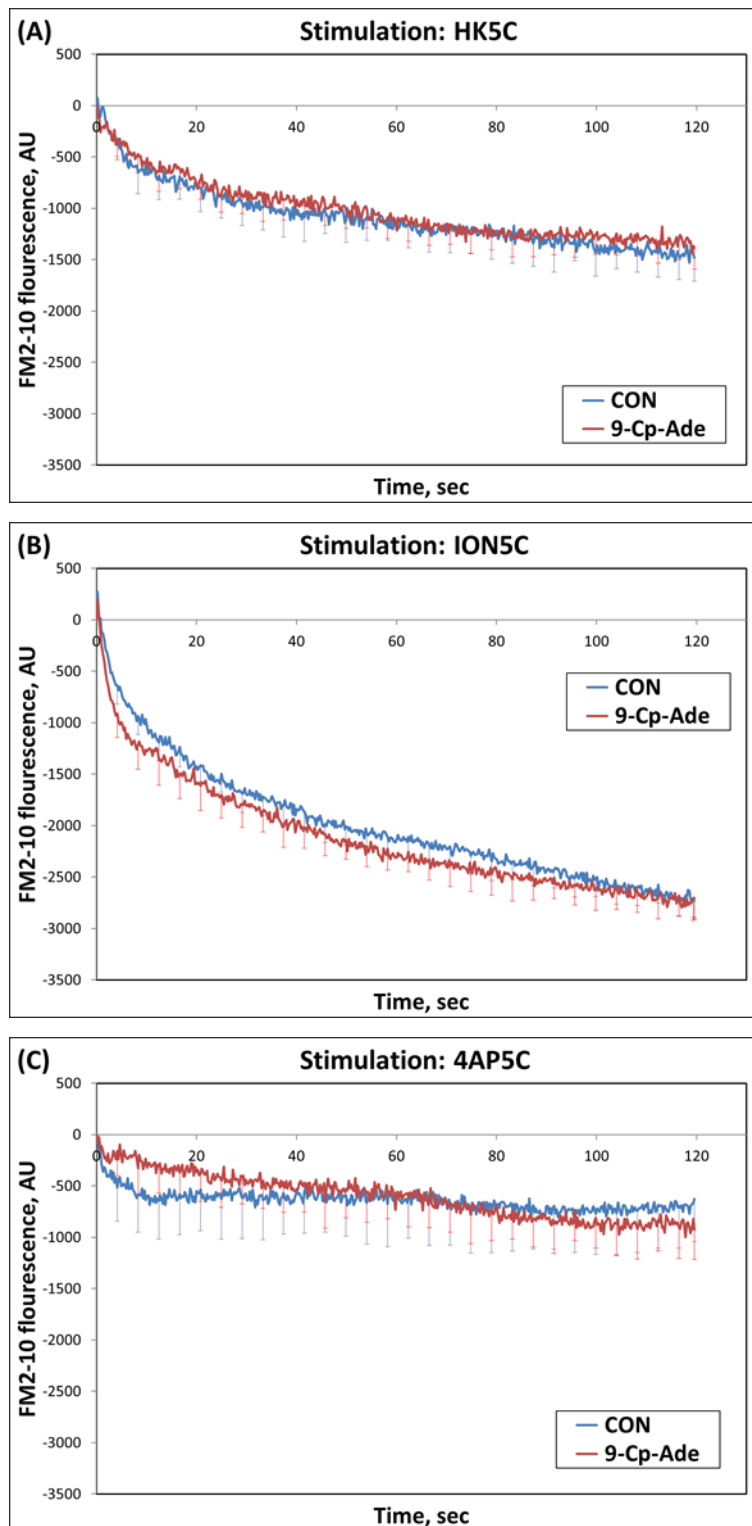


Figure 5.9 The effect of 100 μ M 9-Cp-Ade on FM 2-10 dye release. 9-Cp-Ade had no significant effect on the FM dye release evoked by HK5C, ION5C and 4AP5C. The data points represent the dye released and are expressed as a percentage of maximum control release. The error bars represent S.E.M.. These are the results of 3 independent experiments (i.e performed on different days) with numerous independent sample replicates (i.e. prepared on same day) per experiment and a $p < 0.05$ was considered significant.

[3R-(3 α ,4 α β ,5 β ,6 β ,6 α α ,10 α ,10 α β ,10 β α)]-5-(Acetyloxy)-3ethenyldodecahydro-6,10,10b-trihydroxy-3,4a,7,7,10a-pentamethyl-1Hnaphtho[2,1-b]pyran-1-one (i.e. Forskolin) is a cell permeable adenylate cyclase activator AC activator. The effect of 100 μ M forskolin (Herrero and Sanchez-Prieto, 1996) on the switch in the mode of exocytosis was investigated by measuring glutamate and FM 2-10 dye release Figure 5.10 and Figure. 5.12. Similarly, a 100 μ M 1,9-dideoxyforskolin an inactive homologue of forskolin (Herrero and Sanchez Prieto, 1996) was tested as a control to ensure forskolin is acting specifically on adenylate cyclase (Figure 5.11).

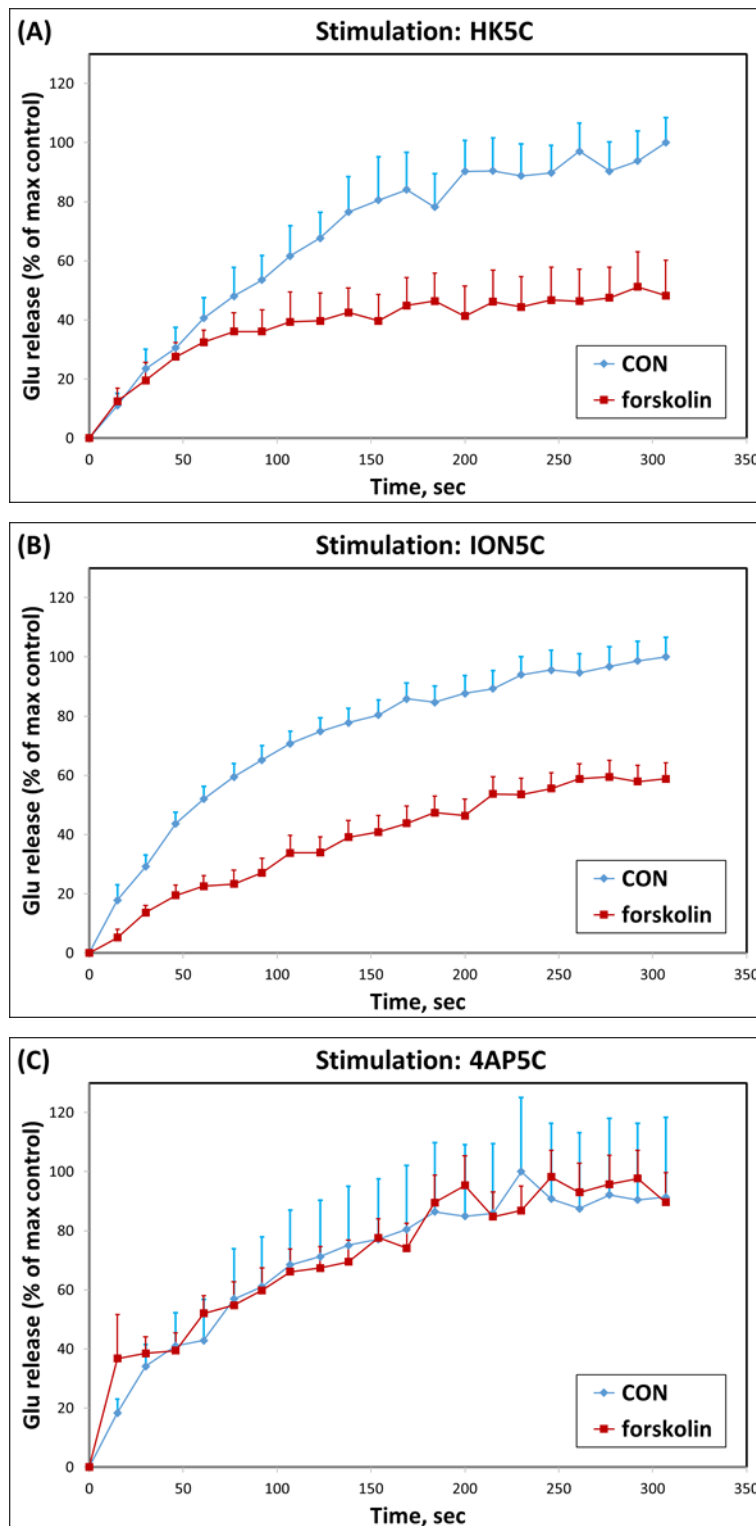


Figure 5.10. The effect of 100 μ M forskolin on glutamate release. No significant difference in the 4AP5C evoked glutamate release was observed between control and forskolin treated terminals. However, when HK5C and ION5C were employed as stimuli the glutamate release for 100 μ M forskolin treated samples was significantly reduced when compared to control: the p value for HK5C was < 0.0002 while the p value obtained for ION5C was < 0.0001 . The data points represent the glutamate released and are expressed as a percentage of

maximum control release. The error bars represent S.E.M.. These are the results of 3 independent experiments (i.e. performed on different days) with numerous independent sample replicates (i.e. prepared on same day) per experiment and a $p < 0.05$ was considered significant.

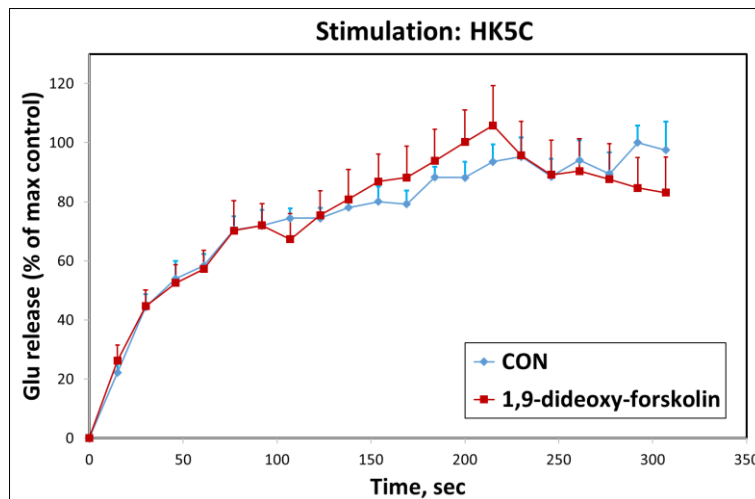


Figure 5.11 The effect of 100 μ M 1,9-dideoxy-forskolin on HK5C evoked glutamate release. 1,9-dideoxy-forskolin is an inactive homologue of forskolin. There was no significant difference in the HK5C evoked glutamate release between this drug treatment and the non-drug treated control. The data points represent the glutamate released and are expressed as a percentage of maximum control release. The error bars represent +S.E.M.. These are the results of 3 independent experiments (i.e. performed on different days) with numerous independent sample replicates (i.e. prepared on same day) per experiment and a $p < 0.05$ was considered significant.

This result emphasizes that the effect of forskolin on HK5C evoked Glu release is specific and is likely to involve changes in cAMP levels (see below for further evidence of this). Although, the forskolin inhibits the release of the RP evoked by ION5C and HK5C it does not block the release of the RRP as shown by the lack of effect of this drug on 4AP5C release. Thus, we can still investigate whether forskolin could possibly have an effect on the mode of exocytosis of the RRP by studying FM dye release induced by 4AP5C.

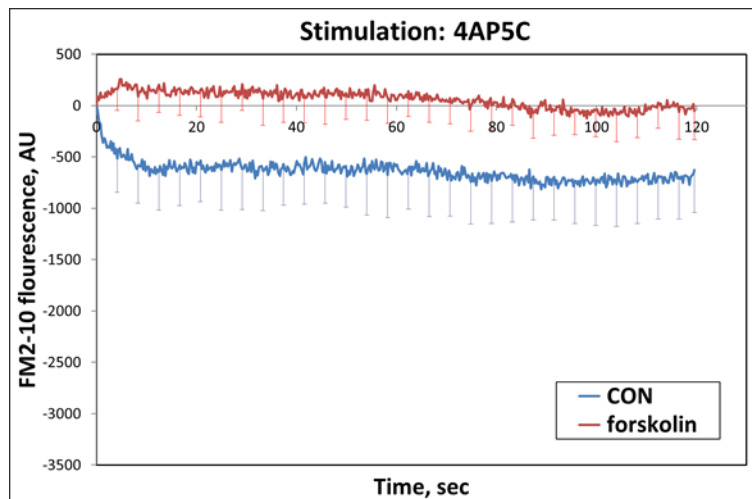


Figure 5.12. The effect of 100 μM forskolin on 4AP5C evoked FM 2-10 dye release. On employing 4AP5C as stimulus, 100 μM forskolin significantly reduces the amount of dye released in comparison to control: the p value was < 0.0001 . The data points represent the FM dye released and are expressed as a percentage of maximum control release. The error bars represent S.E.M.. These are the results of 3 independent experiments (i.e. performed on different days) with numerous independent sample replicates (i.e. prepared on same day) per experiment and a $p < 0.05$ was considered significant.

9-Cp-Ade inhibits activation of adenylate cyclase but has no effect on SV exocytosis including their mode. Thus, we can employ this drug to prove that the action of forskolin on 4AP5C induced SV exocytosis is truly due to activation of adenylate cyclase. The protocol is shown in the time line in Figure 5.13 and Figure 5.14.

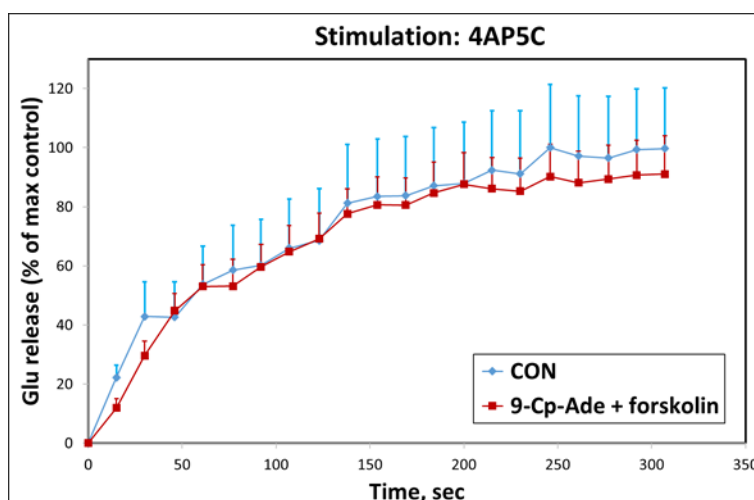


Figure 5.13. The effect of 100 μ M 9-Cp-Ade and 100 μ M forskolin on 4AP5C evoked glutamate release. There is no significant difference in the 4AP5C evoked glutamate release between this double treatment (100 μ M 9-Cp-Ade and 100 μ M forskolin) and non-drug treated control. The data points represent the glutamate released and are expressed as a percentage of maximum control release. The error bars represent S.E.M. These are the results of 3 independent experiments (i.e. performed on different days) with numerous independent sample replicates (i.e. prepared on same day) per experiment and a $p < 0.05$ was considered significant.

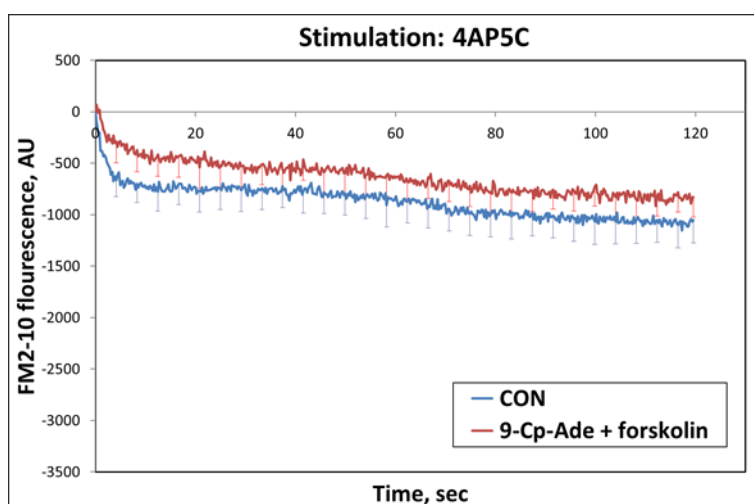


Figure 5.14. The effect of 100 μ M 9-Cp-Ade plus 100 μ M forskolin on 4AP5C evoked FM2-10 release. There is no significant difference in the 4AP5C evoked FM dye release for this double treatment (100 μ M 9-Cp-Ade and 100 μ M forskolin). The data points represent the FM dye released and are expressed as a percentage of maximum control release. The error bars represent S.E.M..

These are the results of 3 independent experiments (i.e performed on different days) with numerous independent sample replicates (i.e. prepared on same day) per experiment and a $p < 0.05$ was considered significant. A timeline for the experiment has been shown above.

The results in Figure 5.14 clearly show that the action of forskolin on switching a majority of the RRP SVs to KR depends upon activation of adenylate cyclase as it fails to act when the enzyme is inhibited by 9-Cp-Ade. This is emphasized even further by plotting the results for forskolin vs 9-Cp-Ade plus forskolin (Figure 5.15).

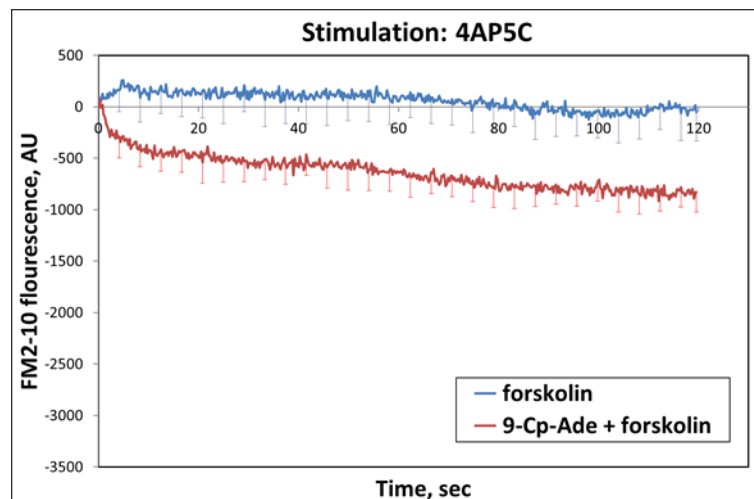


Figure 5.15. Comparing the effect of 100 μM 9-Cp-Ade plus 100 μM forskolin with 100 μM forskolin alone on 4AP5C evoked FM 2-10 dye release. The FM 2-10 dye released for forskolin is significantly lower than the FM 2-10 dye release for 100 μM 9-Cp-Ade and 100 μM forskolin treatment: the p value was < 0.0001 . The error bars represent S.E.M.. These are the results of 3 independent experiments (i.e performed on different days) with numerous independent sample replicates (i.e. prepared on same day) per experiment and a $p < 0.05$ was considered significant.

The results with forskolin are intriguing because increases in cAMP cytosolic levels appears to have two distinct effects: (i) blockade of the RP: (ii) an increase in the KR of the RRP.

Clearly, the activation of adenylate cyclase by forskolin increases the cAMP levels within the nerve terminals. However, whilst an increase in cAMP induces some SVs to switch from FF to KR when exocytosis is evoked by 4AP5C, activation of PKA (a downstream target for cAMP) fails to induce such a switch when 4AP5C is employed as the stimulus. This result suggests that the action of forskolin may be due to cAMP activating a distinct enzyme to PKA. An obvious alternative target is exchange protein directly activated by cAMP (EPAC) Grandoch *et al.*, 2010). To help prove that the action of forskolin is independent of PKA activation, synaptosomes were pre-treated with KT 5720 prior to the addition of forskolin (Figure 5.16).

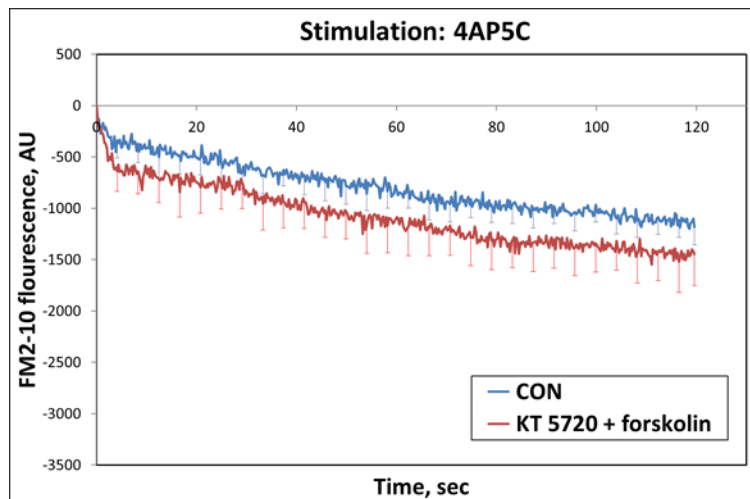


Figure 5.16. The effect of 2 μM KT 5720 followed by 100 μM forskolin on 4AP5C evoked FM2-10 dye release. The FM 2-10 dye released for 2 μM KT 5720 plus 100 μM forskolin is significantly larger than the FM 2-10 dye release for control non-treated terminals. The error bars represent S.E.M. These are the results of 3 independent experiments (i.e. performed on different days) with numerous independent sample replicates (i.e. prepared on same day) per experiment and a $p < 0.05$ was considered significant.

Forskolin does not override KT 5720 action completely as there is much more dye release than with forskolin alone. Similarly, KT 5720 does not completely override the action of forskolin as there is less dye release for the joint treatment than with KT 5720 alone. This may be due to two sub-populations of RRP SVs. This has been discussed in detail later on in the discussion.

Ashton's group have previously shown that 0.8 μM okadaic acid (OA) – by inhibiting protein phosphatase 2A – induces all RRP SVs to switch to FF. This includes those that were undergoing KR following 4AP5C stimulation or all RRP SVs that were originally undergoing KR following HK5C or ION5C stimulation.

Herein, we repeated the experiment for 4AP5C evoked release (Figure 5.17).

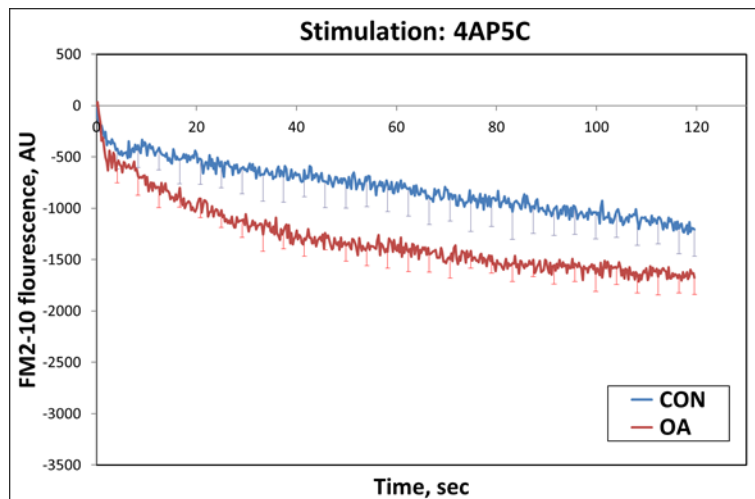


Figure 5.17. The effect of 0.8 μM OA on 4AP5C evoked FM2-10 dye release. The amount of 4AP5C evoked FM 2-10 dye release in terminals treated with 0.8 μM OA is significantly higher than release from controls: p value was < 0.0001 . The error bars represent S.E.M.. These are the results of 3 independent experiments (i.e performed on different days) with numerous independent sample replicates (i.e. prepared on same day) per experiment and a $p < 0.05$ was considered significant.

Thus, as predicted OA switches those SVs undergoing KR to a FF mode. We then tested to see whether OA would still switch these SVs to a FF mode following forskolin treatment (Figure. 5.18).

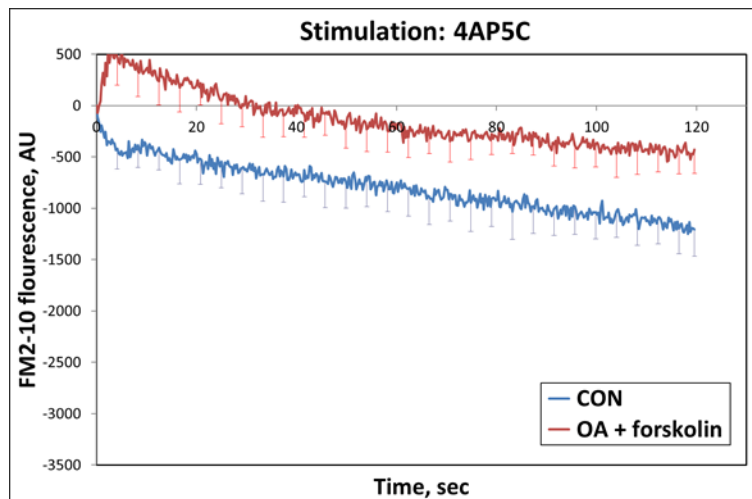


Figure 5.18. The effect of 0.8 μM OA plus 100 μM forskolin on 4AP5C evoked FM2-10 dye release. The amount of FM 2-10 dye released for 0.8 μM OA plus 100 μM forskolin is significantly less than the FM 2-10 dye released from control terminals: p value was < 0.0001 . The error bars represent S.E.M.. These are the results of 3 independent experiments (i.e performed on different days) with numerous independent sample replicates (i.e. prepared on same day) per experiment and a $p < 0.05$ was considered significant.

OA failed to prevent forskolin (via cAMP production) from switching RRP SVs to KR. To emphasize that OA failed to perturb forskolin's action on 4AP5C evoked FM dye exocytosis, forskolin was compared to forskolin plus OA on the same graph (Figure. 5.19).

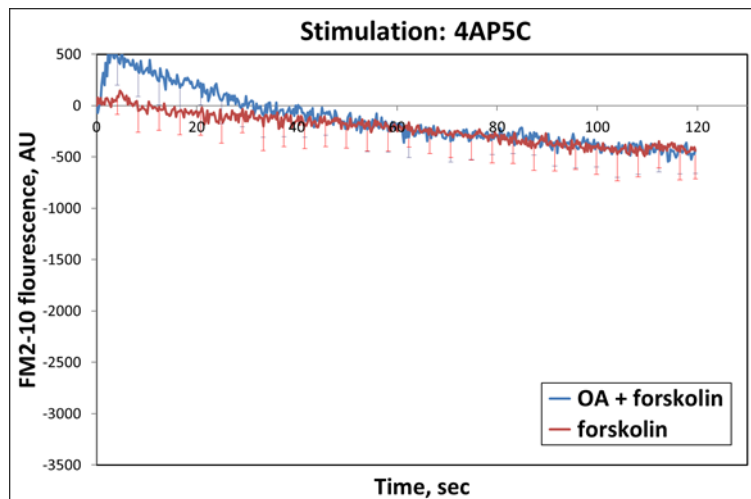


Figure 5.19. A comparison of the effect of 100 μ M forskolin with 100 μ M forskolin plus 0.8 μ M OA on 4AP5C evoked FM 2-10 dye release. There was no change in FM 2-10 dye release when the two drug treatments were compared. Error bars represent S.E.M.. These are the results of 3 independent experiments (i.e. performed on different days) with numerous independent sample replicates (i.e. prepared on same day) per experiment and a $p < 0.05$ was considered significant.

5.3 Discussion

This chapter demonstrates the effect of cAMP and PKA pathways on synaptic vesicular exocytosis and attempts to interpret these results and determine if one can learn more about the protein requirements for the fusion modes.

5.3.1 Effect of Inhibition of PKA using KT 5720

Clearly, inhibition of PKA causes the RRP SVs to undergo more FF for ION5C and 4AP5C (Figure 5.1 and 5.2). This observed effect was similar to the effect produced when the action of dynamins was blocked using 160 μ M DYN (refer to chapter 3). In particular, the specificity for a PKA requirement for ION5C and 4AP5C – but not HK5C – is similar to that specificity of these two stimuli for a dynamin requirement whilst HK5C evoked release for the RRP SVs is dynamin independent. Therefore, there might be an interaction between PKA and dynamins that can regulate the exocytotic mode. Previous data has indicated that dynamin can be phosphorylated on several sites (Graham, *et al.*, 2007) and that certain phosphorylation sites are induced by CDK5 (Cyclin-dependent kinase 5) (Tan *et al.*, 2003), GSK-3 (Glycogen synthase kinase 3) (Clayton *et al.*, 2010) and PKC (Powell, *et al.*, 2000). However, there has been no report of a direct phosphorylation of dynamin (herein, we are discussing dynamin I) by PKA. Thus, it is likely that if the phosphorylation of dynamin is regulated by PKA, this is because PKA regulates another protein that can control the phosphorylation of dynamin (e.g. another kinase or a phosphatase). Alternatively, PKA could control the protein-protein interactions that dynamin participate in (Hill *et al.*, 2001; Clayton *et al.*, 2009; Gonzalez-Jamett *et al.*, 2010) such that dynamin is not available to interact and close the fusion pore.

5.3.2 Effect of activation of PKA using cBIMPS

Results from Figure 5.3 and 5.4 indicate that activation of PKA causes most of the SVs to undergo KR with HK5C and ION5C and that this action is specific for the RP since PKA activation does not affect 4AP5C induced release of SVs (4AP5C only releases the RRP). This is shown by the fact that cBIMPS produces no effect on the sub population of RRP vesicles undergoing exocytosis by FF when 4AP5C is employed as stimuli which demonstrates that the action of cBIMPS by increasing PKA activity is specific for the RP. These observations are similar to the results obtained when the action of PP2B was blocked using 1 μ M cyclosporine A. This may indicate that a substrate phosphorylated by PKA is normally dephosphorylated by PP2B and that such a phosphorylated protein induces the KR mode of the RP of SVs. When comparing results with the inhibition of PKA with the results with activation of PKA it is intriguing that the effects are on distinct pools of SVs. This probably suggests that different proteins are involved in regulating the properties of the two pools. This was the conclusion with studies using cyclosporine A which has a specific action only for the RP of SVs. Thus, PKA induced phosphorylation of a target protein appears to prevent dynamin closing the fusion pore for RRP SVs whilst phosphorylation of a distinct target may allow closure of the fusion pore for RP SVs.

5.3.3 Effect of double treatment of cBIMPS and KT 5720

To ascertain if the effect produced by cBIMPS was due to the activation of PKA, synaptosomes were pre-treated with KT 5720 and then treated with cBIMPS. HK5C induced KT 5720 and cBIMPS FM dye release was similar to HK5C induced control FM dye release. The same result was observed when ION5C was employed as the stimuli as shown in Figure 5.5. There is no

difference in the amount of HK5C induced FM dye release for KT 5720 treatment alone vs the double treatment of cBIMPS plus KT 5720 (Figure 5.6). But when one compares HK5C induced FM dye release for KT 5720 plus cBIMPS with cBIMPS alone, the amount of FM dye for the latter is significantly lower than the former (Figure 5.7). This clearly indicates that the specific activation of PKA can lead to a switch in the mode of some RP SVs. Previously, we have also found such switching with cyclosporine A treatment, but just as here, we do not apparently switch all SVs to a KR mode. This could suggest that there is heterogeneity in the RP of SVs such there are sub-pools of these. However, some previous results from Ashton's laboratory indicate that one possible explanation is that not all RP can undergo SV fusion via KR when all the RRP are already undergoing KR. This may indicate that there is a limit to the number of SVs that can undergo this mode. Such ideas have come about because it would appear that under some conditions where one induces the RRP SVs to undergo FF, then one can then induce all the RPs to undergo KR. This is a complicated issue and will require much further experimentation to fully elucidate.

5.3.4 Effect of activation of adenylate cyclase using Forskolin

The effect of forskolin on HK5C, ION5C and 4AP5C evoked Glu release (Figure 5.10) was similar to the effect produced by blocking the action of CAMKII using 10 μ M KN-93 (Ashton, unpublished observations). This suggests that increased levels of cAMP can prevent the RP of SVs from exocytosing and that this may somehow be related to inhibition of CAMKII. Clearly, this may involve either direct or non-direct interactions between these two kinase pathways. This result does not involve distinctions in the mode of exocytosis but actually involves studying the properties of the different pools. Clearly,

much earlier work has been carried out on what controls release of the two releasable pools of SVs and this has implicated the phospho-protein synapsin I. It is believed that synapsin 1 interacts with both the SV (it is a SV peripheral membrane protein) and the actin cytoskeleton (Cesca *et al.*, 2010). Further, it has been suggested that various phosphorylations on distinct sites on synapsin 1 leads to dissociation of the synapsin I from both SVs (Menegon *et al.*, 2006) and from attachment to the cytoskeleton (Fornasiero *et al.*, 2012). Thus, it is thought that such phosphorylated regulation of SV association with the cytoskeleton and with other SVs can lead to the RP SV being either available or not available for release. Future work on this topic might help reveal the importance of such interactions and possibly reveal other interactions e.g. dynamins are known to interact with the actin cytoskeleton (Gu *et al.*, 2010) and this may have some role to play.

5.3.5 Effect of double treatment of 9-Cp-Ade and Forskolin

Statistically there is no difference between control and 100 μ M 9-Cp-Ade plus 100 μ M forskolin treated terminals (Figure 5.14), although the values for the latter show slightly lower amounts of FM dye release at all time points. This may be because 100 μ M 9-Cp-Ade might have failed to block all the adenylate cyclase in the 5 min treatment period before the addition of forskolin so there might have still been some action of forskolin on residual enzyme activity. However, this result does indicate that forskolin does act via activation of adenylate cyclase and, therefore, through an increase in cAMP levels within the terminal.

5.3.6 Effect of double treatment of KT 5720 and Forskolin

Careful comparison between the action of KT 5720 (Figure 5.2), forskolin (Figure 5.12) and KT 5720 plus forskolin (Figure 5.16) reveal that the latter condition produces a distinct effect from either of the drugs alone. Thus, forskolin does not override KT 5720 action completely as there is much more dye release than with forskolin alone. Similarly, KT 5720 does not completely override the action of forskolin (there is less dye release for the joint treatment than with KT 5720 alone). A possible explanation is that there are two sub-populations of RRP SVs (as has been suggested by many previously) (Neher, 2015). Those SVs that normally undergo KR following 4AP5C stimulation may switch to FF following blockade of PKA. However, those that normally undergo FF may switch to KR when there is an increase in cAMP. Thus, each sub-pool of RRP SVs may have distinct requirements. This is a very interesting possibility as previously Ashton's group had not really considered such diversity between RRP SVs and most results had not revealed this. However, it clearly warrants further research and it may well be that this finding may help to explain other observations which Ashton and his colleagues failed to completely understand. It is apparent that some of the action of forskolin is due to an increase in cAMP but not due to activation of PKA, and, therefore, another enzyme regulated by cAMP may be involved. This data had led to the hypothesis that EPAC enzymes (Grandoch *et al.*, 2010; Schmidt *et al.*, 2013) may be activated by the increase in cAMP induced by forskolin and that these may contribute to the action of forskolin on SV exocytosis. It should be noted that EPAC has been implicated in the regulation neurotransmitter release (Gekel and Neher, 2008) and synaptic plasticity in nerve terminals (Fernandes *et al.*, 2015). Recent experiments in the Ashton laboratory (whilst this thesis was being prepared) have tested whether EPAC plays a role by inhibiting this

with the inhibitor ESI09 (Tsalkova *et al.*, 2012). They have already established that the forskolin induced inhibition of the HK5C evoked release of the RP is actually due to activation of EPAC. This is because pretreatment of the EPAC inhibitor ES109 prior to addition of forskolin prevents the latter from blocking the release of the RP evoked by HK5C. Future experiments will investigate the role of EPAC activation on the modes of the RRP SVs. Clearly, this result may also indicate the heterogeneity in the RRP SVs.

5.3.7 Effect of double treatment of Forskolin and Okadaic acid

The final result in this chapter showed that whilst OA switched the KR SVs evoked by 4AP5C to FF, forskolin prevented this action. Furthermore, forskolin still induced the SVs that usually undergo FF when evoked by 4AP5C to now switch to KR. Thus, forskolin not only reversed the OA action but it also exerted its normal effect. As it is known that OA maintains the phosphorylation of Ser795 on dynamin I molecules, future experiments will ascertain whether this is prevented by forskolin. Clearly, the role of forskolin via PKA or EPAC on the phosphorylation of dynamin I needs to be studied in the future to help us elucidate the mechanisms involved. Indeed, similar experiments need to study the specific phosphorylation sites on myosin-II that might be changed following OA, forskolin or forskolin plus OA in view of the fact that OA normally switches the RRP of SVs induced by HK5C to FF from a KR mode.

5.4 Conclusion

These results clearly indicate that both PKA, and cAMP (via PKA and other enzymes) can regulate the mode of exocytosis. This adds to the knowledge we have already gathered concerning the Ca^{2+} dependent enzymes that also regulate this process. In order to complete this study and interpret all our data correctly, there is a need to measure the effect of the drugs employed in this chapter (KT 5720, cBIMPs, forskolin, 9-Cp-Ade plus various combinations) on stimulus evoked changes in $[\text{Ca}^{2+}]_i$. Such experiments using Fura-2 are already planned (Please refer thesis done by Dilip Bhuvra, 2014). Likewise, it will be necessary to check that the effect of some of the combinations of drugs employed herein are also tested on stimulated evoked Glu release. As most of the drugs employed do not perturb the relevant stimulated release, it is envisaged that the joint treatments will not perturb Glu release but we still have to check this. We have checked in another chapter that the drugs employed herein do not disturb the bioenergetic integrity of the synaptosomes (see chapter 6).

Chapter 6

Bioenergetics

6.1 Introduction

Synaptosomes are isolated nerve terminals or varicosities whose axonal attachments have been severed due to homogenization. Synaptosomes thus function as mini-cells in which mitochondria exist in a physiological cytoplasm, fed by physiological cytoplasmic metabolic pathways and supplying ATP to the cytoplasm and plasma membrane, the latter accommodating a variety of ion channels and pumps as well all the machinery required for exocytosis and recovery. Another advantage of using synaptosomes is that they can be prepared easily from any animal of any age unlike primary neuronal cell cultures (Nicholls, 2003). Mitochondria play a vital role in supporting neuronal energy requirements. Bioenergetics failure may result in impaired neuronal transmission and thereby contribute to neurodegenerative diseases like Parkinson's and Alzheimer's (Pathak *et al*, 2015, Choi *et al* 2009).

Our understanding about synaptosomal bioenergetics has been limited because of the lack of resolution of established assays, this study aims to investigate the change in mitochondrial function on application of various drugs as a change in mitochondrial function would imply a change in synaptic transmission.

6.2 Mitochondrial stress test assay

For this study, the Seahorse XFp flux analyser was used to measure mitochondrial respiration in synaptosomes. Various modulators which act on the electron transport chain were employed to provide an insight of the mitochondrial function (Figure 6.1).

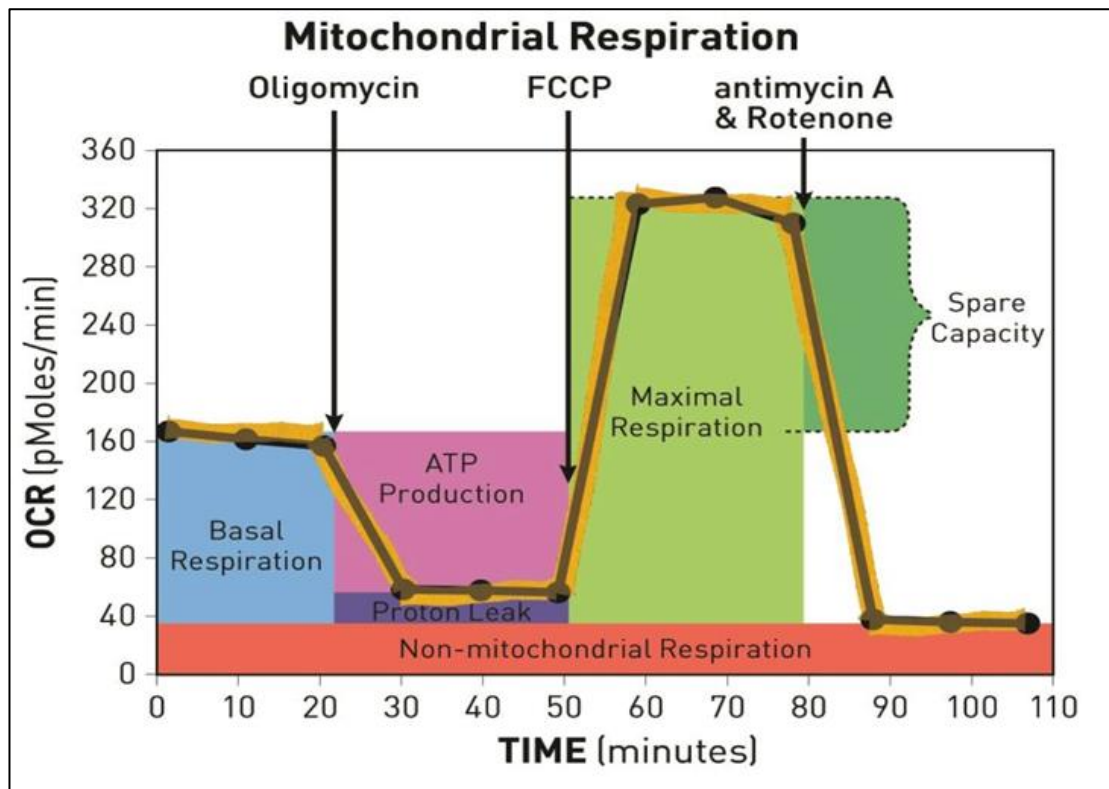


Figure 6.1 Measurement of mitochondrial respiration through sequential injections of various compounds (oligomycin, FCCP, antimycin A and rotenone). Key parameters measured were ATP production, proton leak, maximal respiration, spare respiratory capacity and non-mitochondrial respiration. (Seahorse bioscience, ND)

Oligomycin acts on complex V (ATP synthase) thereby reducing the ATP function and decreasing OCR after it is injected. This effect helps measure ATP production. FCCP (Carbonyl cyanide-4-phenylhydrazone) acts as an uncoupling agent for oxygen from ATP thus collapsing the proton gradient and causing a disruption in the membrane potential. This results in an uninhibited electron flow and maximum consumption of oxygen to complex IV, an increased effect on OCR. This effect of FCCP helps measure the spare respiratory capacity which provides an estimate of the ability of the synaptosome to respond to an increased demand for energy. Rotenone acts as an inhibitor of complex I and antimycin A acts as an inhibitor of complex III, the last injection is a

combination of both of these drugs which shuts down the mitochondrial respiration (see Figure 6.2 and Figure 6.1) and helps calculate non-mitochondrial respiration, which occurs outside the mitochondria. This combination decreases OCR (Figure 6.1). The company that supplies the Seahorse system recommends that one carries out titration of FCCP for the particular cell system/synaptosomes that you are using: refer appendix 1 for titration. Initially, a prepared mixture of the drugs was purchased supplied in a kit but this proved very expensive so these drugs separately were purchased separately. To give the same efficacy as the drugs supplied in the kit the final concentration of the injected drugs used was (in the order oligomycin, FCCP, actimycin A/ rotenone) 4 μM ,2 μM and 0.5 μM ; while the drug concentrations of the kit were 1 μM , 2 μM and 0.5 μM , (refer appendix 1 for graph for the difference in concentration).

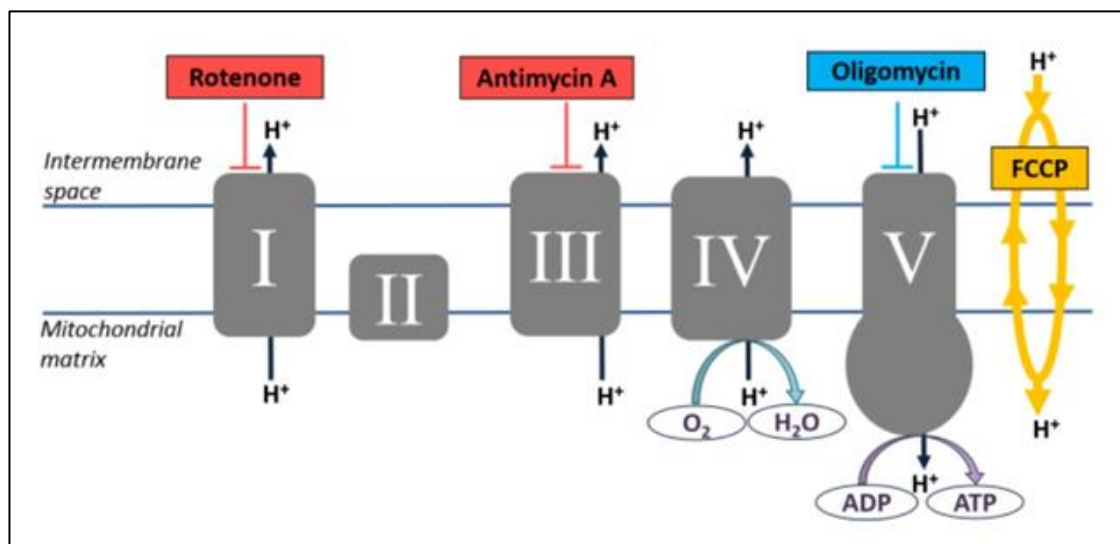


Figure 6.2. The effect of modulators on ETC cycle. See text above (Seahorse bioscience, ND)

In this study, the effect of PAO on bioenergetics of synaptosomes was investigated. This was a prelude to using this drug to investigate the role of phosphatidylinositol 4,5-bisphosphate (PI(4,5)P₂) in synaptic vesicle exocytosis. This is a phospholipid that plays a variety of roles in cell signaling. Phosphorylation of phosphatidylinositol (PI) through PI(4)-kinase (E.C. 2.7.1.64) leads to the synthesis of PI(4)P in turn synthesizing the production of phosphatidylinositol 4,5-bisphosphate synthesis. PAO inhibits the production of PI(4)-kinase by forming stable dithioarsine rings by reacting two thiol groups of closely spaced cystenyl residues (Oda *et al.* 2000). Ashton and Ushkaryov (2005) have shown that 3 μ M PAO apparently did not affect the release of the RRP but it did perturb the release of RP. This indicated that these two pools of SVs had different biochemical requirements. Tarasenko *et al* (2005) have shown that PAO inhibits the SV acidic pool thereby inhibiting the refilling of vesicles and thus reducing the calcium stimulated exocytosis. They also suggested that 1 μ M PAO does not block exocytosis but modifies the endocytic activity while 10 μ M PAO completely inhibits exocytosis. In a preliminary study conducted by Ashton *et. al.*, the effect of PI4- kinase on RRP and RP was investigated and it was found that PAO is not pool dependent but rather mode dependent i.e. its action was not specific to any pool of vesicles but its action inhibits SVs releasing by FF and thereby affecting the glutamate release (Refer appendix 1 for biochemical results). Thus, 3 μ M PAO was used for this study.

6.3 Results

6.3.1 Determining the appropriate concentration of phenylarsine oxide (PAO)

As mentioned earlier through preliminary biochemical studies it was determined that the optimum concentration of PAO is 3 μM and hence this concentration was used for determining the effect of PAO on bioenergetics of synaptosomes using the mito stress test (Figure 6.3). This was done after determining the optimum FCCP concentration.

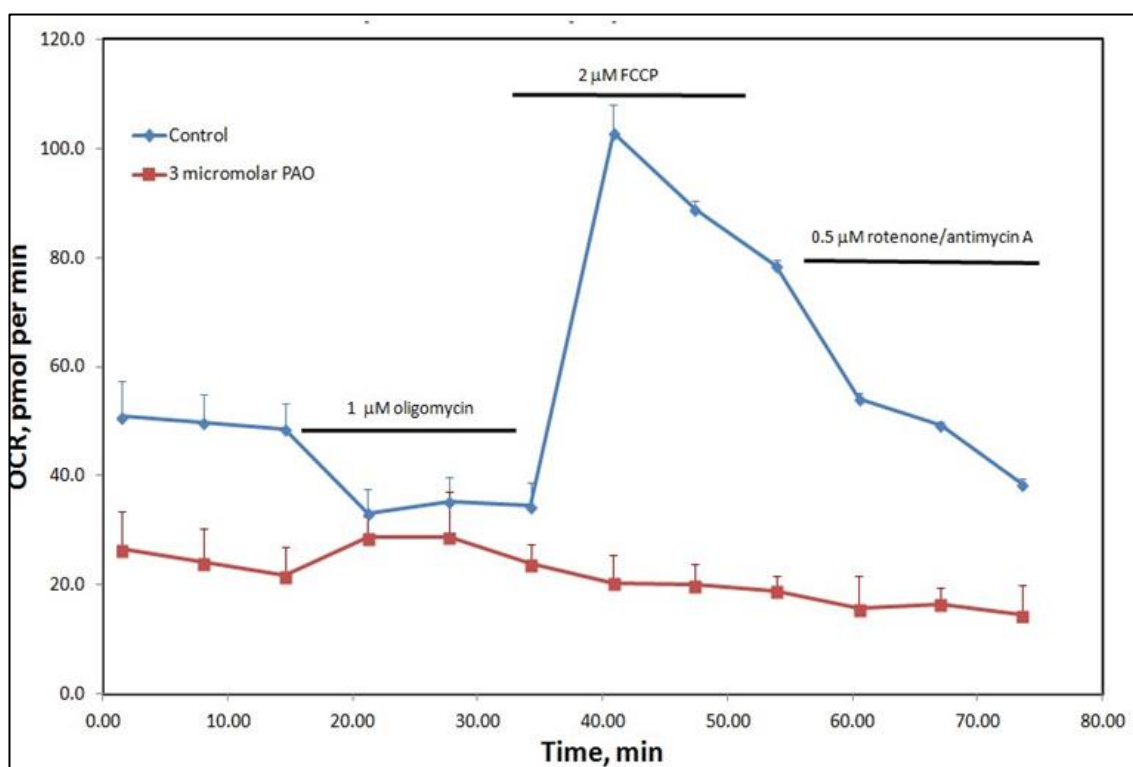


Figure 6.3. The effect of 3 μM PAO on the bioenergetics of synaptosomes. Error bars indicate S.E.M.. These are the results of 3 independent experiments (i.e. performed on different days) with numerous independent sample replicates (i.e. prepared on same day) per experiment. 10 μg of synaptosomes was used per well.

This result clearly shows 3 μM PAO perturbs the bioenergetics of synaptosomes and reduces the OCR in comparison to control. Therefore, the

effect of lower concentrations of PAO on synaptosomes was investigated (Figure 6.4).

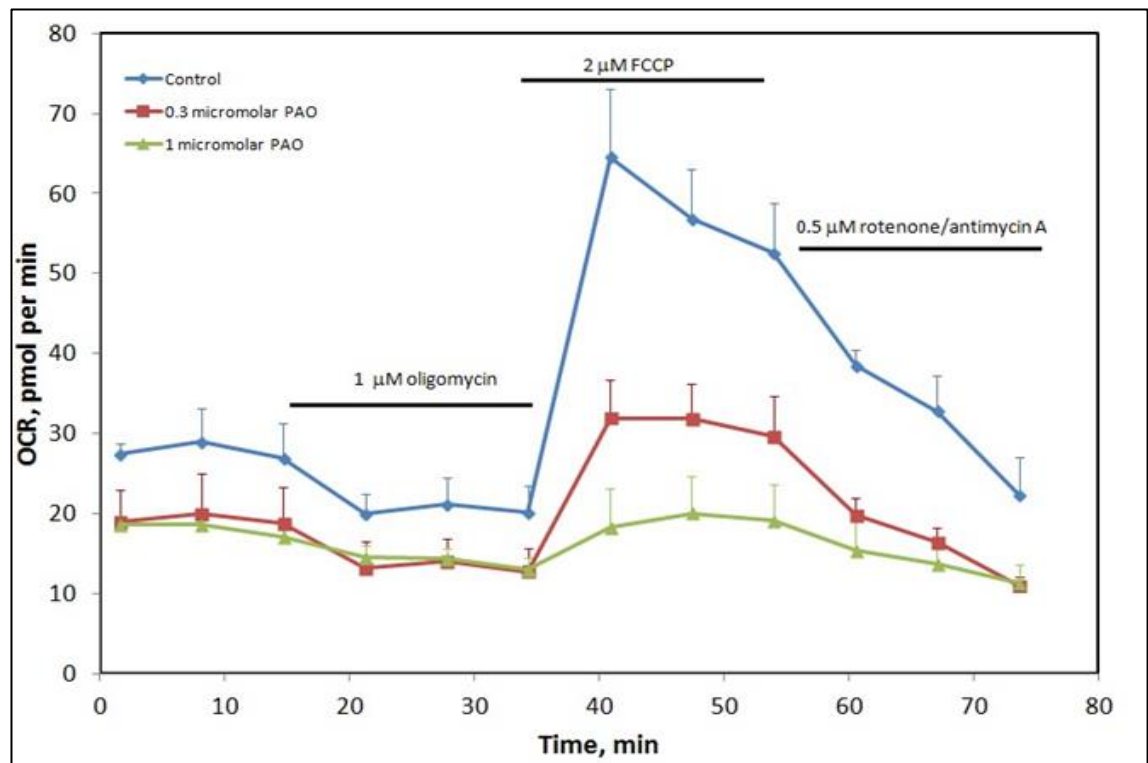


Figure 6.4 Comparison of the effect exerted by 1 μM and 0.3 μM of PAO on the bioenergetics of synaptosomes. Error bars indicate S.E.M.. These are the results of 3 independent experiments (i.e performed on different days) with numerous independent sample replicates (i.e. prepared on same day) per experiment. 10 μg of synaptosomes was used per well.

This result clearly shows 1 μM and 0.3 μM PAO perturbs the bioenergetics of synaptosomes and reduces the OCR in comparison to control. Therefore, the effect of 0.1 μM of PAO on synaptosomes was investigated.

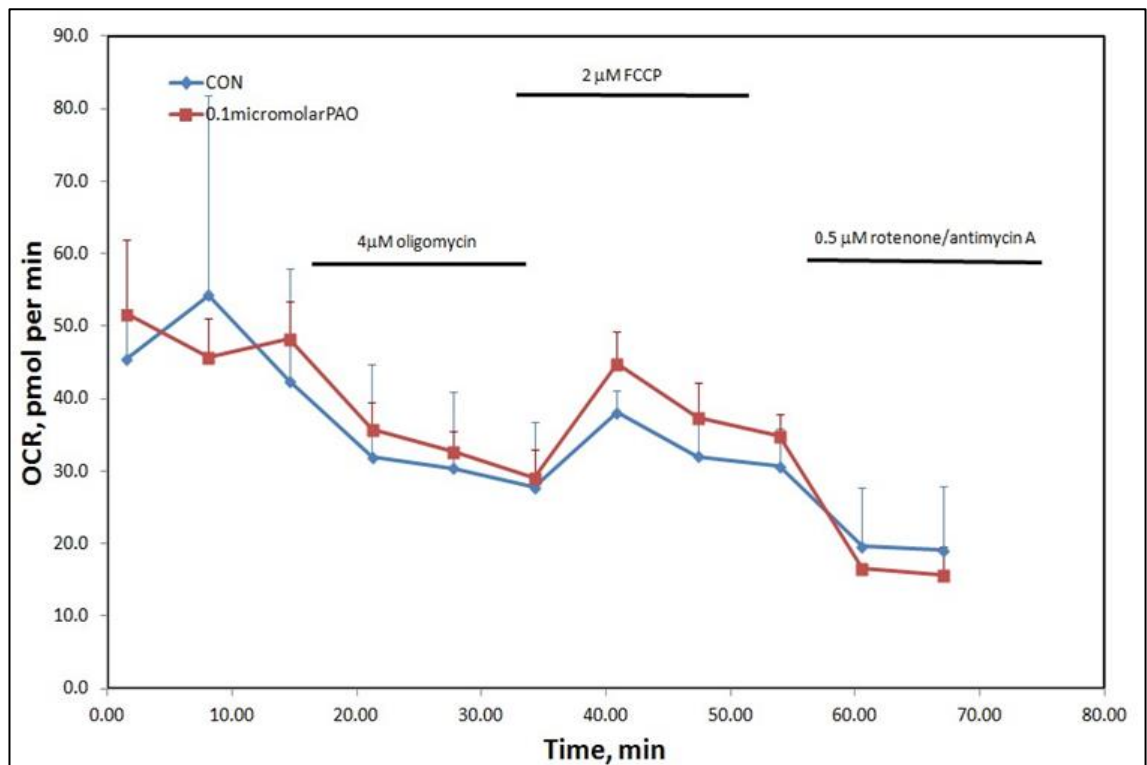


Figure 6.5. The effect of 0.1 μM PAO on the bioenergetics of synaptosomes. Error bars indicate S.E.M.. These are the results of 3 independent experiments (i.e performed on different days) with numerous independent sample replicates (i.e. prepared on same day) per experiment. 10 μg of synaptosomes was used per well.

This result shows that the OCR trace obtained for the action of 0.1 μM PAO on synaptosomes was similar to the control OCR trace and did not exert any detrimental effect.

6.3.2 Effect of various concentrations on mitochondrial respiration parameters

After the mito stress test, various parameters could be directly measured from the traces. The parameters measured were average spare capacity (Figure 6.6), average ATP production (Figure 6.7), average proton leak (Figure 6.8) and average maximum respiration (Figure 6.9).

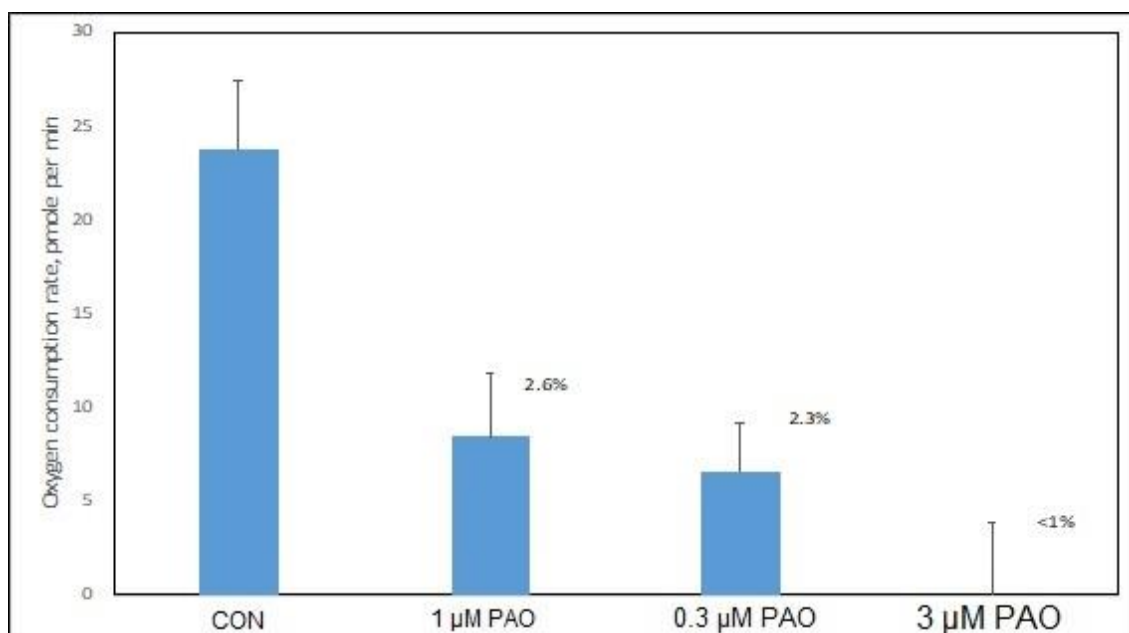


Figure 6.6. Comparison between the effect exerted by 0.1 μ M, 0.3 μ M and 3 μ M PAO and control on the spare respiratory capacity. These are the results of 3 independent experiments (i.e. performed on different days) with numerous independent sample replicates (i.e. prepared on same day) per experiment. $p < 0.05$ was considered significant and expressed as a percentage.

Spare respiratory capacity is an indicator of the cell's flexibility. It measures the capability of the cell to respond to an energy demand and also helps measure how closely the cell respire to its theoretical maximum. In this bar chart, as the dosage of PAO is increased the cell's flexibility is reduced along with the capability of the cell to respond to an energy demand.

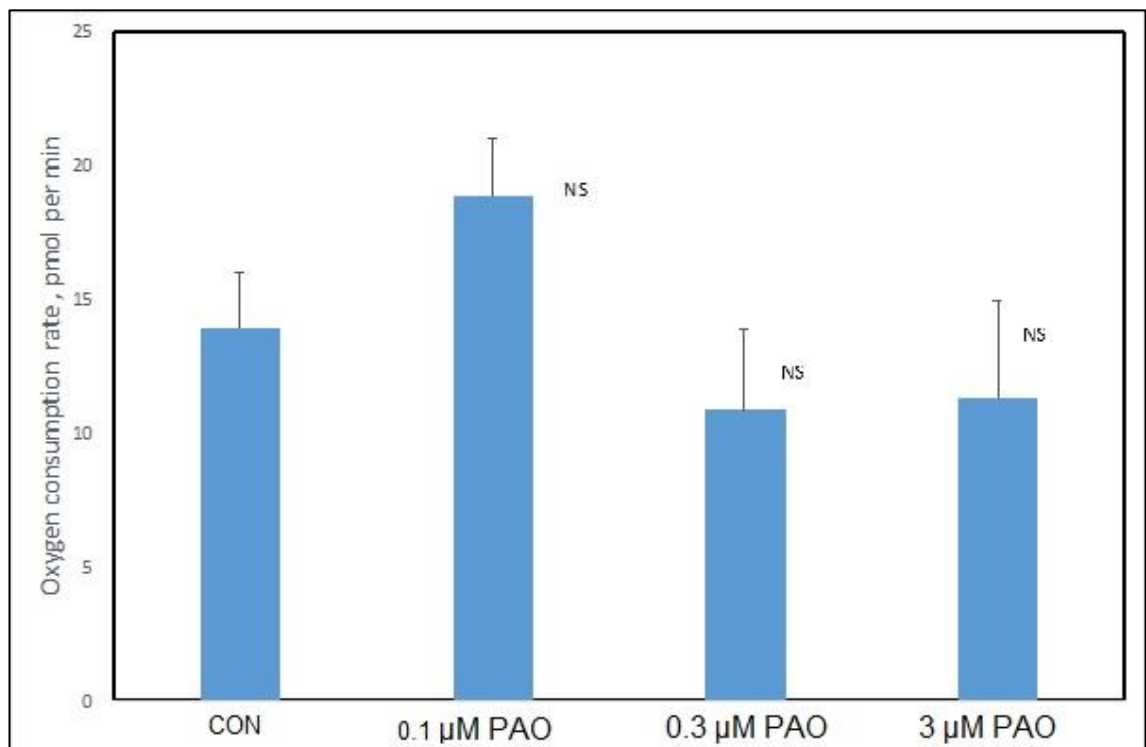


Figure 6.7. Comparison between the effect exerted by 0.1 μ M, 0.3 μ M and 3 μ M PAO and control on the average ATP production. These are the results of 3 independent experiments (i.e performed on different days) with numerous independent sample replicates (i.e. prepared on same day) per experiment. $p < 0.05$ was considered significant and expressed as a percentage.

ATP production helps meet the energy demand of the cell. Upon injection of oligomycin (which blocks the action of complex V) a decrease in the OCR can be observed which represents the portion of the basal respiration being used to

drive ATP production. The graph indicates that there is no significant difference in the ATP production on application of 0.1 μM , 0.3 μM and 3 μM PAO.

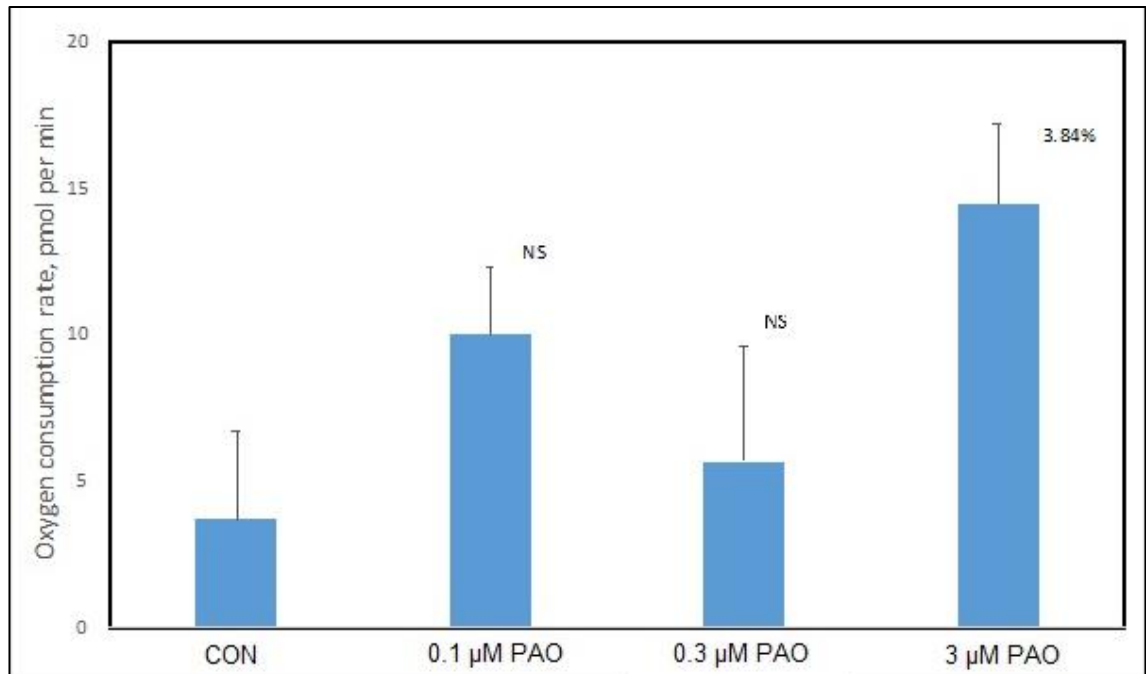


Figure 6.8. Comparison between the effect exerted by 0.1 μM , 0.3 μM and 3 μM PAO and control on the average proton leak. These are the results of 3 independent experiments (i.e performed on different days) with numerous independent sample replicates (i.e. prepared on same day) per experiment. $p < 0.05$ was considered significant and expressed as a percentage.

Proton leak is an indicator of mitochondrial damage or as a mechanism used for regulating mitochondrial ATP production. It is the remaining basal respiration that is not coupled to ATP production.

The graph shows no significant difference in proton leak on application of 0.1 and 0.3 μM PAO. However, a significant increase in proton leak can be observed on application of 3 μM PAO, thereby indicating significant mitochondrial damage.

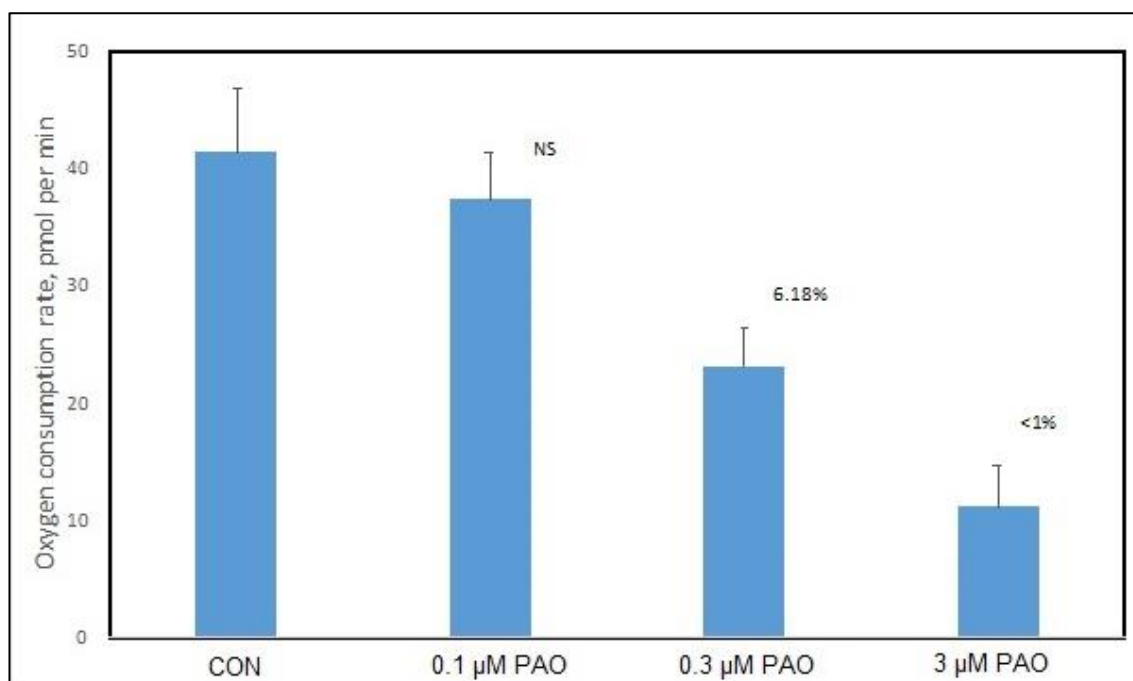


Figure 6.9. Comparison between the effect exerted by 0.1 μM , 0.3 μM and 3 μM PAO and control on the average maximum respiration. These are the results of 3 independent experiments (i.e performed on different days) with numerous independent sample replicates (i.e. prepared on same day) per experiment. $p < 0.05$ was considered significant and expressed as a percentage.

Maximum respiration rate stimulates the respiratory chain to operate at maximum capacity thereby causing rapid oxidation of substrates to meet the high energy demand. The graph shows no significant change in maximum respiration on application of 0.1 μM PAO. However, a significant decrease is observed as the concentration of PAO is increased to 0.3 μM and there is a larger decrease with 3 μM .

The aim of this study was to investigate the effects of varying concentrations (0.1 μM , 0.3 μM and 3 μM) of PAO on the bioenergetics of the cell. The change in bioenergetics of the cell was measured using Seahorse flux analyzer. This study, the first study of its use by Ashton *et al.*, after purchasing the Seahorse

XFp analyzer. This study is completely novel as the effect of blocking PI4-kinase activity on the electron transport chain has never been investigated before. This test measures the oxygen consumption rate to assess the bioenergetics parameters. The results show that 0.1 μ M PAO has the least detrimental effect on the various bioenergetics parameters, when comparing it to the control trace (Figure 6.5 to 6.9). 0.3 μ M PAO in comparison to 0.1 μ M and the control trace showed more of a detrimental effect as shown in Figure 6.4 to Figure 6.9, while Figure 6.3 and Figure 6.5 to 6.9 shows that 3 μ M PAO had the most detrimental effect in comparison to the other two concentrations and the control trace.

Prior to this study, the effect of 3 μ M PAO was investigated on SV exocytosis. However, this assay helped indicated that at such a high concentration the terminals would be bioenergetically compromised. Therefore, it will be essential to repeat such studies at lower PAO concentrations (such as 0.1 μ M which does not compromise its action as a PI(4) kinase inhibitor).

In view of this result, it is essential to determine if any drug that we had used in our SV exocytotic assays and Glu assays to ensure that their actions were not due to compromising the bioenergetics of the synaptosomes. Thus, this assay was used to test the effect of cBIMPS (Figure 6.10), forskolin (Figure 6.11), 9-Cp-Ade (Figure 6.12), Cys A (Figure 6.13), KT 5720 (Figure 6.14), blebb (Figure 6.15), Go 6983 (Figure 6.16) and OA (Figure 6.17) on the bioenergetics of synaptosomes.

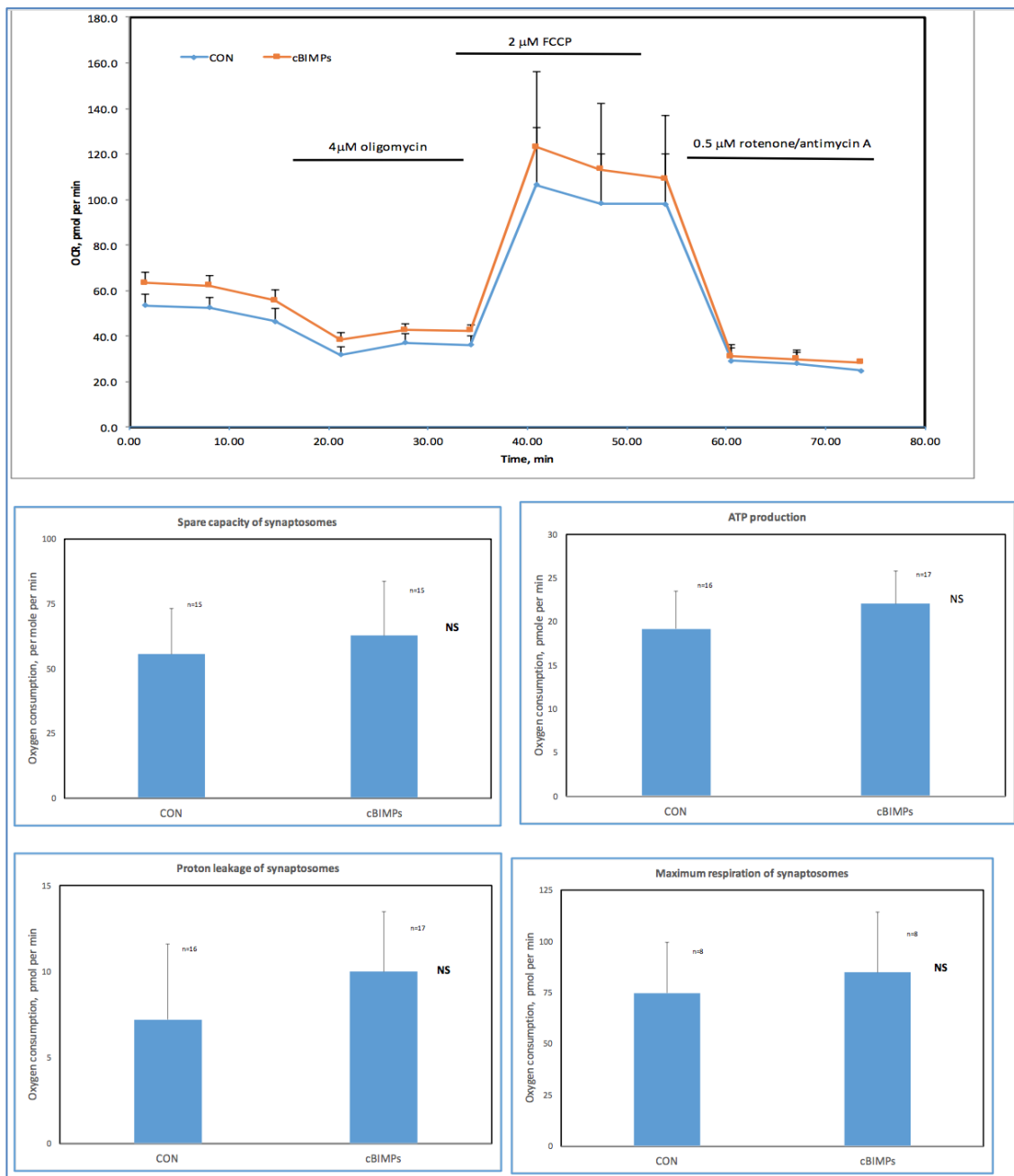


Figure 6.10: Top: effect of 50 μM cBIMPS on synaptosomes as shown by the mito stress test. Bottom (clockwise): Effect of 50 μM cBIMPS on spare capacity, ATP production, maximum respiration and proton leakage. These are the results of 3 independent experiments (i.e performed on different days) with numerous independent sample replicates (i.e. prepared on same day) per experiment. $p < 0.05$ was significant. No significant change can be observed with any parameters, indicating that 50 μM cBIMPS does not perturb the bioenergetics of synaptosomes.

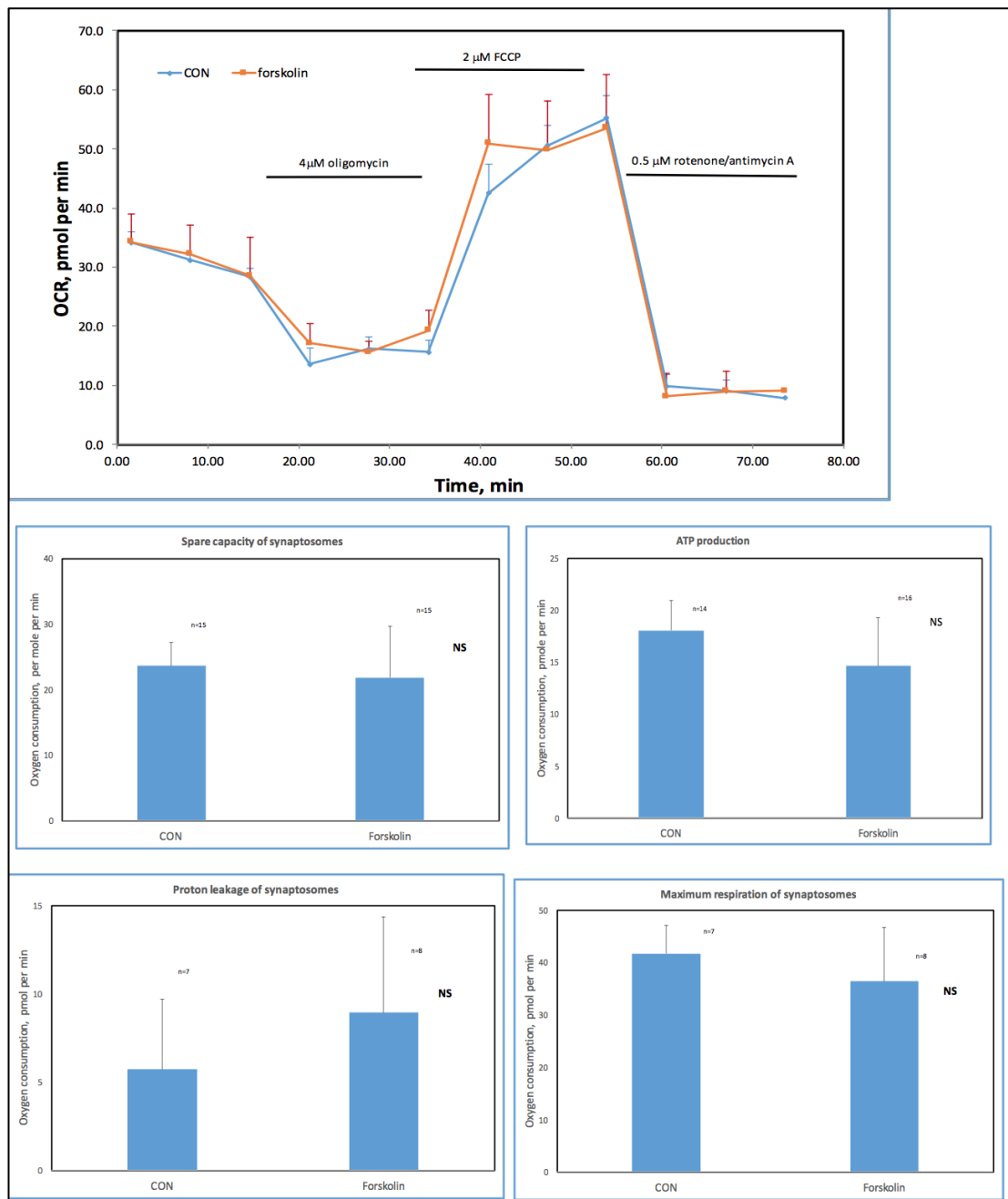


Figure 6.11. Top: effect of 100 μM forskolin on synaptosomes as shown by the mito stress test. Bottom (clockwise): Effect of 100 μM forskolin on spare capacity, ATP production, maximum respiration and proton leakage. These are the results of 3 independent experiments (i.e performed on different days) with numerous independent sample replicates (i.e. prepared on same day) per experiment. $p < 0.05$ was considered significant.

No significant change can be observed with any parameters, indicating that 100 μM forskolin does not perturb the bioenergetics.

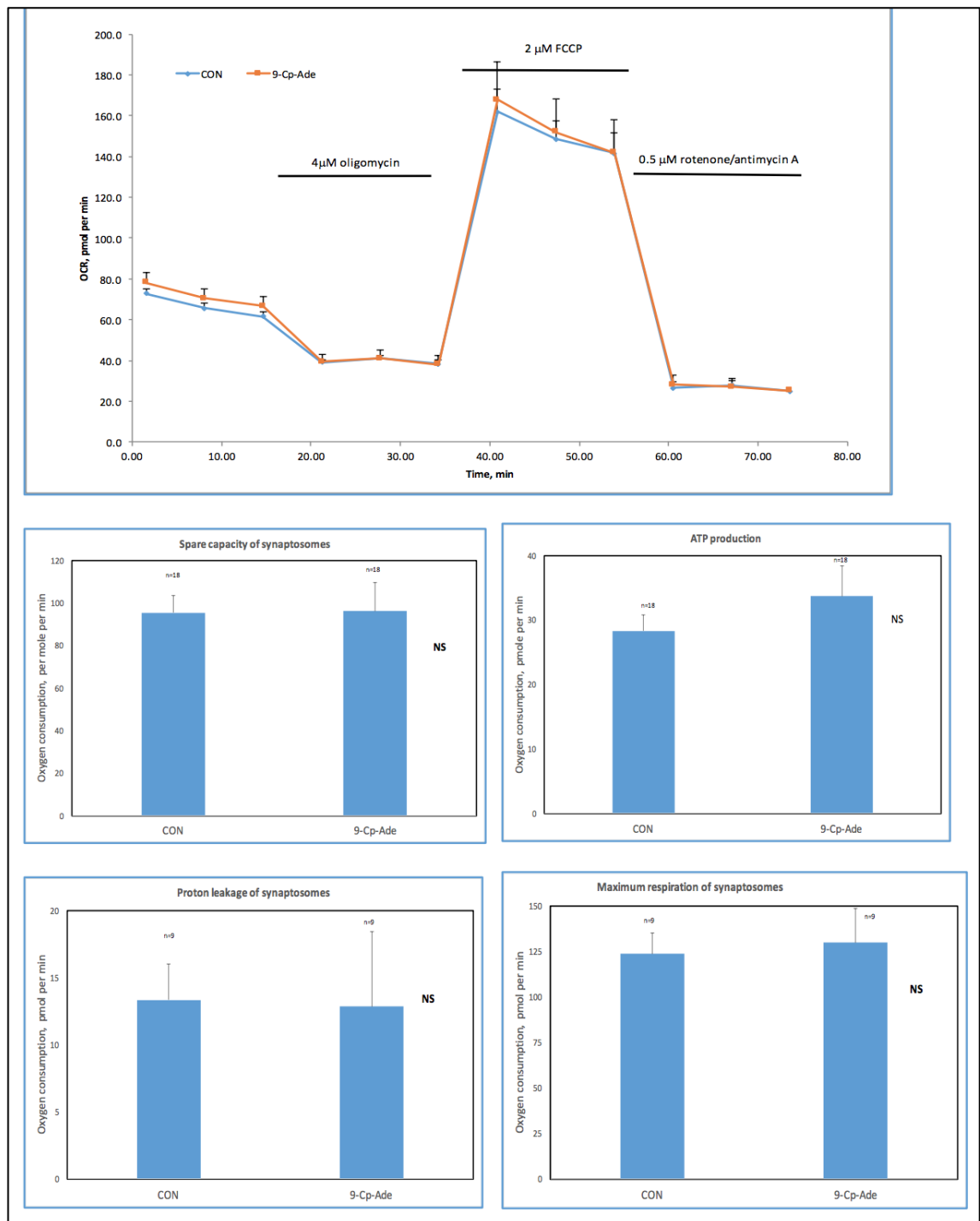


Figure 6.12. Top: effect of 100 μM 9-Cp-Ade on synaptosomes as shown by the mito stress test. Bottom (clockwise): Effect of 100 μM 9-Cp-Ade on spare capacity, ATP production, maximum respiration and proton leakage. These are the results of 3 independent experiments (i.e. performed on different days) with numerous independent sample replicates (i.e. prepared on same day) per experiment. $p < 0.05$ was considered significant.

No significant change can be observed with any parameters, indicating that 100 μM 9-Cp-Ade does not perturb the bioenergetics.

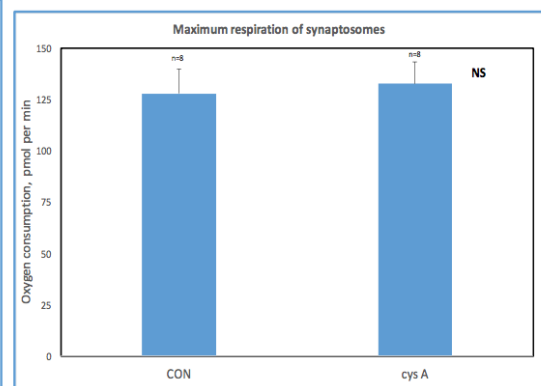
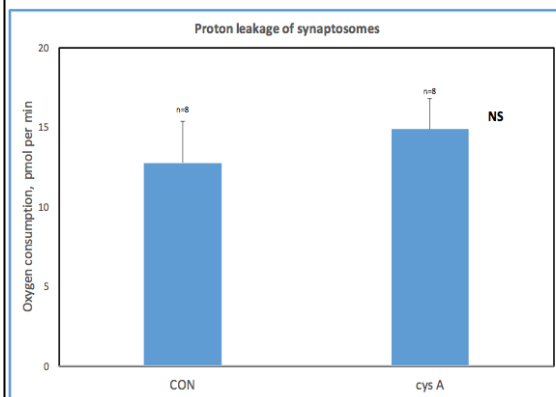
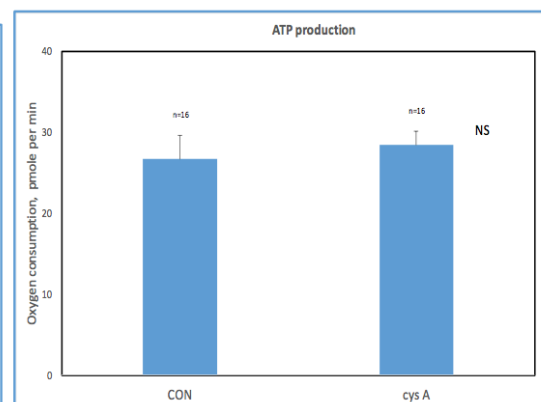
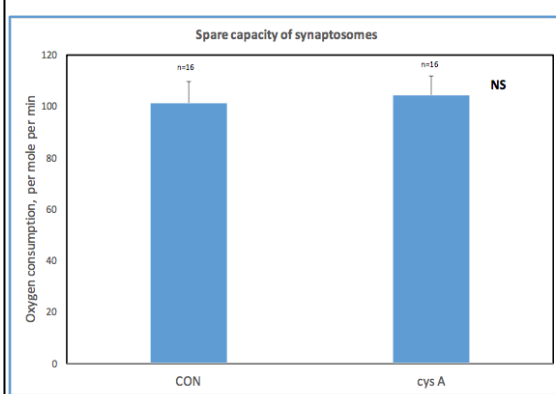
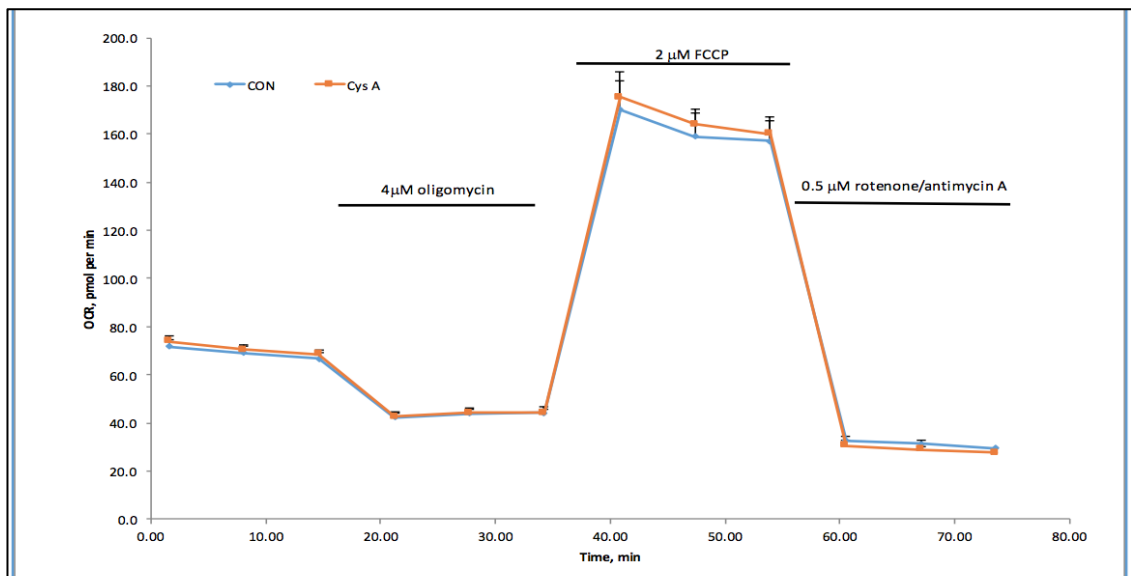


Figure 6.13 Top: effect of 1 μM Cys A on synaptosomes as shown by the mito stress test. Bottom (clockwise): Effect of 1 μM Cys A on spare capacity, ATP production, maximum respiration and proton leakage. These are the results of 3 independent experiments (i.e performed on different days) with numerous independent sample replicates (i.e. prepared on same day) per experiment. $p < 0.05$ was considered significant. No significant change can be observed with any parameters, indicating that 1 μM Cys A does not perturb the bioenergetics.

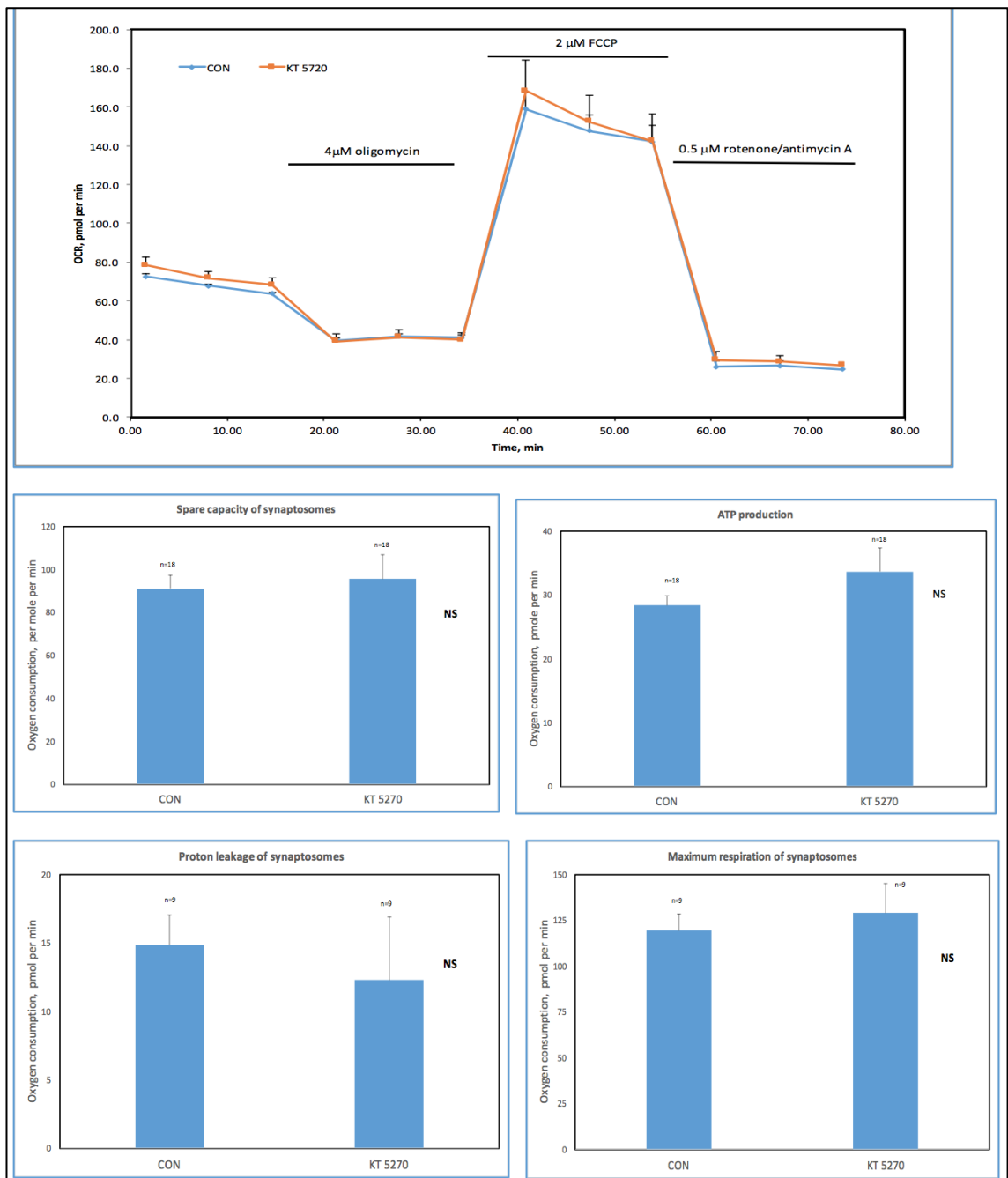


Figure 6.14 Top: effect of 2 μM KT 5720 on synaptosomes as shown by the mito stress test. Bottom (clockwise): Effect of 2 μM KT 5720 on spare capacity, ATP production, maximum respiration and proton leakage. These are the results of 3 independent experiments (i.e performed on different days) with numerous independent sample replicates (i.e. prepared on same day) per experiment. $p < 0.05$ was considered significant.

No significant change can be observed with any parameters, indicating that 2 μM KT 5720 does not perturb the bioenergetics.

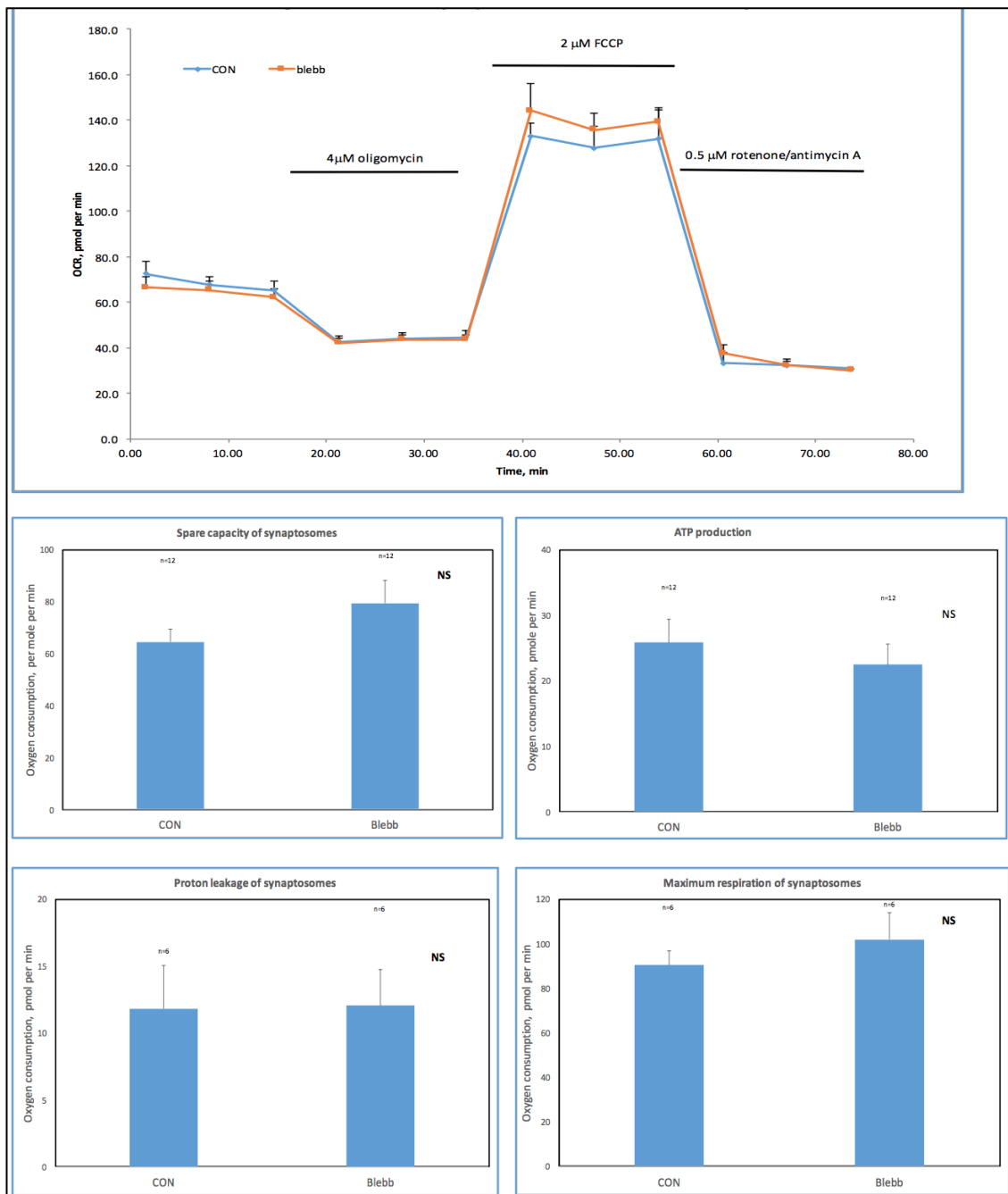


Figure 6.15 Top: effect of 50 μM blebb on synaptosomes as shown by the mito stress test. Bottom (clockwise): Effect of 50 μM blebb on spare capacity, ATP production, maximum respiration and proton leakage. These are the results of 3 independent experiments (i.e performed on different days) with numerous independent sample replicates (i.e. prepared on same day) per experiment. $p < 0.05$ was considered significant. No significant change can be observed with any parameters, indicating that 50 μM blebb does not perturb the bioenergetics.

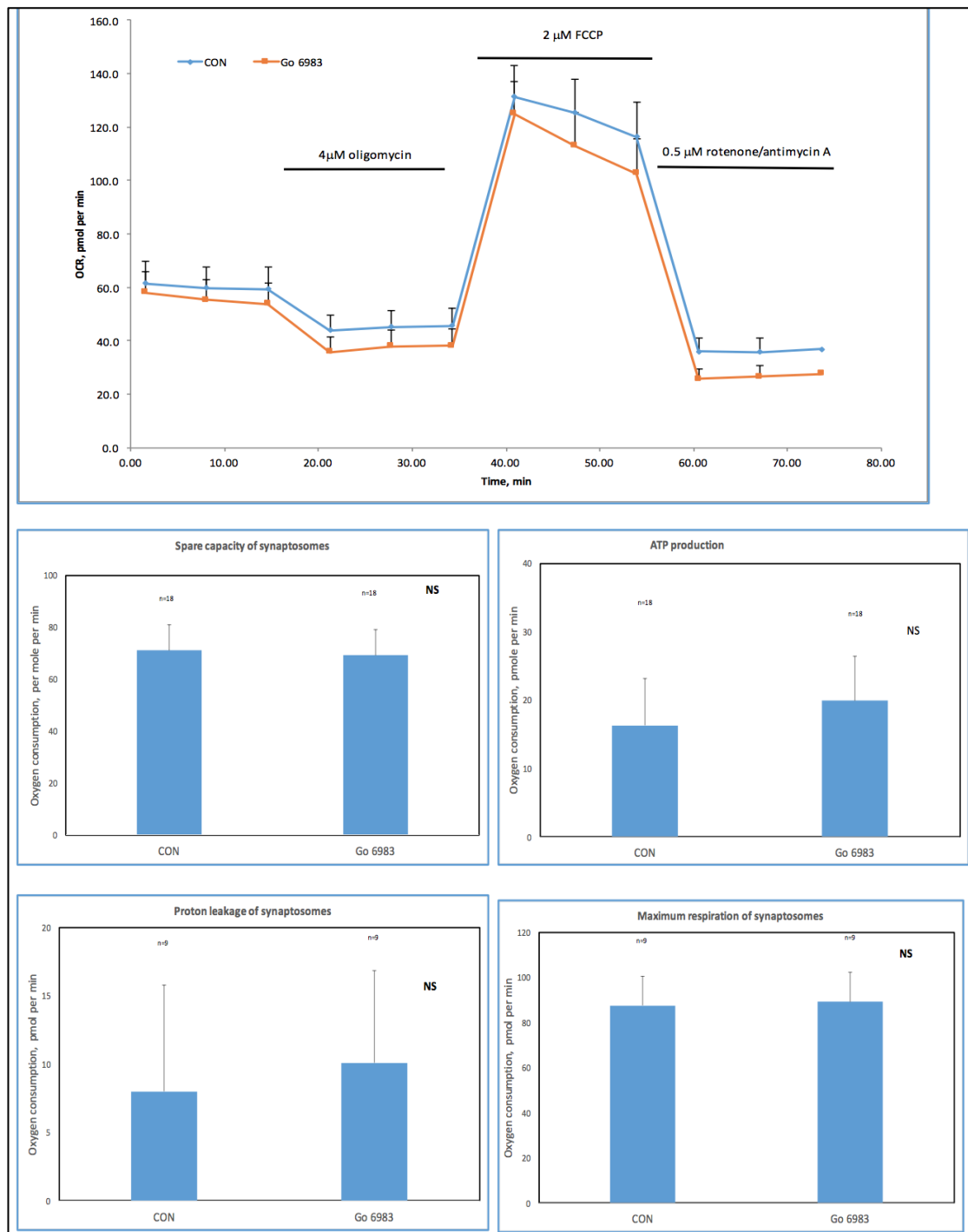


Figure 6.16. Top: effect of 1 μM GO 6983 on synaptosomes as shown by the mito stress test. Bottom (clockwise): Effect of 1 μM GO 6983 on spare capacity, ATP production, maximum respiration and proton leakage. These are the results of 3 independent experiments (i.e performed on different days) with numerous independent sample replicates (i.e. prepared on same day) per experiment. $p < 0.05$ was considered significant.

No significant change can be observed with any parameters, indicating that 1 μM GO 6983 does not perturb the bioenergetics.

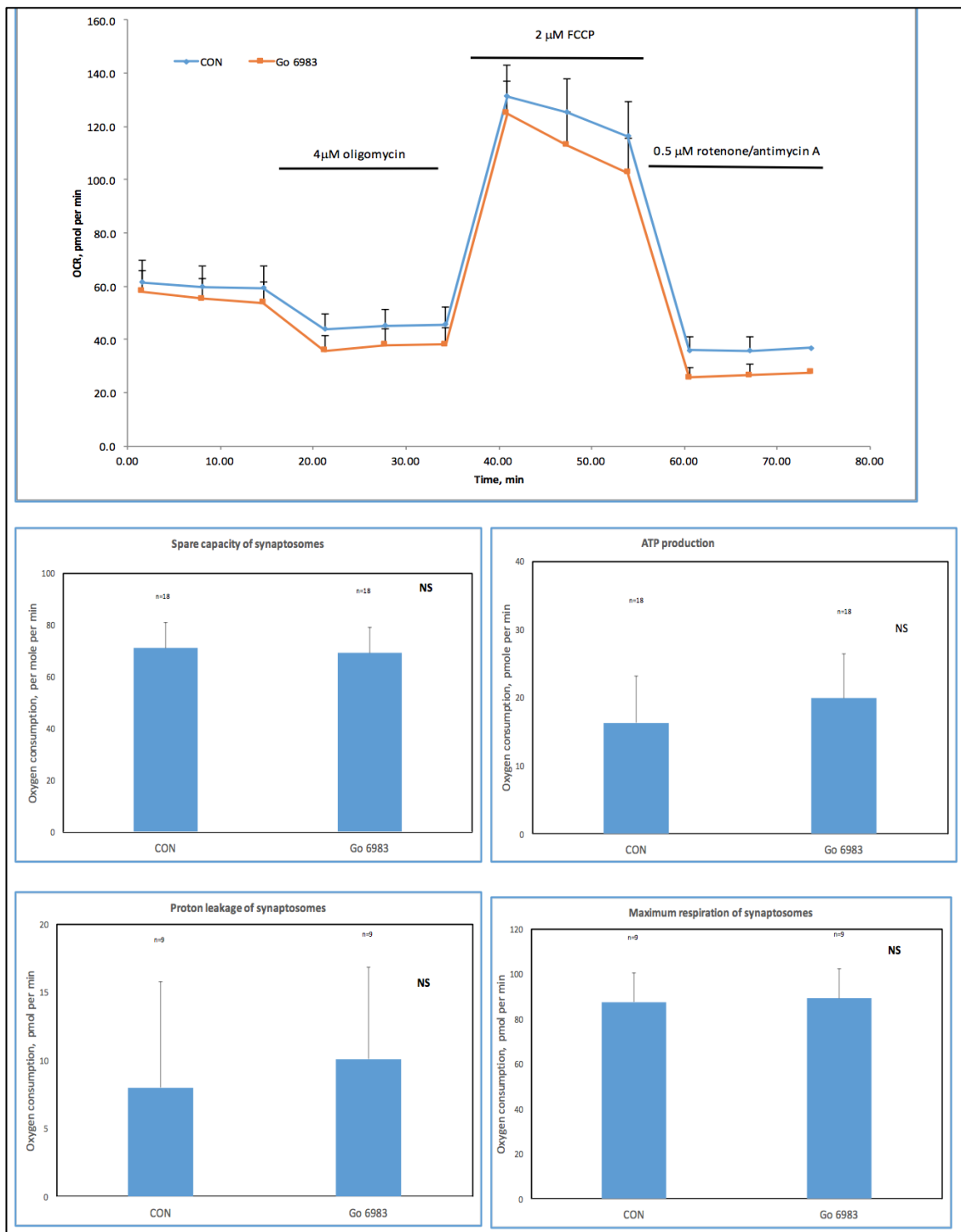


Figure 6.17. Top: effect of 0.8 μM OA on synaptosomes as shown by the mito stress test. Bottom (clockwise): Effect of 0.8 μM OA on spare capacity, ATP production, maximum respiration and proton leakage. These are the results of 3 independent experiments (i.e performed on different days) with numerous independent sample replicates (i.e. prepared on same day) per experiment. $p < 0.05$ was considered significant.

No significant change can be observed with any parameters, indicating that 0.8 μM OA does not perturb the bioenergetics.

6.4 Discussion

The nature of the results in this chapter actually represent an important set of controls that probably should be carried out with any drug that one investigates in this system. There is an assumption that the drug employed does not have a detrimental effect on the bioenergetics of the tissue being used in the study and that its action can be completely explained by the specificity that has been described in the literature. However, the first drug that was tested was PAO (Figure. 6.3 to 6.9) which showed that the concentration being used would perturb many more parameters in the synaptosomes than just regulating the fusion mode. Indeed, many of the studies that were carried out using 3 μM PAO must now have to be performed using a lower concentration such that the drug concentration will still perturb the PIP_2 production but not bioenergetics. However, it was reassuring that many of the drugs that we have been employing in our studies do not have such detrimental effects to the bioenergetics of the synaptosomes.

50 μM cBIMPS had no effect on spare capacity, ATP production, maximum respiration and proton leakage and this indicates that activation of PKA does not perturb the bioenergetics of the nerve terminals (Figure 6.10). The effect of activation of PKA on the bioenergetics of synaptosomes has previously not been investigated.

100 μM forskolin had no effect on spare capacity, ATP production, maximum respiration and proton leakage (Figure 6.11). This indicates that activation of AC does not perturb the bioenergetics of synaptosomes. Again, this is a novel result.

100 μ M 9-Cp-Ade had no effect on spare capacity, ATP production, maximum respiration and proton leakage (Figure 6.12). Therefore, inhibition of AC does not perturb the bioenergetics of synaptosomes. Again, this is a novel result.

1 μ M Cys A had no effect on spare capacity, ATP production, maximum respiration and proton leakage (Figure 6.13). This novel result demonstrates that the inhibition of PP2B does not perturb bioenergetics of the nerve terminals.

2 μ M KT 5720 had no effect on spare capacity, ATP production, maximum respiration and proton leakage (Figure 6.14). Therefore, this original observation indicates that inhibition of PKA bioenergetics of the nerve terminals.

50 μ M blebb had no effect on spare capacity, ATP production, maximum respiration and proton leakage (Figure 6.15). The novel conclusion is that the inhibition of myosin-II does not perturb the bioenergetics of synaptosomes.

1 μ M GO 6983 had no effect on spare capacity, ATP production, maximum respiration and proton leakage (Figure 6.16) thereby suggesting that inhibition of PKCs does not perturb the bioenergetics of synaptosomes. This result is novel as the effect of inhibition of PKCs on bioenergetics of synaptosomes has never been investigated before.

Finally, 0.8 μ M OA had no effect on spare capacity, ATP production, maximum respiration and proton leakage (Figure 6.17). This indicates that inhibition of PP2A does not perturb the bioenergetics of synaptosomes and this result has not been previously reported.

Due to time constraints, this bioenergetics assay could not be carried out the other drugs employed in this thesis. However, subsequently many of these have been tested and have been shown to have negligible effects on the bioenergetics of the synaptosomes (e.g. PMA, DYN). Herein, we did not report the effect of the drugs on the basal respiration but it would appear that some of the other drugs actually make the terminals work harder after their addition such that the basal respiration increases. This normally indicates that the drug causes an increase in ATP production. However, in every case whilst the maximal respiration is similar the spare capacity has been reduced as some of this is being used because of the drug addition.

One problem with this assay is that to measure all the bioenergetic parameters of the synaptosomes using the 'mito stress test' assay takes 100 min. In all the experiments reported, herein, this test has been carried out at 37°C. Normally in our SV exocytotic studies the synaptosomes were treated with the drugs for 5 min (10 min when carrying various double drug additions) at 37°C, but the Glu release and FM dye release are measured at room temperature (20 to 24°C) within 30 min of the drug application. This has not proven to be a problem for all the drugs tested that had negligible effects but may prove problematic for some drugs such as PAO which affect glutamate release (3 µM PAO treated synaptosomes show a decrease in the glutamate release on comparison to control synaptosomes while the rest of the drugs that were utilised for this study did not perturb the glutamate release on comparison to control synaptosomes). Very recently, Seahorse have introduced an adaptor that allows one to carry out the experiments at lower temperatures than at 37°C. Ashton and colleagues have now reproduced the normal conditions for release assays for measurement of the bioenergetics of synaptosomes and have shown that the

prolonged 37°C temperature exposure may produce results that are not applicable at lower temperatures i.e. there may be spontaneous release of the RRP (Ashton *et al.*, unpublished). In particular, they have recently discovered that whilst 3 µM PAO is still detrimental to nerve terminals with the modified temperatures, 0.3 µM PAO does not interfere with the bioenergetics of the synaptosomes. This indicates that this concentration could be employed to reinvestigate SV exocytosis modes. Also, the author of this thesis would like to remind the reader that these particular bioenergetics study is completely novel and thus there is a lack of citations in text.

Chapter 7

Phosphorylation Studies

7.1 Investigating the role of phosphorylation of dynamins in switching the mode of synaptic vesicular exocytosis

7.1.1 Introduction

Eddie Fischer and Ed Krebs in 1955 discovered phosphorylation as a regulatory physiological mechanism (reviewed by Johnson, 2009). It is a molecular mechanism through which protein function can be regulated in response to stimuli present inside the cell or outside the cell. Most of the neuronal proteins are regulated via phosphorylation as stated in chapter 1. Proteins are known to undergo covalent modification in many ways for e.g. ADP-ribosylation, acylation, carboxymethylation, tyrosine sulphation and glycosylation. However, none of these modification pathways are as widespread and readily subject to regulation in response to physiological stimuli as phosphorylation. Thus, regulation of protein phosphorylation is important for neuronal function (Siegel *et al.*, 1999). Phosphatases and kinases mediate protein phosphorylation. Protein kinases can be classified as serine-threonine kinases (which phosphorylate serine or threonine residues), tyrosine kinases (which phosphorylate tyrosine residues) and kinases that perform dual function of phosphorylating serine-threonine and tyrosine residues. Over 95% of protein phosphorylation occurs at serine-threonine residues and less than 1% at tyrosine residues. Phosphate groups carry a negative charge, and phosphorylation of proteins results in a conformational change by altering the localized charge on the protein at the phosphorylated amino acid. This conformational change can alter the functional activity of the protein. There are

various ways in which extracellular signals can regulate neuronal function via protein phosphorylation.

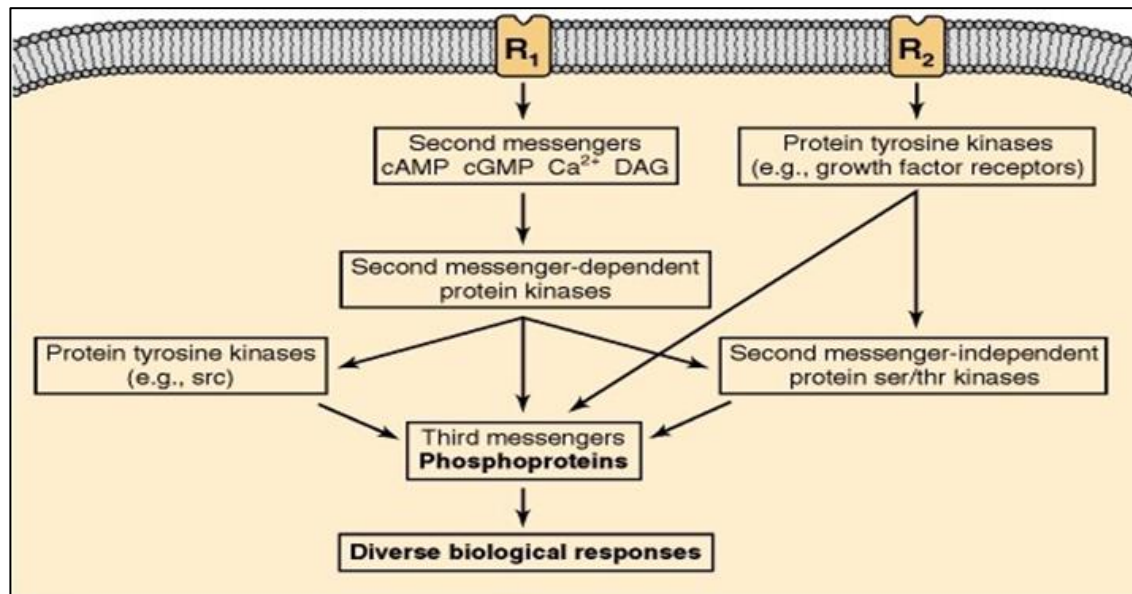


Figure 7.1. Schematic representation of the various ways in which biological responses can be altered. Second messengers include cAMP, cGMP, Ca²⁺ and DAG. Major second messenger-dependent protein kinases include PKC, PKA, Ca²⁺ / calmodulin kinases, CDKs, MAP kinases. Major second messenger-independent protein ser/thr kinases include CMGC kinases, CK1 kinases, STE kinases. Third messengers include DNA-binding proteins. There exists molecular cross-talk between different signalling pathways. (Siegel *et al.*, 1999).

Exocytosis of SVs is mediated by protein complexes that are regulated in a Ca²⁺ dependent manner. Dynamins are well characterized members of the dephosphin family. They are one of the most prominent nerve terminal proteins regulated in response to changes in Ca²⁺ concentrations. Dynamin can be phosphorylated on numerous sites in its amino acid sequence and these phosphorylations affect the properties of the protein. Huang *et al* (2004) have suggested that phosphorylation of serine residue 857 by Dyrk 1A (Dual specificity tyrosine-phosphorylation-regulated kinase 1A) reduces the binding of

dynamin I to amphiphysin I and Grb 2 (Growth factor receptor-bound protein 2). Chircop et al (2011) have suggested that Ser-512, Ser-851, Ser-822 and Ser-347 can regulate the activity of dynamin I and Ser-853 for dynamin III. However, the exact function of these sites is still unknown. Also, these authors showed that phosphorylation of dynamin II at Ser-764 by CDKI (Cyclin Dependent Kinase I) is associated with cytokinesis.

Graham *et. al.*, (2007) have identified two serine residues- Ser774 and Ser-778 in the PRD of dynamin 1 and 3 (for dynamin 3 the equivalent sites are Ser-759 and Ser-763 respectively) which act as substrates for calcineurin and CDK5 and GSK3. The phosphorylation/ dephosphorylation of dynamin 1 on Ser-774 and Ser-778 play an important part in their actions on CME and ADBE. The role of dynamin 1 and its phosphorylation in this latter process, which is also called bulk endocytosis, is controversial and this has been discussed in other chapters of this thesis. Ser-774 and Ser-778 are known to regulate the GTPase activity of dynamins which is absolutely essential for dynamins function (Smillie and Cousin, 2005). Phosphorylation of Ser-774 and Ser-778 stimulates the recruitment of syndapin I (Anggono and Robinson, 2007). Powell *et. al.*, (2000) have shown that phosphorylation of dynamin I on Ser-795 by PKC blocks its association with phospholipids. In this study the effect of phosphorylation of serine residues 774, 778 and 795 on dynamin I in KR mode of exocytosis has been investigated. This study is completely novel as the role of the aforementioned sites has never been implicated in KR mode of exocytosis.

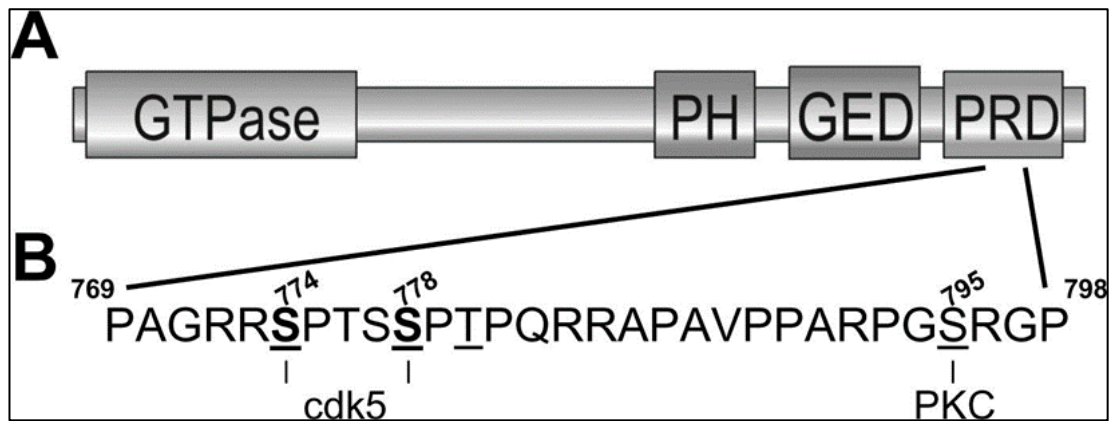


Figure 7.2. Schematic diagram showing the domain structure and phosphorylation sites for dynamin 1 A. Schematic diagram showing the domain structure of dynamin 1. B. Phosphorylation sites present *in vitro* and *in vivo* on dynamin 1. Ser774 and Ser-778 indicate GSK3 and CDK5 phosphorylation sites. Ser-795 has been shown to undergo phosphorylation by PKC *in vitro* but not *in vivo* under conditions tested by these authors. (Smillie and Cousin, 2005).

In this study the effect of various kinases and phosphatases on the phosphorylation of Ser-774, Ser-778 and Ser-795 were investigated by using site-specific antibodies.

7.2 Results

7.2.1 Investigating the role of Ser-774, Ser-778 and Ser-795 in KR exocytosis.

In order to investigate the possible role of ser-774, ser-778 and ser-795 of dynamin 1 in the KR mode of exocytosis, the change in phosphorylation level of each serine residue was determined upon the application of various drug treatments. These included treatments with OA, Cys A, KN-93, active phorbol ester which is PMA (Ph est) and Blebb. As RRP would have released within 2 sec and RP would start to release after 2 sec the stimulation time chosen for

analysis was 15 sec. However, most experiments involved a time course varying from 2 sec to 300 sec.

For HK5C stimulation, RRP exocytoses via KR and RP by FF. 0.8 μ M OA blocks the effect of PP2A and induces the release of RRP and RP by full fusion (Ashton *et. al.*, unpublished). 1 μ M Cys A blocks the action of PP2B and induces the release of RRP and RP by KR. 10 μ M KN-93 blocks the effect of CAMKII and this blocks the release of RP but it converts RRP SVs to FF (Ashton *et. al.*, unpublished). 1 μ M Ph est supra-maximally all terminal PKCs and this actually induces RRP and RP by FF. This is distinct from the use of 40 nM Ph est that activates some PKCs (at the active zone) which can regulate the properties of both dynamins and myosin-II (chapter 3). 50 μ M Blebb inhibits the action of myosin-II. As shown earlier this drug has different effects depending upon the stimulation employed. With HK5C Blebb induces RRP to release by FF and RP by FF whilst it does not perturb ION5C or 4AP5C effects on the mode. 1 μ M Go 6983 inhibits all PKCs, it can change the requirement for the different proteins for closing the fusion pore (chapter 3) and it also inhibits the action of Ph est. (Ashton *et. al.*, unpublished) Results from Ashton and colleagues have shown that many of these drugs that induce changes in protein phosphorylation also induced changes in the mode of exocytosis. The aim here was to determine if phosphorylation changes of dynamin-1 are related to these changes in mode of exocytosis.

Western blotting was carried out using the respective primary and secondary antibodies against each of the aforementioned phospho-serine residues. For recognising phospho-serine-774, the primary antibody used was 1:1000 p-Dynamin (ser-774) while the secondary antibody used was 1:5000 donkey anti-

sheep HRP conjugate. For recognising phospho-serine-778, the primary used was 1:400 p-Dynamin (ser-778) while the secondary antibody used was 1:5000 donkey anti-sheep HRP conjugate. For recognising phospho-serine-795, the primary used was 1:100 p-Dynamin (ser-795) while the secondary antibody used was 1:5000 donkey anti-goat HRP conjugate. Later these blots were reprobed with 1:1000 dynamin 4E67 (a pan-dynamin antibody that recognizes all the dynamin 1 protein whether phosphorylated or not) and the secondary antibody used was 1:5000 of goat anti-mouse HRP conjugate. This antibody serves as an internal control for investigating the total dynamin 1 protein content. In the histograms produced after statistical analysis the change in the amount of phosphorylation was expressed as a percentage of the maximum L_0 + control and the error bars represent S.E.M..

7.2.2 Phospho-serine-778 content of dynamin 1

Synaptosomes were treated with the various drugs for 5 min at 37°C and following washing steps samples were taken and stimulated for 15 s with HK5C (Figure. 7.3). The actual protocol was identical to that employed in the release studies except release was terminated with the SDS-sample buffer. This denatures all the kinases and phosphatases and effectively maintains the phosphorylated state of proteins at the precise time just before solubilisation with this sample buffer.

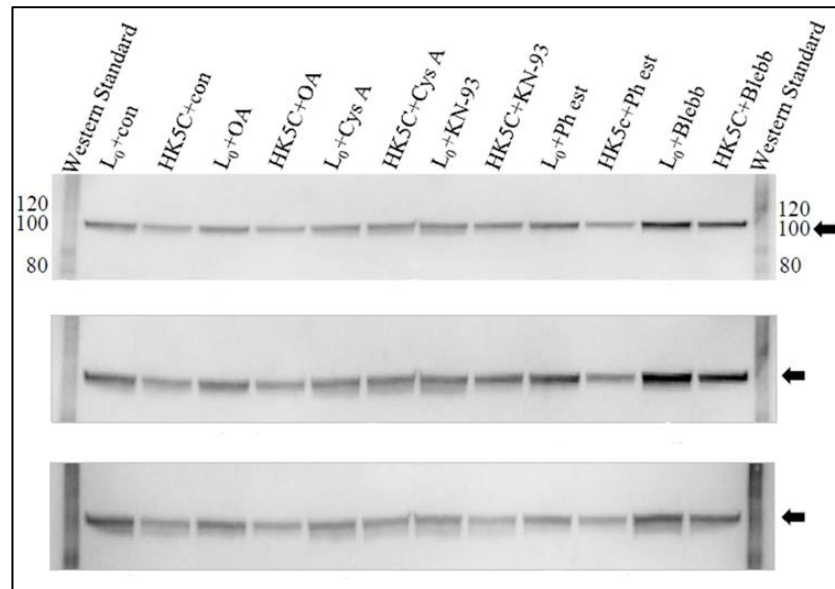


Figure 7.3. The effect of OA, Cys A, KN-93, Ph est, and Blebb drug treatments on phosphorylation of ser-778 of dynamin 1 following the application of HK5C stimulation for 15 sec. The three blots are from 3 independent experiments. The representative blots are indicative of different sample sets with the same drug and stimulation conditions. The protein ladder represents the weight of protein in kilo Dalton (kDa).

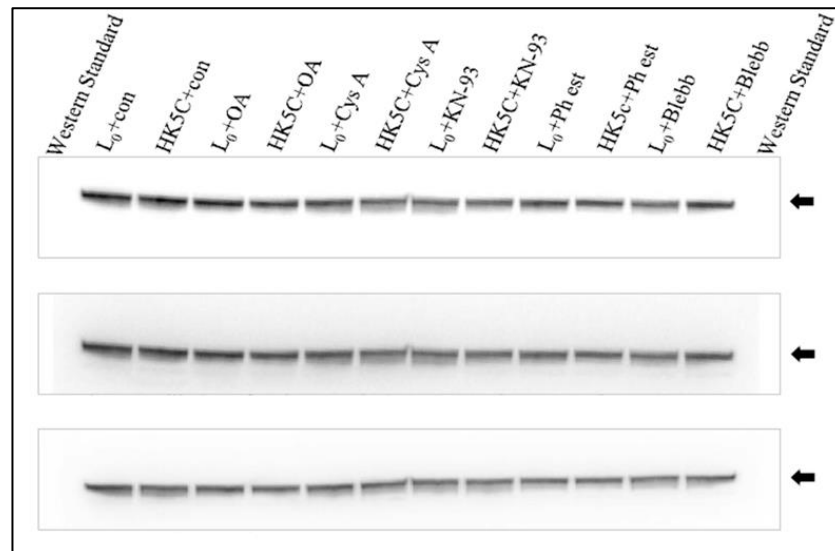


Figure 7.4. Reprobing blots presented in Figure 7.3 with anti-dynamin 4E67.

All the blots show same levels of intact dynamin 1. The three blots are from 3 independent experiments shown in Figure 7.3.

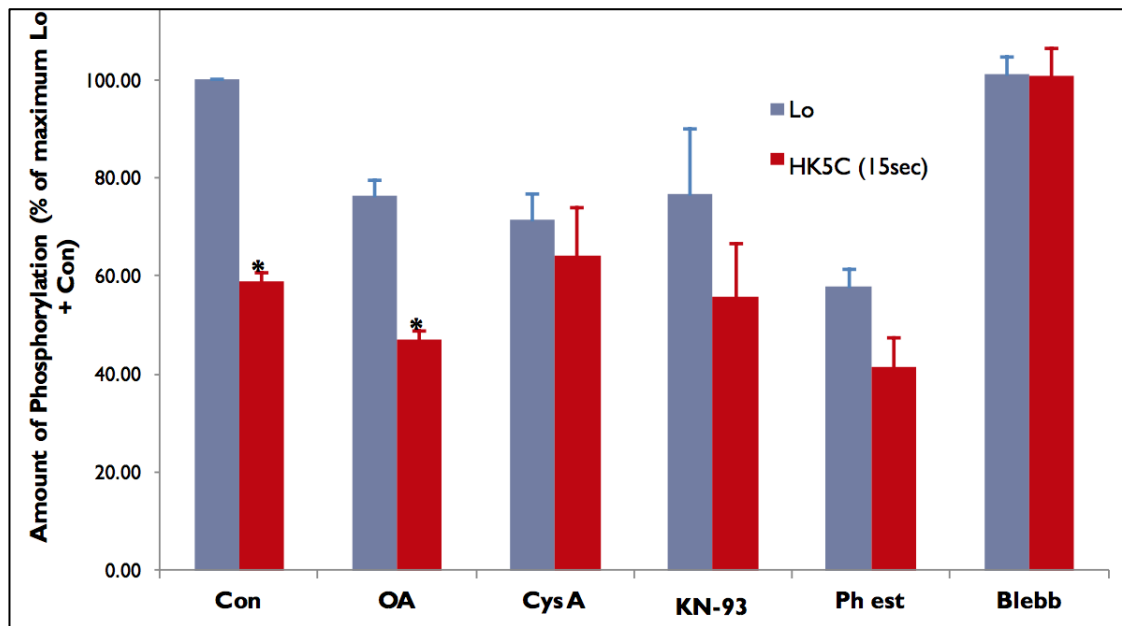


Figure 7.5 Bar chart showing changes produced in p-Dyn778 phosphorylation after the various drug treatments and comparing basal (Lo to HK5C). Data are mean and S.E.M, n=3. $p < 0.05$ for HK5C compared to control.

Figure. 7.5 shows changes in p-Dyn778 following various drug treatments and stimulation. It can be observed that following various drug treatments and upon stimulation with HK5C, all drug treatments show a decrease in phosphorylation at the Ser-778 site on dynamin compared to the basal Lo apart from Blebb treatment which seems to have no effect. However, only the control and samples treated with Okadaic Acid show a statistically significant decrease.

7.2.3 Phospho-serine-774 content of dynamin 1

Synaptosomes were prepared exactly as outlined for phospho-ser-778 except these samples were probed with an antibody specifically recognizing phosphoserine -774 of dynamin 1 (Figure 7.6).

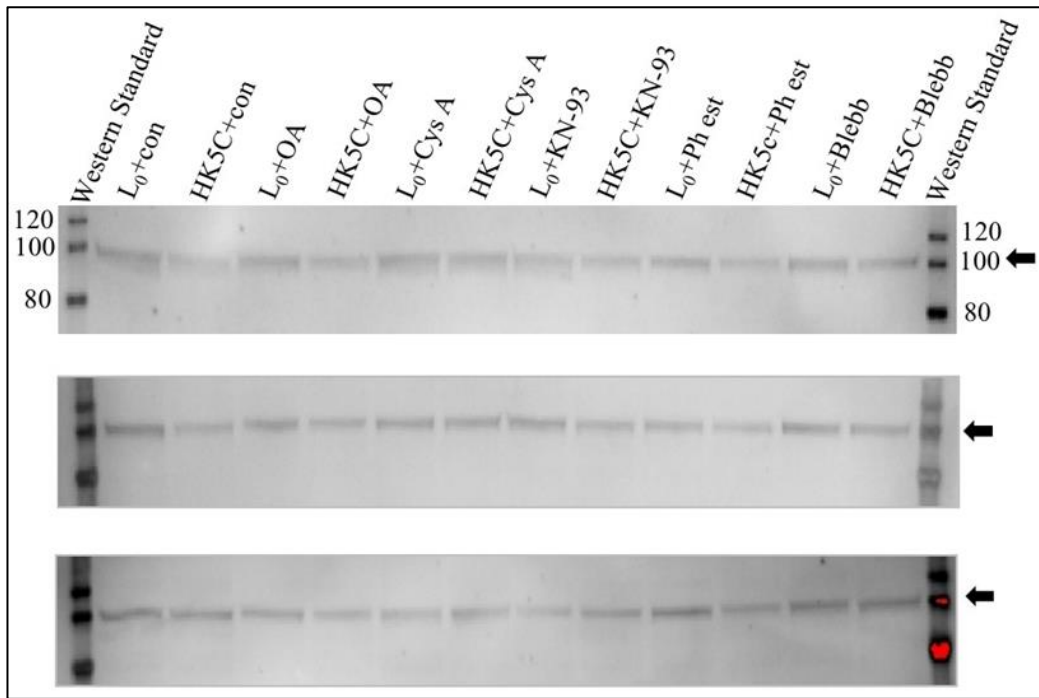


Figure 7.6. The effect of OA, Cys A, KN-93, Ph est, and Blebb drug treatments on phosphorylation of ser-774 of dynamin 1 following the application of HK5C stimulation for 15 sec. The three blots are from 3 independent experiments. The representative blots are indicative of different sample sets with the same drug and stimulation conditions.

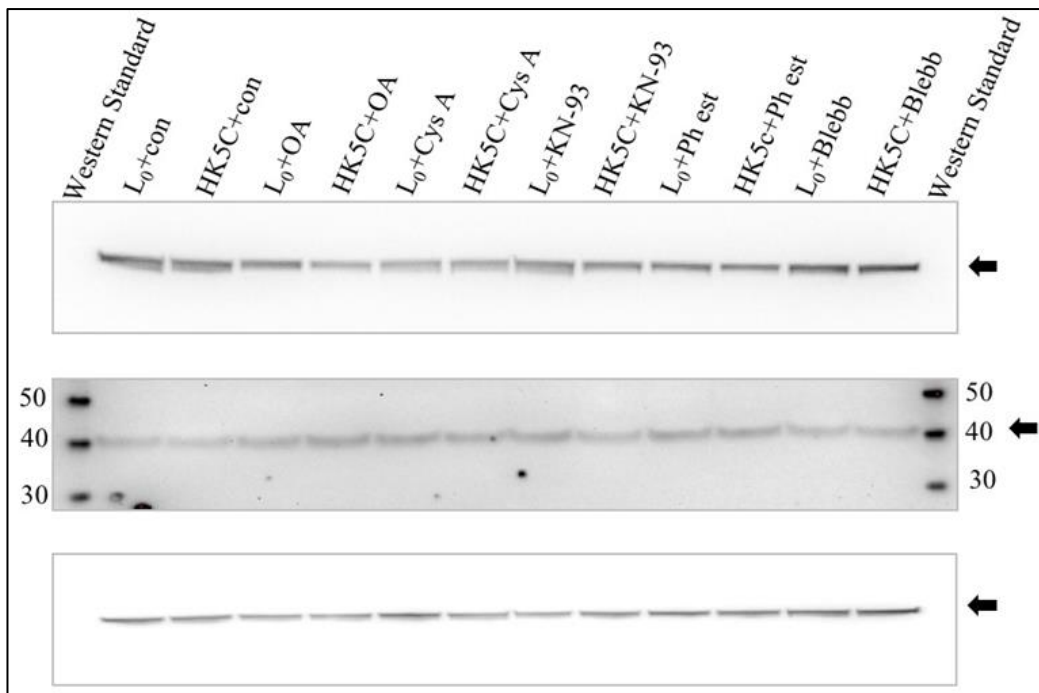


Figure 7.7. Reprobing blots presented in Figure 7.6 with anti-dynamin 4E67 (top and bottom blot) or anti-synaptophysin (middle blot).

Top and bottom blots show the level of dynamin 1 in each track. A second control was used wherein the middle blot was probed with 1:1000 antisynaptophysin antibody.

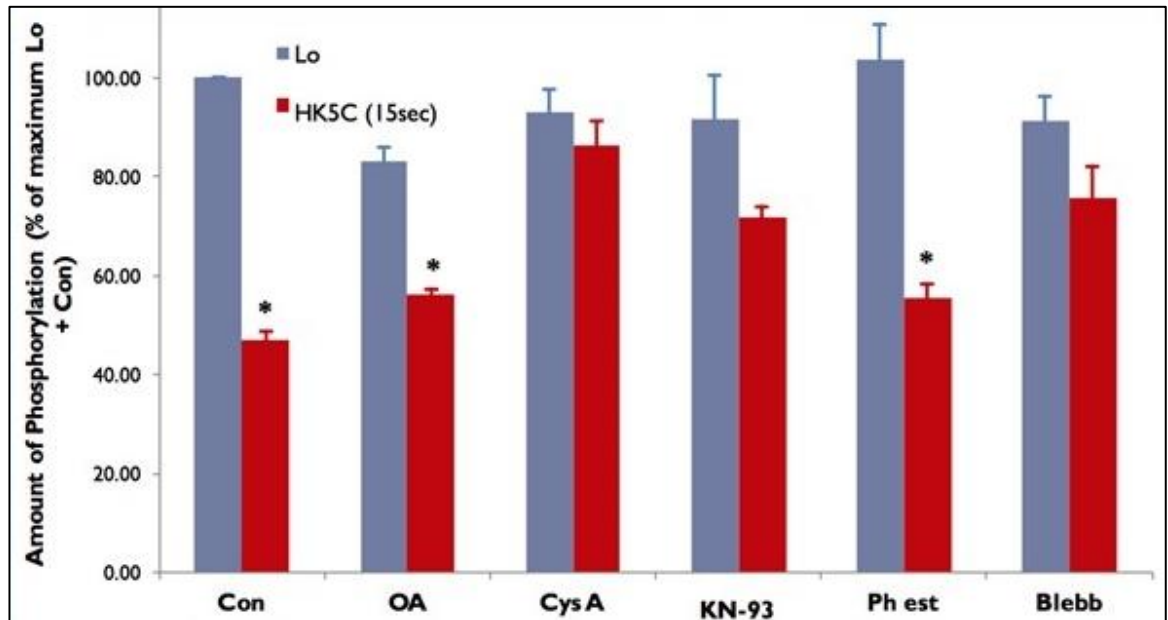


Figure 7.8. Bar chart showing changes produced in p-Dyn774 phosphorylation after the various drug treatments and comparing basal (Lo to HK5C). Data are mean and S.E.M, n=3. $p < 0.05$ for HK5C compared to control.

Figure 7.8 shows changes in p-Dyn774 following various drug treatments and stimulation. It can be observed that following various drug treatments and upon stimulation with HK5C, many samples show a decrease in phosphorylation at the Ser-774 site on dynamin compared to the basal Lo.

Whilst the control and samples treated with OA and Ph est show a significant decrease those treated with KN-93 show some reduction which is not statistically significant whilst both Blebb and Cys A may actually prevent this stimulation induced dephosphorylation.

7.2.4 Phospho-Ser-795

Synaptosomes were prepared exactly as outlined for phospho-ser-778 except these samples were probed with an antibody specifically recognizing phosphoserine-795 of dynamin 1 (Figure 7.9).

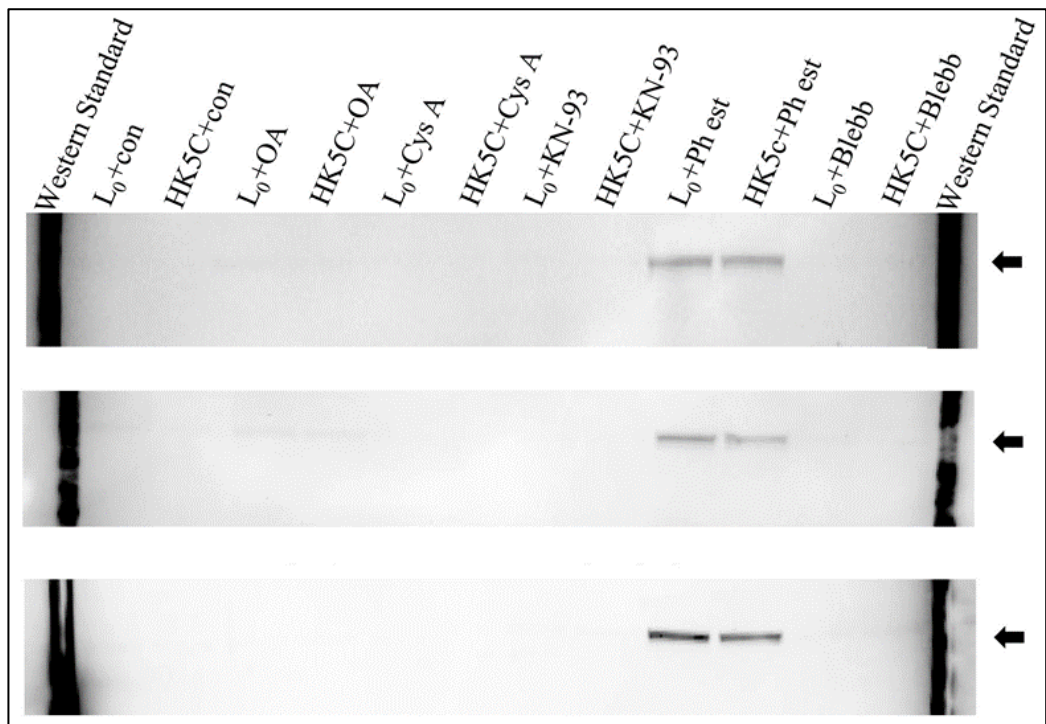


Figure 7.9. The effect of OA, Cys A, KN-93, Ph est, and Blebb drug treatments on phosphorylation of ser-795 of dynamin 1 following the application of HK5C stimulation for 15 sec. The three blots are from 3 independent experiments. The representative blots are indicative of different sample sets with the same drug and stimulation conditions. It can be observed that bands appear only for the samples treated with Ph est and faint bands can be observed for samples treated with OA (see over-exposed image of bottom blot in Figure 7.9.a).

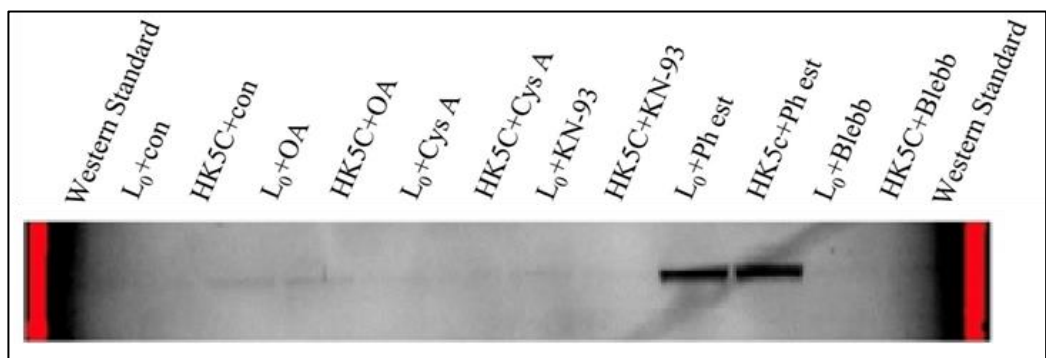


Figure 7.9a. Over-exposed image of bottom blot in Figure 7.9. Faint bands can be observed with OA treated samples and dark bands can be observed with Ph est treated samples.

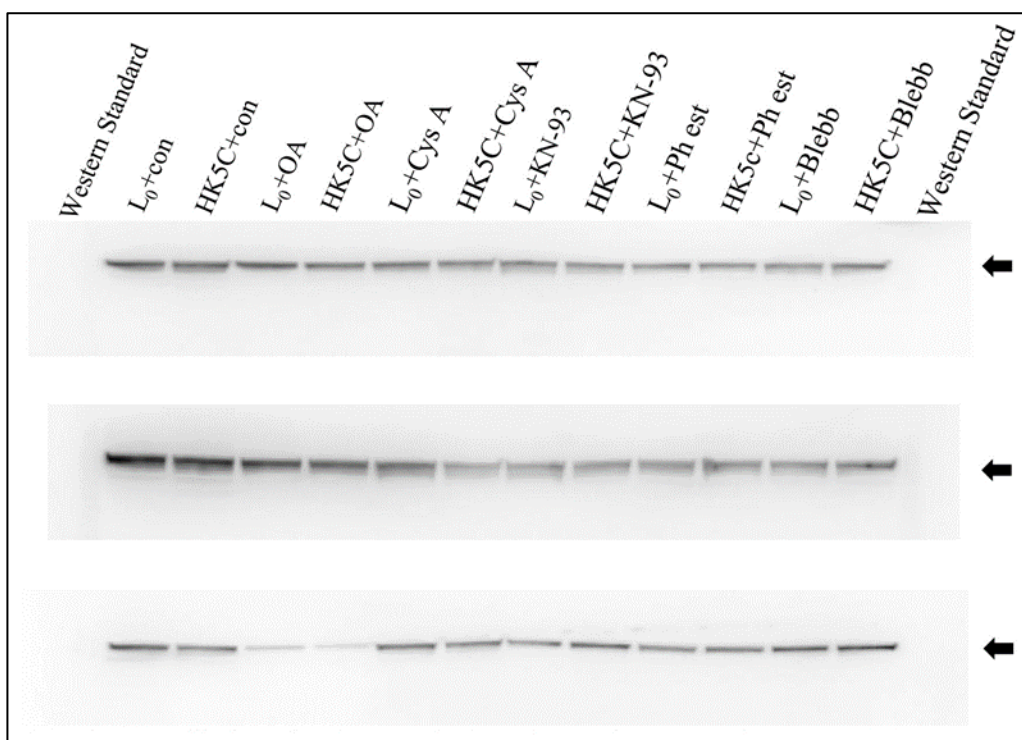


Figure 7.10. Reprobing blots presented in Figure 7.9 with anti-dynamin 4E67. All the blots show same levels intact dynamin 1 except for the OA samples in the bottom gel which seemed to contain less total dynamin 1. The three blots are from 3 independent experiments shown in Figure 7.9.

7.2.5 Regulation of phospho-Ser 795 on dynamin 1 by Ph est and determination as to whether this is due to activation PKC

The large phosphorylation of Ser-795 of dynamin 1 induced by 1 μ M Ph est was assumed to be due to activation of PKCs but this was determined using a double drug treatment (similar to that outlined in earlier chapters) where in some cases the PKC inhibitor Go 6983 (1 μ M) was incubated with synaptosomes prior to the addition of Ph est with subsequent stimulation with basal or HK5C for 15 sec prior to the addition of SDS-sample buffer.

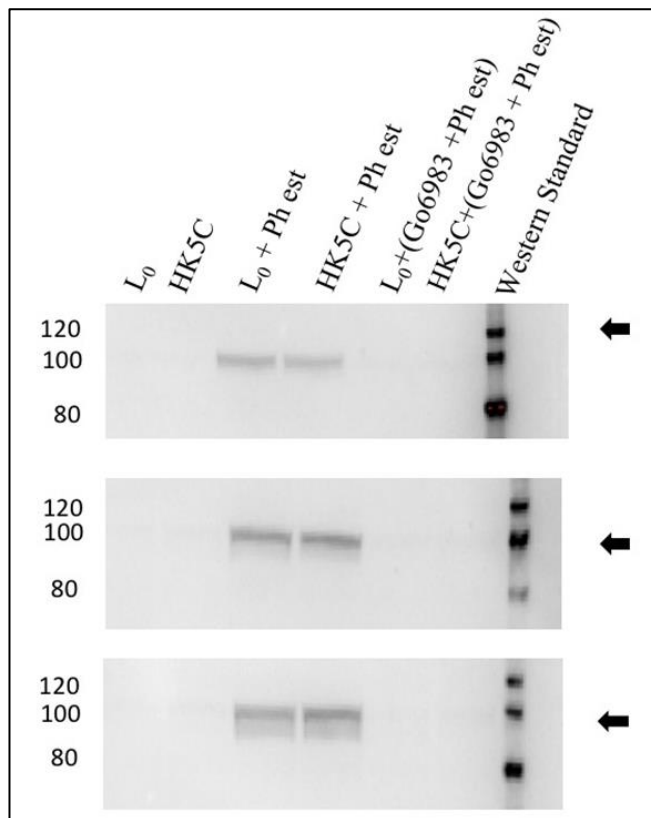


Figure 7.11: Effect of Ph est and GO 6983 + Ph est treatment on phosphorylation of Ser-795 on dynamin 1 following the application of HK5C stimulation for 15 sec. The three blots are from 3 independent experiments. The representative blots are indicative of different sample sets with the same drug and stimulation conditions.

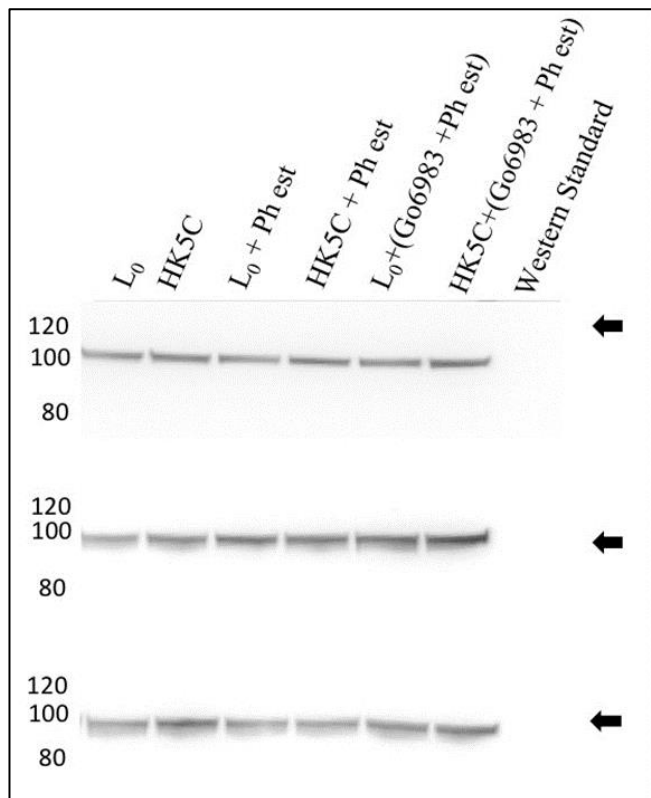


Figure 7.12. Reprobing blots presented in Figure 7.11 with anti-dynamin 4E67. All the blots show similar levels intact dynamin 1. The three blots are from the 3 independent experiments shown in Figure 7.11.

A large phospho-Ser-795 content of dynamin 1 was found following pretreatment with 1 μ M Ph est but there was no phosphorylation at this site if terminals were treated with Go 6983 prior to the addition of Ph est. This indicates that Ph est act by activating PKCs which then regulate the phosphorylation of Ser-795.

7.2.6 The effect that pre-treatment with the conventional PKC inhibitor, Go 6976, has on phosphorylated Ser795 of dynamin as revealed by OA treatment

Synaptosomes were treated, using various conditions (as outlined in results below) and were analysed using western blotting (Figure 7.13). The three blots shown represent different stimulation times induced by the addition of Lo, HK5C and ION5C: top blot (2 s); middle blots (15 s); bottom blot (120 s).

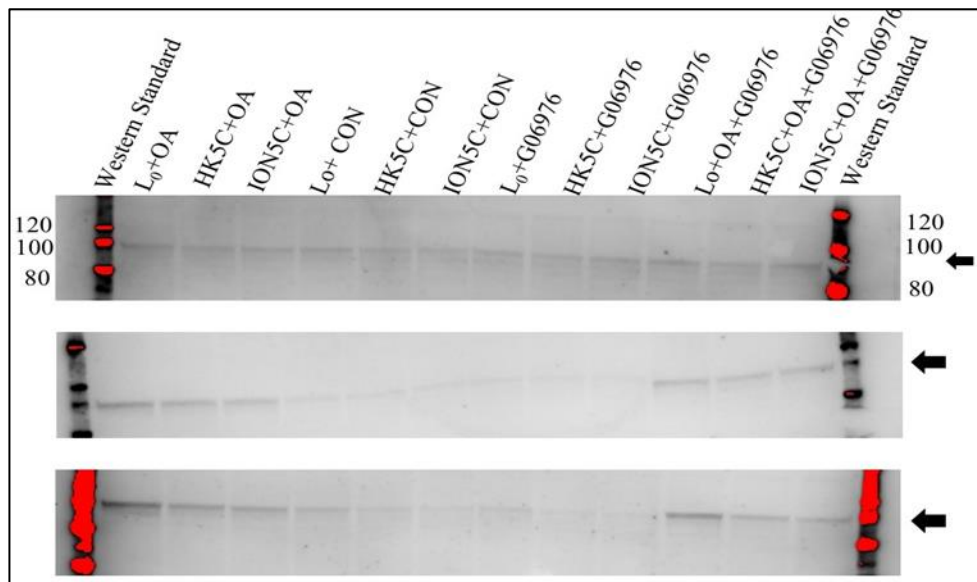


Figure 7.13 The effect of OA, GO 6976, OA+Go 6976 drug treatments on the phosphorylation of Ser-795 on dynamin 1 seen after stimulation. This experiment was repeated 3 times with representative blots being indicative of different sample sets with the same drug and stimulation conditions. Top blot represents the 2 sec stimulation time point blot. Middle blot represents the 15 s stimulation time point. Bottom blot represents the 120 secs stimulation time point

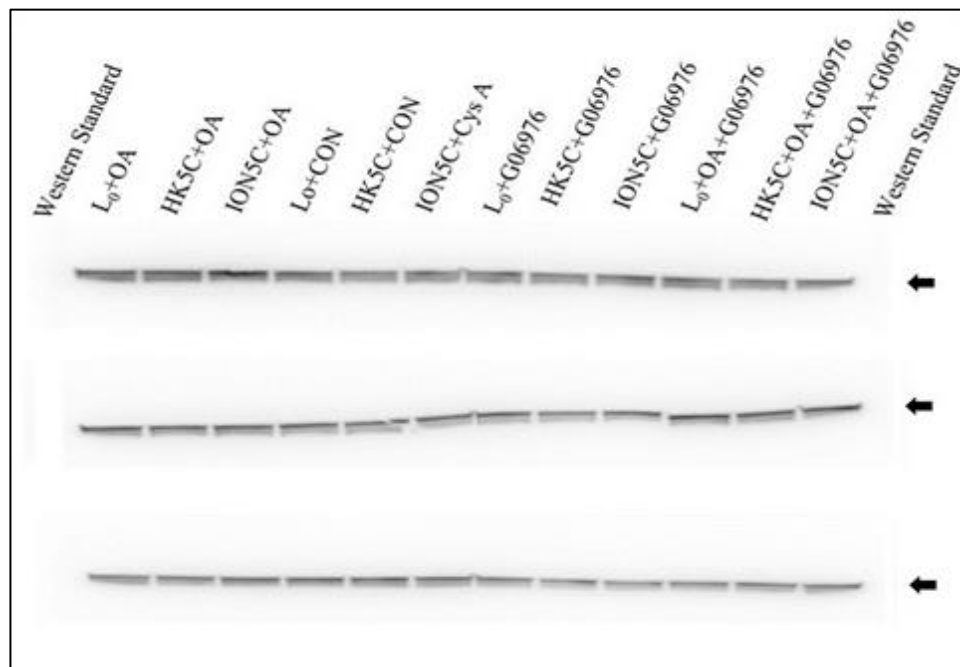


Figure 7.14. Reprobing blots shown in Figure 7.13 with anti-dynamin 4E67. This indicates that there are similar amounts of total dynamin protein in each track for the 2 s time point (top blot), 15 s time point (middle blot) and 120 s time point (bottom blot).

By comparing Figure 7.13 and Figure 7.14 we can make some observations. It would appear that after 2 s of stimulation there is some phospho-Ser795 present in dynamin 1 even in the non-OA treated samples. However, this did not seem to be reduced by the pre-treatment with the Go 6976 inhibitor. There is a slight increase in the amount of phospho-Ser795 in those samples also treated with OA and this increase was still prevalent in samples treated with both Go 6976 and OA. Clearly at later times there appears to be greater amounts of phosphorylated Ser795 dynamin 1 in all those samples treated with OA with or without pre-treatment with Go 6976. However, there is still a small amount of phosphorylation at this site for controls or those treated with the PKC inhibitor.

Neither 15s or 120 s reveal any real difference between control samples and Go 6976 samples. This indicates that in the time scale of this experiment endogenous conventional PKCs are not causing the phosphorylation of Ser795 on dynamin 1.

What is interesting is that there appears to be stimulated mediated reduction in the phosphorylation of Ser795 on dynamin 1 that is time dependent and stimulus dependent. This is difficult to study in any of the samples without OA but is very clear in those samples that were treated with OA. These changes can be quantitated at the different time points when comparing basal stimulation (Lo) with HKC and ION5C at 2 s (Figure 7.15), 15 s (Figure 7.16) and 120 s (Figure 7.17).

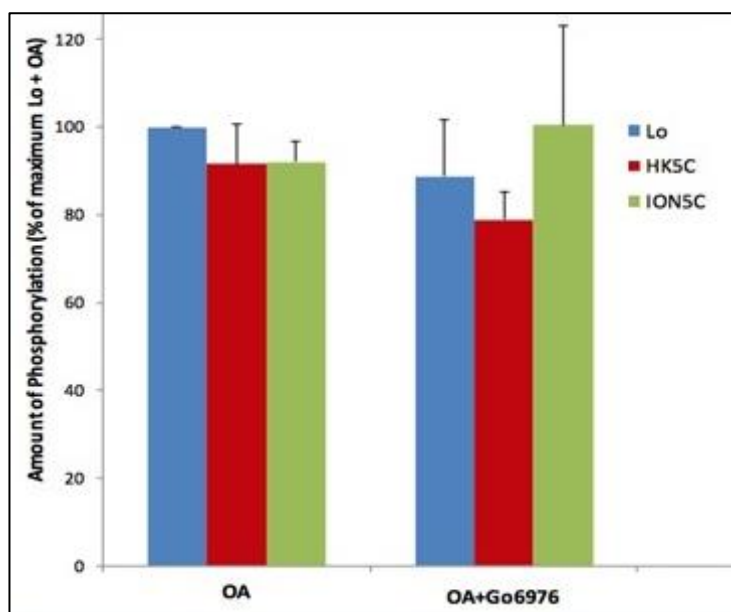


Figure 7.15 Bar chart showing the changes produced in p-Dyn795 phosphorylation following 2 s stimulation in samples treated with OA or OA plus Go 6976. Data are mean and the S.E.M. from 3 independent experiments. There was no significant difference between HK5C or ION5C when compared to the control basal ($p < 0.05$ was considered as significant)

Figure 7.15 indicates that following a 2 s stimulus, there is no difference in the amount of phospho-Ser795 present in the OA treated synapsotomes for HK5C or ION5S stimulus compared to the basal stimulus. Futhermore, this also applied to samples treated with Go 6976 and then OA. Finally, there is no difference between the samples that did or did not have a pre-treatment with Go 6976. This S.E.M.i-quantitative analysis reinforces the comment above that inhibition of conventional PKCs does not prevent OA revealing phosphorylation of Ser795 on dynamin 1.

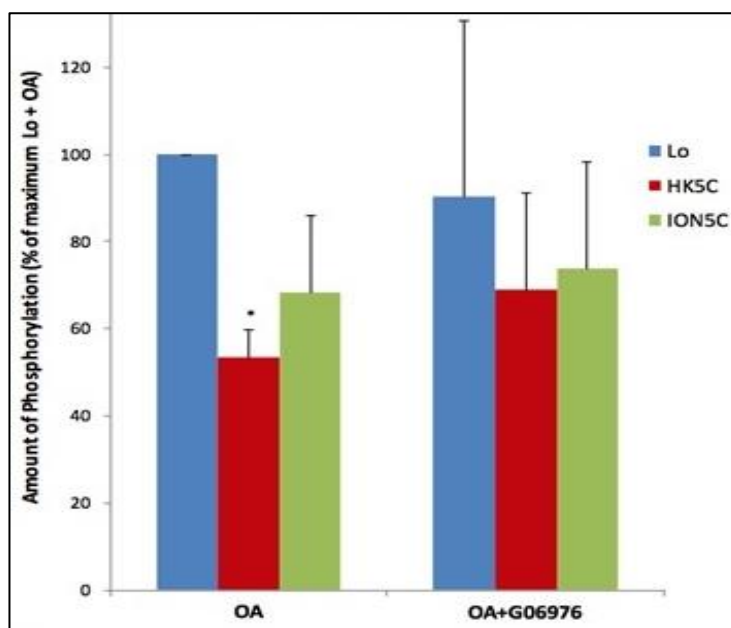


Figure 7.16 Bar chart showing the changes produced in p-Dyn795 phosphorylation following 15 s stimulation in samples treated with OA or OA plus Go 6976. Data are mean and the S.E.M. from 3 independent experiments. There is a significant difference only for the HK5C stimulated sample in the OA treated synaptosome when compared to the basal ($p < 0.05$).

Comparing Figure 7.15 and Figure 7.16, there appears to be a quantitative decrease in the amount of phosphorylated Ser795 in dynamin 1 following a 15 s stimulus with HK5C or ION5C compared to negligible change found in 2 s. However, statistically only the HK5C stimulated sample for OA treated synaptosomes showed a significant decrease.

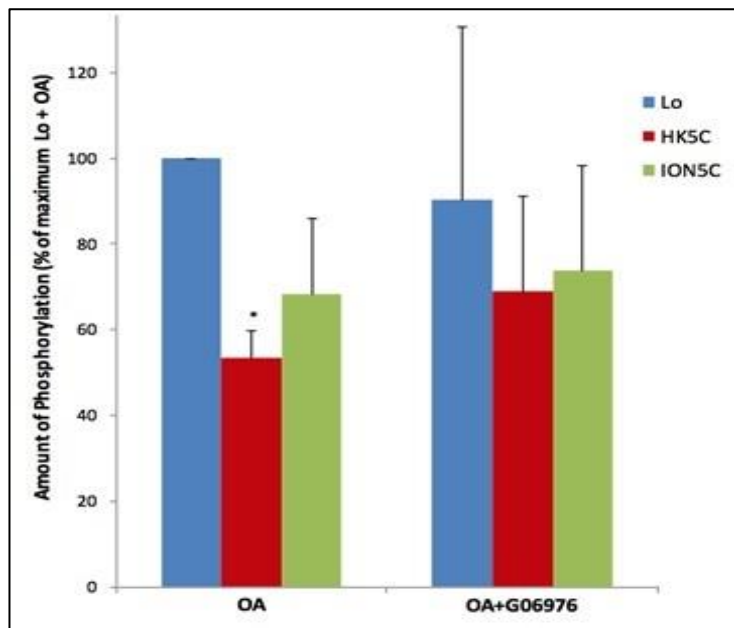


Figure 7.17 Bar chart showing the changes produced in p-Dyn795 phosphorylation following 120 s stimulation in samples treated with OA or OA plus Go 6976. Data are mean and the S.E.M. from 3 independent experiments. There is a significant difference for ION5C and HK5C stimulated sample in both the OA treated and OA plus Go 6976 treated synaptosome when compared to the basal ($p < 0.05$).

There is clearly a significant decrease in the amount of phosphorylated Ser795 dynamin 1 following the applications of either HK5C or ION5C for 120 s compared to the basal control. This applies to synaptosomes treated with OA alone or treated with OA plus Go 6976. Thus, phospho-Ser795 is capable of being regulated in vivo inside the terminals even when PP2A is blocked by OA. However, it is apparent that Go 6976 neither inhibits the amount of phosphorylated Ser795 present in OA treated terminals nor does it prevent the reduction of this phosphorylation following relevant application of the stimuli.

7.2.7 The effect that pre-treatment with the broad spectrum PKC inhibitor Go 6983 has on phospho-Ser795 of dynamin as revealed by OA treatment.

Synaptosomes were treated as outlined above except the broad spectrum PKC inhibitor Go 6983 was employed. The various conditions were run on western blots (Figure 7.18). The three blots shown represent different stimulation times induced by the addition of Lo, HK5C and ION5C: top blot (2 s); middle blots (15 s); bottom blot (120 s).

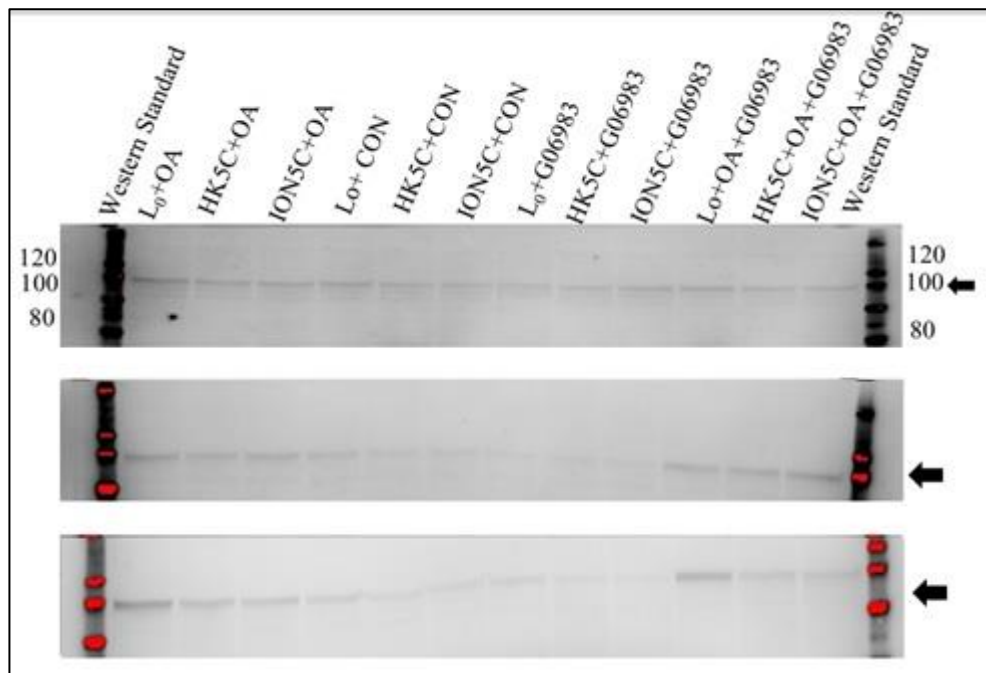


Figure 7.18. The effect of OA, GO 6983, OA+Go 6983 drug treatments on the phosphorylation of Ser-795 on dynamin 1 seen after stimulation. This experiment was repeated 3 times with representative blots being indicative of different sample sets with the same drug and stimulation conditions. Top blot represents the 2 sec stimulation time point blot. Middle blot represents the 15 s stimulation time point. Bottom blot represents the 120 secs stimulation time point.

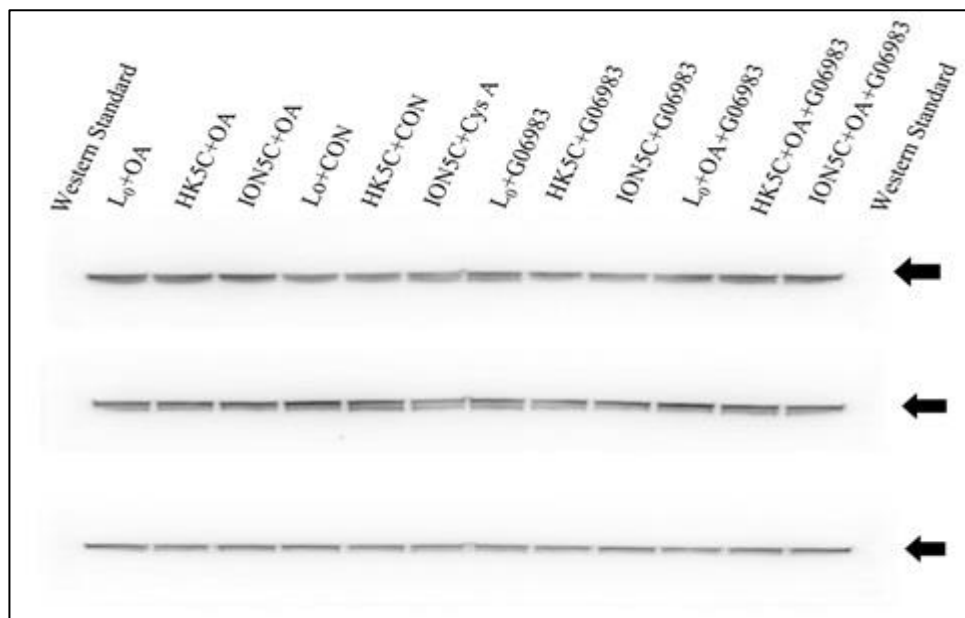


Figure 7.19. Reprobing blots shown in Figure 7.18 with anti-dynamin 4E67. This indicates that there are similar amounts of total dynamin protein in each track for the 2 s time point (top blot), 15 s time point (middle blot) and 120 s time point (bottom blot).

By comparing Figure 7.18 and Figure 7.19 we can make some observations. It would appear that after 2 s of stimulation there is some phospho-Ser795 present in dynamin 1 even in the non-OA treated samples. This did seem to be reduced slightly by the pre-treatment with the Go 6983 inhibitor. There is an increase in the amount of phospho-Ser795 in those samples also treated with OA and this increase was still prevalent in samples treated with both Go 6983 and OA. Clearly at later times there appears to be a greater amounts of phosphorylated Ser795 dynamin 1 in all those samples treated with OA with or without pretreatment with Go 6983. However, there is still a small amount of phosphorylation at this site for controls or those treated with the PKC inhibitor.

15s or 120 s may reveal a slight difference between control samples and Go 6983 samples with the latter containing slightly less phospho-Ser795. This is not perfect and some specific lanes do not appear to agree with this idea. However, it could be that in the time scale of this experiment some endogenous PKCs are causing the phosphorylation of Ser795 on dynamin 1 but these are not the conventional PKCs whose action were not perturbed by treatment with Go 6983. However, this difference is not really revealed when you compare the OA versus OA plus Go 6983.

Again as expected from Figure 7.13, there appears to be stimulated mediated reduction in the phosphorylation of Ser795 on dynamin 1 that is time dependent and stimulus dependent shown in Figure 7.18. This is very clear in those samples that were treated with OA. These changes can be quantitated at the different time points when comparing basal stimulation (Lo) with HKC and ION5C at 2 s (Figure 7.20), 15 s (Figure 7.21) and 120 s (Figure 7.22).

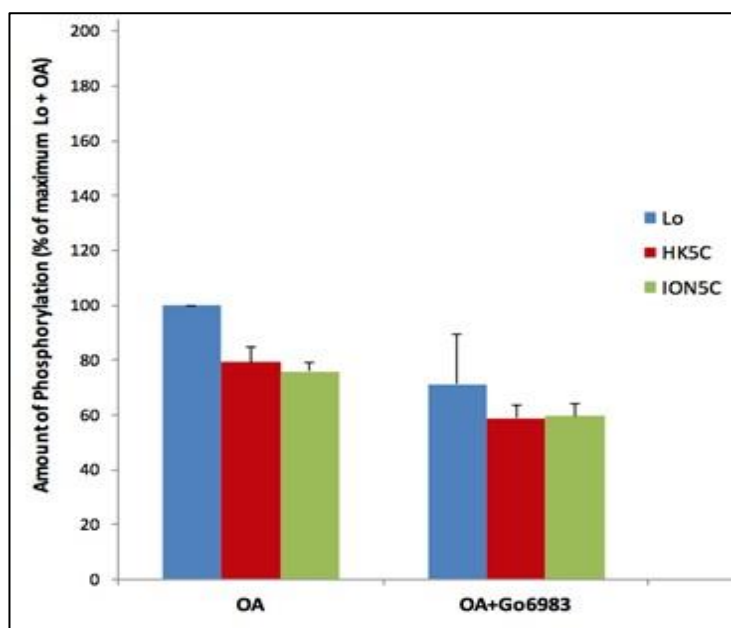


Figure. 7.20. Bar chart showing the changes produced in p-Dyn795 phosphorylation following 2 s stimulation in samples treated with OA or OA plus Go 6983. Data are mean and the S.E.M. from 3 independent experiments. There was no significant difference between HK5C or ION5C when compared to the control basal ($p < 0.05$ was considered as significant).

Although, we were unable to prove statistically that there was a difference between OA and OA plus Go 6983, the values for basal, HK5C and ION5C are all lower for the double treatment than in the equivalent OA treated samples.

However, 2 s did not appear to induce only evoked change in the phospho-Ser795 content of dynamin 1.

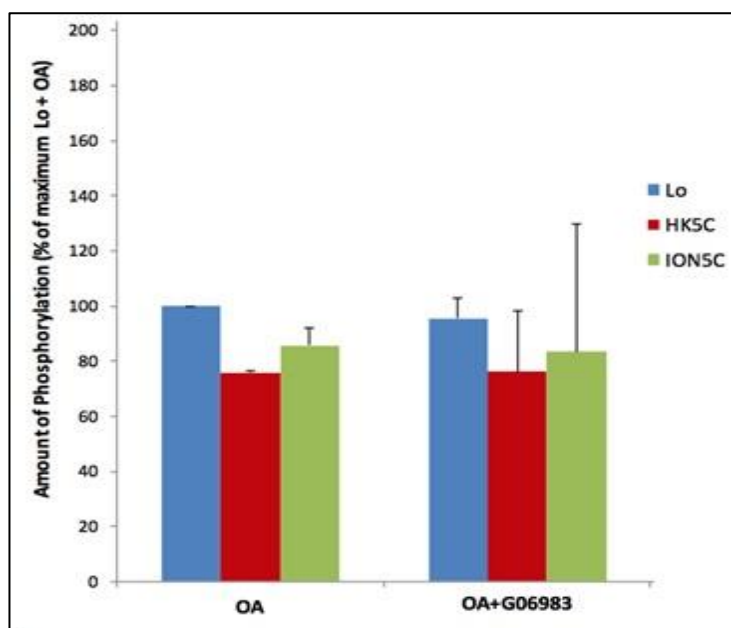


Figure 7.21 Bar chart showing the changes produced in p-Dyn795 phosphorylation following 15 s stimulation in samples treated with OA or OA plus Go 6983. Data are mean and the S.E.M. from 3 independent experiments. There appears to be no significant difference between stimuli and the basal condition ($p < 0.05$).

There appears to be no difference between OA and OA plus Go 6983 in the 15 s stimulated samples (Figure. 7.21) which may infer that the 2 s time point (Figure 7.20) may be incorrect. Furthermore, 15 s did not appear to induce only evoked change in the phospho-Ser795 content of dynamin 1 for any of the stimuli. This is also different from the results reported earlier for OA alone (Figure 7.16). However, the only difference was for the HK5C sample. Clearly, more of these types of experiments need to be carried out to sort out such discrepancies.

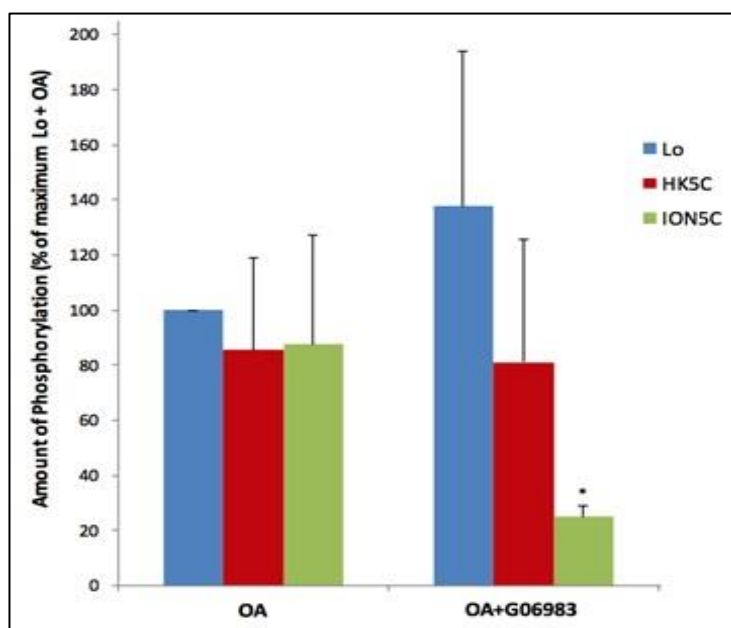


Figure 7.22. Bar chart showing the changes produced in p-Dyn795 phosphorylation following 120 s stimulation in samples treated with OA or OA plus Go 6983. Data are mean and the S.E.M. from 3 independent experiments. There is only a significant difference for ION5C stimulated sample for OA plus Go 6976 treated synaptosome when compared to the basal ($p < 0.05$).

The results for OA treated synaptosomes look very different between Figure 7.17 and 7.22. This indicates the difficulty of quantitating the amounts of phosphorylated Ser795 on dynamin 1. Visual inspection of the blots shown in.

Figure 18 would suggest that there is a stimulus dependent decrease in the phosphorylation of Ser795 after 120 s exposure for both HK5C and ION5C in OA treated terminals. This suggests that one of the three independent experiments may not have worked correctly and so such quantitation does not reveal the correct result. Again, this suggests that this type of experiment may need to be done many more times. Intriguingly, in the blots in Figure 7.17, one can see some stimulus evoked decrease in phospho-Ser795 even in the non-drug treated terminals and this also occurs in the Go 6983 treated terminals.

However, these changes were not quantitated as there is large variation between experiments when one is looking at such low levels of phosphorylation.

7.2.8 Investigating the role of PKA on phosphorylation of Ser-778 and Ser-774 on Dynamin 1

From the results reported in this chapter we found no correlation between changes in phosphorylation of Ser774 and Ser778 on dynamin 1 and the mode of SV exocytosis. Interestingly, we found some interesting observations with phospho-Ser795 that need to be further studied. One problem we had with this site is that we could not determine what the endogenous kinase was that phosphorylated it. It was clear that exogenous activation of PKCs with 1 μ M Ph est could phosphorylate Ser795 on dynamin 1 but when we inhibited PKCs with inhibitors (Go 6983 or Go 6976) we did not seem to reduce the amount of phosphorylation of Ser795. This problem led us to determine whether there may be other kinases that can regulate the mode of exocytosis and also the phosphorylation of dynamin (see earlier chapters). It was clear that both changes in cAMP and PKA could regulate the mode. Therefore, in an initial attempt to discover whether PKA could regulate the mode of exocytosis by changing the phosphorylation state of dynamin 1, we investigated whether PKA could regulate the phosphorylation of Ser774 and Ser778. This was done initially to perhaps show that these sites were not involved before the more difficult experiments on phosphorylation of Ser795 could be attempted.

As we were investigating these pathways, it seemed relevant to mention a few properties about PKA. PKA (E.C. 2.7.11.11) functions as a canonical signal transducer of cAMP and plays a vital role in neuronal outgrowth, survival and regeneration and in axonal growth. Based on the regulatory subunit, the PKA

isoforms can be classified into two categories type I and type II, with type II specifically IIb existing as the predominant form in neurons (Zhong *et. al.*,2009). PKA exerts its regulatory effect through phosphorylation of proteins. Abel and Ngyen have suggested that phosphatases like PP1 and calcineurin can dephosphorylate the proteins which have been previously phosphorylated by PKA, thus reversing the effect exerted by phosphorylation of PKA. Cribbs and Strack (2007) have shown that reversing the phosphorylation of Drp1 (dynamaminrelated protein1) on Ser 656 by PKA and calcineurin helps regulate mitochondrial fission and cell death. The function of PKA has been well described in regulating SNARE complex and thus modulating synaptic function (Baba *et. al.*,2005) The role of PKA has been well described in neurosecretory pathway, it affects the size of RRP in adrenal chromaffin cells by phosphorylating SNAP-25, thus altering the rate of vesicle depriming (Heidelberger and Matthews, 2004). However, the role of PKA in KR mode of exocytosis of synaptic vesicles has not been investigated before.

The aim of this study was to investigate the role of PKA in phosphorylation of ser-778 and ser-774 on dynamin I. The drug treatments employed for the study were 2 μ M KT 5720 (PKA inhibitor), 50 μ M cBIMPS (PKA activator) and 1 μ M Cys A (PP2B inhibitor). It seems relevant just to remind ourselves as to what these drugs do in terms of regulating the mode of SV exocytosis. 1 μ M Cys A blocks the action of PP2B and induces the release of the RP by KR. Inhibition of PKA via 2 μ M KT 5720 causes the SVs of the RRP to undergo more FF for ION5C and 4AP5C, however no change is observed with HK5C. Activation of PKA by 50 μ M cBIMPS induces the release of RP by KR on employing HK5C and ION5C as stimulus. The effect produced by 50 μ M cBIMPS is similar to the effect exerted by 1 μ M CysA. The stimulation employed for this study were

ION5C and HK5C and the timepoints used for this study were 2 secs, 15 secs, 30 secs and 120 secs which should encompass both the time required for the RRP release (2 s) and the RP (complete by about 2 mins). Following the relevant stimulation time point the reactions were terminated with SDS-sample buffer and samples were used to carry out western blotting using the relevant antibodies (as highlighted above).

In the histograms produced after the S.E.M.i-quantitative densitometric analysis the change in the amount of phosphorylation was expressed as a percentage maximum of respective control. Due to time constraint, this study could only be carried out with one sample set. Therefore, no statistical analysis could be employed and there are no measures for S.E.M..

7.2.9 Phospho-serine -774 content of dynamin 1 following manipulation of PKA and PP2B

Synaptosomes were treated as outlined above and the various conditions were run on western blots (Figure 5.13). The four blots shown represent different stimulation times induced by the addition of Lo, HK5C and ION5C: first blot (2 s); second blot (15 s); third blot (30 s); fourth blot (120 s).

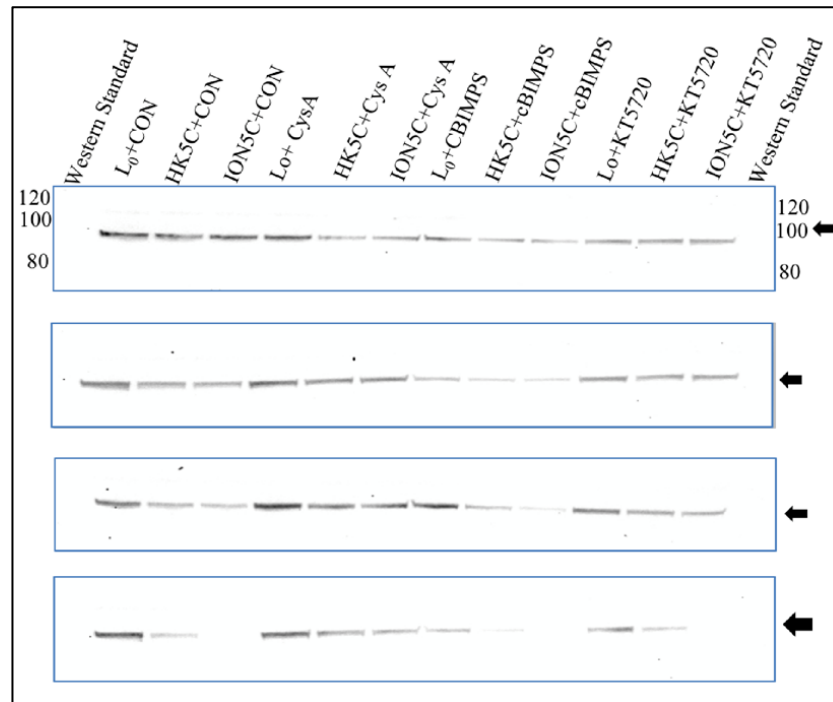


Figure 7.23 The effect of Cys A, cBIMPS, KT 5720 drug treatments on phosphorylation of Ser-774 in dynamin 1 following the application of basal (Lo), HK5C and ION5C stimuli for the time in s: 2 (first blot); 15 (second blot); 30 (third blot); 120 (fourth blot).

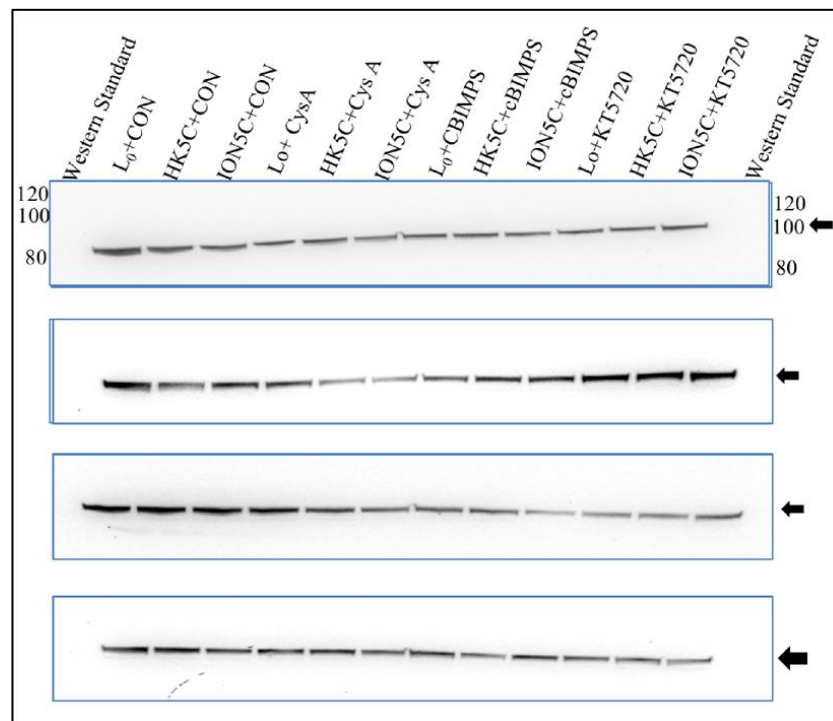


Figure 7.24. Reprobing blots presented in Figure 7.23 with anti-dynamin 4E67. The blots show similar levels of total dynamin.

There is clearly a time dependent decrease in phosphorylation of ser-774 when synaptosomes are stimulated with HK5 or ION5C relative to control. In general, it would appear that there is more dephosphorylation induced by ION5C than by HK5C. All these blots underwent some S.E.M.i-quantative analysis (see below) but it is clear that Cys A inhibits the action PP2B (calcineurin) and prevents to a large extent the dephosphorylation of Ser-774. This result has been well categorised previously. However, it is interesting since it means that dynamin.1 will not be available to contribute to CME or bulk endocytosis (with the caveats already discussed throughout this thesis) and this could possibly explain why the RP SVs which normally require such pathways for recycling may switch to KR as they don't have the same requirement for Ser774 phosphorylation of dynamin 1.

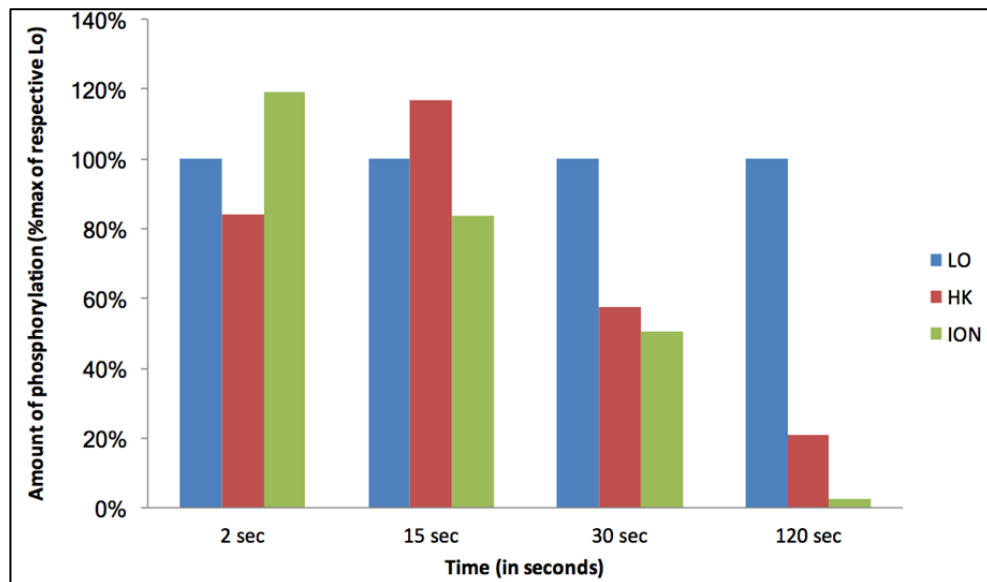


Figure 7.25. Bar chart showing the stimulus evoked time dependent reduction in phospho-Ser774 in non-drug treated synaptosomes. Note in this graphic the basal sample at the different time points is used to normalise the results for the other two stimuli.

Both HK5C and ION5C stimulation induced a time dependent reduction in phosphorylation of Ser774 on dynamin 1 but ION5C seems to act more quickly (change by 15 s for this but not for HK5C) and it also seems to lead by 120s to a greater reduction in the content of this phosphorylated site.

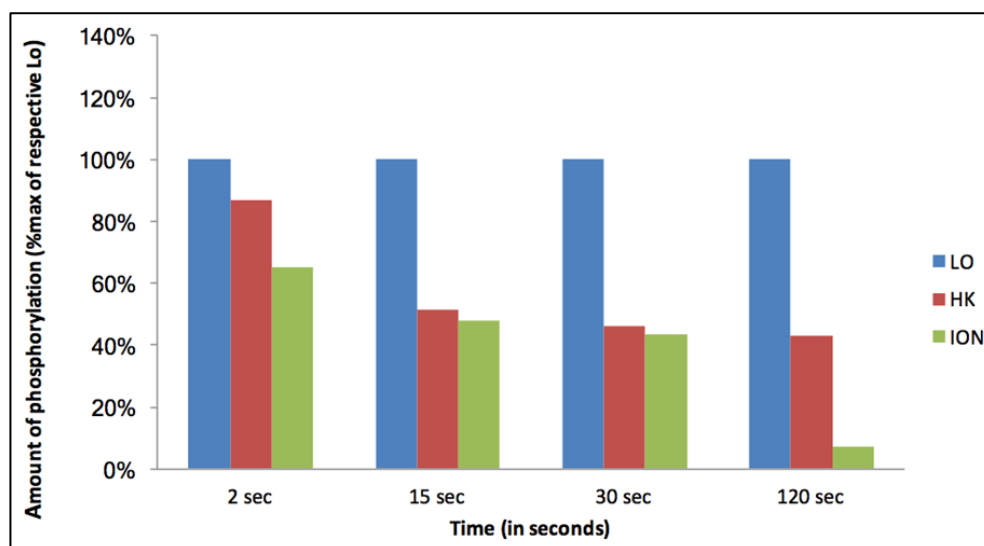


Figure 7.26. Bar chart showing the stimulus evoked time dependent reduction in phospho-Ser774 in Cys A treated synaptosomes. Note in this graphic the basal sample at the different time points is used to normalise the results for the other two stimuli.

For both HK5C and ION5C stimulation, Cys A pretreatment by inhibiting PP2B prevents the dephosphorylation of ser-774 for the first three time points although there is reduction by 120 s when compared to the results for non-drug treated terminals (Figure 7.25). The result for this 2 min time point may reflect that other phosphatases or pathways can reduce this phosphorylation by this time. There are some values which reduce and then gain following longer incubation time points which is not really possible and this just reflects the fact that the experiment needs to be done many more times.

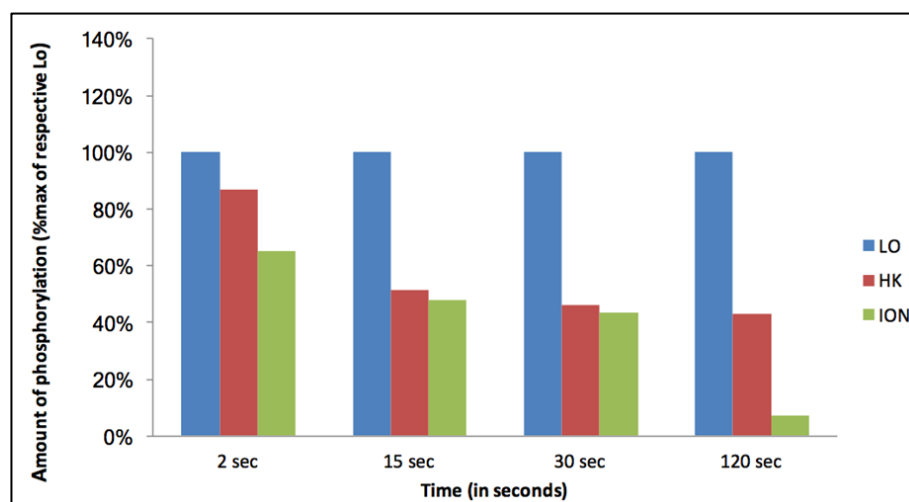


Figure 7.27. Bar chart showing the stimulus evoked time dependent reduction in phospho-Ser774 in cBIMPS treated synaptosomes. Note in this graphic the basal sample at the different time points is used to normalise the results for the other two stimuli.

The results when terminals are treated with cBIMPs is that the two stimuli each reduce the phosphorylation content of Ser774 from 15 s onwards and from these results there seems to be already a reduction by 2 s. Whereas HK5C seems to reduce the level of Ser774 until it reaches a level that does not change.

The results when terminals are treated with cBIMPs is that the two stimuli each reduce the phosphorylation content of Ser774 from 15 s onwards and from these results there seems to be already a reduction by 2 s. Whereas HK5C seems to reduce the level of Ser774 until it reaches a level that does not change (approx. 50%) even after 120 s, the ION5C continues to decrease the level. Comparing these results (Figure 7.27) with the non-drug treated control synaptosomes might suggest (Figure 7.25) that the activation of PKA by cBIMPS actually leads to a greater stimulated reduction in phospho-Ser774 in

dynamamin 1 than with control terminals. This does not fit in with the results with Cys A treated terminals (Figure 7.26) in which there is a great reduction in the stimulus evoked decrease in phosphor-Ser-774 in dynamamin 1 (Figure 7.26). This may be very significant as both treatments switched the mode of the RP of SVs to KR and yet they induce completely different patterns of phosphorylation changes in Ser774. This may well indicate that the changes in phospho-Ser-774 are not related to the modes of exocytosis. This was the conclusion of studies using other drug treatments not connected to PKA pathways.

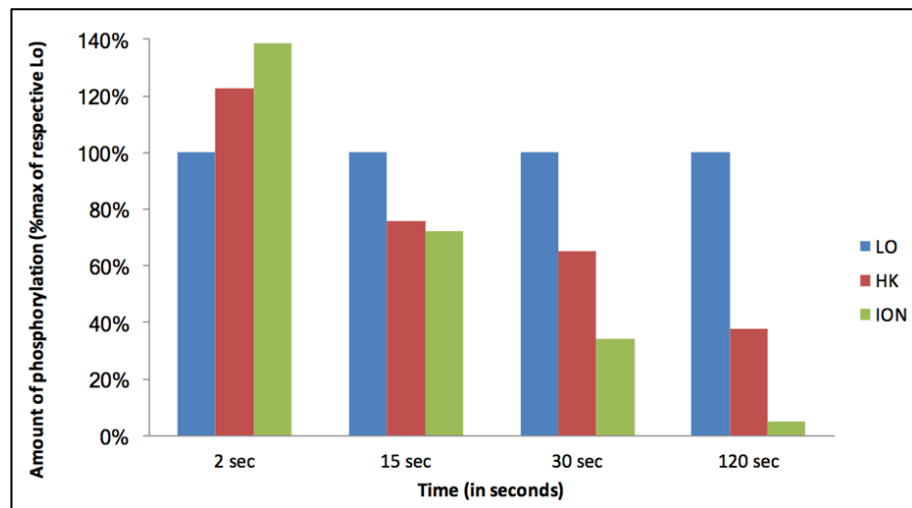


Figure 7.28. Bar chart showing the stimulus evoked time dependent reduction in phospho-Ser774 in KT 5720 treated synaptosomes. Note in this graphic the basal sample at the different time points is used to normalise the results for the other two stimuli.

Figure 7.28 indicates that there is a time dependent stimulus evoked reduction of the content of phospho-Ser774 dynamin in terminals treated with the PKA inhibitor KT 5720. As with other treatments the ION5C seems to cause a larger reduction in phosphor-Ser775 in dynamin 1 than HK5C does. However, comparison between Figure. 7.25 for non-drug treated terminals and Figure 7.28 for KT 5270 treated terminals indicate that these changes look very similar i.e. inhibition of PKA does not affect the phosphorylation changes induced in this phosphorylation site. KT 5720 can switch the RRP SVs to a FF mode for ION5C but not for HK5C but this treatment appears to not affect dynamin 1 phosphorylation at Ser774 may also suggest that this site is not relevant for defining the mode of exocytosis that maybe controlled by dynamin.

7.2.10 Phospho-serine -778 content of dynamin 1 following manipulation of PKA and PP2B

Synaptosomes were treated as outlined above and the various conditions were run on western blots (Figure 7.29) and probed with the antibody to phospho-Ser-778 and for pan-dynamin. The four blots shown represent different stimulation times induced by the addition of Lo, HK5C and ION5C: first blot (2 s); second blot (15 s); third blot (30 s); fourth blot (120 s).

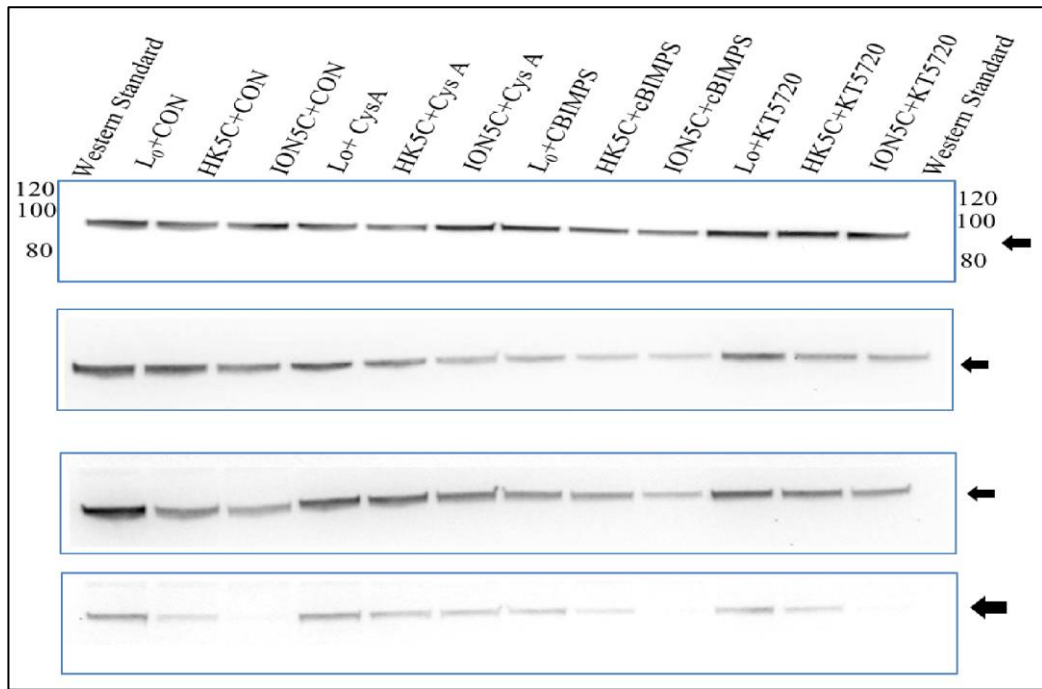


Figure 7.29 The effect of Cys A, cBIMPS, KT 5720 drug treatments on phosphorylation of Ser-778 in dynamin 1 following the application of basal (Lo), HK5C and ION5C stimuli for the time in s: 2 (first blot); 15 (second blot); 30 (third blot); 120 (fourth blot).

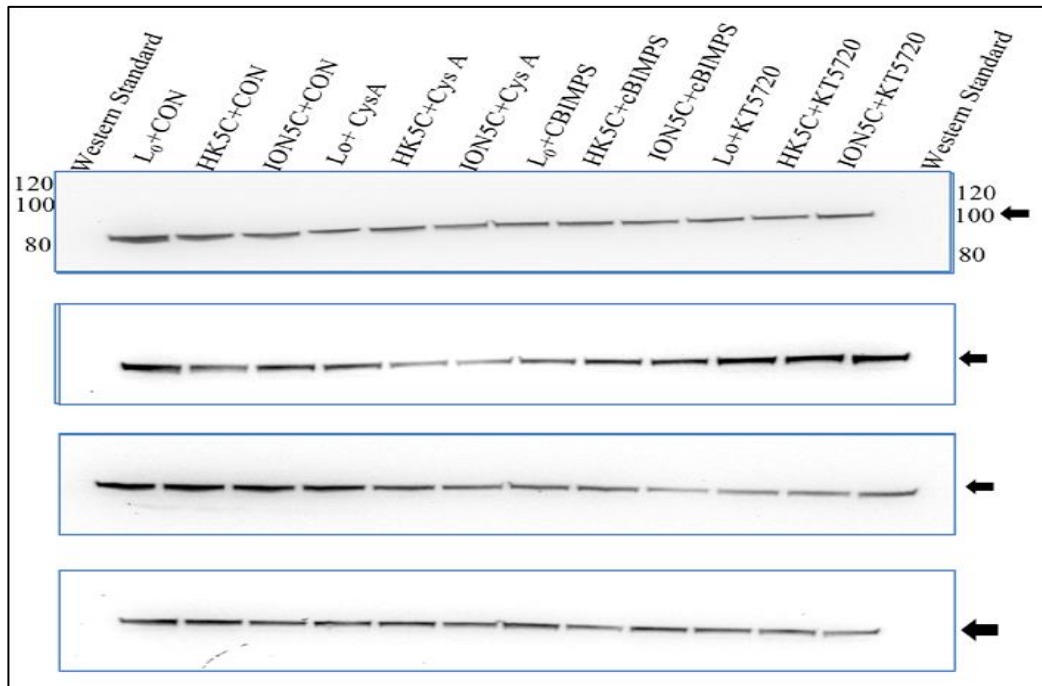


Figure 7.30. Reprobing blots presented in Figure 7.29 with anti-dynamin 4E67. The blots show similar levels of total dynamin.

By comparing Figure. 7.29 and 7.30 one can determine that there is a stimulus evoked time dependent decrease in phosphorylation of ser-778 on dynamin 1 can be observed. Both HK5C and ION5C induce this but just as for the phospho-Ser-774 site, it would appear that ION5C has a larger effect in reducing the phosphorylation. Again, it would appear that Cys A can greatly reduce the dephosphorylation of this site although there is some reduction after 120 s which could be due to the same reasons mentioned above for the Ser774 site. S.E.M.i-quantative analysis of these blots was performed to see if this could reveal some information that was not so obvious from just examining the blots visually.

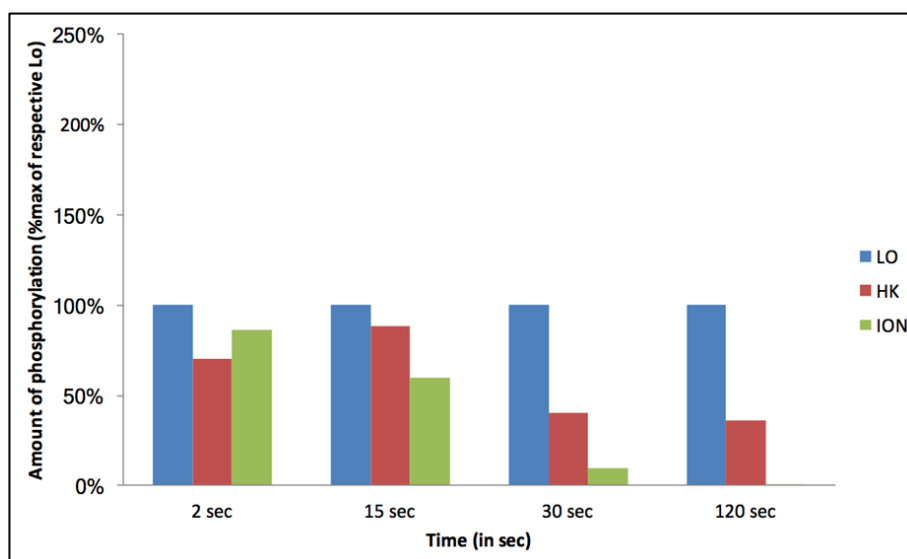


Figure 7.31. Bar chart showing the stimulus evoked time dependent reduction in phospho-Ser778 in non-drug treated synaptosomes. Note in this graphic the basal sample at the different time points is used to normalise the results for the other two stimuli.

Figure 7.31 reveals simply that in non-drug treated terminals there is a stimulus evoked reduction the phosphorylation of ser-778 of dynamin 1 and that this comes mainly apparent after 30 s. However, ION5C seems to induce a faster and stronger reduction in this phosphorylation than does HK5C. This is similar to what occurs with phospho-Ser774 (Figure. 7.25).

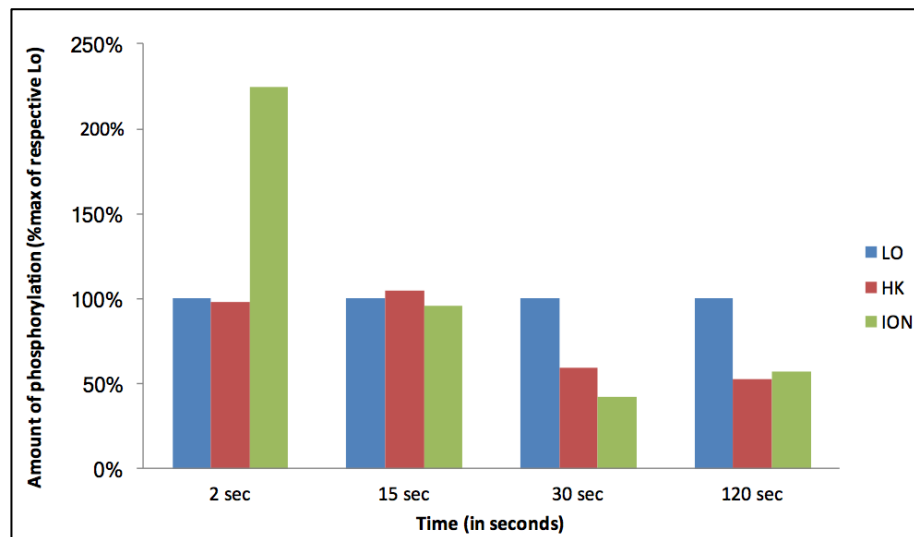


Figure 7.32. Bar chart showing the stimulus evoked time dependent reduction in phospho-Ser778 in Cys A treated synaptosomes. Note in this graphic the basal sample at the different time points is used to normalise the results for the other two stimuli.

It would appear that the sample for 2 s ION5C stimulation in Figure.7.32 might be wrong since this appears to induce an increase in the phosphorylation of Ser788 in dynamin 1. However, if you take this as an error then the first two stimulation time points (2 and 15 s) do not cause a change in this phosphorylation site in synaptosomes in which PP2B is inhibited. However, by 30 s there is a substantial reduction in the phosphorylation of Ser778 for both HK5C and ION5C stimulation although this does not decrease much further after 120 s stimulation. This result for phospho-Ser778 is reminiscent of the result for phospho-Ser774 (Figure. 7.26) although the former seems to undergo some dephosphorylation earlier than the latter site. Note that there is still some substantial amount of phospho-Ser778 even after 120 s stimulation and this is most certainly not the case in the non-drug treated terminals with the ION5C stimulus.

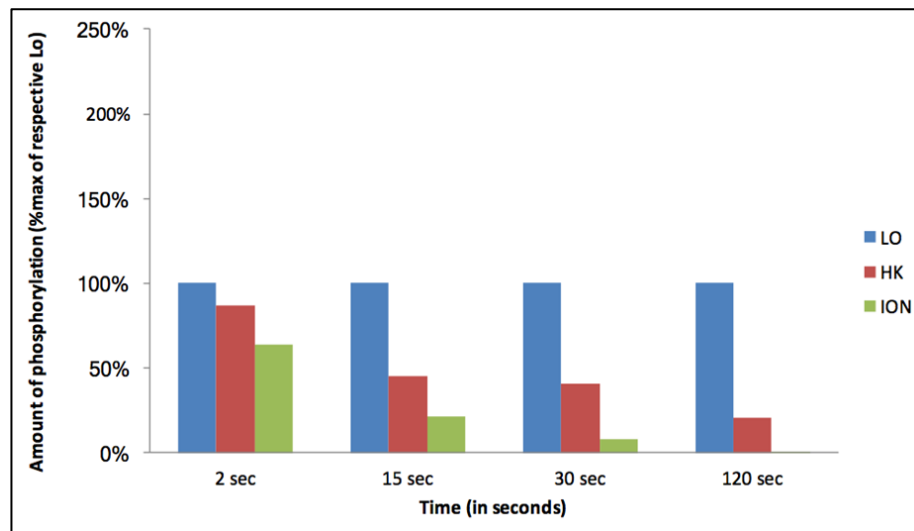


Figure 7.33. Bar chart showing the stimulus evoked time dependent reduction in phospho-Ser778 in cBIMPS treated synaptosomes. Note in this graphic the basal sample at the different time points is used to normalise the results for the other two stimuli.

The activation of PKA with cBIMPs induces the stimuli (HK5C and ION5C) to cause a quicker reduction in phospho-Ser778 (Figure 7.33) than found in the control (Figure 7.31). Again this is completely different to the effect seen for Cys A treated terminasl (Figure. 7.32) even though both drug treatments convert RR SVs to a FF mode. Again, this could rule out a role of phospho-Ser778 in regulation the mode of the fusion pore.

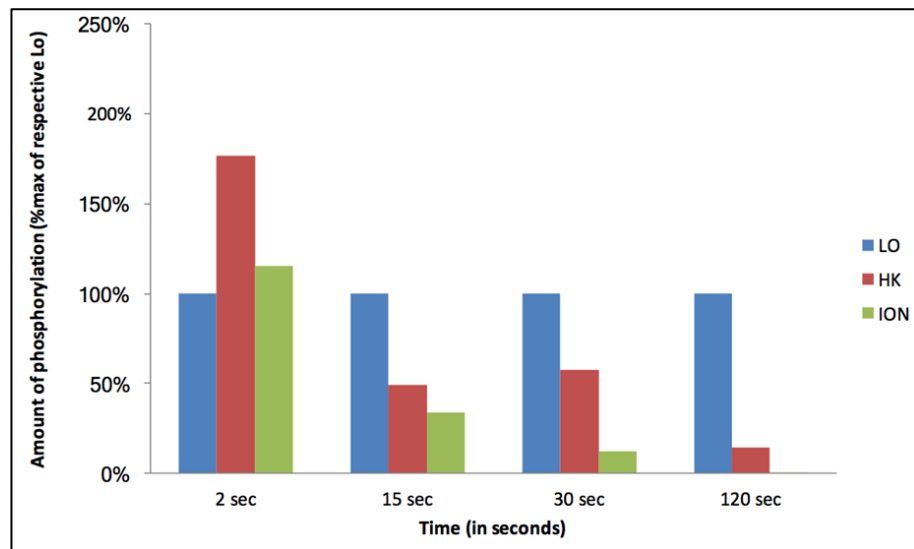


Figure 7.34. Bar chart showing the stimulus evoked time dependent reduction in phospho-Ser778 in KT 5720 treated synaptosomes. Note in this graphic the basal sample at the different time points is used to normalise the results for the other two stimuli.

It would appear that there is an error for the HK5C sample for 2 s stimulation in KT 5720 treated synaptosomes since this appears to induce an increase in the phosphorylation of Ser788 in dynamin 1. For all other time points both HK5C and ION5C induce a dephosphorylation of Ser778 of dynamin 1. Indeed, this might be slightly faster than that in the control samples (Figure 7.31). In fact, this result looks quite similar to the one obtained in synaptosomes treated with cBIMPs (Figure 7.33). This pattern of dephosphorylation of Ser778 is distinct from the change seen for phospho-Ser774 in the KT 5720 treated terminals (Figure. 7.28). In the case of phospho-Ser778 we have an inhibitor of PKA and an activator of PKA actually gives you quite similar phosphorylation changes upon the application of a stimulus. However, these two conditions work on different pools and cause opposite switches in the mode.

7.3 Discussion

Much of the results in this chapter were discussed during the result section as this led onto the next set of experiments. Manipulation of synaptosomes with the various drugs that regulate PKC, Blebb, PP2B and PP2A failed to really show any correlation between the phosphorylated state of dynamin 1 at Ser774 or Ser-778 and the specific mode of certain pools of SVs that these various drugs induced. Likewise, initial studies with manipulation of PKA failed to show a correlation with the mode of exocytosis and the phosphorylation state of Ser774 and Ser778 of dynamin 1. Data herein was able to show stimulation specific reduction in these sites which may be important for CME and bulk endocytosis but clearly these sites do not seem to be involved in defining the mode of exocytosis.

The results with OA and with PKC and PKC blockers on the phosphorylation of Ser795 seemed more promising as there were conditions in which the mode of exocytosis was switched to FF which corresponded to phosphorylation of this site. Recent experiments carried out in the lab definitely suggest that normally the stimuli employed may only work on a sub-population of SVs. This is probably those SVs at the AZ. This could explain why it is so difficult to find a substantial change in say Ser795 if only a small population of this is being phosphorylated. Immunoprecipitation of such a phosphorylated pool of dynamin may prove useful although if it is so low this still may present problems of detection.

The use of Ph est may phosphorylate the Ser-795 of all the dynamin 1 in the terminal. Ashton's group have recently obtained good data for a correlation between this exogenous activated PKC phosphorylation and the modes. Clearly, this treatment will work not only on the relevant pool of dynamin 1 (e.g.

those at the AZ or associated with the pools of SVs) but on all the rest of the dynamin throughout the terminal. Hence, this will be easy to detect unlike perhaps the stimulus induced change in Ser795 of a sub pool of dynamin 1.

A big question that needs to be answered to clarify the situation is what do these drug treatments do to the various phosphorylation sites on non-muscle myosin-II. Clearly, there has to be conditions where a drug that switches both ION5C and HK5C evoked SV exocytosis either to FF (e.g. OA acting on the RRP SVs) or to KR (e.g. Cys A acting on the RP of SVs) must act both on dynamin 1 and on myosin-II. There is currently a large research effort in the Ashton lab to establish these sites on myosin-II that maybe important in mode switching (remember our wdata suggest that myosin-II is activated by a PKC mediated phosphorylation). There needs to be a good correlation between activation of myosin-II by specific phosphorylation sites and inactivation of dynamin 1 on specific phosphorylation sites (Ser795). This research has obtained some very interesting preliminary data about phospho-Ser sites on the myosin-II HC (e.g. Ser1943, Ser1916) that could play a role. Just like the Ser795 site it would appear that drug treatments such as activation of PKC with Ph est can show this important change under conditions where ION5C can switch its requirements from dynamin 1 to myosin-II to close the RRP SVs fusion pore (using 40 nM PMA, see earlier chapters for discussion about this). However, it has proven much more difficult to see HK5C phosphorylating dynamin 1 at Ser795 and inactivating it and at the same time activating the phosphorylation of various sites on the myosin-II molecule. This may also be to do with the fact that there may be only a sub pool of myosin-II within the terminal that is acted upon by HK5C but this is located at the relevant site (e.g.

AZ, SVs) whilst a large amount of myosin-II may not be phosphorylated by HK5C.

Chapter 8

General Discussion and Conclusion

8.1 General discussion and conclusion

SVs can exocytose via FF or by the highly debated mechanism KR. This study presents strong evidence to prove the existence of KR. Elegant studies conducted by Ashton et al have established that a switch in the mode of exocytosis can be brought about by regulating the intracellular calcium levels or by protein phosphorylation. Cerebrocortical synaptosomes derived from adult male Wistar rats have been used as model system.

HK5C, ION5C and 4AP5C induce SV exocytosis through distinct mechanisms in a Ca^{2+} -dependent manner. HK5C produces a relatively fast and large increase in $[\text{Ca}^{2+}]_i$ in comparison to ION5C and 4AP5C which do not produce such a large increase in Ca^{2+} at this region. This is due to the strategic localization of voltage-dependent Ca^{2+} channels here. However, HK5C and ION5C induce release of both releasable SV pools with exocytosis of RRP by KR and the RP undergoing FF, whilst 4AP5C results in the exocytosis of RRP by a mixture of KR and FF.

In this study, the role of two major proteins, dynamins and non-muscle myosin-II involved in KR mode of exocytosis has been investigated. It has been shown here, in the results presented in chapter 3, the activity of both these proteins in regulating the fusion pore can be mediated through the action of PKCs and through the increase in $[\text{Ca}^{2+}]_i$ at the AZ (see diagram 8.1).

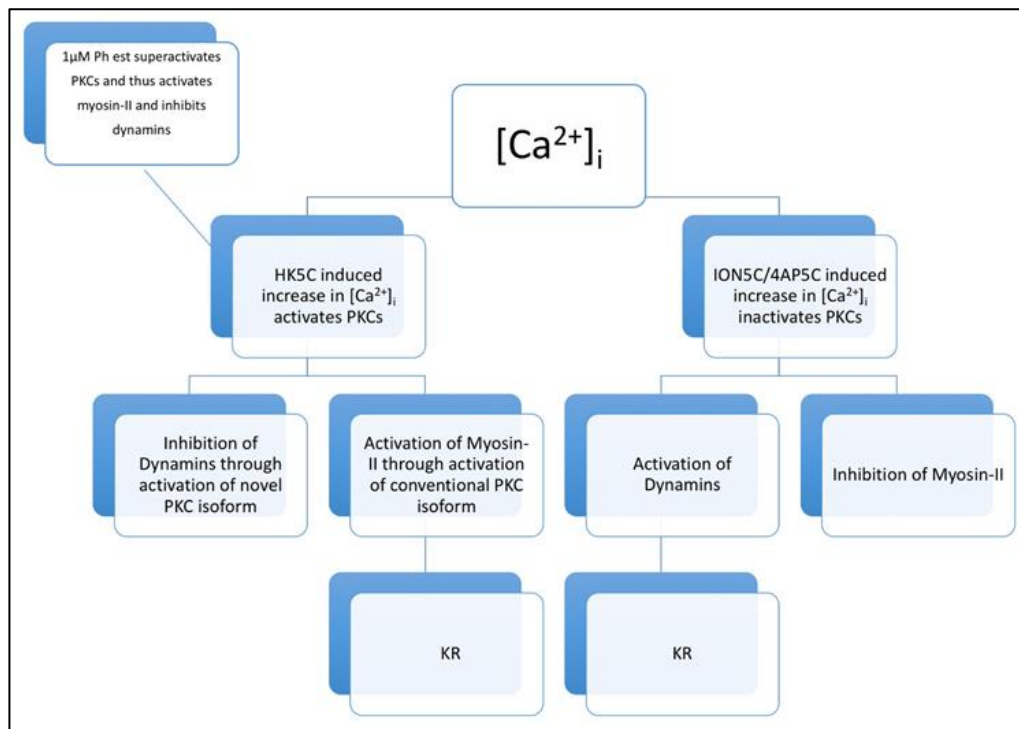


Figure 8.1. A schematic representation of the action of PKCs. HK5C induced increase in $[Ca^{2+}]_i$ results in activation of PKCs which results in inactivation of dynamins through activation of a novel PKC isoform and activation of myosin II via conventional PKC isoform. Thus myosin-II mediates the action of the fusion pore causing the vesicles to KR. $1\mu\text{M}$ Ph est superactivates PKCs resulting in inhibition of dynamins and activation of myosin-II. For ION5C and 4AP5C the action of the fusion pore is dynamin-dependent resulting in KR of SVs. The figure suggests that the $[Ca^{2+}]_i$ induced at the AZ may actually lead to an inhibition of PKCs. However, it is more likely that it just does not activate PKCs so dynamin is not inactivated whilst myosin-II is not activated.

Chapter 6, elucidates the importance of bioenergetics assay which helped decipher the optimum concentration of PAO. Thus, the bioenergetics observations for the other drugs help conclude that the drugs are target specific and do not perturb the mitochondrial respiration.

The last part of the study was investigating the role of phosphorylation of Ser778, Ser-774 and Ser-795 on dynamins. It was concluded that Ser-774 and Ser-778 may play a role in CDE and bulk endocytosis (the changes in phosphorylation of these sites correspond nicely with possible pathways involving these two processes) as previously documented but these sites do not show any correlation with dynamin's activity towards regulating closure of the fusion pore. However, the results also suggest that the phosphorylation of Ser-795 may play an important role in the inhibition of dynamin's activity and thereby preventing it from closing the fusion pore of exocytosing vesicles.

Phosphorylation studies involving the combination treatment of Ph est and Go 6983 indicated that the phosphorylation of Ser-795 may be under the regulation of PKC. It is possible that PKC may phosphorylate this site when a very high $\Delta[\text{Ca}^{2+}]_i$ is achieved at the active zone. Furthermore, on investigating the role of PKCs on the phosphorylation of ser-795 on dynamin-I, it was observed that due to the low phosphorylation levels obtained on employing Go 6983 and Go 6976 drug treatments, it was difficult to obtain a conclusion as to which PKC isoform could regulate the mode of SV exocytosis by phosphorylation of Ser795. This could of course mean that there is a distinct phosphorylation site on dynamin 1 that is regulated but which we have not investigated. For the phosphorylation studies conducted to decipher the role of PKA on the phosphorylation of ser-774 and ser-778 on dynamin 1, it was observed that again ser-774 and ser-778 do not show any correlation with dynamin's activity

towards regulating closure of the fusion pore for PKA drug treatments. The experiment needs to be repeated to confirm these findings.

8.2 Future directions

This study gives an insight into the activity of PKA and PKC in regulating the mode of synaptic vesicle fusion. However, a substantial amount of work still needs to be undertaken to elucidate the mechanism of SV exocytosis.

- a) The effect of HK5C and ION5C on ser-774 and ser-778 phosphorylation for PKA drug treatments needs to be repeated to provide a definitive conclusion about the role of regulation of PKA on Ser-774 and Ser-778 in phosphorylation of dynamin 1. One also needs to investigate the role of PKA drug treatments on the phosphorylation of Ser-795. The experiments also need to be carried out with 4AP5C stimulation. After the role of dynamins has been elucidated, it is important to elucidate the role of myosin-II phosphorylation sites. If we are unable to prove that the well-characterised phosphorylation sites play a role then we need to find evidence that other phosphorylation sites are involved. This can be investigated by immunoprecipitating dynamins or myosin II by using antibodies that specifically recognise phosphorylated serine residues. Alternatively, further analysis could be carried out by using phosphoproteomic techniques to enrich the phosphorylated proteins and utilising mass spectrometry to determine the phosphorylation sites.
- b) Immunoprecipitation of the distinct dynamin isoforms may help elucidate the specific phosphorylation changes. Although, not discussed herein there are some splice variants of dynamin 1 and it may be a specific type that plays a role in modulating the mode of exocytosis.

- c) To carry out bioenergetics assay for the rest of the drug treatments so as to investigate their effects on mitochondrial respiration. In particular, we have not tested the double drug treatments and as this may provide some essential information we need to make sure that such treatments are not actually detrimental to the bioenergetics integrity of the nerve terminals.
- d) To repeat the biochemical experiments carried out with 0.3 μ M PAO instead of 3 μ M PAO so as to elucidate the role of inhibition of PI(4)kinase on regulation of SV exocytosis.
- e) To establish the role of EPACS in the mode of release and also establish its role in conjunction with other drug treatments.
- f) To investigate the role of dynamin 1 by using dynole-34-2TM (since 20 μ M dynole specifically blocks dynamin 1). Also, to investigate the role of dynamin 2 using dyngo, as 50 μ M specifically blocks dynamin 2. This has already been performed for simply measuring ION5C evoked release but more can be done (see below).
- g) To investigate further the role of dynamin 2 by comparing the actions of dyngo on 4AP5C and HK5C. Our argument about dynamin 1 not being active at active zone with HK5C due to PKC stimulation should not apply to the RP which sees a lot less calcium and PKC should not be activated. So dyngo may be able to regulate RP stimulation by HK5C and should have no effect on 4AP5C which doesn't release the RP.
- h) To investigate the PKC isoform involved in mode switching and also the myosin-II isoform and sub-units that are involved in this process. This would be an exciting set of experiments which can be done. There are several isoforms of PKC and these can be inhibited by specific inhibitors against those

isoforms. So rather than using GO 6983 which blocks all PKC isoforms, specific inhibitors can be used to determine which PKC isoform phosphorylates dynamin and which phosphorylates myosin-II. This may reveal that distinct PKCs regulate these two different proteins. HK5C.

References

- Alabi, A.A. and Tsien, R.W. (2013). 'Perspectives on kiss-and-run: role in exocytosis, endocytosis, and neurotransmission'. *Annu Rev Physiol.* 75, 393-422.
- Andreas, W.H., Kang, G. and Kornhuber, J. (2001). 'A common molecular machinery for exocytosis and the 'kiss-and-run' mechanism in chromaffin cells is controlled by phosphorylation'. *Journal of Cell Science.* 114, 4613-4620.
- Armbruster, M., Messa, M., Ferguson, S.M., De Camilli, P. and Ryan, T.A. (2013). 'Dynamin phosphorylation controls optimization of endocytosis for brief action potential bursts'. *eLife.* 2, e00845.
- Ashton, A.C. and Ushkaryov, Y.A. (2005). Properties of synaptic vesicle pools in mature central nerve terminals. *The journal of Biological Chemistry.* 280 (44), 37278-37288.
- Baba, T., Sakisaka, T., Mochida, S. and Takai, Y. (2005). 'PKA-catalyzed phosphorylation of tomosyn and its implication in Ca²⁺-dependent exocytosis of neurotransmitter'. *The Journal of Cell Biology.* 170(7), 1113-1125.
- Bangalore, L. (2009). *Brain Development.* Infobase Publishing.
- Brady, S.T, Siegel, G., Albers, R.W. and Price, D. (2005). *Basic Neurochemistry: Molecular, Cellular and Medical Aspects.* 7th ed. Academic Press.
- Brady, S.T. and Siegel, G.J. (2012). *Basic Neurochemistry: Principles of Molecular, Cellular and Medical Neurobiology.* Academic Press.
- Brand, M.D. and Nicholls, D.G. (2011). Assessing mitochondrial dysfunction in cells. *Biochem J.* 435 (Pt 2), 297-312.
- Calejo, A.I., Jorgačevski, J., Rituper, B., Guček, A., Pereira, P.M., Santos, M.A.S., Potokar, M., Vardjan, N., Kreft, M., Gonçalves, P.P. and Zorec, R. (2014). 'Hyperpolarization-Activated Cyclic Nucleotide-Gated Channels and cAMP-Dependent Modulation of Exocytosis in Cultured Rat Lactotrophs'. *The Journal of Neuroscience.* 34(47), 15638-15647.
- Cesca, F., Baldelli, P., Valtorta, F. and Benfenati, F. (2010). 'The synapsins: key actors of synapse function and plasticity'. *Prog. Neurobiol.* 91, 313-348.
- Chandrasekar, I., Huettner, J.E., Turney, S.G. and Bridgman, P.C. (2013). 'Myosin II regulates activity dependent compensatory endocytosis at central synapses'. *J. Neurosci.* 33, 16131-16145.

- Chandrasekar, I., Huettner, J.E., Turney, S.G. and Bridgman, P.C. (2013). 'Myosin II Regulates Activity Dependent Compensatory Endocytosis at Central Synapses'. *The Journal of Neuroscience*. 33(41), 16131-16145.
- Chang, C.-R., and Blackstone, C. (2007). 'Drp1 phosphorylation and mitochondrial regulation'. *EMBO Reports*. 8(12), 1088–1089.
- Cheung, G. and Cousin, M.A. (2013). 'Synaptic vesicle generation from activity dependent bulk endosomes requires calcium and calcineurin'. *Journal of Neuroscience*. 33, 3370-3379.
- Chircop, M., Sarcevic, B., Larsen, M.R., Malladi, C.S., Chau, N., Zavortink, M., Smith, C.M., Quan, A., Anggono, V., Hains, P.G., Graham, M.E. and Robinson, P.J. (2011). 'Phosphorylation of dynamin II at serine-764 is associated with cytokinesis'. *Biochimica et Biophysica Acta (BBA) - Molecular Cell Research*. 1813(10), 1689-1699.
- Cho, S. and von Gersdorff, H. (2013). 'Neuroscience: Faster than kiss-and-run'. *Nature*. 504, 220-221.
- Clayton, E.L. and Cousin, M.A. (2009). 'The Molecular Physiology of ActivityDependent Bulk Endocytosis of Synaptic Vesicles'. *Journal of Neurochemistry*. 111, 901-914.
- Clayton, E.L., Anggono, V., Smillie, K.J., Chau, N., Robinson, P.J. and Cousin, M.A. (2009). 'The phospho-dependent dynamin-syndapin interaction triggers activity-dependent bulk endocytosis of synaptic vesicles'. *J. Neurosci*. 29, 7706-7717.
- Clayton, E.L., Sue, N., Smillie, K.J., O'Leary, T., Bache, N., Cheung, G., Cole, A.R., Wyllie, D.J., Sutherland, C., Robinson, P.J. and Cousin, M.A. (2010). 'Dynamin I phosphorylation by GSK3 controls activity-dependent bulk endocytosis of synaptic vesicles'. *Nat Neurosci*. 13(7), 845-851.
- Clementi, F. (2012). *Neurotransmitter Release the Neuromuscular Junction*. Elsevier.
- Cocucci, E., Gaudin, R. and Kirchhausen, T. (2014). 'Dynamin recruitment and membrane scission at the neck of a clathrin-coated pit'. *Mol Bio Cell*. 25, 35953609.
- Cousin, M.A., Tan, T.C. and Robinson, P.J. (2001). 'Protein phosphorylation is required for endocytosis in nerve terminals: potential role for the dephosphins dynamin I and synaptojanin, but not AP180 or amphiphysin'. *J. Neurochem*. 76(1), 105-116.
- Crawford, D.C. and Mennerick, S. (2012). 'Presynaptically Silent Synapses: Dormancy and Awakening of Presynaptic Vesicle Release'. *The Neuroscientist*. 18(3), 216-223.

- Cribbs, J.T. and Strack, S. (2007). 'Reversible phosphorylation of Drp1 by cyclic AMP-dependent protein kinase and calcineurin regulates mitochondrial fission and cell death'. *EMBO Rep.* 8(10). 939-944.
- Denker, A. and Rizzoli, S.O. (2010). 'Synaptic vesicle pools: an update'. *Front synaptic neuroscience.* 2,135.
- Doreian, B.W., Fulop, T. and Smith, C. (2008). 'Regulation of activity dependent transmitter release from chromaffin cells by F-actin and non-muscle myosin II'. *FASEB.* 22(1195.2).
- Doussau, F., Humeau, Y., Benfenati, F. and Poulain, B. (2010). 'A Novel Form of Presynaptic Plasticity Based on the Fast Reactivation of Release Sites Switched Off during Low-Frequency Depression'. *The Journal of Neuroscience.* 30(49), 16679-16691.
- Earnest, S., Khokhlatchev, A., Albanesi, J.P. and Barylko, B. (1996). 'Phosphorylation of dynamin by ERK2 inhibits the dynamin-microtubule interaction'. *FEBS Lett.* 396(1), 62-66.
- Fà, M., Staniszewski, A., Saeed, F., Francis, Y.I. and Arancio, O. (2014). 'Dynamin 1 is required for memory formation'. *PLoS ONE.* 9, e91954.
- Fasshauer, D., Sutton, R.B., Brunger, A.T. and Jahn, R. (1998). 'Conserved structural features of the synaptic fusion complex: SNARE proteins reclassified as Q- and R-SNAREs'. *Proc Natl Acad Sci USA.* 95, 15781-15786.
- Ferguson, S.M. and Camili P.D. (2012). 'Dynamin, a membrane remodelling GTPase'. *Nat Rev Mol Cell Biol.* 13, 75-78.
- Fernandes, H.B., Riordan, S., Nomura, T., Remmers, C.L., Kraniotis, S., Marshall, J.J., Kukreja, L., Vassar, R. and Contractor, A. (2015). 'Epac2 Mediates cAMP-Dependent Potentiation of Neurotransmission in the Hippocampus'. *The Journal of Neuroscience.* 35(16), 6544-6553.
- Fesce, R., Grohovaz, F., Valtorta, F. and Meldolesi, J. (1994). 'Neurotransmitter release: fusion or 'kiss-and-run'?' *Trends Cell Biol.* 4, 1-4.
- Fornasiero, E., Raimondi, A., Guarnieri, F.C., Orlando, M., Fesce R., Benfenati, F. and Valtorta, F. (2012). 'Synapsins Contribute to the Dynamic Spatial Organization of Synaptic Vesicles in an Activity-Dependent Manner'. *The Journal of Neuroscience.* 32(35), 12214-12227.
- Fraga, D., Sehring, I.M., Kissmehl, R., Reiss, M., Gaines, R., Hinrichsen, R. and Plattner, H. (2015). 'Protein phosphatase 2B (PP2B, Calcineurin) in Paramecium: Partial characterization reveals that two members of the unusually large catalytic subunit family have distinct roles in calcium-dependent processes'. *American Society for Microbiology.* 9, 1049-1063.

- Freeley, M. and Long, A. (2012). 'Regulating the Regulator: Phosphorylation of PKC θ in T Cells'. *Frontiers in Immunology*. 3, 227.
- Freeley, M., Kelleher, D. and Long, A. (2011). 'Regulation of Protein Kinase C function by phosphorylation on conserved and non-conserved sites'. *Cellular Signalling*. 23(5), 753-762.
- Fresco, P., Diniz, C. and Gonçalves, J.G. (2004). 'Facilitation of noradrenaline release by activation of adenosine A2A receptors triggers both phospholipase C and adenylate cyclase pathways in rat tail artery'. *Cardiovascular Research*. 63, 739-746.
- Gao, J., Hirata, M., Mizokami, A., Zhao, J., Takahashi, I., Takeuchi, H., Hirata, M. (2016). 'Differential role of SNAP-25 phosphorylation by protein kinases A and C in the regulation of SNARE complex formation and exocytosis in PC12 cells'. *Cellular Signalling*. 28, 425-437.
- Gekel, I. and Neher, E. (2008). 'Application of an Epac Activator Enhances Neurotransmitter Release at Excitatory Central Synapses'. *The Journal of Neuroscience*. 28(32), 7991-8002.
- Ghosh, A. and Giese, K.P. (2015). 'Calcium/calmodulin-dependent kinase II and Alzheimer's disease'. *Molecular Brain*. 8, 78.
- Gonzalez-Jamett, A.M., Baez-Matus, X., Hevia, M.A., Guerra, M.J., Olivares, M.J., Martinez, A.D., Neely, A. and Cardenas, A.M. (2010). 'The association of dynamin with synaptophysin regulates quantal size and duration of exocytotic events in chromaffin cells'. *J. Neurosci*. 30, 10683-10691.
- Graham, M.E., Anggono, V., Bache, N., Larsen, M.R., Craft, G.E. and Robinson, P.J. (2007). 'The in vivo phosphorylation sites of rat brain dynamin 1'. *J. Biol. Chem*. 282, 14695-14707.
- Graham, M.E., O'Callaghan, D.W., McMahon, H.T. and Burgoyne, R.D. (2002). 'Dynamin-dependent and dynamin-independent processes contribute to the regulation of single vesicle release kinetics and quantal size'. *PNAS*. 99(10), 7124-7129.
- Grandoch, M., Roscioni, S.S. and Schmidt, M. (2010). 'The role of Epac proteins, novel cAMP mediators, in the regulation of immune, lung and neuronal function'. *BJP*. 159, 265-284.
- Granseth, B., Odermatt, B., Royle, S.J. and Lagnado, L. (2006). 'Clathrin-mediated endocytosis is the dominant mechanism of vesicle retrieval at hippocampal synapses'. *Neuron*. 51, 773-786.
- Griffith, L.C. (2004). 'Calcium/Calmodulin-Dependent Protein Kinase II: An Unforgettable Kinase'. *Journal of Neuroscience*. 24, 8391-8393.

- Gross, O.P. and von Gersdorff, H. (2016). 'Recycling at Synapses: Synaptic vesicles in rodent neurons are recycled using at least two distinct mechanisms'. *eLife*. 5, e17692.
- Gu, C., Yaddanapudi, S., Weins, A., Osborn, T., Reiser, J., Pollak, M., Hartwig, J. and Sever, S. (2010). 'Direct dynamin-actin interactions regulate the actin cytoskeleton'. *EMBO J*. 29, 3593-3606.
- Guan, J.S., Su, S.C., Gao, J., Joseph, N., Xie, Z., Zhou, Y., Durak, O., Zhang, L., Zhu, J.J., Clauser, K.R., Carr, S.A. and Tsai, L.H. (2011). 'Cdk5 is required for memory function and hippocampal plasticity via the cAMP signaling pathway'. *Plos one*. 6, e25735.
- Guillery, R.W. (2005). 'Observations of synaptic structures: origins of the neuron doctrine and its current status'. *Philos Trans R Soc Lond B Biol Sci*. 360, 1281-1307.
- Heidelberger, R. and Matthews, G. (2004). 'Vesicle Priming and Depriming: A SNAP Decision'. *Neuron*. 41(3), 311-313.
- Hemmings, H.C. and Hopkins, P.M. (2000). *Foundations of Anaesthesia: Basic Sciences for Clinical Practice*. 2nd ed. Elsevier Mosby.
- Herrero, I. and Sánchez-Prieto, J. (1996). 'cAMP-dependent Facilitation of Glutamate Release by β -Adrenergic Receptors in Cerebrocortical Nerve Terminals'. *J. Biol. Chem*. 271, 30554-30560.
- Hill, E., van der Kaay, J., Downes, C.P. and Smythe, E. (2001). 'The Role of Dynamin and Its Binding Partners in Coated Pit Invagination and Scission'. *The Journal of Cell Biology*. 152(2), 309-323.
- Huang, Y., Chen-Hwang, M.-C., Dolios, G., Murakami, N., Padovan, J.C., Wang, R. and Hwang, Y.-W. (2004). 'Mnb/Dyrk1A Phosphorylation Regulates the Interaction of Dynamin 1 with SH3 Domain-Containing Proteins'. *Biochemistry*. 43(31), 10173-10185.
- Huang, Y., Martin, K.C. and Kandel, E.R. (2000). 'Both Protein Kinase A and Mitogen-Activated Protein Kinase Are Required in the Amygdala for the Macromolecular Synthesis-Dependent Late Phase of Long-Term Potentiation'. *The Journal of Neuroscience*. 20(17), 6317-6325.
- Ikeda, K. and Bekkers, J.M. (2009). 'Counting the number of releasable synaptic vesicles in a presynaptic terminal'. *Proc. Natl. Acad. Sci. USA*. 106, 2945-2950.
- Jackson, J., Papadopoulos, A., Meunier, F.A., McCluskey, A., Robinson, P.J. and Keating, D.J. (2015). 'Small molecules demonstrate the role of dynamin as a bi-directional regulator of the exocytosis fusion pore and vesicle release'. *Mol. Psychiatry*. 20, 810-819.

- Johnson, L.N. (2009). 'The regulation of protein phosphorylation'. *Biological Society Transactions*. 37(4), 627-641.
- Johnson, R.A., De'Saubry, L., Bianchi, G., Shoshani, I., Lyons, E., Taussigi, R., Watson, P.A., Cali, J.J., Krupinski, J., Pieroni, J.P. and Iyengar, R. (1997).
- 'Isozyme-dependent Sensitivity of Adenylyl Cyclases to P-site mediated Inhibition by Adenine Nucleosides and Nucleoside 3*-Polyphosphates'. *The Journal of Biological Chemistry*. 272(14). 8962-8966.
- Junge, H.J, Rhee, J.S., Jahn, O., Varoqueaux, F., Spiess, J., Waxham, M.N., Rosenmund, C. and Brose, N. (2004). 'Calmodulin and Munc13 form a Ca²⁺ sensor/effector complex that controls short-term synaptic plasticity'. *Cell*. 118(3), 389-401.
- Kandel, E. and Schwartz, J. (2013). *Principles of Neural Science*. 5th ed. McGraw Hill Professional.
- Kidokoro, Y., Kuromi, H., Delgado, R., Maureira, C., Oliva, C. and Labarca, P. (2004). 'Synaptic vesicle pools and plasticity of synaptic transmission at the *Drosophila* synapse'. *Brain Research Reviews*. 47, 18-32.
- Kittel, R.J. and Heckmann, M. (2016). 'Synaptic vesicle proteins and active zone plasticity'. *Front Synaptic Neuroscience*. 8(8).
- Kohansal-Nodehi, M., Chua, J.J.E., Urlaub, H., Jahn, R. and Czernik, D. 'Analysis of protein phosphorylation in nerve terminal reveals extensive changes in active zone proteins upon exocytosis.' *eLife*.
- Kononenko, N.L. and Haucke, V. (2015). 'Molecular mechanisms of presynaptic membrane retrieval and synaptic vesicle reformation'. *Neuron*. 85, 484-496.
- Kononenko, N.L., Pechstein, A. and Haucke, V. (2013). 'The tortoise and the hare revisited'. *eLife*. 2, e01233.
- Lanuza, M.A., Santafe, M.M., Garcia, N., Besalduch, N., Tomàs, M., Obis, T., Priego, M., Nelson, P.G. and Tomàs, J. (2014). 'Protein Kinase C isoforms at the neuromuscular junction: localization and specific roles in neurotransmission and development'. *J. Anat.* 224, 61-73.
- Lee, S., Jung, K.J., Jung, H.S. and Chang, S. (2012). 'Dynamics of Multiple Trafficking Behaviors of Individual Synaptic Vesicles Revealed by QuantumDot Based Presynaptic Probe'. *Plos one*. 7, e38045.
- Leenders, A.G. and Sheng, Z.H. (2005). 'Modulation of neurotransmitter release by the second messenger-activated protein kinases: implications for presynaptic plasticity'. *Pharm. Ther.* 105, 69-84.
- Leitz, J. and Kavalali, E.T. (2014). 'Fast retrieval and autonomous regulation of single spontaneously recycling synaptic vesicles'. *eLife*. 3, e03658.

- Liu, J.P., Sim, A.T. and Robinson, P.J. (1994). 'Calcineurin inhibition of dynamin 1 GTPase activity coupled to nerve terminal depolarization'. *Science*. 265, 970-973.
- Liu, Y.W., Neumann, S., Ramachandran, R., Ferguson, S.M., Pucadyil, T.J. and Schmidt, S.L. (2011). 'Differential curvature sensing and generating activities of dynamin isoforms provide opportunities for tissue-specific regulation'. *Proc Natl Acad Sci USA*. 108, E234-242.
- Lou, X., Korogod, N., Brose, N. and Schneggenburger, R. (2008). 'Phorbol esters modulate spontaneous and Ca²⁺-evoked transmitter release via acting on both Munc13 and protein kinase C'. *J. Neurosci*. 28, 8257-8267.
- Lou, X., Paradise, S., Ferguson, S.M. and De Camilli, P. (2008). 'Selective saturation of slow endocytosis at a giant glutamatergic central synapse lacking dynamin 1'. *Proc. Natl. Acad. Sci. USA*. 105, 17555-17560.
- Macia, E., Ehrlich, M., Massol, R., Boucrot, E., Brunner, C. and Kirchhausen, T. (2006). 'DYN, a cell-permeable inhibitor of dynamin'. *Dev. Cell*. 10, 839850.
- Maeno-Hikichi, Y., Polo-Parada, L., Kastanenka, K.V. and Landmesser, L.T. (2011). 'Frequency-dependent modes of synaptic vesicle endocytosis and exocytosis at adult mouse neuromuscular junctions'. *J Neurosci*. 31, 10931105.
- Marois, R. and Ivanoff, J. (2005). 'Capacity limits of information processing in the brain'. *Trends in cognitive sciences*. 9, 296-305.
- Menegon, A., Bonanomi, D., Albertinazzi, C., Lotti, F., Ferrari, G., Kao, H., Benfenati, F., Baldelli, P. and Valtorta, F. (2006). 'Protein Kinase A-Mediated Synapsin I Phosphorylation Is a Central Modulator of Ca²⁺-Dependent Synaptic Activity'. *J. Neurosci*. 26(45), 11670-11681.
- Mettlen, M., Pucadyil, T., Ramachandran, R. and Schmidt, S. (2009). 'Dissecting dynamin's role in clathrin-mediated endocytosis'. *Biochem Soc Trans*. 37, 1022-1026.
- Mochida, S. (2015). *Presynaptic Terminals*. Springer.
- Morgan, J.R., Augustine, G.J. and Lafer, E.M. (2002). 'Synaptic vesicle endocytosis: the races, places, and molecular faces'. *Neuromolecular medicine*. 2, 101-114.
- Nagy, G., Matti, U., Nehring, R.B., Binz, T., Rettig, J., Neher, E. and Sorenson, J.B. (2002). 'Protein kinase C-dependent phosphorylation of synaptosome-associated protein of 25kDa at Ser187 potentiates vesicle recruitment'. *The Journal of Neuroscience*. 22, 9278-9286.

- Ñeco, P., Fernández-Peruchena, C., Navas, S., Gutiérrez, L.M., Álvarez de Toledo, G. and Alés, E. (2007). 'Myosin II Contributes to Fusion Pore Expansion during Exocytosis'. *The Journal of Biological Chemistry*. 283(16), 10949-10957.
- Neher, E. (2015). 'Merits and Limitations of Vesicle Pool Models in View of Heterogeneous Populations of Synaptic Vesicles'. *Neuron*. 87(6), 1131-1142.
- Nestler, E.J. and Greengard, P. (1999). 'Protein Phosphorylation is of Fundamental Importance in Biological Regulation'. *Basic Neurochemistry: Molecular, Cellular and Medical Aspects*. 6th ed. Lippincott-Raven, Philadelphia.
- Nguyen, T.H., Maucort, G., Sullivan, R.K., Schenning, M, Lavidis, N.A., McCluskey, A., Robinson, P.J. and Meunier, F.A. (2012). 'Actin- and dynamindependent maturation of bulk endocytosis restores neurotransmission following synaptic depletion'. *Plos One*. 7, e36913.
- Nicholls, D. G. (2003). 'Bioenergetics and transmitter release in the isolated nerve terminal'. *Neurochemical Research*. 28(10), 1433-1441.
- Oda, M., Sakitani, K., Kaibori, M., Inoue, T., Kamiyama, Y. and Okumura, T. (2000). 'Vicinal Dithiol-binding Agent, Phenylarsine Oxide, Inhibits Inducible Nitric-oxide Synthase Gene Expression at a Step of Nuclear Factor- κ B DNA Binding in Hepatocytes'. *The Journal of Biological Chemistry*. 275, 4369-4373.
- Okamoto, Y., Lipstein, N., Hua, Y., Lin, K.H., Brose, N., Sakaba, T. and Midorikawa, M. 'Distinct modes of endocytotic presynaptic membrane and protein uptake at the calyx of Held terminal of rats and mice'. *Elife*. 5, e14643.
- Parfitt, K.D. and Madison, D.V. (1993). 'Phorbol esters enhance synaptic transmission by a presynaptic, calcium-dependent mechanism in rat hippocampus'. *Journal of Physiology*. 471, 245-268.
- Pickel, V.M. and Segal, M. (2013). *The Synapse: Structure and Function*. Elsevier.
- Powell, K.A., Valova, V.A., Malladi, C.S., Jensen, O.N., Larsen, M.R. and Robinson, P.J. (2000). 'Phosphorylation of dynamin I on Ser-795 by protein kinase C blocks its association with phospholipids'. *J. Biol. Chem*. 275, 11610-11617.
- Raimondi, A., Ferguson, S.M., Lou, X., Armbruster, M., Paradise, S., Giovedi, S., Messa, M., Kono, N., Takasaki, J. and Cappello, V. (2011). 'Overlapping role of dynamin isoforms in synaptic vesicle endocytosis'. *Neuron*. 70, 1100-1114.
- Rizzoli, S.O. and Betz, W.J. (2005). 'Synaptic vesicle pools'. *Nature reviews neuroscience*. 6, 57-69.

- Robertson, M.J., Deane, F.M., Robinson, P.J. and McCluskey, A. (2014). 'Synthesis of Dynole 34-2, Dynole 2-24 and Dyngo 4a for investigating dynamin GTPase'. *Nature Protocols*. 9, 851-870.
- Rosen, D.M., Das, K. and Grimes, K.V. (2013). 'Protein kinase C, an elusive therapeutic target?'. *Nat Rev Drug Discov*. 11, 937-957.
- Ryan, T.A. (2003). 'Kiss-and-run, fuse-pinch-and-linger, fuse-and-collapse: The life and times of a neurosecretory granule'. *Proc Natl Acad Sci USA*. 100, 2171-2173.
- Saheki, Y. and De Camilli, P. (2012). 'Synaptic vesicle endocytosis'. *Cold Spring Perspect Boil*. 4, a005645.
- Santafé. M.M., Garcia, N., Lanuza, M.A., Tomàs, M. and Tomàs, J. (2009). 'Interaction Between Protein Kinase C and Protein Kinase A Can Modulate Transmitter Release at the Rat Neuromuscular Synapse'. *Journal of Neuroscience Research*. 87, 683-690.
- Schmidt, M., Dekker, F.J. and Maarsingh, H. (2013). 'Exchange protein directly activated by cAMP (epac): a multidomain cAMP mediator in the regulation of diverse biological functions'. *Pharmacol. Rev*. 65, 670-709.
- Seabrooke, S., Qiu, X, and Stewart, B.A. (2010). 'Nonmuscle Myosin II helps regulate synaptic vesicle mobility at the Drosophila neuromuscular junction'. *BMC Neuroscience*. 11(37).
- Seino, S. and Shibasaki, T. (2005). 'PKA-Dependent and PKA-Independent Pathways for cAMP-Regulated Exocytosis'. *Physiological Reviews*. 85(4), 1303-1342.
- Shepherd, G.M. (2015). *Foundations of the Neuron Doctrine: 25th Anniversary Edition*. Oxford University Press.
- Shpetner, H.S. and Vallee, R.B. (1989). 'Identification of dynamin, a novel mechanochemical enzyme that mediates interactions between microtubules'. *Cell*. 59, 421-432.
- Shupliakov, O.L. and Brodin, L. (2010). 'Recent insights into the building and cycling of synaptic vesicles'. *Exp Cell Res*. 316, 1344-1350.
- Shupliakov, O.L., Bloom, O., Gustafsson, J.S., Kjaerulff, O., Low, P., Tomilin, N., Pieribone, V.A., Greengard, P. and Brodin, L. (2002). 'Impaired recycling of synaptic vesicles after acute perturbation of the presynaptic actin cytoskeleton'. *Proc Natl Acad Sci USA*. 99, 14476-14481.
- Sim, A.T.R., Baldwin, M.L., Rostas, J.A., Holst, J. and Ludowyke, R.I. (2003). 'The role of serine/ threonine protein phosphatases in exocytosis'. *Biochem J*. 373, 641-659.

- Sims, C. (2007). Differential Modulation of Glutamatergic Synaptic Transmission by Polysialic Acid. ProQuest.
- Smillie, K.J. and Cousin, M.A. (2005). 'Dynamin I Phosphorylation and the Control of Synaptic Vesicle Endocytosis'. Biochemical Society symposium. 72, 87-97.
- Soderling, T.R. and Derkach, V.A. (2000). 'Postsynaptic protein phosphorylation and LTP'. Trends Neurosci. 23,75–80.
- Stanley, E.F. (2016). 'The nanophysiology of fast transmitter release'. Trends Neurosci. 39, 183-197.
- Sudhof, T.C. (2004). 'The synaptic vesicle cycle'. Annual review neuroscience. 27, 509-547.
- Sudhof, T.C. (2012). 'The presynaptic active zone'. Neuron 75, 11-25.
- Takamori, S., Holt, M., Stenius, K., Lemke, E.A., Grønborg, M., Riedel, D.,
- Urlaub, H., Schenck, S., Brügger, B., Ringler, P., Müller, S.A., Rammner, B.,
- Gräter, F., Hub, J.S., De Groot, B.L., Mieskes, G., Moriyama, Y., Klingauf, J., Grubmüller, H., Heuser, J., Wieland, F. and Jahn, R. 'Molecular anatomy of a trafficking organelle'. Cell 127, 831-846.
- Takei, K. and Haucke (2001). 'Clathrin-mediated endocytosis: membrane factors pull the trigger'. Trends in cell biology. 11, 385-391.
- Takei, K., Yoshida, Y. and Yamada, H. (2005). 'Regulatory Mechanisms of Dynamin-Dependent Endocytosis'. J. Biochem. 137, 243-247.
- Tan, T.C., Valova, V.A., Malladi, C.S., Graham, M.E., Berven, L.A. and Jupp, O.J. (2003). 'Cdk5 is essential for synaptic vesicle endocytosis'. Nature Cell Biology. 5(8), 701-710.
- Tsalkova, T., Meia, F.C., Li, S., Chepurny, O.G, Leech, C.A., Liu, T., Holz, G.G., Woods, V.L. and Cheng, X. (2012). 'Isoform-specific antagonists of exchange proteins directly activated by cAMP'. PNAS. 109, 18613–18618.
- Turner, K.M., Burgoyne, R.D. and Morgan, A. (1999). 'Protein phosphorylation and the regulation of synaptic membrane traffic'. Trends in Neuroscience. 22(10), 459-464.
- Vicente-Manzanares, M., Ma, X., Adelstein, R.S. and Horwitz, A.R. (2010). 'Non-muscle myosin II takes centre stage in cell adhesion and migration'. Nat Rev Mol Cell Biol. 10, 778-790.
- Von Kleist, L., Stahlschmidt, W., Bulut, H., Gromova, K., Puchkov, D., Robertson, M.J., MacGregor, K.A., Tomilin, N., Pechstein, A., Chau, N.,

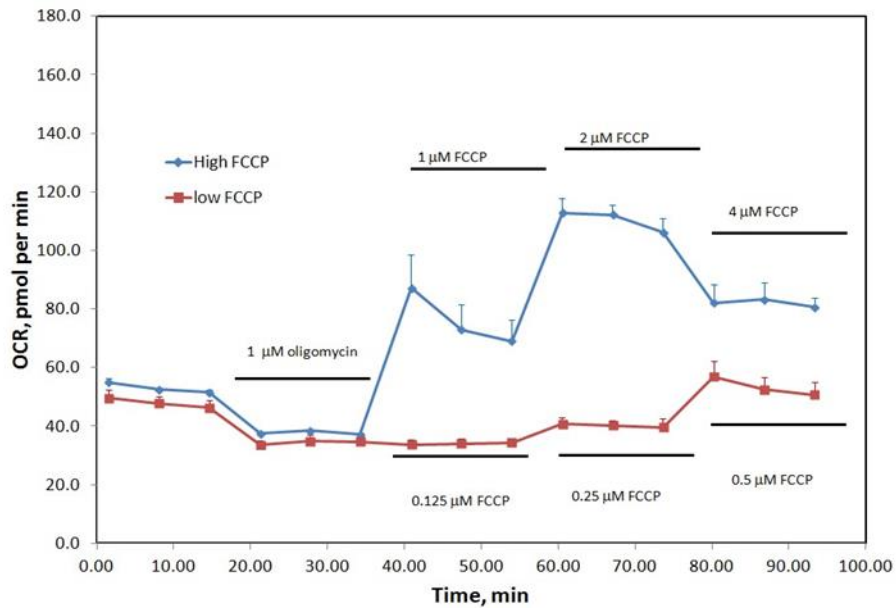
Chircop, M., Sakoff, J., von Kries, J.P., Saenger, W., Kräusslich, H., Shupliakov, O., Robinson, P.J., McCluskey, A. and Haucke, V. (2011). 'Role of the Clathrin Terminal Domain in Regulating Coated Pit Dynamics Revealed by Small Molecule Inhibition'. *Cell*. 146, 471-484.

- Voronov, S.V., Frere, S.G., Giovedi, S., Pollina, E.A., Borel, C., Zhang, H., Schmidt, C., Akeson, E.C., Wenk, M.R., Cimasoni, L., Arancio, O., Davisson, M.T., Antonarakis, S.E., Gardiner, K., De Camilli, P. and Di Paolo, G. (2008). 'Synaptojanin 1-linked phosphoinositide dyshomeostasis and cognitive deficits in mouse models of Down's syndrome'. *PNAS*. 105, 9415-9420.
- Wang, J. and Richards, D.A. (2011). 'Spatial regulation of exocytic site and vesicle mobilization by the actin cytoskeleton'. *Plos one*. 6, e29162.
- Wang, H. and Sieburth, D. (2013). 'PKA Controls calcium influx into motor neurons during a rhythmic behavior'. *PLOS Genetics*. 9, e1003831.
- Watanabe, S., Liu, Q., Davis, M.W., Hollopeter, G., Thomas, N., Jorgensen, N.B. and Jorgensen, E.M. (2013). 'Ultrafast endocytosis at *Caenorhabditis elegans* neuromuscular junctions'. *Elife*. 2, e00723.
- Watanabe, S., Rost, B.R., Camacho-Pérez, M., Davis, M.W., Söhl-Kielczynski, B., Rosenmund, C. and Jorgensen, E.M. (2013). 'Ultrafast endocytosis at mouse hippocampal synapses'. *Nature*. 504, 242-247.
- Watanabe, S., Trimbuch, T., Camacho-Pérez, M., Rost, B.R., Brokowski, B., Söhl-Kielczynski, B., Felies, A., Davis, M.W., Rosenmund, C. and Jorgensen, E.M. (2014). 'Clathrin regenerates synaptic vesicles from endosomes'. *Nature*. 515, 228-233.
- Wilhelm, B.G., Mandad, S., Truckenbrodt, S., Krohnert, K., Schafer, C., Rammner, B., Koo, S.J., Claben, G.A., Krauss, M., Haucke, V., Urlaub, H., Rizzoli, S.O. (2014). 'Composition of isolated synaptic boutons reveals the amounts of vesicle trafficking proteins'. *Science*. 344, 1023-1028.
- Wu, L.G., Ryan, T.A. and Lagnardo, L. (2007). 'Modes of vesicle retrieval at ribbon synapses, calyx-type synapses, and small central synapses'. *J Neurosci*. 27, 11793-11802.
- Wu, Y., O'Toole, E., Girard, M., Ritter, B., Messa, M., Liu, X., McPherson, P.S., Ferguson, S.M. and De Camilli, P. (2014). 'A dynamin 1-, dynamin 3- and clathrin independent pathway of synaptic vesicle recycling mediated by bulk endocytosis'. *eLife*. 3, e01621.
- Wu-Zhang, A.X. and Newton, A.C. (2014). 'Protein kinase C pharmacology: Refining the toolbox'. *Biochem J*. 452, 195-209.

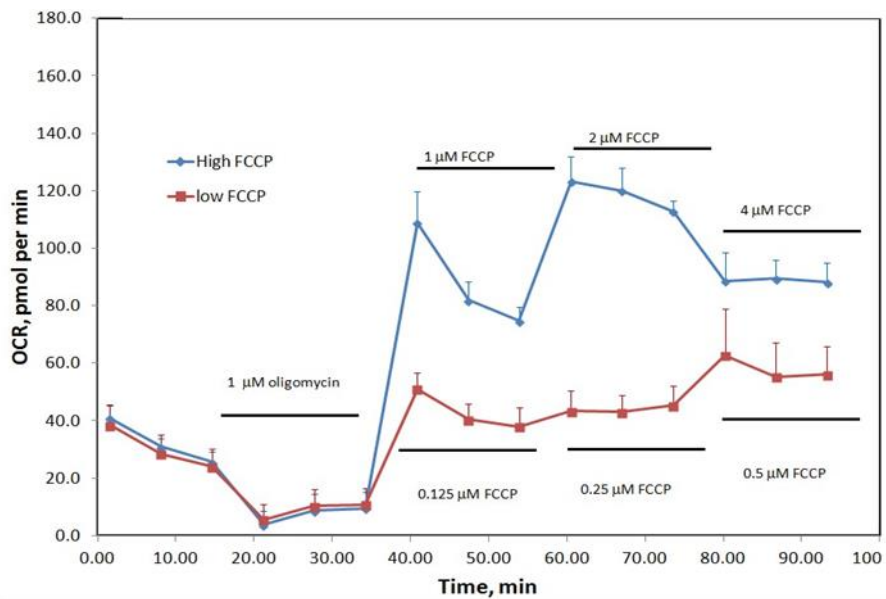
- Xiong, W., Liu, T., Wang, Y., Chen, X., Sun, L., Guo, N., Zheng, H., Zheng, L., Ruat, M., Han, W., Zhang, C.X. and Zhou, Z. (2011). 'An inhibitory effect of extracellular Ca²⁺ on Ca²⁺-dependent exocytosis'. *Plos One*. 6, e24573.
- Xue, J., Graham, M.E., Novelle, A.E., Sue, N., Gray, N., McNiven, M.A., Smillie, K.J., Cousin, M.A. and Robinson, P.J. (2011). 'Calcineurin Selectively Docks with the Dynamin Ixb Splice Variant to Regulate Activity-dependent Bulk Endocytosis'. *The Journal of Biological Chemistry*. 286, 30295-30303.
- Yamamori, S., Sugaya, D., Lida, Y., Kokubo, H., Itakura, M., Suzuki, E., Kataoka, M., Miyaoka, H. and Takahashi, M. (2014). 'Stress-induced phosphorylation of SNAP-25.' *Neuroscience Letters*. 561, 182-187.
- Yao, L. and Sakaba, T. (2010). 'cAMP Modulates Intracellular Ca²⁺ Sensitivity of Fast-Releasing Synaptic Vesicles at the Calyx of Held Synapse'. *Neurophysiol*. 104, 3250-3260.
- Young, L.H., Balin, B.J. and Weis, M.T. (2005). 'Go 6983: a fast acting protein kinase C inhibitor that attenuates myocardial ischemia/reperfusion injury'. *Cardiovasc. Drug Rev*. 23(3), 255-272.
- Yuste, R. (2015). 'From the neuron doctrine to neural networks'. *Nature reviews neuroscience*. 16, 487–497.
- Zhong, H., Sia, G.M., Sato, T.R., Gray, N.W., Mao, T., Khuchua, Z., Huganir, R.L. and Svoboda, K. (2009). 'Subcellular Dynamics of Type II PKA in Neurons'. *Neuron*. 62(3), 363-374.
- Zhou, L., McInnes, J. and Verstreken, P. (2014). 'Ultrafast synaptic endocytosis cycles to the center stage'. *Dev cell*. 28, 5-6

Appendix 1

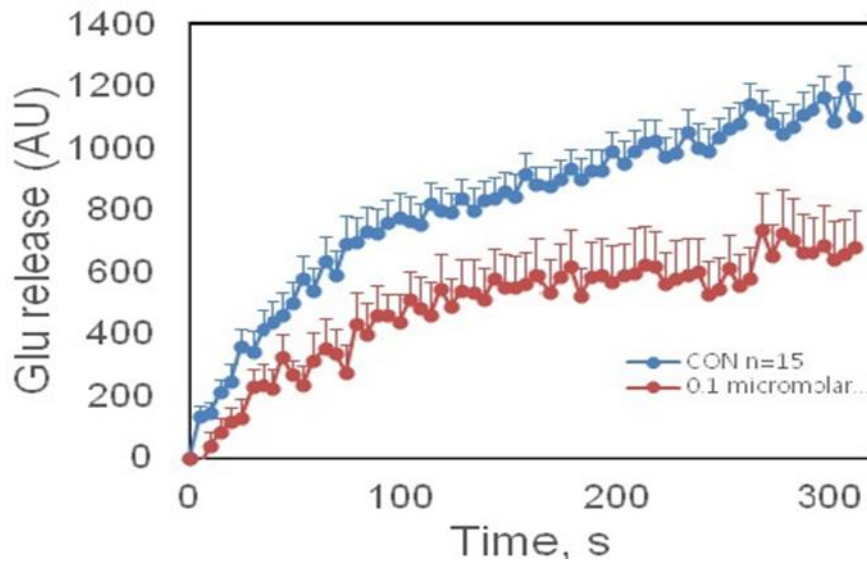
FCCP titration



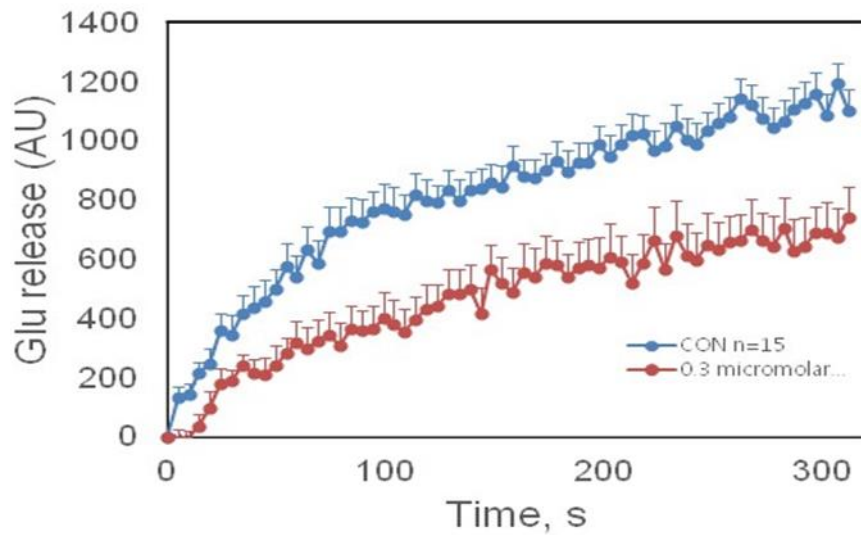
FCCP titration using initial 10 μg of immobilised synaptosome from freshly prepared terminals.



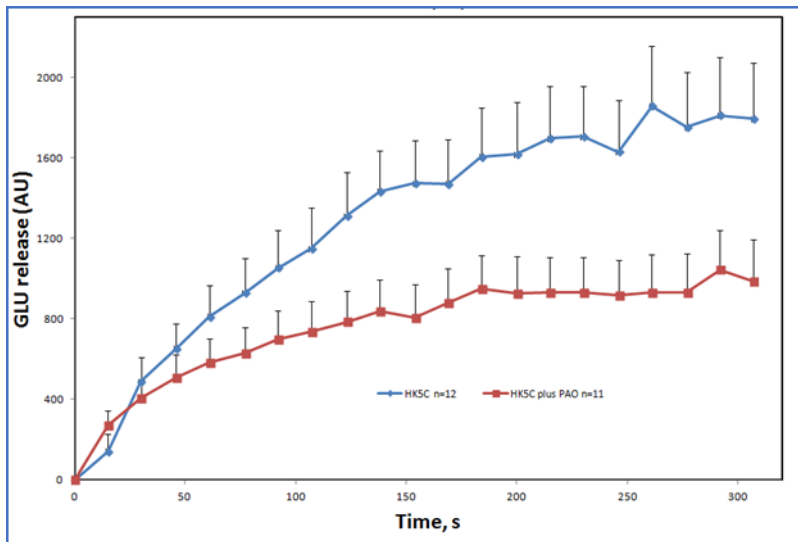
FCCP titration using 10 μg of immobilised synaptosomes prepared from stock.



The effect of 0.1 μM PAO pre-treatment on HK5C evoked Glu release.



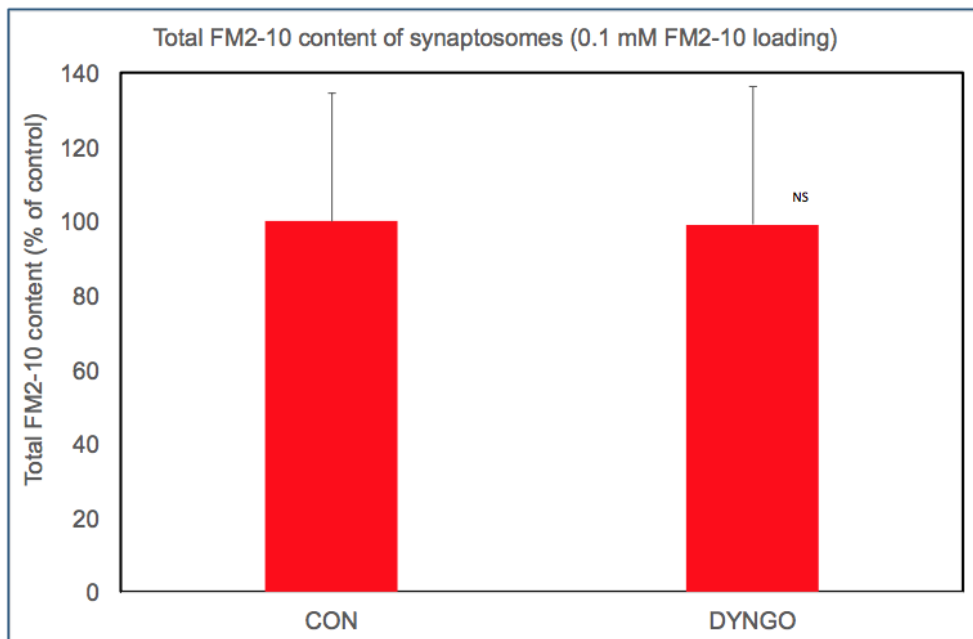
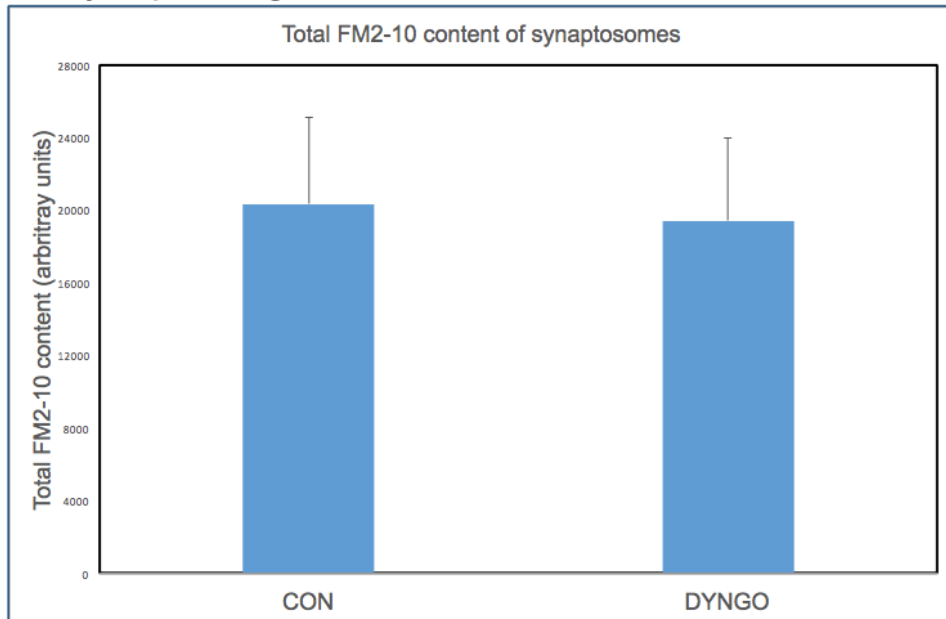
0.3 μM PAO pre-treatment on HK5C evoked Glu release.

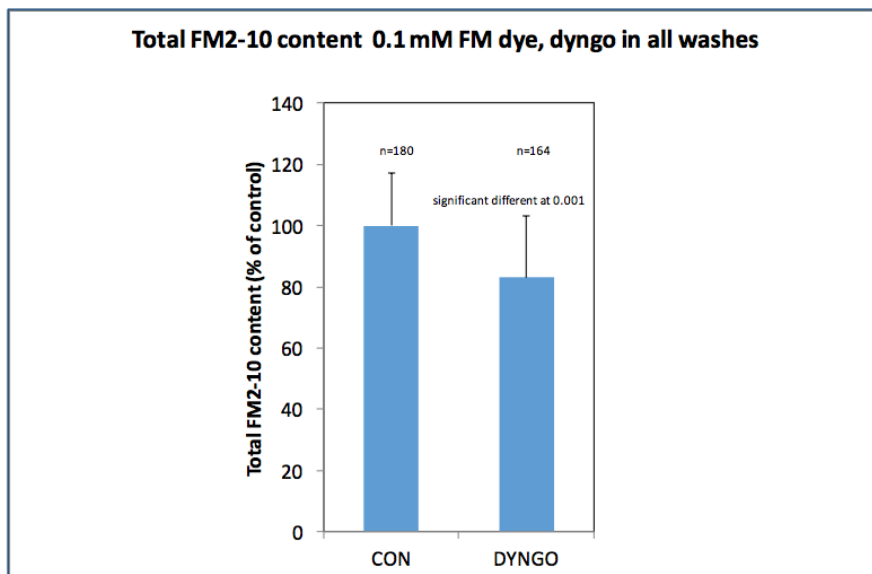
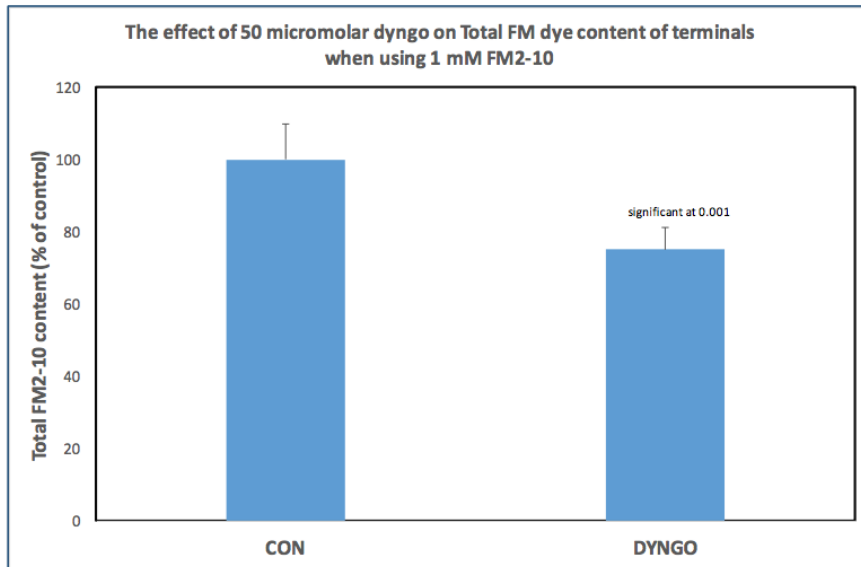


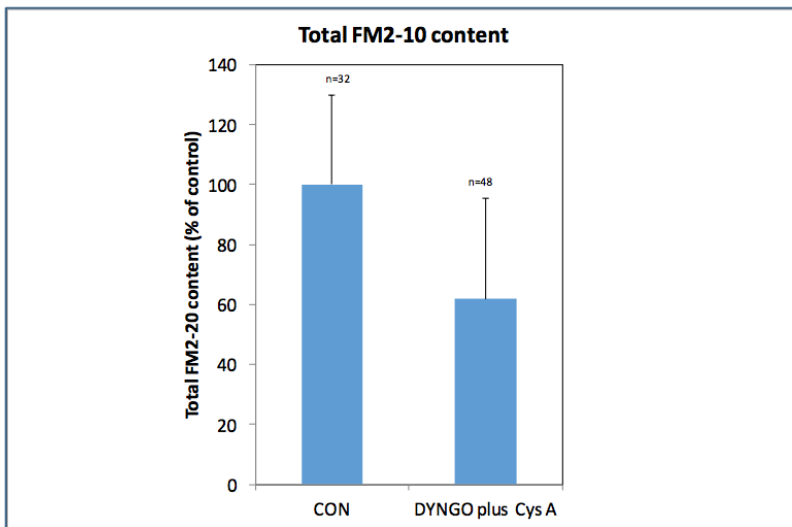
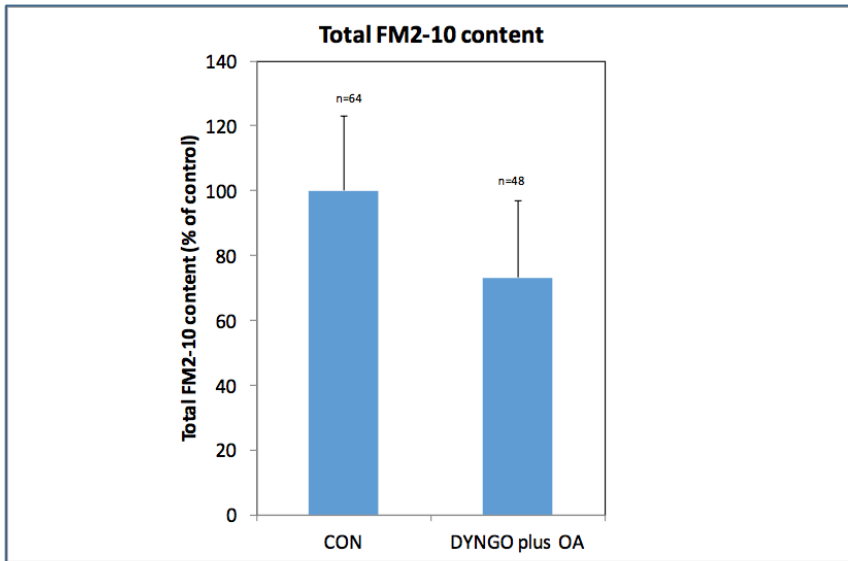
Effect of 3 micromolar PAO on glutamate release using HK5C stimulation.

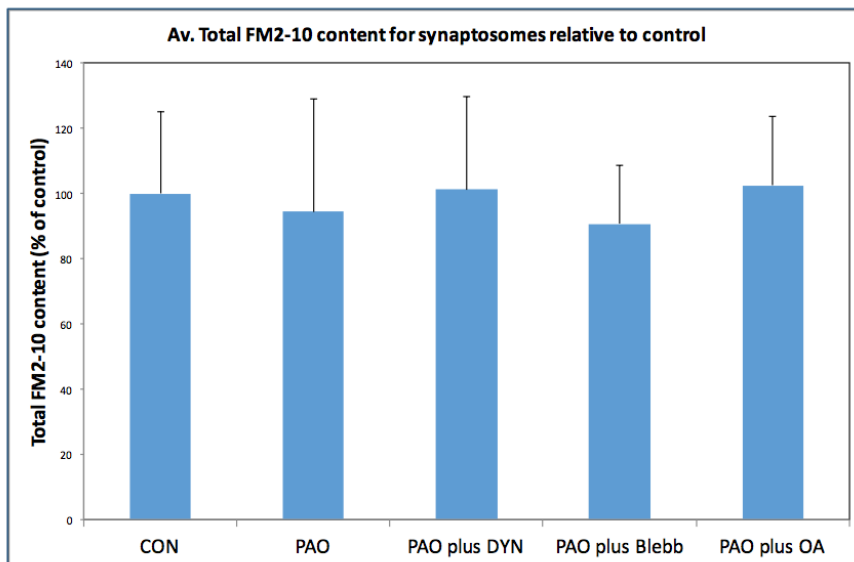
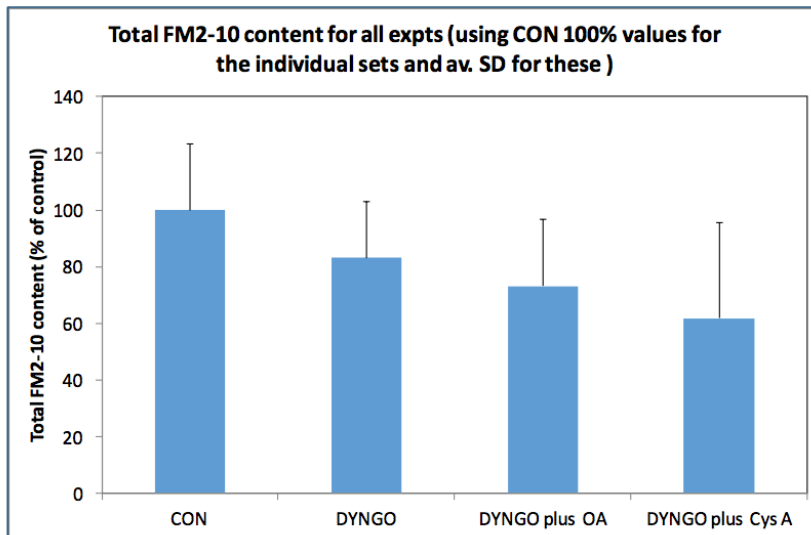
Appendix 2

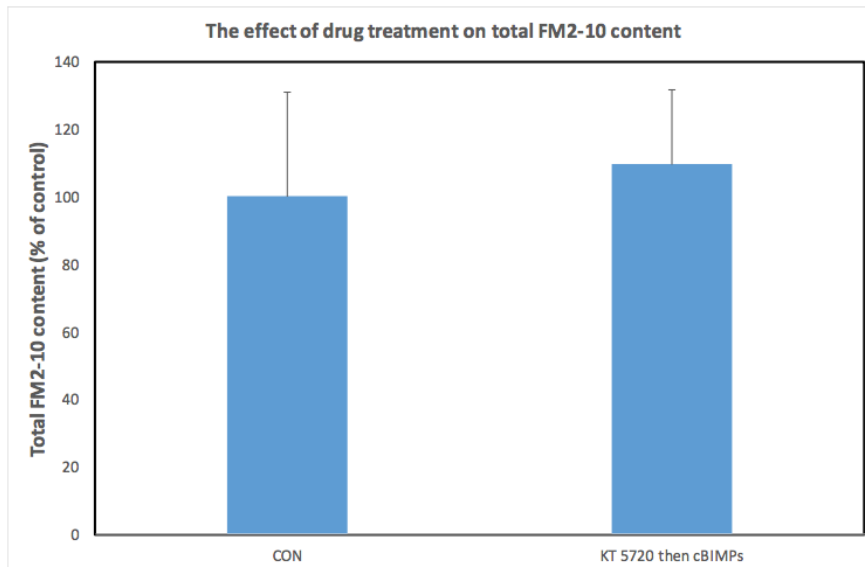
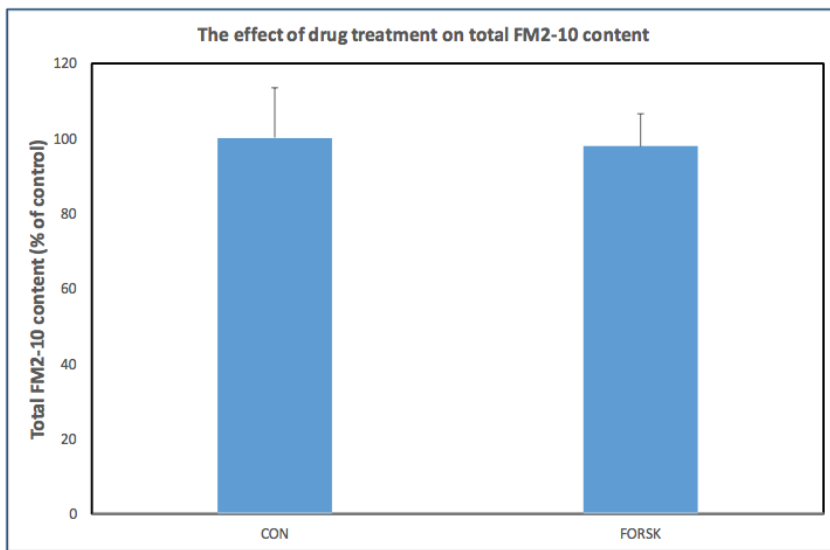
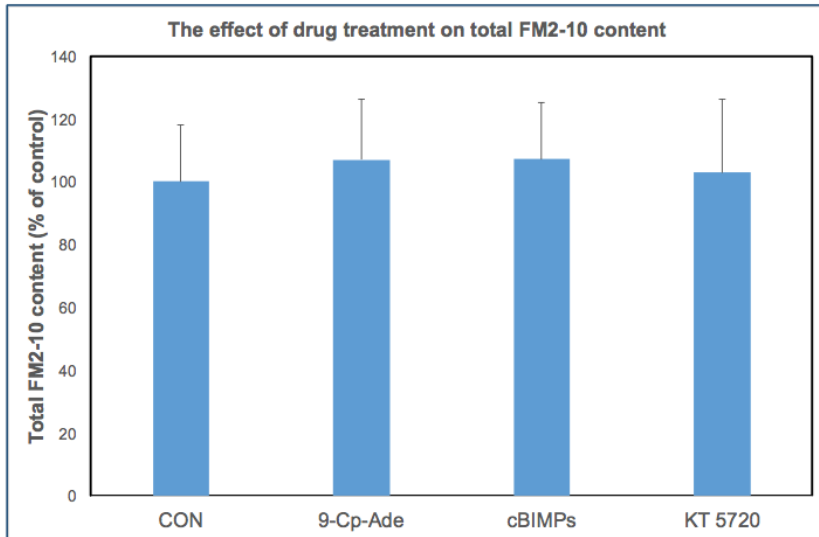
FM dye uptake figures

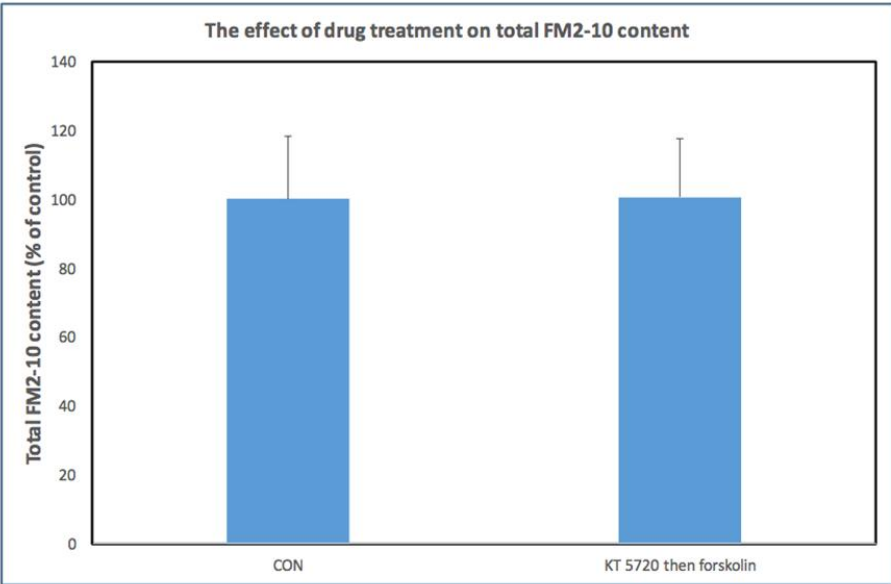
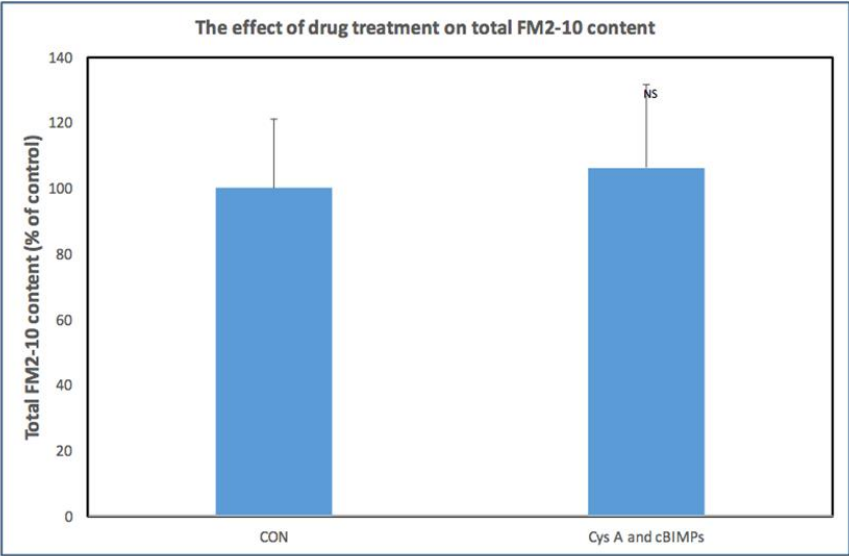










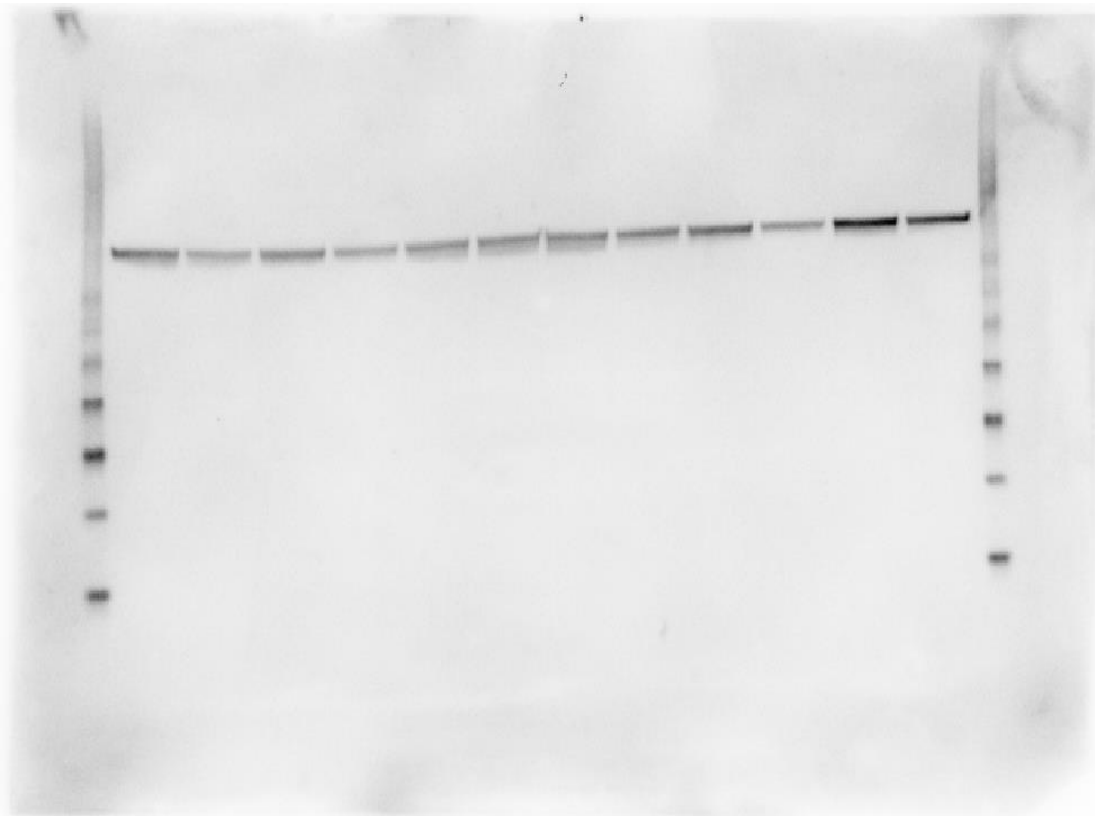


Appendix 3

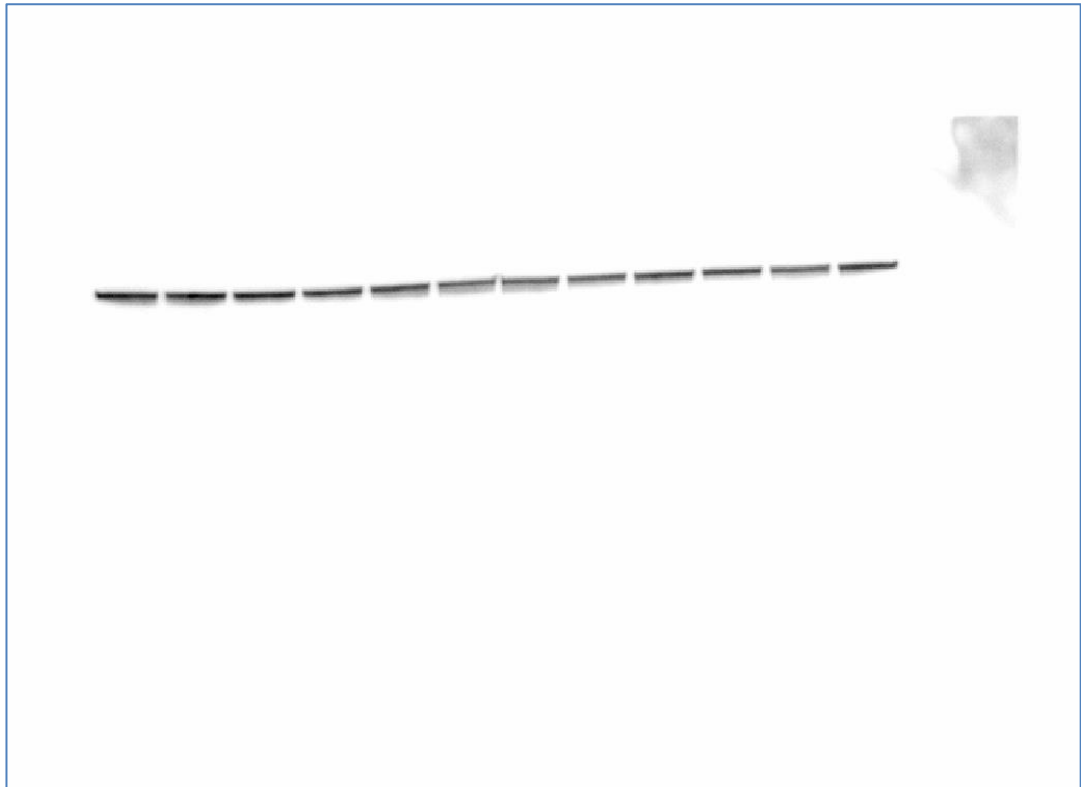
For ease of presentation, full sized blots were not presented, only the region that contained the band of interest were presented. However, full sized blots can be obtained by emailing the author on the email address: singhdeeba@gmail.com

A representative blot has been shown below

(A) Using antibody against phosphorylated ser-778 residue on dynamin I



(B) The above blot was stripped and probed with Dynamin-I (4E67)



Dynamin-I (4E67) binds to dynamin-I and helps estimate the total amount of dynamin-I present in the synaptosomes. Please note that this antibody does not bind to the western standard loaded into wells present on both end of the gels.

Appendix 4

The step by step guideline for the calculations please refer to appendix 6c of MSc thesis by Pooja M Babar. Due to the extensively long text which represents 46 pages, it was deemed considerable to omit the information and cite the work by Pooja Babar.